Wisconsin Highway Delay Causation Study

Final Report

Prepared by

Yongju Kim, Zhaoxiang He, Yingying Pang,
Anupam Srivastava, Soyoung Ahn (PI), Steven Parker
University of Wisconsin-Madison

In collaboration with

Pei Li
University of Wyoming

Jerry Shadewald, Jason Matson, Jonathan Riehl
HNTB Corporation

WISCONSIN
UNIVERSITY OF WISCONSIN–MADISON

July 3, 2026

Table of Contents

Executive Summary

This study aimed to develop a reproducible framework for analyzing highway delay causation in Wisconsin. The objective was to measure recurrent and non-recurrent delays, and link non-recurrent delay to available causal factors.

The framework integrated 15-minute travel time data from the National Performance Management Research Data Set (NPMRDS) with traffic volume estimates, crash records, non-crash incident data, lane closure records, weather data, holiday information, traffic signal information, and roadway attributes. Delay was measured using vehicle-hours of delay (VHD) for each Traffic Message Channel (TMC) segment in 15-minute intervals. VHD was calculated by multiplying the per-vehicle delay relative to an adjusted free-flow travel time by the corresponding 15-minute traffic volume. Delay was then separated into recurrent and non-recurrent components using a historical recurrent baseline derived from event-free observations. Observed delay below this baseline was classified as recurrent delay, while observed delay above this baseline was classified as non-recurrent delay and matched to available causal factor indicators, including crashes, non-crash incidents, work zones, special events, holidays, and weather. Delay that exceeded the recurrent baseline but did not match an available event indicator was retained as unclassified. Recurrent and unclassified delay were further separated into delay on signalized TMCs and delay on non-signalized TMCs based on the signal indicator.

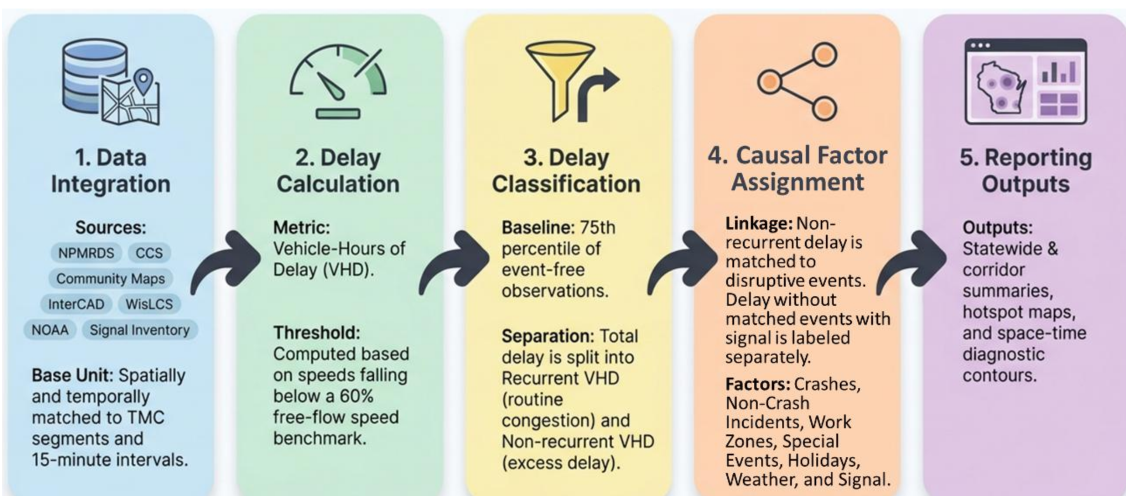

Figure 1: Wisconsin Highway Delay Causation Methodology Summary.

Note: AI-assisted graphic prepared and reviewed by the research team.

At the statewide level, non-recurrent delay accounted for the larger share of total delay across the analysis years: 2019, 2023, and 2024 (Figure 2). Statewide total VHD was 33.2 million vehicle-hours in 2019, increased to 34.9 million vehicle-hours in 2023, and decreased to 32.6 million vehicle-hours in 2024. Non-recurrent delay represented approximately 73–75 percent of statewide VHD across the three years, indicating that delay above the recurrent baseline accounted for most of the observed delay. However, year-to-year comparisons involving 2023 and 2024 should be interpreted with caution because changes in NPMRDS data supply and abnormal observation coverage patterns may have affected delay estimates.

(a) 2019 (b) 2023 (c) 2024

Figure 2: Monthly Statewide Recurrent and Non-Recurrent Delay.

Delay was spatially concentrated. In 2024, the Southeast region accounted for 58 percent of statewide VHD, followed by the Southwest region at 19 percent. At the Metropolitan Planning Area (MPA) level, the Southeastern Wisconsin MPA accounted for the largest share of total delay, followed by the Madison MPA. When MPA areas are treated as urban and non-MPA areas as rural, urban areas accounted for 81 percent of statewide VHD, while rural areas accounted for 19 percent. These results show that statewide delay is concentrated in the state's largest urbanized and high-demand areas.

Causal factor assignment results further show that delay is not attributable to a single cause. As shown in Figure 3, work-zone-related delay was the most prominent identifiable contributor, representing approximately 24 percent of annual statewide VHD in 2024. Unclassified delay on signalized TMCs and recurrent delay on signalized TMCs together accounted for 51 percent of annual VHD in 2024, indicating the significance of signalized facilities in statewide delay patterns. Heavy weather, crash-related, and holiday-related delay each accounted for less than 5 percent of statewide delay.

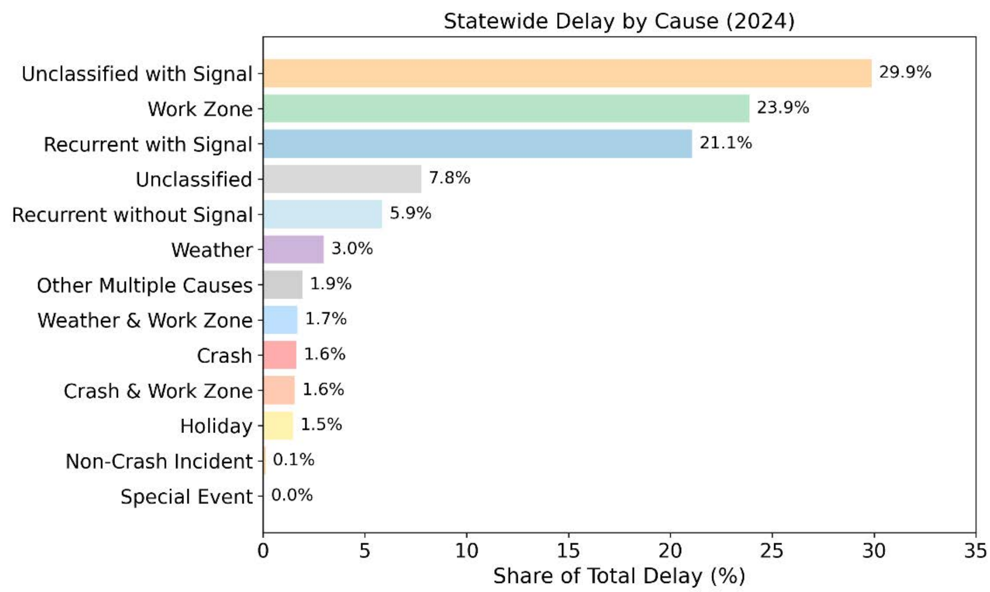

Figure 3: Statewide Delay Composition by Cause in 2024.

The corridor-level application examined 12 selected corridors identified through data-driven screening and WisDOT input. Across these corridors, non-recurrent delay generally accounted for the larger share of total delay, although the share of recurrent delay varied by corridor. For example, I-94 showed a relatively large recurrent component, while WI-172 showed a higher non-recurrent delay share. Delay was often concentrated in localized hotspots rather than being evenly distributed along an entire corridor. These hotspots were generally observed in urban or interchange areas. Several localized delay concentrations also appeared in smaller communities or non-urban corridor sections, such as the US-53 Spooner-to-Haugen section.

Corridor-level cause attribution showed that work-zone-related delay was the most common major cause across the selected corridors. In 2024, work-zone delay was the largest category in 7 of the 12 selected corridors and the second-largest category in 2 corridors. Signal-related recurrent delay and unclassified delay were especially important for 'principal arterial' and 'other principal arterial' corridors, where delay was often concentrated on signalized TMCs. Representative case studies showed that event impacts can remain localized or propagate upstream depending on event type, severity, location, and corridor structure. For example, the US-53 from I-94 to WI-29 case showed upstream-propagating delay associated with a crash, while the US-51 from Beltline to I-39/90/94 interchange case illustrated how signalized-segment delay and queue spillback can contribute to unclassified delay on non-signalized upstream TMCs.

Regression and machine-learning models were used as supplementary diagnostics. Statewide models showed that traffic demand, signal presence, work-zone closure severity, crash indicators, and heavy vehicle ratio were important predictors of delay. Corridor-level models showed that short-term temporal correlation in delay was especially important, as lagged delay variables substantially improved model fit. Roadway geometry variables provided modest improvement. Machine-learning models improved explanatory power by capturing nonlinear relationships, particularly in interstate corridors, while probabilistic models showed that the likelihood of non-recurrent delay varies by corridor and operating condition.

Overall, the study provides WisDOT with a repeatable framework for quantifying delay, separating recurrent and non-recurrent components, assigning delay to available causal factor categories, identifying unclassified delay, and generating statewide and corridor-level reporting outputs. The results demonstrate that delay causation is geography-specific and corridor-specific, requiring both systemwide summaries and localized diagnostics. Accompanying scripts and examples are provided to help WisDOT reproduce the delay causation outputs in the future.

1. Introduction

Transportation agencies use delay, travel time reliability, and related mobility measures to monitor system performance, identify operational needs, and support planning and investment decisions. Vehicle-hours of delay (VHD) is a useful metric because it combines congestion intensity with the number of vehicles affected. However, delay magnitude alone does not explain why delay occurs. Similar levels of delay may result from routine peak-period congestion, crashes, work zones, special events, weather, traffic signals, or combinations of these factors.

Wisconsin's highway system serves daily commuting, freight movement, intercity travel, tourism, and local access. Delay patterns vary across regions, facility types, and corridors. Urban interstate and arterial facilities may experience recurring peak-period congestion, while other corridors may be more affected by work zones, crashes, weather, special events, or localized bottlenecks. These differences require a framework that can classify delay consistently while still supporting localized interpretation.

This study develops and applies a delay causation methodology for Wisconsin highways. The methodology integrates NPMRDS travel time data with traffic volume estimates, crash and incident records, lane closure and work-zone data, special event information, weather data, holiday indicators, signal information, and roadway attributes. The base unit of analysis is a TMC segment during a 15-minute interval.

The methodology calculates VHD, separates delay into recurrent and non-recurrent components using a historical recurrent delay baseline, and assigns non-recurrent delay to available causal factor categories. Delay above the recurrent baseline that cannot be matched to an available causal factor is retained as unclassified delay. This category is important because it may reflect unreported events, event impacts outside the matching buffers, queue spillbacks, local demand variations, or data limitations.

The resulting outputs are designed to support delay diagnosis at multiple spatial and temporal scales. At the statewide level, the methodology produces annual and monthly summaries of total, recurrent, and non-recurrent delay by region, MPA, and causal factor category. At the corridor and selected-section levels, the outputs include recurrent and non-recurrent delay shares, monthly and hourly delay profiles, direction-specific spatial delay distributions, hotspot maps, and space-time contour diagnostics. These outputs allow delay patterns to be examined from broad statewide trends to localized corridor and segment-level conditions.

Regression and machine-learning models are also used as supplementary diagnostic tools. Regression models provide interpretable estimates of how delay is associated with traffic demand, event indicators, and signal presence, while Light Gradient-Boosting Machine (LightGBM) is used to capture nonlinear relationships and interaction patterns that may not be represented in the linear models. These models complement the causal factor assignment framework.

The report is organized as follows. Chapter 2 reviews literature, current practice, and potential data sources. Chapter 3 describes data sources and preparation. Chapter 4 presents the delay causation methodology. Chapter 5 applies the methodology statewide. Chapter 6 applies the methodology to selected corridors. Chapter 7 summarizes the major findings, limitations, and implementation implications.

2. Literature Review

This chapter reviews current practices for estimating highway delay and attributing delay to contributing factors. The review covers definitions of highway congestion and delay, State DOT delay causation practices, relevant academic studies, and commonly used data sources. The findings from this review are used to establish the methodological basis for the delay causation framework applied in this study.

2.1. Highway Delay and Congestion

Highway delay or congestion indicates deteriorating driving conditions, typically characterized by reduced speed, increased density, and a higher probability of unstable traffic flow. Although the definitions of delay and congestion vary across agencies and are sometimes used interchangeably, this study uses the term "delay" to represent travel conditions in which observed travel time exceeds an expected or reference travel time.

In terms of specific definitions of delay and congestion, MnDOT defines freeway congestion as traffic flowing at speeds less than or equal to 45 mph. This speed limit was selected since it is the speed at which "shock waves" can propagate. In contrast, Oregon and PennDOT adopt definitions from INRIX. While INRIX's exact algorithms are proprietary, PennDOT suggested that delay starts when speeds fall below 65% of free-flow for at least two minutes, with recovery marked when speeds rise above 70% of free-flow. Oregon DOT's application of INRIX probe data considers delay events when speeds drop below 60% of historical free-flow speed for at least five minutes. Moreover, Oregon DOT also adopts the Travel Time Index (TTI) to quantify congestion by comparing travel during the most congested hour of a weekday with free-flow travel. Thresholds are then applied to classify congestion severity; for instance, TTIs below 1.2 are considered uncongested, while TTIs above 2.0 indicate severe congestion.

WisDOT uses two delay-related measures: VHD and excessive delay. VHD is calculated as a product of the number of vehicles on the roadway and their individual delay in hours. At the segment level, VHD can be calculated for a roadway segment over a specified time interval. It is essentially the number of vehicles on the road multiplied by the time delay between the current NPMRDS-reported travel time and the travel time at the 85th percentile speed. For example, the equation for VHD is:

$$VHD_{s,t} = \sum_{i} V_i \cdot (TT_i - TT_2) \cdot \frac{1}{12}$$

where $VHD_{s,t}$ is vehicle-hours of delay for segment during a specific time interval, in vehicle-hours. V_i is traffic volume in a single direction, in number of vehicles for one-hour period. TT_i is the NPMRDS travel time for the current time interval i, in hours. TT_2 is the free-flow travel time for the segment, in hours. 1/12 converts the volume from a one-hour interval to a 15-minute interval.

Excessive delay is defined as the travel time in excess of the travel time at a threshold speed. The threshold speed is the greater (faster) of 20 mph or 60% of the posted speed limit (PSL) [1]. The excessive delay ($EXDELAY$) is calculated using the travel time for all vehicles (TT_ALL), in seconds, every 15 minutes on every TMC for which a PSL is provided. Non-negative delay values are enforced, and the resulting measure is expressed in hours.

$$EXDELAY = max\left\{0, \left[\frac{TT\_ALL}{3600} - \frac{MILES}{max(20, 0.6 \times PSL)}\right]\right\}$$

2.2. **Current Practice**

An important step in estimating contributing factors to delay is to link observed congestion events to other data on incidents, work zones, weather, or recurring demand. This process requires integrating multiple data sources and applying attribution rules that ensure each delay event is assigned to a likely cause.

These processes vary across agencies. Oregon DOT uses a structured prioritization framework. Once an instance of delay is identified using INRIX probe data, the vehicle hours of delay are allocated to the most likely explanatory factor with the order of incidents, work zones, weather, signal operations, holiday travel, recurring congestion, and unclassified. Similarly, VDOT quantifies delay by cause, separating recurring congestion from non-recurring sources such as incidents, work zones, and weather. Its statewide congestion reports present pie charts that show the proportion of delay attributable to each factor, based on INRIX probe data and DOT-maintained work zone and incident records.

PennDOT provides more detailed correlation rules. Crashes are linked to delay when occurring within two miles and 30 minutes of a congestion event, weather events are linked if within 15 miles and 15 minutes, and work zones are linked if they fall within three miles and the active time window. Waze alerts are also used with a one-mile, 30-minute buffer. When multiple causes overlap, PennDOT applies a priority hierarchy of crash, road work, and weather, ensuring that each delay incident is classified to a single primary cause.

At the national scale, the UMD Transportation Disruption and Disaster Statistics (TDADS) project developed a standardized methodology using INRIX probe data, Waze reports, NOAA radar, and DOT databases. Delay events are verified following a similar order to Oregon DOT.

The following subsections summarize selected delay causation practices and related studies that informed the methodology developed for this study.

FHWA Causes of Congestion in Urban Areas

FHWA published the “Traffic Congestion and Reliability: Trends and Advanced Strategies for Congestion Mitigation” report in 2020 [2]. The report examines national traffic congestion and delay trends and summarizes major sources of congestion in the U.S.

The report synthesizes findings from previous studies and identifies seven root causes of congestion, grouped into three broad categories:

1. **Category 1 – Traffic-Influencing Events**
   This category groups congestion that can be attributed to specific external trigger events and can occur with otherwise normally operating roadway conditions.
   a. **Traffic Incidents** – Events that disrupt the normal flow of traffic, usually through physical impedance in roadway lanes. These would include events such as vehicular crashes, breakdowns, and debris.
   b. **Work Zones** – Construction activities on the roadway that result in physical changes to the highway environment. These include reduction in the number or width of lanes, lane "shifts", lane diversions, reduction, or elimination of shoulders, and temporary roadway closures.
   c. **Weather** – Environmental conditions leading to changes in driver behavior and traffic flow. These include reduced visibility, heavy precipitation and snow, and wet or icy roadway surface.
2. **Category 2 – Traffic Demand**
   This category groups congestion and delay that is attributable to increases in traffic demand beyond roadway capacity (sudden increases as well as rush-hour traffic).
   a. **Fluctuations in Normal Traffic** – Day-to-day variations in demand leading to fluctuations in travel times, and thus delays and decreased travel time reliability.
   b. **Special Events** – Special case of demand fluctuations brought on by special events. These events can cause surges in demand that overwhelm the system and can lead to significant congestion and delays.
3. **Category 3 – Physical Roadway Features**
   This category groups congestion and delay attributable to physical features that make up the roadway including the roadway itself and control devices deployed.

a. **Traffic Control Devices** – Control devices such as signals, ramp-meters, at-grade railroad crossings that can lead to delays. The impact from such controls can escalate further if their design is suboptimal.
b. **Physical Bottlenecks ("Capacity")** – Situations where roadway capacity is not large enough to accommodate demand. Usual cause of recurring congestion.

In addition, the report also produces national estimates of congestion by source for urban (Figure 2-1) and for rural areas (Figure 2-2). These estimates were generated by combining findings from two previous studies: Texas Transportation Institute's annual Urban Mobility Study [3], and an Oak Ridge National Laboratory study [4]. The TTI study reported a breakdown on vehicle-hours of congestion delay by recurring and non-recurring sources for highways across all urbanized areas in the country. The Oak Ridge National Lab study investigated highway capacity losses and delay caused by temporary capacity-reducing events, studying all urban and rural freeways and principal arterials across the nation. The causes assessed in the study were: crashes, breakdowns, work zones, weather, sub-optimal signal timing, railroad crossings, toll facilities, and commercial truck pickup and delivery activities.

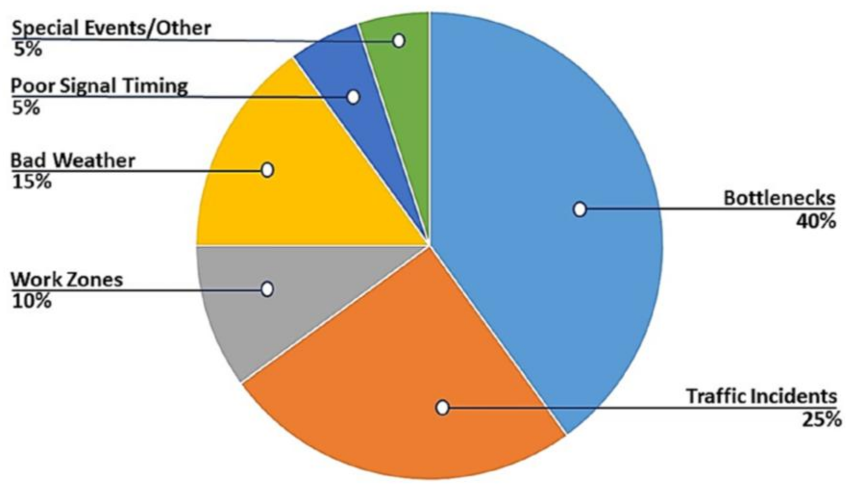

Figure 2-1: National Summary of Sources of Congestion for Urban Areas [2].

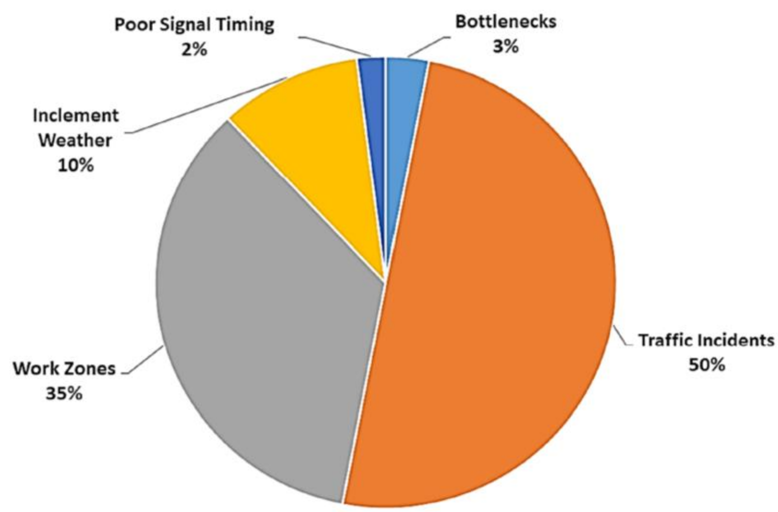

Figure 2-2: National Summary of Sources of Congestion for Rural Areas [2].

RITIS Delay Causation Module

The Regional Integrated Transportation Information System (RITIS) framework [5] was developed by The Center for Advanced Transportation Technology (CATT Lab) at the University of Maryland. RITIS is an automated, large-scale transportation data sharing system that provides dashboards and visualization tools for transportation data and performance measures, including delay.

The Causes of Congestion Graphs tool within RITIS identifies and quantifies congestion and delay using six primary categories and several combined secondary categories. The six primary categories are:

1. Recurrent Bottlenecks,
2. Weather,
3. Work Zones,
4. Incidents,
5. Signal Timing, and
6. Holidays.

In addition to the six primary categories, congestion may also be attributed to combination causes such as: incident and weather, signal and weather, incident and work zone, and recurrent and incident; as well as in an "unclassified" category. RITIS uses a multitude of data sources for mapping causes of delay including Waze (for incidents and work zones), NOAA Radar data (for weather), and OpenStreetMap (OSM traffic signal database).

Congestion delay is first categorized as recurrent or non-recurrent delay based on comparison with historic data. The cause of non-recurrent congestion delay is then identified by matching the observed delay against spatiotemporal mapping of relevant weather, incident, work zone, holiday, and signal location data. When observed delay overlaps spatially and temporally with a known event, the delay is attributed to the corresponding cause or combination of causes. For example, congestion/delay observed within 1 mile and within 30 minutes from a recorded traffic incident would be attributed to the incident in the absence of other similar event overlaps (in which case it may be categorized to a combination cause). Figure 2-3 shows a data flow and logic diagram for the Causes of Congestion Graphs module.

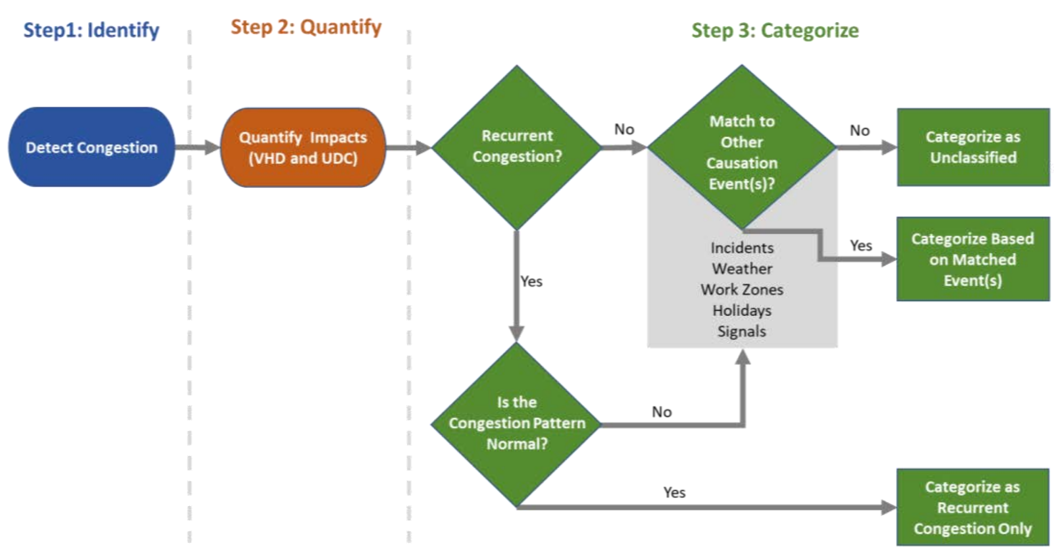

Figure 2-3: Data Flow and Logic for RITIS Causes of Congestion Graphs Module [6].

<u>Oregon Delay Study</u>

Oregon's 2024 Statewide Congestion Overview [7] examines causes of congestion and delay in Oregon at the statewide level, and for each of the 8 counties in Oregon with MPOs. It was reported that the 8 MPO counties represented 78% of statewide population and accounted for about 85% of congestion delay in the state. Data used for the analysis included Interstates, U.S. routes, Oregon routes, interchanges, and city and county arterials where sufficient data was available for analysis and reporting. The analysis included all hours of all days in 2023.

Oregon's delay causation analysis was conducted using the RITIS platform and INRIX speed data.

Congestion, in this study, was defined as the period starting when speed drops below 60% of free-flow speed for a duration of at least 5 continuous minutes. Delay was calculated as the difference between observed travel times and free-flow travel times. Delay was classified into 7 categories including the 6 primary causes defined by RITIS and the "unclassified" category. Delays that were attributed to a combination of causes were reassigned to a singular cause using a priority order (deemed the most explanatory cause): Incidents, work zones, weather, signal operations, holidays, recurring, and unclassified. Figure 2-4 shows the distribution of delay by cause reported at the statewide level, and for one of the 8 counties assessed.

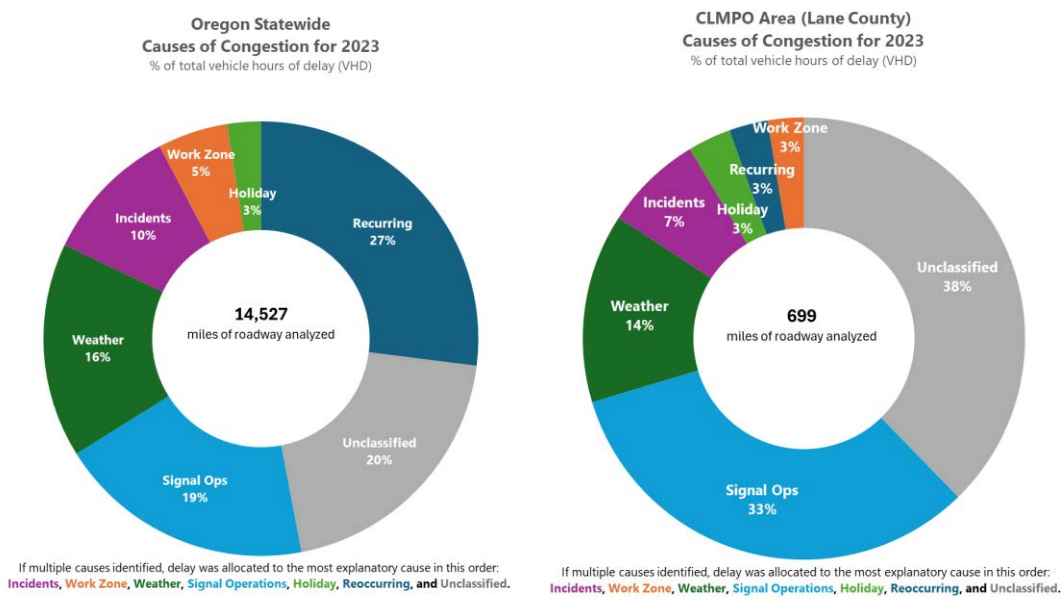

Figure 2-4: Oregon Causes of Congestion Study at the Statewide Level and for One Studied County [7].

<u>Pennsylvania Delay Study</u>

Pennsylvania's Transportation Systems Management and Operations Performance Report (TSMO) 2024 [8] analyzes congestion delay, travel time reliability, and causes of congestion for the state. Pennsylvania first published a statewide congestion pie chart (by cause of congestion) in 2020 using data from 2018. This analysis was updated in 2022 (and part of the 2024 report) with data from 2022 and with pie charts made available at municipality level in addition to statewide charts.

Pennsylvania TSMO report considers 8 causes of congestion:

1. Recurring,
2. Crash,
3. Minor Crash,

4. Other Incidents,
5. Roadwork,
6. Weather,
7. Rubbernecking, and
8. Unknown

Unique to the TSMO study are a breakdown of the “incidents” category into “Crash”, “Minor Crash”, and “Other Incidents” subdivisions, and the inclusion of “Rubbernecking” as a cause. Crash and incident data is obtained through a combination of PennDOT sources such as the Road Condition Reporting System (RCRS), and the Crash Reporting System (CRS), as well as Waze. Access to these internal reporting databases allows the analysis to be broken down into incident subdivisions. Work zone (WZ) information is obtained through PennDOT’s maintenance database, RCRS, and Waze. The Roadway Weather Information System (RWIS) acts as the primary source of weather data for the analysis.

Pennsylvania’s analysis uses traffic speeds available through INRIX for defining congestion / flow incidents (instances marking reduced speeds) starting when speeds drop below 65% of free-flow speed for at least 2 minutes, and ending when speeds have returned to 70% of free-flow speed. Delay due to congestion is classified as recurrent or non-recurrent through comparison against historical travel times for similar time-of-day and day-of-week candidates. Non-recurrent delay is then mapped against a buffer around known causal events (crash, roadway, weather) to assign cause for the congestion. Table 2-1 shows the buffers used for each data type to correlate causes to congestion. When multiple causes are identified for a given congestion event, the causation is attributed based on a priority order: Crash, Roadwork, Weather. Figure 2-5 shows Congestion Pie Charts for two Urban areas in Pennsylvania from the 2024 report.

Table 2-1: Distance and Time Buffers for Correlation between Events and Delay by Data Source [8].

Data Type	Distance Buffer	Time Buffer
Crashes (RCRS + CRS)	2 miles	30 minutes
Weather (RWIS)	15 miles	15 minutes
Work Zones (RCRS)	3 miles	Within start-end of WZ
Work Zones (Maintenance Database)	3 miles	30 minutes
All Waze Alerts	1 mile	30 minutes

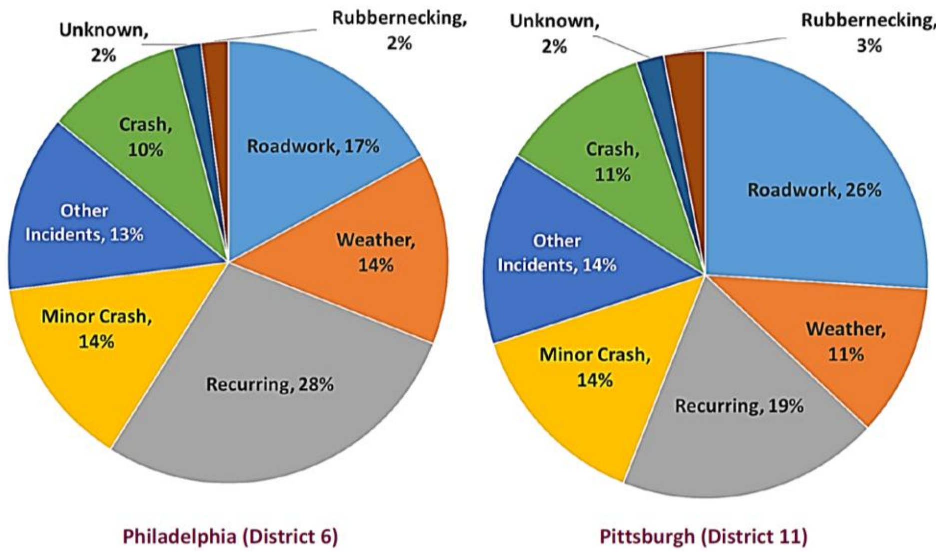

Figure 2-5: Congestion Pie Charts for Urban Areas in Pennsylvania [8].

Virginia Delay Study

Virginia's Freeway Operations and Special Facilities Performance Report was published in 2025 [9]. The VDOT Operations Performance report provided analysis of congestion and delay in Virginia at the statewide and district levels for calendar year 2024. This report provides an analysis of overall delays on interstate highways (in vehicle-hours), summary on reported incidents on all roads in the state (and by district), and breakdown of delay by cause of congestion (recurrent, incident, work zones, and weather) estimated at a planning level. The publication also reports detailed statistics on incidents, work zones and weather events through the year including information on number of incidents, number of lane-impacting incidents, incident clearing time, incident detection statistics, number of work zones, and number of weather events by type of event (fog, high wind, icy conditions, standing water, and other). The detailed process of identifying and quantifying delay by cause is not clearly mentioned in the report. Figure 2-6 and Figure 2-7 show statewide congestion causes in Virginia from 2021 to 2024 and cause-specific delay estimates for major interstates in 2024, respectively.

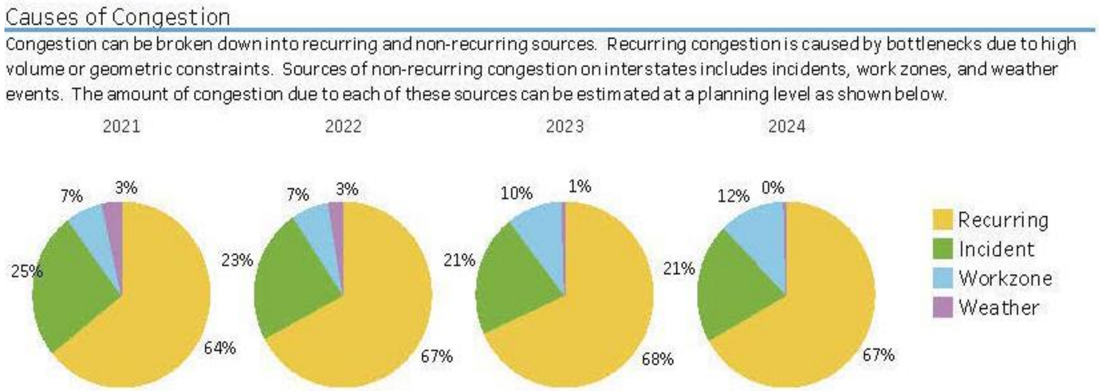

Figure 2-6: Virginia Statewide Causes of Congestion 2021-2024 [9].

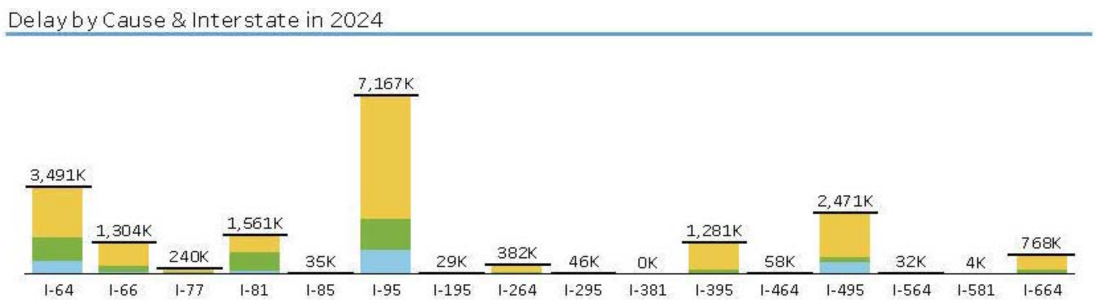

Figure 2-7: Causes of Delay Graphs for Interstates in Virginia, 2024 [9].

Academic Literature

In addition to State DOT delay causation reports, academic studies that assess delay causes for specific corridors were reviewed. This section reviews two such relevant studies: an exploration of an arterial in Florida; and a study focusing on delays caused by collisions and recurring delays that can be mitigated through optimal ramp metering on a freeway section in California. These studies provide examples of corridor-level delay attribution using regression-based modeling and theoretical congestion analysis.

Florida Case Study - Delay on Arterial

Soltani-Sobh et al. [10] investigated causes of delay on major arterial corridors in 2017. They considered 6 main causes of delay on arterials: delay due to demand, delay due to presence of signals, delay due to suboptimal signal timings, delay due to work zones and incidents, delay due to weather, and delay due to number of access points on the arterial.

The study considered a 3.6-mile arterial corridor, Broward Boulevard, in Fort Lauderdale, Florida. Soltani-Sobh et. al. define delay as the difference between observed travel time through a section of the roadway, and the free flow travel time as determined by the posted speed limit. For the study area, average expected delays for each delay cause are computed either theoretically, empirically or through simulation (such as average delay due to suboptimal signals through Synchro modeling). A multivariate linear regression model is then trained to break down delay observed for spatiotemporal blocks by contributing factors. The model is calibrated separately for the AM peak, midday, and PM peak periods (Figure 2-8). Figure 2-9 presents the congestion pie chart obtained for the AM peak period studied at the location.

Scenario	Factor	Average value	Maximum value	Coefficient	$Delay^{0.5}$ Contribution	Average Delay (%)
	Other (Intercept)	NA	NA	0.346	0.346	5.87
	Demand	228.9	772.56	0.014	3.2	54.35
	Signal Existence	8.85	44.28	0.105	0.93	15.77
	Suboptimal Signal Timing	19.8	147.8	0.041	0.81	13.79
AM peak	Weather	0.008	0.46	2.014	0.016	0.28
	Work Zone	-	-	-	-	-
	Traffic Incident	0.0044	1	1.656	0.0074	0.13
	Number of Access Points	4.1	13	0.141	0.58	9.81
	Other (Intercept)	NA	NA	0.385	0.385	7.65
	Demand	222. 93	679.76	0.011	2.45	48.7
	Signal Existence	10.47	44.28	0.088	0.92	18.3
	Suboptimal Signal Timing	11.97	97.1	0.033	0.39	7.84
Mid-day	Weather	0.0046	0.36	7.7	0.035	0.7
	Work Zone	0.037	1	0.841	0.031	0.62
	Traffic Incident	0.0019	1	2.09	0.004	0.08
	Number of Access Points	4.1	13	0.198	0.81	16.12
	Other (Intercept)	NA	NA	1.313	1.325	21.28
	Demand	264	661	0.014	3.52	56.52
	Signal Existence	10.33	44.28	0.93	0.88	14.18
	Suboptimal Signal Timing	-	-	-	-	-
PM peak	Weather	0.009	1.18	1.086	0.01	0.17
	Work Zone	0.007	1	1.412	0.0098	0.16
	Traffic Incident	-		-	-	-
	Number of Access Points	4.1	13	0.085	0.48	7.69

Figure 2-8: Regression Calibration Results and Delay Contributions from Various Causes for Broward Blvd., Fort Lauderdale, Florida [10].

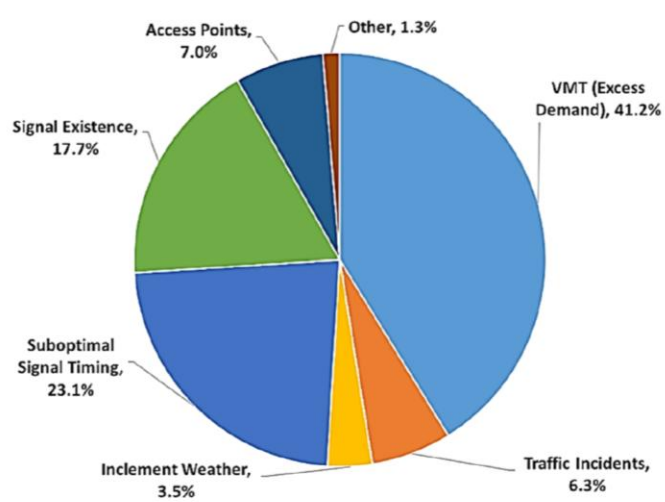

Figure 2-9: Congestion Pie Chart for AM Peak Period on Broward Blvd., Fort Lauderdale,

Florida [10].

California Case Study – I-15N

In 2005, Kwon and Varaiya investigated recurrent and collision caused delays on a 22-mile-long section of I-15 N in California [11]. The study considered daytime (5am to 8pm) traffic data on 44 weekdays from September to October of 2002. The study focused on estimating delay on a freeway due to collisions, and potentially sub-optimal ramp metering. Delay was first quantified as the difference in cumulative observed travel times and free-flow travel times along the study section. This total delay is then divided into three components, one each for delay due to collisions, potential delays that can be eliminated with optimal ramp metering, and residual delay attributed to excess demand. The results from the case study were used to generate a congestion pie chart for the location (Figure 2-10).

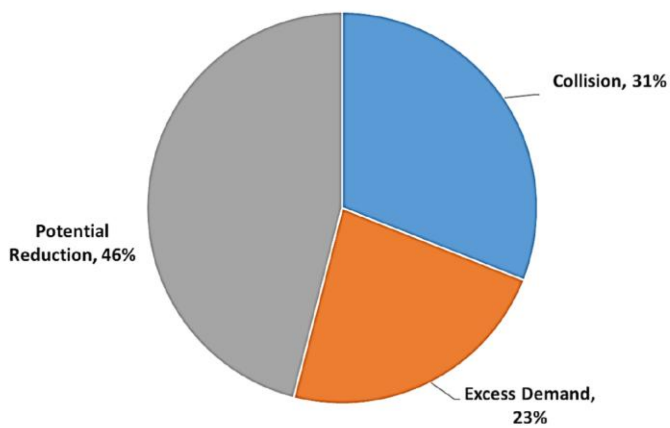

Figure 2-10: I-15N Congestion Pie for Studied I-15N Section by Kwon and Varaiya [11].

2.3. <u>Data Sources Used in Existing Practices</u>

State DOT delay causation analyses generally rely on traffic speed, volume, work zone, incident, signal, and weather data to estimate delay and identify contributing factors. As shown in Table 2-2, these data are obtained using a combination of third-party probe data, crowdsourced platforms, federal datasets, and DOT-maintained databases.

- **Traffic data**: Most DOTs use INRIX probe data from the RITIS platform for obtaining speed and congestion metrics. Some DOTs, such as Oregon DOT and MnDOT, supplement INRIX data with internal loop detector and radar detector data. Nationally, volume data are also available from the FHWA Highway Performance Monitoring System (HPMS).
- **Incident, crash, and work zone data**: DOTs use crowdsourced platforms and

internal databases to collect these data. Waze allows users to report crashes, disabled vehicles, and work zones, making it a useful crowdsourced source for incident and work zone information. Moreover, DOT-owned systems also play an important role, including incident logs, crash reporting databases, and work zone plans. For example, VDOT integrates Waze with its internal work zone database for a comprehensive work zone dataset.

- **Weather data**: The National Oceanic and Atmospheric Administration (NOAA) is the primary source for national and state-level weather data. PennDOT supplements this with its Road Weather Information System (RWIS), which provides roadway-level detail on precipitation, temperature, visibility, and surface conditions.
- **Roadway and signal data**: OpenStreetMap (OSM) is commonly used to extract signal locations and roadway geometry attributes, enabling analysis of the impact of signals and network bottlenecks.

Table 2-2: Data Types and Sources.

Data Type	Data Source
Speed and volume	INRIX and DOT Database
Crash and incident	Waze and DOT Database
Work Zone	Waze and DOT Database
Weather	NOAA and RWIS
Signal locations	OSM

2.4. <u>Summary of Literature Review Findings</u>

Causes of Delay

Based on the reviewed practices and literature, this study considers the following primary delay causation categories: recurrent congestion, crashes and other incidents, work zones, weather, special events, holidays, and signal operations. Delay that cannot be associated with an identified causal factor is retained as unclassified delay.

RITIS Modeling

The RITIS delay causation framework provides a useful reference for developing a repeatable Wisconsin-specific methodology. In particular, its use of probe speed data, historical comparisons, spatiotemporal event matching, and causal factor categories informed the structure of the methodology developed in this study. RITIS's Causes of Congestion Graphs Module allows analysis of delay by causation. Publicly available RITIS congestion cause summaries for the NHS were used as a reference point where applicable, particularly for comparing broad statewide delay patterns.

Regression Modeling for Delay Causation

In addition to rule-based delay classification, this study applies regression-based modeling to examine the relationship between observed delay and potential causal factors. The modeling framework uses variables representing the occurrence, frequency, and intensity of causal events to evaluate their association with observed delay. In doing so, observed delay can be attributed to multiple causes when relevant (such as occurrence of an incident within a WZ) along with attributing what portion of the delay was experienced due to each causal factor. This modeling component complements rule-based attribution methods by allowing multiple causal factors to be evaluated simultaneously, rather than assigning each delay observation to only one primary cause based on a fixed priority order. Additionally, unlike existing methodology that uses a fixed spatiotemporal buffer to determine correlation to events, and thus likely cause of delay, the framework also allows sensitivity testing of spatial and temporal influence ranges for selected causal factors. Depending on event type and intensity, influence buffers will be set with their likelihood of being a trigger for a delay scaling inversely by distance from event to delay. This has the potential for better identifying delay causes that would otherwise (using existing methodologies) be categorized as “unknown/other causes”.

Data Sources

The methodology developed in this study uses the following data sources:

1. Traffic data: travel time data were obtained from NPMRDS data archived by the TOPS Lab.
2. Crash data were obtained from WisTransPortal safety data applications.
3. Incident data were obtained from the InterCAD Traffic Incident Data system in WisTransPortal.
4. Lane closure data, including work zones, special events, and other lane-impacting activities, were obtained from the Wisconsin Lane Closure system in WisTransPortal.
5. Weather data were obtained from NOAA weather records.
6. Signal locations were compiled using OSM and WisDOT sources.

3. Data Sources and Preparation

This chapter describes the Wisconsin-specific datasets used to implement the delay causation methodology and the procedures used to align them within a common TMC-level, 15-minute analysis framework. The chapter focuses on the role of each dataset in delay calculation and causal factor matching. Detailed input file names and required fields are provided in the Appendices.

3.1. Analysis Years and Base Unit

This study covers the recent analysis years 2023 and 2024, along with 2019 as a comparison year consistent with the RITIS analysis. The base unit of analysis is a TMC segment observed over a 15-minute interval. This 15-minute resolution was adopted for the reproducible workflow because it reduces short-term volatility relative to the 5-minute series while preserving the timing of short-duration disturbances and delay patterns.

3.2. Data Sources

This study uses a set of datasets representing highway delay and its major contributing factors. These datasets cover travel time and road network information, traffic volume, crash occurrences, roadway incidents, weather conditions, lane closures including work zones and special events, and traffic signal information. The data were obtained from WisDOT systems, national data archives, and validated geospatial sources. Table 3-1 summarizes the data sources and key attributes, with additional details provided in the following sections.

Table 3-1: Summary of Data Sources and Key Attributes.

Data Type	Source	Key Attributes
Travel Time & Road Network	NPMRDS	15-min speed/travel time, TMC network
Traffic Volume	NPMRDS AADT & WisDOT Hourly Volume Adjustment Factor	Hourly traffic volume
Safety	Community Maps	Crash location, time, severity
Incidents	InterCAD	Non-crash events (e.g., disabled vehicles, debris)
Work Zones/Special Events	WisLCS	Closure type, duration, lanes closed
Weather	NOAA (GHCN)	Station location, daily precipitation, snow
Traffic Signal	WisDOT Inventory & OSM	Signal locations

Travel Time & Road Network

Travel time data were obtained from the National Performance Management Research Data Set (NPMRDS) (https://auth.ritis.org/npmrds), archived by the TOPS Lab for the full study period. The dataset provides 15-minute travel times and speeds for Traffic Message Channel (TMC) segments on Wisconsin's National Highway System (NHS) and serves as the primary input for delay estimation in the MAPSS and MAP-21 PM3 reporting. Roadway network shapefiles corresponding to the travel time data for each year were also obtained from the NPMRDS website. Supporting datasets, including crash records, non-crash incidents, weather information, lane closure information, and traffic signal locations, were spatially matched to the TMC segments in the NPMRDS roadway network.

Traffic Volume

Traffic volume was estimated using Annual Average Daily Traffic (AADT) from the NPMRDS dataset for each TMC segment, supplemented with hourly volume adjustment factors provided by WisDOT. NPMRDS AADT is used as the base volume measure because it is available for all directional TMC segments statewide and is directly aligned with the travel time and delay analysis framework. To capture temporal variations in traffic demand, hourly volume profiles developed based on the WisDOT continuous count site (CCS) data were applied to the TMC-level AADT values. These profiles express typical directional hourly traffic volumes as a percentage of AADT and are stratified by month, day of week, and holiday condition. Using the CCS–TMC profile assignment, directional hourly volumes were estimated by multiplying the NPMRDS AADT for each TMC by the corresponding hourly percentage factor. This approach provides a consistent method for estimating hourly traffic volume across the statewide TMC network.

Crash Records

Crash data were collected through WisTransPortal's Community Maps (https://transportal.cee.wisc.edu/services/crash-data/), maintained by the TOPS Lab in collaboration with WisDOT. Crash information used in this study includes crash date and time, location, and severity. Crashes occurring on private property or in parking lots were excluded from the analysis.

Non-Crash Incident Records

Non-crash incident data were collected from WisTransPortal's InterCAD system (https://transportal.cee.wisc.edu/applications/intercad-data/), also maintained by the TOPS Lab in collaboration with WisDOT. These data include timestamps, durations, and narrative descriptions of incident types. Crash-related incidents were removed to avoid duplication with the DT4000 crash dataset. The remaining incident records, such as disabled vehicles and debris, were retained to account for non-crash contributors to delay.

Lane Closure Records

Lane closure data were collected from the Wisconsin Lane Closure System (WisLCS) (https://transportal.cee.wisc.edu/closures/). The WisLCS records provide detailed information on planned and unplanned roadway closures, including closure type (construction, maintenance, emergency, special event, and permit-related activities), lane configuration, roadway status, and begin and end timestamps. These data were used to identify the location, timing, duration, and type of lane restrictions that may contribute to non-recurrent delays.

Weather Data

Two weather data sources were evaluated. The National Oceanic and Atmospheric Administration (NOAA) Global Historical Climatology Network Daily (GHCNd) dataset provides daily precipitation, snowfall, temperature, and other atmospheric measures from weather stations across Wisconsin. These data provide broad spatial coverage and consistent historical records (https://www.ncei.noaa.gov/products/land-based-station/global-historical-climatology-network-daily). WisDOT Road Weather Information System (RWIS) was also explored but ultimately not adopted for this study. The RWIS dataset includes roughly 60 stations statewide and is extremely large (approximately 80

GB). During the exploration, the research team found that many of the most useful operational weather variables such as precipitation, pavement condition, and visibility had substantial missing data for extended time periods in RWIS. Due to limited station coverage, high computational cost associated with the large file size, and a high proportion of missing values, the RWIS dataset was not used for the statewide or corridor-level delay causation analysis. Instead, NOAA data served as the weather data source in this study.

Traffic Signal Data

Traffic signal locations were compiled from two sources: WisDOT's statewide signal inventory and traffic signal points extracted from OpenStreetMap (OSM). The WisDOT dataset contains 4,754 records, with one signal record per intersection, and reflects the official statewide signal inventory used for planning and operations. In contrast, the OSM dataset includes 22,408 directional records corresponding to 9,714 unique signal nodes, with multiple signal nodes at each intersection, resulting in several closely overlapping points for the same location. Accordingly, the WisDOT signal dataset was used as the primary source for traffic signal information, with the OSM dataset used as a supplemental source. The two inventories were therefore treated as complementary: (i) at intersections present in the WisDOT inventory, OSM provided additional directional signal information; and (ii) at intersections not covered by the WisDOT inventory, OSM signal nodes identified additional signalized locations.

Together, these datasets provide the inputs needed to characterize recurrent and non-recurrent delay sources across Wisconsin's freeway and arterial networks. The following section describes the data preparation and integration procedures used to create a unified analytical dataset for subsequent delay causation modeling. Because the NPMRDS TMC network is updated annually, the data were prepared separately for each analysis year. The data cleaning and spatial matching examples presented below are based on the 2024 dataset. The same process was applied to the 2019 and 2023 datasets.

3.3. Data Cleaning and Spatial Matching

Data Cleaning

Travel Time & Road Network

Travel time data were obtained from NPMRDS and verified through the PM3/MAPSS project workflows to ensure consistency with established performance-measure practices. The dataset provides 15-minute travel times and speeds for NHS highways in Wisconsin, including freeways and key arterials. The corresponding TMC shapefile was filtered to retain only primary segments (isprimary =1), resulting in 10,697 out of 10,986 TMCs in

2024; the remaining 289 secondary segments represent overlapping roadways and were excluded to avoid duplicative delay accounting. The final travel time dataset and TMC network provide a clean, non-duplicative spatial–temporal base layer for the delay analysis.

Crash

Crash data were cleaned to ensure complete and valid spatiotemporal records for spatial and temporal matching. Records with invalid GPS coordinates or time information were removed. Date and time fields were standardized into a unified timestamp; roadway names were normalized to reduce formatting inconsistencies. After cleaning, 109,023 of 111,203 crash records remained for the 2024 analysis.

Non-Crash Incident

Incident data were filtered and cleaned to ensure a valid, non-duplicative incident inventory. Crash-related incidents were removed to avoid overlapping with police-reported crashes, leaving 6,663 out of 8,897 records in 2024. Additional cleaning focused on temporal and spatial validity. Records with unusable or missing time information or GPS coordinates were removed, resulting in 6,571 non-crash incident records available for spatial and temporal matching.

Lane Closure

Lane closure records were first checked for valid time and location information. Most lane closure records include usable spatial coordinates; however, 439 out of 18,871 records lack GPS coordinate information, which cannot be spatially matched directly. As a mitigation strategy, an automated approach using the Google Maps API was explored to infer approximate start and end coordinates from roadway names and descriptive location fields wherever feasible. However, none of the 439 records could be successfully geocoded; therefore, 18,432 of the 18,871 lane closure records were included in the 2024 analysis.

Weather

NOAA weather data provide station metadata (location and period of record) and daily weather measurements, including precipitation and snowfall. The data were used to characterize prevailing weather conditions affecting roadway segments rather than event-specific conditions at exact times. Initial screening focused on station coverage and data completeness. Stations were filtered to retain those geographically relevant to the Wisconsin TMC network and with sufficient temporal coverage during the study period. 598 out of 749 weather stations were retained based on the temporal coverage in 2024.

Traffic Signal

Prior to spatial integration, both the WisDOT and OSM signal inventories were reviewed for completeness and positional accuracy. To preserve full spatial coverage of the signal network, all records from both the WisDOT and OSM inventories were retained for spatial matching rather than deduplicated at the inventory level. After this review, 4,754 WisDOT signal intersections and 9,714 OSM signal nodes, corresponding to 22,408 OSM directional records, were carried forward for spatial matching.

Spatial Matching

To integrate these datasets into a unified analysis framework, spatial matching was performed to assign crash records, non-crash incidents, weather stations, lane closures, and traffic signal locations to corresponding NPMRDS TMC segments. Spatial matching methods for each data type are described in the following subsections.

Crash

Crash locations were linked to the TMC network using a proximity-based spatial matching approach. Roadway attributes such as road name and direction were checked for consistency and manual review was conducted when feasible. During manual review, a match was accepted only when no nearby non-TMC roadway provided a more plausible location match. Each crash was first spatially joined to up to two nearest TMC segments within a 50-meter buffer, resulting in 51,892 spatially joined crashes in 2024. After review, one primary TMC match was retained for each crash, with an additional overlapping TMC retained where applicable. Selecting two candidate matches helps avoid errors that can occur when the closest match corresponds to different roadway names or directions between the TMC segment and crash record. For crashes located around an intersection, the road name reported for the crash (the road on which the first harmful event occurred) was used to identify the affected TMC segments, so intersection and non-intersection crashes were filtered through the same road-name and direction consistency checks. The spatial matching procedure was divided into the following cases.

Case 1: High confidence matches (within 20 meters)

49,433 crashes fell within a 20-meter buffer and were treated as high-confidence matches. These cases were resolved using proximity, roadway name, and direction consistency.

a) For two non-overlapping matched segments or one single matched segment, matches were automatically assigned when road name and direction were consistent; otherwise, assignments were made to the closest segment within a narrow buffer (<=5 meters), with manual review conducted for cases with unmatched road names or directions for a broader buffer (5-20 meters). The matched TMC segments were then examined for the presence of an overlapping segment. If an overlapping segment existed, the crash was also assigned to that segment to account for potential traffic impacts in both travel directions.

b) For two overlapping matched segments in opposite directions, records were assigned to both travel directions on undivided facilities when road names were matched. Manual reviews were conducted for those with unmatched road names.

Case 2: Plausible matches (20–50 meters)

2,958 crashes fell between 20 and 50 meters from the nearest TMC segment. Records with unmatched road names or directions were excluded directly, while manual reviews were conducted for the remaining cases.

After applying these rules and manual review, 49,433 crash records were successfully matched to TMC segments. Figure 3-1 shows the matched crash locations in 2024.

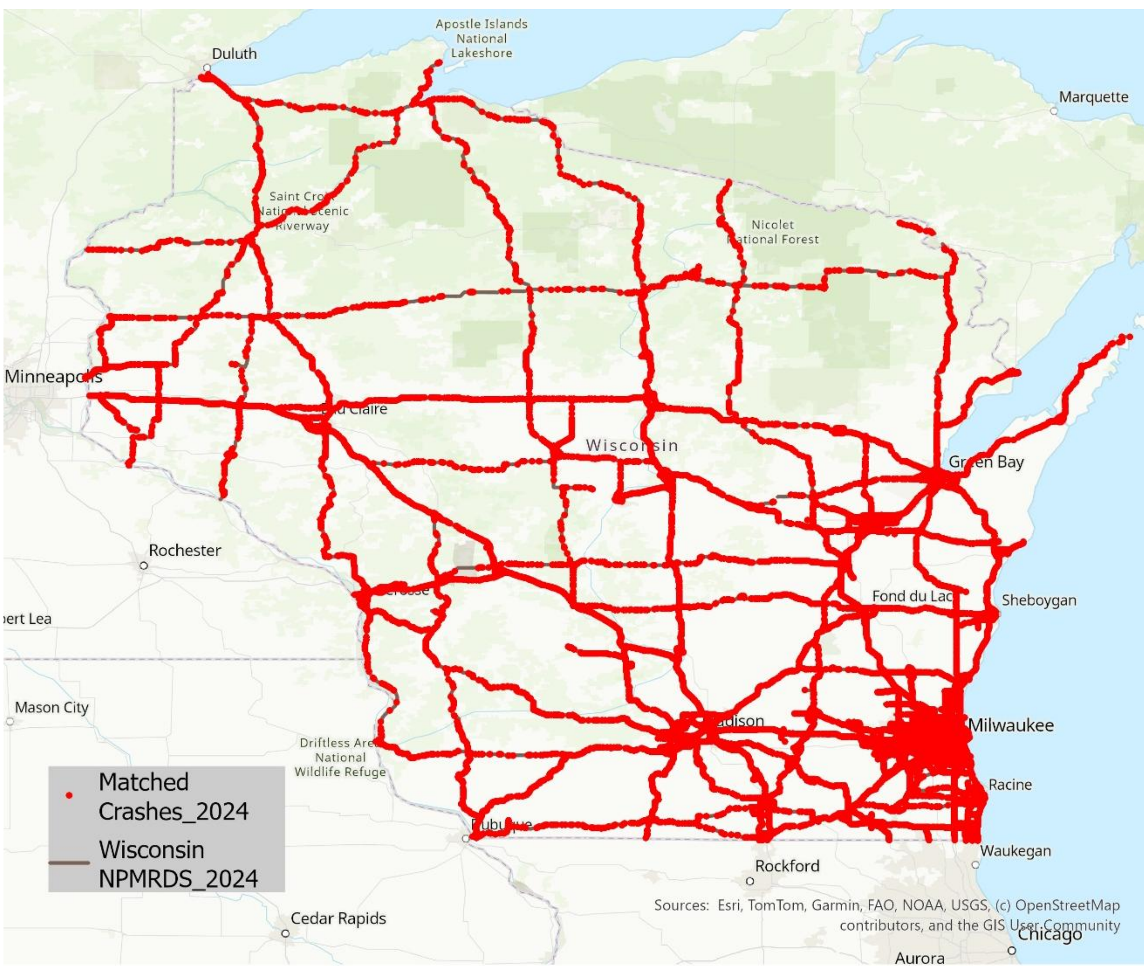

Figure 3-1: Crash Data Matching.

Non-Crash Incident

Non-crash incident data were linked to the TMC network using the same proximity-based spatial matching approach described for crash records. 5,539 non-crash incidents in 2024 were successfully matched to the TMC segments. Figure 3-2 shows the matched non-crash incident locations in 2024.

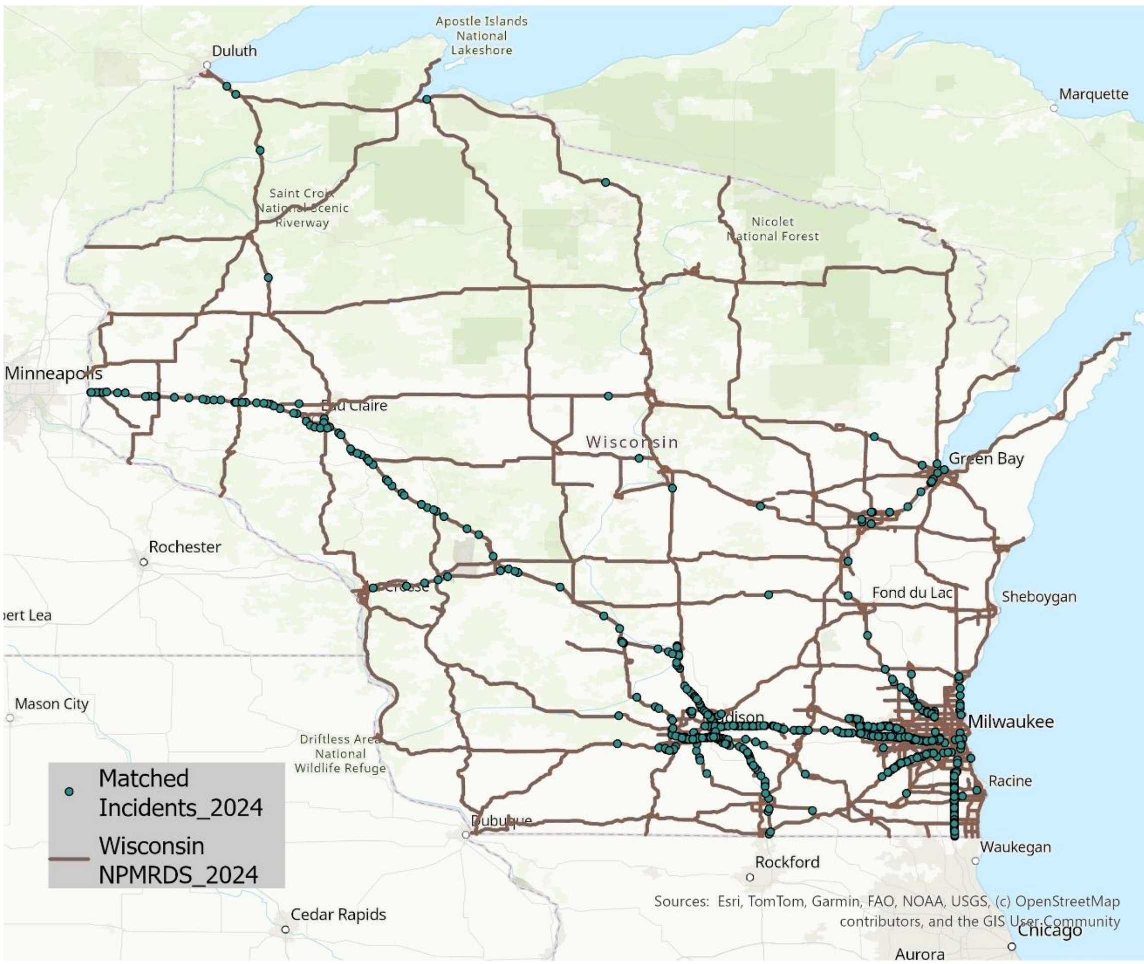

Figure 3-2: Non-Crash Incident Matching.

Lane Closure

All lane closures were included in the matching process, including those related to construction, maintenance, and special events. First, upstream and downstream endpoints were extracted for each lane closure record and spatially linked to the statewide TMC network. For each endpoint, the two nearest TMC segments were identified as candidate matches, and the final endpoint match was selected based on road name and direction consistency. Lane closures were then evaluated based on the correspondence between endpoints and TMCs, with eligible closures expanded into ordered sequences of affected TMC segments. The spatial matching details for different cases are described below.

Case 1: Both endpoints matched to the same TMC corridor.
Endpoints of 13,048 lane closures were matched to the same TMC corridors. Because TMC segments within a single TMC corridor (tmclinear) can be ordered using the road_order attribute in the NPMRDS roadway network, these closures were expanded into ordered TMC sequences by identifying all segments between the two endpoint positions along the TMC corridor.

Case 2: Endpoints matched to different TMC corridors.
Endpoints of 1,768 lane closures were matched to different TMC corridors. For each lane closure, the two TMC corridors were connected based on the shared endpoint coordinates to ensure continuity across different corridors, with manual review applied when the automated approach did not produce a valid continuous path. Once the start and end corridors were established, all intermediate TMC segments between the two endpoints were identified to form a continuous affected path.

Case 3: Only one endpoint matched to the TMC network.
For 723 lane closures, only one endpoint could be matched to the TMC network. These records were processed using a direction-based inference approach: the lane closure direction and the matched TMC direction were compared to expand affected segments forward or backward along the same TMC corridor. When closure length information was available, expansion was constrained by cumulative segment length. The matching was initially processed using the automated rules, followed by manual review to resolve ambiguous locations.

Case 4: No endpoint matched to the TMC network.
For 2,893 lane closures, neither endpoint was mapped to the TMC network. These closures were excluded from the analysis.

In total, 15,442 lane closure records were successfully matched to TMC segments, with each lane closure record linked to an ordered list of affected TMC segments. Consistent with the crash matching procedure, each matched TMC segment was then examined for the presence of an overlapping segment. These overlapping segments were flagged to account for potential effects of unidirectional lane closures on traffic in both travel directions. Figure 3-3 shows the matched lane closure records in 2024.

Figure 3-3: Lane Closure Data Matching.

Weather

Weather conditions were linked to roadway segments by associating each TMC with observations from nearby weather stations. Each TMC segment was linked to the three nearest weather stations to provide redundancy and improve the robustness of weather assignment. The distance between each TMC and the associated weather stations was retained for filtering purposes. Retaining this distance allows weather assignments to be filtered using an acceptable maximum distance (10,578 out of 10,697 TMCs have the nearest weather station within 15 miles for 2024). If station-level daily observations were unavailable for a given TMC and date, a backup protocol was applied using NOAA weather information from a broader jurisdictional area, such as the county level. Figure 3-4 shows the matched NOAA weather stations.

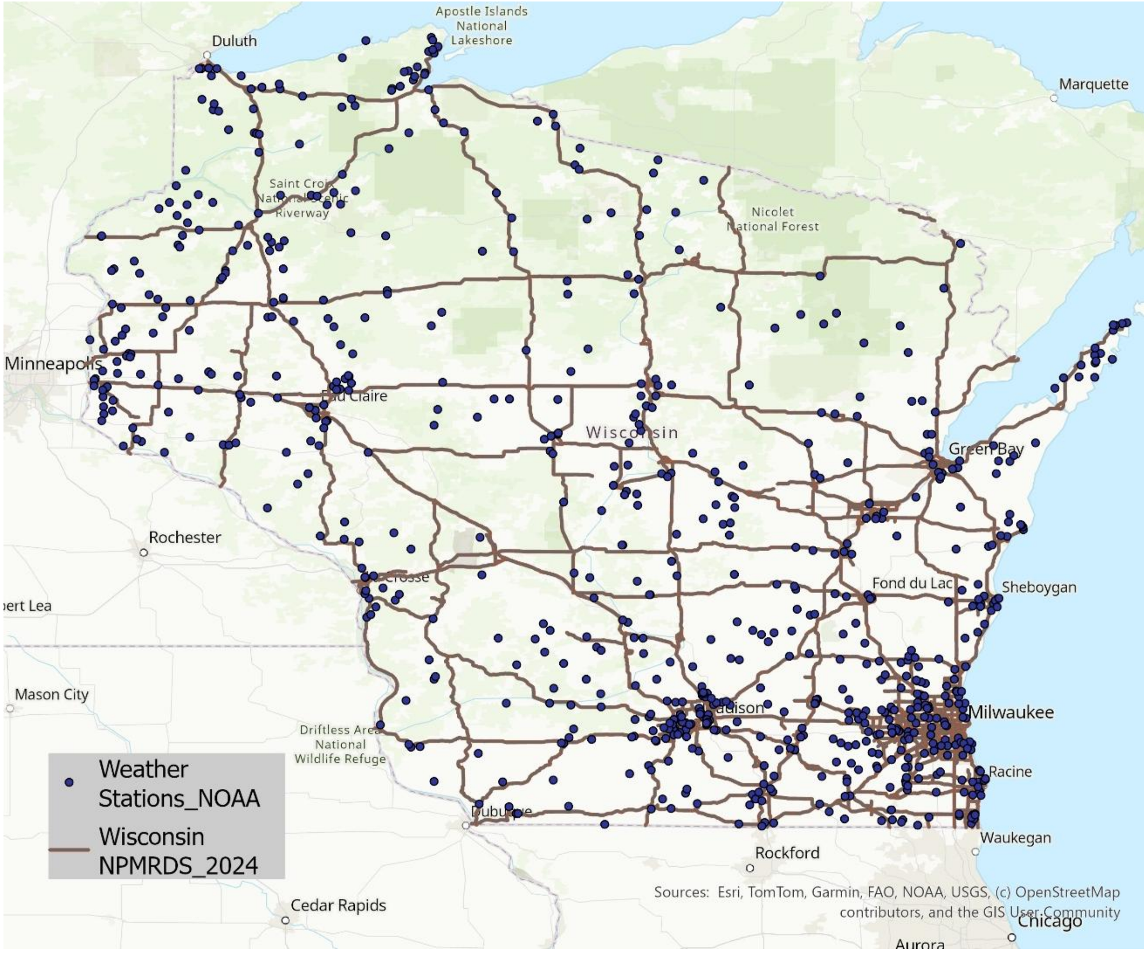

Figure 3-4: Weather Station Matching.

Traffic Signal

Using a similar proximity-based spatial matching approach, each TMC segment was buffered by 50 meters and spatially joined with the combined signal point dataset. Only signals located at the downstream endpoint or within the segment were retained, while signals at the upstream endpoint were excluded because signal-related delay is attributed to the approaching segment. Each candidate signal-TMC pair was then verified through a road-name matching step that compared the TMC's road and intersection names against the signal's name components, with separate rules applied to ramp and non-ramp segments. Interstate mainline segments were classified as non-signalized, and TMCs were reclassified as non-signalized when OSM bridge data indicated that the TMC bridges over the matched signal. This produces a many-to-many relationship: a TMC may include multiple signals along its length, and a single signal at an intersection may be matched to multiple intersecting TMCs because it produces delay on all approaching cross-roads. Through this procedure, 4,444 TMC segments in 2024 were identified as having at least one associated traffic signal. Figure 3-5 shows the signalized TMC segments identified through this matching procedure.

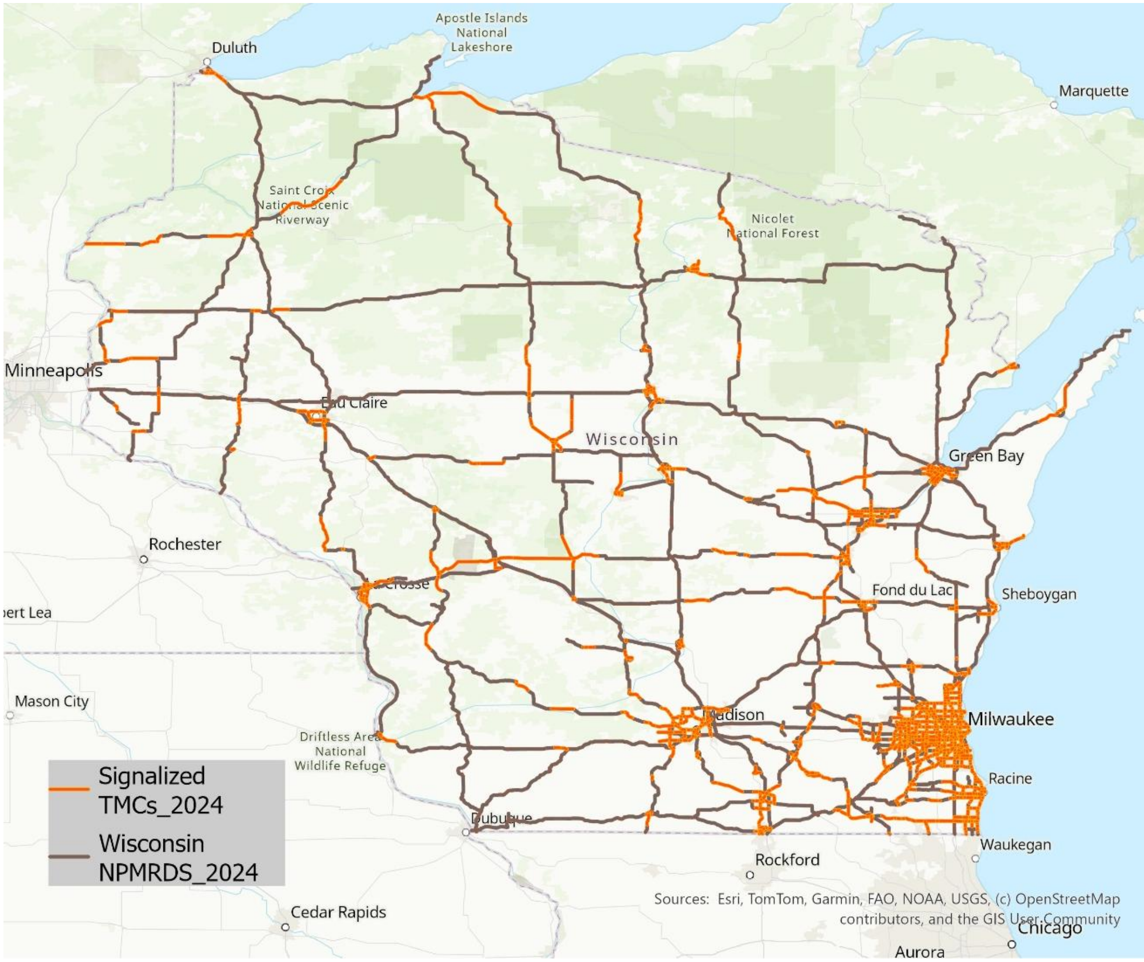

Figure 3-5: Traffic Signal Matching.

Spatial Matching Results

Table 3-2 summarizes the 2024 data processing results, including the number of raw records, the number retained after cleaning, and the number used in the analysis after spatial matching. For the weather data, 749 weather stations were initially available, of which 580 were retained after excluding stations with no observations in 2024. For traffic signal data, 4,754 WisDOT signal intersections and 9,714 OSM signal nodes were obtained and all records remained. After spatial matching and road-name verification, 2,615 unique WisDOT signal locations and 4,932 unique OSM signal nodes were spatially associated with at least one TMC segment and used in the analysis. Some WisDOT intersections and OSM signal nodes may refer to the same physical signal location; however, both sources were retained to preserve available signal information and maximize spatial coverage.

Table 3-2: Data Processing Results for 2024.

Dataset	# of Raw Records	# of Cleaned Records	# of Spatially Matched Records
Crash	111,203	109,023	49,433
Incident	8,897	6,571	5,539
Lane Closure	18,871	18,432	15,442
Weather Station	749	598	580
Traffic Signal	4,754 (WisDOT) + 9,714 (OSM)	4,754 (WisDOT) + 9,714 (OSM)	2,615 (WisDOT) + 4,932 (OSM)

3.4. Analysis Dataset and TMC Coverage

All calculations begin with an analysis dataset at the TMC level. Each record represents one TMC segment during a 15-minute interval and contains travel time, estimated hourly traffic volume, and causal factor information, including severity or type where available. This dataset is the base input for delay calculation, recurrent and non-recurrent delay classification, causal factor assignment, statewide summaries, corridor-level diagnostics, and delay causation modeling.

Table 3-3: Key Variables in the Analysis Dataset.

Dataset	Data Item	Data Type
NPMRDS Data	TMC ID	String
	Time (Start time of the 15-minute interval)	Timestamp
	Travel Time	Numeric
	Travel Speed	Numeric
	Length	Numeric
Traffic Volume	Hourly Volume	Numeric
Crash Data	Crash ID	String
	Injury Severity	Categorical
Non-crash Incident Data	Incident ID	String
	Incident Type	Categorical
Lane Closure Data	Closure ID	String
	Closure Type (construction, special events, maintenance, emergency, permit)	Categorical
	Duration (continuous, daily, weekly)	Categorical
	Roadway Status	Categorical
	Lane Description	Text
Weather Data	Precipitation (mm)	Numeric
	Snowfall (mm)	Numeric
	Snow depth (mm)	Numeric
Traffic Signal Data	Signal indicator	Binary

TMC Lookup Tables

Annual TMC lookup tables provide the common spatial reference for the analysis dataset. The lookup process starts from the annual NPMRDS TMC identification file and appends WisDOT region, MPA, AADT, heavy vehicle ratio, and other TMC attributes. These fields are retained for aggregation, corridor segmentation, modeling, and mapping.

The number of TMCs included in the final analysis varies by year because the NPMRDS network changes over time and because some TMCs do not have valid travel time coverage. Table 3-4 summarizes TMC coverage by processing stage. The final analysis TMCs consist of primary TMCs with valid NPMRDS travel time coverage.

Table 3-4: TMC Coverage by Processing Stage.

Processing Stage	**2019**	**2023**	**2024**
Raw TMC inventory	10,371	10,821	10,986
Primary TMCs	10,094	10,534	10,697
TMCs with valid NPMRDS coverage	9,789	10,517	10,680
TMCs with CCS profile coverage	9,932	10,257	10,697
Final analysis TMCs	9,789 (94.4%)	10,517 (97.2%)	10,680 (97.2%)

Note: CCS profile coverage was assessed using the annual TMC inventory before filtering for valid NPMRDS travel time coverage. Therefore, CCS coverage counts may exceed the number of TMCs with valid NPMRDS observations.

4. Delay Causation Methodology

This chapter describes the methodology used to calculate total delay, separate delay into recurrent and non-recurrent components, and associate non-recurrent delay with causal factor categories. The methodology combines a historical recurrent baseline with spatiotemporal event matching and serves as the basis for the delay causation outputs presented in this report.

Figure 4-1 summarizes the overall delay causation methodology. After total VHD is calculated for each TMC and 15-minute interval, observations with positive delay are compared with the recurrent baseline, represented by the 75th percentile of event-free delay. Delay within the baseline is classified as recurrent delay and separated into signalized and non-signalized categories. Delay exceeding the baseline is classified as non-recurrent delay and matched to crash, non-crash incident, work zone, special event, holiday, and weather indicators. When no matching event is identified, the excess delay is retained as unclassified, with a separate category for signalized TMCs.

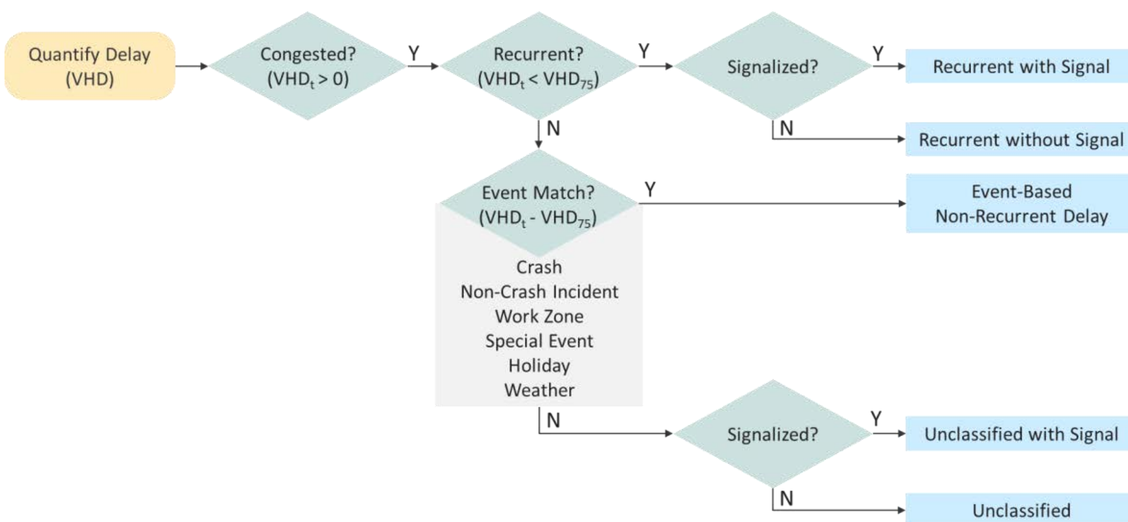

Figure 4-1: Delay Causation Methodology Flowchart.

4.1. Traffic Volume Estimation

Traffic volume is estimated for each TMC and time period using TMC-level AADT and WisDOT CCS-based hourly volume profiles. When CCS profile data are available, directional hourly volume is estimated by scaling the TMC AADT using the corresponding hourly profile. For 2019 and 2023, year-specific AADT values are combined with the 2024 CCS hourly profiles. This assumes that hourly traffic distribution patterns are transferable across the analysis years. For TMCs without CCS profile coverage, AADT is distributed uniformly across 24 hours and two directions as a fallback approximation. The fallback rule is applied to 260 TMCs in 2023, representing approximately 2.5 percent of the 2023 analysis TMCs not covered by the 2024 CCS profiles. For future applications, an hourly distribution curve may be used instead of uniform distribution, and CCS profiles for the corresponding analysis year should be reviewed and used when available.

4.2. **Delay Definition and Calculation**

Delay is measured using vehicle-hours of delay (VHD). VHD represents the total delay experienced by vehicles traveling on a roadway segment during a given time interval. At the base level, VHD is calculated for each TMC segment and 15-minute interval.

Delay is calculated relative to an adjusted free-flow travel time. In this study, delay is identified when observed speed falls below 60 percent of free-flow speed, consistent with the threshold-based delay definition used by Oregon DOT. The adjustment factor used for this threshold is 0.6. This threshold is intended to capture operationally meaningful delay rather than minor speed reductions near free-flow conditions.

For TMC segment s and 15-minute interval t, VHD is calculated as:

$$VHD_{s,t} = \frac{1}{4} V_{s,t} \cdot max\left(ATT_{s,t} - \frac{FTT_s}{\alpha}, 0\right)$$

where:

- $VHD_{s,t}$ is vehicle-hours of delay for TMC segment s during 15-minute interval t;
- $V_{s,t}$ is the directional hourly traffic volume for TMC segment s during interval t;
- $ATT_{s,t}$ is the actual (observed) travel time for TMC segment s during interval t;
- FTT_s is the free-flow travel time for TMC segment s;
- α is the free-flow speed adjustment factor set to 0.6; and
- ¼ converts hourly traffic volume to a 15-minute equivalent.

For each 15-minute interval, per-vehicle delay is calculated as the positive difference between actual (observed) travel time and the adjusted free-flow travel time. Negative delay values are set to zero. The per-vehicle delay is then multiplied by the estimated 15-minute traffic volume to produce VHD.

To summarize, the calculation procedure consists of the following steps:

1. Estimate directional hourly volume for each TMC and hour.
2. Convert hourly volume to a 15-minute volume using a factor of $1/4$.
3. Calculate adjusted free-flow travel time using the 60 percent free-flow speed

threshold.

4. Calculate per-vehicle delay as the positive difference between observed and adjusted free-flow travel time.
5. Multiply 15-minute volume by per-vehicle delay to obtain VHD.

The resulting 15-minute TMC-level VHD values serve as the base unit for all subsequent delay classification and aggregation.

4.3. <u>**Data Quality Treatment**</u>

The final methodology retains high travel time observations rather than applying outlier capping. This approach preserves high-delay values that may represent severe congestion or event-related disturbances. Negative delay values are replaced with zero after comparing observed travel time with the adjusted free-flow benchmark.

Missing observations are treated using a conservative interpolation rule. Short missing gaps in the 15-minute travel speed series are filled using linear interpolation, and the interpolated speeds are used for delay calculation. Gaps longer than one hour are retained as missing. The procedure is applied separately for each TMC time series. Each observation receives an imputation label indicating whether it is observed or linearly interpolated.

Table 4-1: Missing Data Imputation Rule.

Gap Length	Treatment	Reason
15 to 60 minutes	Linear interpolation	Preserves continuity for short gaps without reconstructing long periods
Longer than 60 minutes	Retain as missing	Avoids excessive smoothing and artificial delay creation over extended gaps

Table 4-2 summarizes the number of observed, interpolated, and retained missing 15-minute observations by year after applying the imputation rule.

Table 4-2: Summary of Missing Data Imputation Outcomes.

Category	2019	2023	2024
Total 15-minute slots	343,006,560	368,515,680	375,252,480
Observed	137,794,199 (40.2%)	167,182,167 (45.4%)	202,391,820 (53.9%)
Linearly interpolated	49,894,374 (14.5%)	57,531,235 (15.6%)	51,309,078 (13.7%)
Retained as missing	155,317,987 (45.3%)	143,802,278 (39.0%)	121,551,582 (32.4%)

Table 4-3 summarizes the observed, interpolated, and missing 15-minute records by time-of-day period (5 AM–10 PM and 10 PM–5 AM). Daytime (5 AM to 10 PM) showed a higher observation ratio and a lower missing ratio than nighttime (10 PM to 5 AM). This contrast was especially pronounced in 2024, when the share of retained missing records during the daytime period decreased to approximately 21%.

Table 4-3: Summary of Observed, Interpolated, and Missing Records by Time-of-Day Period.

Time Window	Category	2019	2023	2024
5 AM to 10 PM	Observed	47.9 %	56.2 %	65.2 %
	Linearly interpolated	16.9 %	18.1 %	14.1 %
	Retained as missing	35.2 %	25.7 %	20.7 %
10 PM to 5 AM	Observed	21.4 %	19.0 %	26.4 %
	Linearly interpolated	8.8 %	9.5 %	12.7 %
	Retained as missing	69.8 %	71.5 %	60.9 %

4.4. **Causal Factor Matching**

This section describes how causal factor records are converted into TMC-level, 15-minute indicators and integrated with the delay dataset. These matched indicators provide the basis for identifying event-free observations, assigning non-recurrent delay to available causal factors, and preparing the analysis dataset for aggregation and reporting.

In this documentation, causal factor matching refers to the process of linking external event or roadway status records to TMC-time observations. Spatial and temporal buffer rules define the range of TMCs and 15-minute intervals over which each matched record is assumed to affect delay.

Delay Causation Factors Considered

Based on the literature review and available datasets, this study considers eight primary categories of delay causation factors. These factors represent either recurring operational conditions or external events that may contribute to delay.

The eight causal factor categories include recurring operational conditions and external event-related factors:

1. Traffic demand and recurring bottlenecks
2. Traffic signal operation
3. Crashes
4. Non-crash incidents including emergencies
5. Work zones
6. Special events
7. Holidays
8. Weather events

Causal factor variables are developed from crash records, non-crash incident data, lane closure data, weather data, holiday information, and traffic signal inventory data. Work zones, emergencies, and special events are derived from lane closure records based on closure type information because they are interpreted as distinct delay contributors.

Temporal Alignment and Spatial/Temporal Buffer Rules for Causal Factors

Causal factor matching converts external event and roadway status records into TMC-time indicators. Causal factor indicators are joined to the 15-minute TMC-level delay dataset using TMC identifiers and timestamps. Most factors are represented by binary event flags denoting whether the event is present during a given 15-minute interval, with severity, type, or intensity attributes retained where available. Weather variables are treated differently from most other event indicators. Rain and snow measurements are converted into categorical severity flags to distinguish weather intensity. Because NOAA GHCN provides daily precipitation and snowfall totals, daily values were converted to approximate hourly intensities before applying the severity thresholds. Table 4-4 summarizes the severity-based weather flags.

Table 4-4: Weather Event Flags by Severity.

Weather Event	Flag and Definition
Rain	1: light rain < 0.1 mm/h
	2: moderate rain 0.1-8 mm/h
	3: heavy rain 8-16 mm/h
	4: extreme rain > 16 mm/h
Snow	1: light snow < 0.1 mm/h
	2: moderate snow 0.1-1.5 mm/h
	3: heavy snow 1.5-3 mm/h
	4: extreme snow > 3 mm/h

Note: The weather severity thresholds are based on and modified from the FHWA empirical study [12] on weather-related traffic impacts.

A 3-mile upstream impact buffer is applied to crashes, non-crash incidents, and lane closures to represent the potential upstream spatial extent of delay impacts. For crash data, which do not include an explicit end time, a severity-based temporal buffer is applied following the reported crash start time to approximate the duration of crash-related impacts. A 90-minute buffer is applied to no-apparent-injury, possible-injury, and minor-injury crashes (O, C, and B), and a 120-minute buffer is applied to serious-injury and fatal crashes (A and K). Weather conditions are assigned at the daily level based on nearby weather stations, while traffic signals are treated as static segment attributes.

Table 4-5: Spatial and Temporal Buffer Rules for Causal Factors.

Factor	Temporal Resolution	Spatial Buffer	Temporal Buffer
Crash	15-minute	3 miles upstream	O, C, B: 90-minute A, K: 120-minute
Non-crash incident	15-minute	3 miles upstream	Observed event duration
Lane closure	15-minute	3 miles upstream	Observed closure duration
Weather	Daily	15 miles from weather station	Daily assignment
Holiday	Daily	-	Full day
Traffic signal	Static	165 ft (50 meters)	-

Note: The spatial and temporal buffer settings are based on Penn DOT practice [8] and are refined using the project data analysis to better reflect the observed duration and spatial extent of delay impacts.

Spatial and temporal buffers are rounded to the analysis units used in this study. A 15-minute interval is included if any portion of the interval overlaps the event duration or buffer, and a TMC segment is included if any portion of the segment overlaps the spatial impact buffer. This conservative rule ensures that potentially affected time intervals and TMC segments are retained in the analysis.

Analysis Data Structure

The causal factor matching steps result in a set of analysis-ready datasets at the 15-minute TMC level. Each record represents a 15-minute observation for a specific TMC segment and includes delay metrics, quality flag, and causal factor indicators with severity or type.

Table 4-6: Key Variables in the 15-Minute TMC-Level Analysis Dataset.

Data Item		Data Type	Source Dataset
Identifier	TMC code	String	TMC Data
	Time	Timestamp	NPMRDS Data
	Hour	Numeric	
Traffic state	Hourly volume	Numeric	
	Vehicle-hours of delay (VHD)	Numeric	
	Heavy vehicle ratio	Numeric	
Quality	Imputation flag	Categorical	-
Causal factor	Crash flag	Binary	Crash Data
	Injury severity	Categorical	
	Crash upstream flag	Binary	
	Number of overlapping crashes	Numeric	
	Incident flag	Binary	Non-crash Incident Data
	Incident type	Categorical	
	Incident upstream flag	Binary	
	Work zone flag (construction, maintenance, permit)	Binary	Lane Closure Data
	Work-zone road status	Categorical	
	Emergency flag	Binary	
	Emergency road status	Categorical	
	Special event flag	Binary	
	Special event road status	Categorical	
	Lane closure upstream flag	Binary	
	Weather rain flag	Categorical	Weather Data
	Precipitation (mm)	Numeric	
	Weather snow flag	Categorical	
	Snowfall (mm)	Numeric	
	Snow depth (mm)	Numeric	
	Holiday flag	Binary	Holiday Data
	Signal flag	Binary	Traffic Signal Data

Detailed variable names and definitions are provided in the Appendices.

4.5. Recurrent and Non-Recurrent Delay Classification

For classification and reporting, causal factors are grouped into recurrent and non-recurrent delay contributors.

Recurrent delay contributors are:

- Traffic demand and recurring bottlenecks
- Traffic signal operation

Traffic demand and signal control are treated as routine operational conditions. Traffic signal presence is treated as a persistent segment attribute rather than a discrete event because the analysis uses annual signal inventories and does not include signal timing, cycle length, coordination, or temporary signal malfunctions. Therefore, signal-related effects are incorporated into the recurrent delay framework rather than treated as discrete non-recurrent events.

Non-recurrent delay contributors are:

- Crashes
- Non-crash incidents
- Work zones
- Special events
- Holidays
- Weather events

These factors represent discrete events or external conditions that may introduce additional delay beyond the recurrent baseline.

Recurrent delay is estimated from event-free observations. Event-free observations are defined as 15-minute TMC intervals with no matched crashes, non-crash incidents, work zones, special events, holidays, or weather events. Traffic signal presence is not used to exclude observations from the event-free set because it is treated as a persistent recurrent condition rather than a discrete event. These observations represent conditions not directly linked to recorded non-recurrent disruptions.

For each TMC, event-free VHD observations are grouped by year, season, day of week, and hour of day to construct the recurrent baseline. This grouping accounts for regular variation in traffic demand and operating conditions by season, day of week, and time of day. For each TMC and temporal group, the 75th percentile of event-free VHD is used as the recurrent delay baseline. This threshold is selected based on comparison with the 50th percentile and reflects the rationale that one week in a typical four-week month may experience delay from unobserved or short-term disturbances. The 75th percentile therefore represents the upper range of typical event-free delay and provides a conservative recurrent baseline while reducing the influence of isolated extreme observations.

Once the recurrent baseline is constructed, it is applied to all 15-minute TMC observations. Total delay is decomposed as:

$$\text{Total Delay} = \text{Recurrent Delay} + \text{Non-Recurrent Delay}$$

For each 15-minute TMC observation:

$$\text{Recurrent Delay} = \min(\text{Observed Delay}, \text{Recurrent Baseline})$$
$$\text{Non-Recurrent Delay} = \max(\text{Observed Delay} - \text{Recurrent Baseline}, 0)$$

This procedure produces recurrent and non-recurrent delay values for each 15-minute TMC observation. The non-recurrent component is then used for causal factor assignment.

4.6. **Causal Factor Assignment**

After total delay is separated into recurrent and non-recurrent components, non-recurrent delay is assigned to causal factor categories using the matched event indicators.

If non-recurrent delay occurs without a matched causal factor, the delay is retained as unclassified. This category represents delay that exceeds the recurrent baseline but cannot be linked to a recorded crash, incident, work zone, special event, holiday, or weather event using the available datasets and matching rules. Unclassified non-recurrent delay on signalized TMCs is reported separately because it may include signal-related effects not captured by the event indicators. When multiple causal factor indicators are active for the same TMC and 15-minute interval, the observation is retained as a multiple-cause case rather than assigned to a single cause using a priority rule. This approach preserves information about overlapping conditions, such as a crash occurring within a work zone or incident occurring during a weather event.

To summarize, the causal factor assignment procedure is:

1. Start with the 15-minute TMC-level dataset containing total, recurrent, and non-recurrent delay.
2. Identify observations with positive non-recurrent delay.
3. Check whether each observation overlaps with matched causal factor indicators.
4. Assign non-recurrent delay to the matched causal factor category or categories.
5. Label observations with positive non-recurrent delay and no matched causal factor as unclassified.
6. Retain multiple-cause observations where more than one factor is active.

The resulting dataset contains total delay, recurrent delay, non-recurrent delay, cause-specific delay indicators, and unclassified delay indicators. These values are used for statewide summaries and corridor-level diagnostics.

Table 4-7: Causal Factor Assignment Categories.

Reporting Category	Classification Rule	Interpretation
Recurrent without signal	Recurrent VHD on non-signalized TMCs	Routine delay not associated with a signalized segment
Recurrent with signal	Recurrent VHD on signalized TMCs	Routine delay occurring on TMCs with nearby traffic signals
Crash	Non-recurrent VHD with crash indicator active	Excess delay overlapping crash temporal/spatial buffer
Non-crash incident	Non-recurrent VHD with incident or emergency indicator active	Excess delay overlapping non-crash incident or emergency records
Work zone	Non-recurrent VHD with work-zone indicator active	Excess delay overlapping construction, maintenance, or permit lane-closure activity
Special event	Non-recurrent VHD with special-event indicator active	Excess delay overlapping special-event-related closure or event records
Holiday	Non-recurrent VHD with holiday indicator active	Excess delay occurring on holiday dates
Heavy weather	Non-recurrent VHD with heavy or extreme rain/snow indicator active	Excess delay overlapping high-intensity weather conditions
Unclassified	Non-recurrent VHD with no matched event factor	Excess delay above baseline that cannot be linked to available factor records
Unclassified with signal	Non-recurrent VHD with no matched event factor on signalized TMCs	Excess delay above baseline on signalized TMCs, not linked to recorded events
Multiple causes	Non-recurrent VHD with more than one active factor	Overlapping conditions, such as crash plus work zone or weather plus incident

4.7. <u>**Aggregation and Reporting Outputs**</u>

This section describes how classified 15-minute TMC-level delay records are aggregated into reporting outputs for statewide, regional, MPA-level, corridor-level, and selected-section analyses. Aggregation translates TMC-level time-series records into interpretable summaries, figures, maps, and diagnostic plots.

Temporal and Spatial Aggregation

Delay and causal factor variables are first developed at the 15-minute TMC level and then aggregated to broader temporal and spatial levels depending on the reporting purpose. Daily summaries are used primarily for corridor diagnostics and case studies. Monthly summaries are used to examine temporal patterns and delay composition across geographies. Annual summaries are used for year-to-year comparison, corridor screening, TMC-level delay maps, and summary reporting.

Spatial summaries are produced at the TMC, corridor, selected-section, MPA, WisDOT region, and statewide levels. For additive measures such as VHD, values are summed across selected TMCs and time intervals. The same summation rule is applied to total VHD, recurrent VHD, non-recurrent VHD, unclassified VHD, and cause-specific VHD.

Table 4-8: Reporting Output Levels and Uses.

Output Level	Primary Use	Meaning of Output
Daily	High-delay date screening and case-study selection	Shows when unusual or event-related delay occurred on specific TMCs or sections
Monthly	Seasonal and temporal reporting	Shows how total, recurrent, non-recurrent, and cause-specific delay vary over the year
Annual	Statewide/corridor summaries and screening	Shows total annual delay and cause composition for comparison across locations and years
TMC	Mapping and hotspot identification	Shows where delay is spatially concentrated at the segment level
Corridor/section	Corridor diagnostics and selected case studies	Shows delay composition and spatial-temporal patterns for operationally relevant corridors
Region/MPA/statewide	Agency-level reporting	Shows aggregate delay patterns and cause shares for broader planning and performance monitoring

Cause-Based Reporting Outputs

Cause-based summaries are generated using causal factor indicators assigned to each 15-minute TMC observation. Two levels of cause-based reporting are retained. First, raw cause-combination tables preserve the original combination of active causal factor indicators. Second, reporting summary tables convert the raw combinations into readable cause categories for figures and interpretation.

The main delay measures included in reporting tables are total VHD, recurrent VHD, non-recurrent VHD, unclassified VHD, cause-specific VHD, and cause-specific delay shares. These outputs allow users to identify not only where and when delay occurred, but also whether delay was primarily recurrent, event-related, unclassified, or associated with multiple conditions. Example reporting tables and output formats are provided in the Appendix.

Mapping

Maps are generated to show the spatial distribution of delay across the statewide network, regions, MPAs, corridors, and selected sections. TMC-level annual delay summaries are joined to the NPMRDS TMC geometry and mapped using TMC-level VHD. The maps support the identification of high-delay hotspots and comparison of delay concentrations across geographies and corridors.

4.8. Corridor-Level Diagnostics

Corridor-level diagnostics examine delay patterns at a finer spatial and temporal resolution than statewide or regional summaries. For each selected corridor, TMC-level records are aggregated by month, year, and causal factor category. These outputs identify where delay is concentrated along the corridor, whether it is primarily recurrent or non-recurrent, and which causal factors are most relevant for each selected location.

The corridor-level outputs include:

- Annual TMC-level delay summaries;
- Monthly corridor delay summaries;
- Recurrent and non-recurrent delay component plots;
- Selected-section datasets; and
- Diagnostic figures for high-delay days or selected case studies.

Case Study Outputs

Selected case study panels demonstrate how the methodology can be applied to specific corridors or corridor sections. Each case study combines annual delay summaries, spatial maps, temporal profiles, cause composition summaries, and space-time contour plots. The purpose is to show how the methodology identifies delay locations, separates recurrent and non-recurrent components, and links excess delay to reported causal factors.

Space-time contour plots use 15-minute TMC-level delay data and preserve the spatial sequence of TMCs along the corridor. For each selected section, TMCs are ordered by direction using the corridor road-order sequence. Where necessary, the order is manually reviewed so that the contour reflects the actual spatial progression of the study section. Delay values are displayed by time of day and TMC order to show the timing, location, and progression of delay.

The case study diagnostics support two types of interpretation: recurrent congestion diagnostics based on typical weekday periods, and event-driven diagnostics based on selected high-delay dates or known event periods. Case study locations can be selected based on high annual delay, localized corridor hotspots, notable work zone or incident influence, recurring peak-period delay, or WisDOT review priorities.

4.9. **Delay Causation Modeling**

Regression and machine-learning models are used as supplementary analyses to examine associations between delay and selected explanatory variables and to support interpretation. The modeling is used for two purposes:

- to review whether event severity or type provides useful distinctions in delay impacts; and
- to support interpretation of key contributing factors at statewide and corridor levels.

Use of Modeling

Delay causation modeling is used to guide interpretation of the application results. It helps assess whether the signs and relative importance of selected factors are consistent with the event-indicator-based attribution results. However, the primary delay causation outputs are based on the recurrent baseline, event matching, and causal factor assignment procedures described earlier in this chapter.

Event vs. Non-Event Comparison of Non-Recurrent Delay

To further examine the contribution of individual event types, the mean non-recurrent 15-minute VHD was compared under two conditions: when a specific event is present and when no events are present (event-free baseline).

As shown in Table 4-9, crashes and work zones show higher mean non-recurrent delay during event occurrences, suggesting measurable event-related delay effects. When evaluated relative to the event-free baseline, crashes, work zones, non-crash incidents, and emergency activities all show increases on the order of 0.05 vehicle-hours or more.

For several other event categories, the differences in mean delay are relatively small. It is important to note that these comparisons are based on simple averages; therefore, the magnitudes should be interpreted as preliminary indicators of relative influence rather than precise impact estimates. Given these observations, certain event types were aggregated in the modeling framework to improve interpretability:

- Emergency and Non-Crash Incidents: Combined into a single category as both involve similar operational responses (e.g., temporary lane closures or traffic control).
- Weather-related events: Rain and snow indicators were aggregated into a unified heavy-weather factor because their mean delay differences were similar and because higher-intensity weather conditions are most relevant for delay causation modeling.

Table 4-9: Comparison of Mean Non-Recurrent VHD With and Without Event.

Event	With Event	No Event	Difference (With – No Event)
Crash	0.8976	0.0690	0.8286
Non-crash incident	0.5256	0.0690	0.4566
Work zone	0.1342	0.0690	0.0652
Weather rain	0.1120	0.0690	0.0430
Weather snow	0.1289	0.0690	0.0599
Emergency	0.1277	0.0690	0.0587
Special event	0.0978	0.0690	0.0287
Holiday	0.0762	0.0690	0.0072

Event Severity and Variable Simplification

Event severity and type are reviewed where such information is available. The purpose is to determine whether detailed event attributes should be retained in the delay causation modeling or simplified into broader categories.

For crashes, injury severity is grouped as minor crashes (O, C, and B) and major crashes (A and K). This grouping preserves a distinction between lower- and higher-severity crashes while reducing the influence of sparse observations and higher missing-data rates for severe crashes.

For non-crash incidents and emergency lane closures, detailed type distinctions are not retained because these categories have relatively limited statewide delay contributions and many detailed subtypes are sparse. These records are represented using a single incident or emergency indicator.

For work zones, closure intensity is retained because delay increased with the extent of lane closure. Work zone variables distinguish between partial lane closures and full closures.

Weather indicators are simplified to focus on higher-intensity conditions. Rain and snow are combined into a general heavy-weather category, and only heavy or extreme rain or snow conditions are retained as active weather-event indicators in the modeling.

The final event variables used for the modeling are summarized in Table 4-10.

Table 4-10: Final Event Variables Included in Delay Modeling.

Event	Final Model Variable	Data Type
Crash	Minor crash (O, C, B)	Binary
	Major crash (A, K)	Binary
Non-crash incident	Incident flag	Binary
Work zone	Partial work-zone closure	Binary
	Full work-zone closure	Binary
Special event	Special event flag	Binary
Holiday	Holiday flag	Binary
Weather	Heavy weather flag (rain/snow severity ≥3)	Binary

Modeling Framework

The primary dependent variable is total delay, defined as total 15-minute TMC-level VHD. Non-recurrent delay is also modeled as a supporting dependent variable to examine factors more directly associated with event-related delay above the recurrent baseline. These models are used as supplementary diagnostics and are not used as the primary basis for delay classification or causal factor assignment.

The unit of analysis is the TMC-level 15-minute interval. This resolution is used to preserve short-duration event effects associated with crashes, non-crash incidents, and other events, while maintaining a consistent structure for combining traffic, event, weather, signal, and roadway attribute variables. Although coarser temporal resolutions may improve predictive fit, the 15-minute level is retained to preserve operational detail for corridor-level causation analysis.

Table 4-11 summarizes the dependent and explanatory variables used in the delay causation models. The explanatory variables reflect the severity-based distinctions, particularly for crashes, work zones, and weather conditions. Most event-related variables are expected to be positively associated with delay because they may reduce roadway capacity or disrupt traffic flow. Holidays may have a negative or context-dependent relationship with delay because regular commuter demand may decrease, while localized recreational demand may increase in some corridors. Traffic signal operation is expected to increase delay because signals require periodic stops and interruptions to traffic flow. Heavy vehicle ratio, defined as the combined share of single-unit trucks and buses and combination trucks, is included as a traffic composition variable. Its expected relationship with delay is not fixed because it may be correlated with hourly volume, facility type, lane configuration, and work-zone conditions.

Table 4-11: Modeling Variables Used in Delay Causation Modeling.

Variable Group	Variable	Temporal Resolution	Expected Relationship
Dependent variable	Total delay	15-minute	-
	Non-recurrent delay	15-minute	-
Crash	Minor crash with severity O/C/B	15-minute	Positive
	Major crash with severity A/K	15-minute	Positive
Incident	Non-crash incident or emergency	15-minute	Positive
Work zone	Partial work-zone closure	15-minute	Positive
	Full work-zone closure	15-minute	Positive
Special event	Special-event-related lane closure	15-minute	Positive
Holiday	Holiday indicator	Daily	Negative
Heavy weather	Heavy rain/snow event	Daily	Positive
Signal	Traffic signal indicator	Yearly	Positive
Traffic demand	Hourly volume	Hourly	Positive
	Heavy vehicle ratio	Monthly	Varies

Baseline Regression Modeling

A baseline regression model is estimated as a diagnostic check to examine whether selected event and traffic variables are associated with 15-minute delay. The main purpose of this model is to identify statistically significant variables and compare broad patterns across regions. The ordinary least squares (OLS) model uses delay as the dependent variable and includes event indicators, signal presence, traffic volume, and heavy vehicle ratio as explanatory variables.

The model can be summarized as:

$$\ln(\text{Delay}+1) = \beta_0 + \sum_i \beta_i \text{Event}_i + \beta_s \text{Signal} + \beta_v \ln(\text{Volume} + 1) + \beta_h \text{HV}_{\text{ratio}} + \epsilon$$

where:

- Event indicators include crash (minor/major), non-crash incident, work zone (partial/full closure), special event, holiday, and heavy weather conditions;
- Signal indicates signalized TMCs;
- Volume captures hourly traffic demand;
- HV ratio represents the heavy vehicle share.

A natural log transformation is applied to delay because the delay distribution is strongly right-skewed. Because hourly volume spans a wider numeric range than the other covariates, a natural log transformation, $\ln(\text{Volume} + 1)$, is applied to reduce scale effects and improve numerical stability. Standard errors are clustered at the TMC level to account for within-segment correlation across observations. A p-value threshold of 0.05 is used to determine statistical significance, and predictive performance is evaluated using a 70:30 train-test split.

The regression results are used as a supporting diagnostic and are not used to assign delay to causes. The results help confirm whether selected variables are associated with total and non-recurrent delay. In particular, event indicators, signal presence, and traffic conditions are interpreted as supporting evidence for the event flag-based attribution results, rather than as direct causal estimates. To account for heterogeneous TMC geometry attributes and delay propagation, extended corridor-level models include additional geometry variables and lagged delay variables.

Impact Size Interpretation

Because the regression uses a log-transformed dependent variable, coefficients represent the marginal association between each explanatory variable and $\ln(\text{Delay}+1)$, holding other variables constant. However, coefficient magnitude alone does not reflect how frequently the factor occurs across the network.

To compare relative model contributions on the transformed scale, an average modeled contribution is calculated as:

$$Average\ Impact_j = \beta_j \times \bar{X}_j$$

where

- β_j is the regression coefficient from the log-delay model, and
- $\bar{X}_j$ is the sample mean of the variable or the mean occurrence rate for binary indicators.

This value is used for relative comparison only and should not be interpreted as observed VHD directly. In this study, the impact size interpretation is conducted for the non-recurrent delay model to focus on delay above the recurrent baseline.

Contribution Decomposition

To quantify the total modeled contribution of each factor at the statewide level, the modeled contribution attributable to factor j is computed across time as:

$$Modeled\ Contribution_j = \beta_j \sum X_{jt}$$

The share of each factor is calculated as:

$$\mathrm{Share_j} = \frac{Modeled\ Contribution_{\mathrm{j}}}{\sum Modeled\ Contribution} \times 100$$

This decomposition aggregates the modeled contribution of each explanatory variable on the regression scale. Because the dependent variable is log-transformed, these modeled shares should be interpreted as relative diagnostic indicators rather than direct decompositions of observed VHD. These modeled shares differ from the flag-based pie charts, which summarize observed delay by event-flag categories.

Machine Learning Model

In addition to linear regression, a Gradient Boosting Machine (GBM) model [13] is used to capture potential nonlinear relationships and interaction effects. GBM is an ensemble learning method that builds prediction models sequentially using decision trees. Unlike linear regression, GBM does not assume linear relationships or additive marginal effects. LightGBM [14] is an efficient implementation of GBM designed for large-scale datasets and is well-suited for this application given the size of the dataset. The analysis is implemented using the open-source LightGBM library in Python.

Linear regression is utilized to quantify interpretable marginal effects of event types, while LightGBM is used to examine whether a larger share of delay variability can be explained when nonlinear structures are allowed. Given the 15-minute temporal resolution, stochastic variability in traffic conditions – such as fluctuations in traffic demand and localized speed changes associated with signal cycles – and substantial heterogeneity across statewide TMCs, the linear regression model yields a relatively low R^2; however, it still provides useful, interpretable estimates of the marginal associations between causal factors and delay. Together, these approaches provide complementary insights: OLS supports interpretable estimates of marginal associations, while LightGBM supports evaluation of nonlinear structure and predictive performance.

5. Statewide Application

This chapter applies the delay causation methodology to all primary TMCs statewide. Aggregated delay metrics and causal factor summaries are presented at the statewide, WisDOT region, and MPA levels across multiple temporal resolutions, providing a consistent view of statewide delay patterns and contributing factors.

5.1. <u>**Delay Classification**</u>

This section summarizes the classification of statewide delay into recurrent and non-recurrent components. The results are presented at the statewide, WisDOT region, and MPA levels to show how delay magnitude and delay composition vary across geography and time.

<u>***Statewide***</u>

Table 5-1 summarizes statewide VHD by recurrence type for 2019, 2023, and 2024. Across all three years, non-recurrent delay accounts for the majority of total delay, representing approximately 75 percent of statewide VHD. Recurrent delay accounts for the remaining 25 percent.

Between 2019 and 2023, total VHD increased substantially, with the non-recurrent component rising in magnitude. In 2024, total delay decreased compared to 2023 and fell below 2019 levels. This change may be influenced by changes in the NPMRDS travel time data supply, including the loss of a major data provider during the period from approximately June 2023 to July 2024 and abnormal increases in observation coverage from August to November 2024 (Figure 5-1). This issue may have affected reported travel time estimates and delay calculation, with impacts especially noticeable on non-interstate facilities. As a result, 2024 delay may be systematically underestimated relative to other years, and year-to-year comparisons involving 2023 and 2024 should be interpreted with this data limitation in mind. Despite these fluctuations in total delay, the proportional split between recurrent and non-recurrent components remains relatively stable across the three analysis years.

Table 5-1: Statewide Vehicle-Hours of Delay by Recurrence Type (unit: veh-hr)

Year	Total VHD	Recurrent VHD	Non-Recurrent VHD
2019	33,212,446	8,705,748 (26.2%)	24,506,698 (73.8%)
2023	34,938,463	8,582,558 (24.6%)	26,355,905 (75.4%)
2024	32,583,838	8,781,503 (27.0%)	23,802,334 (73.0%)

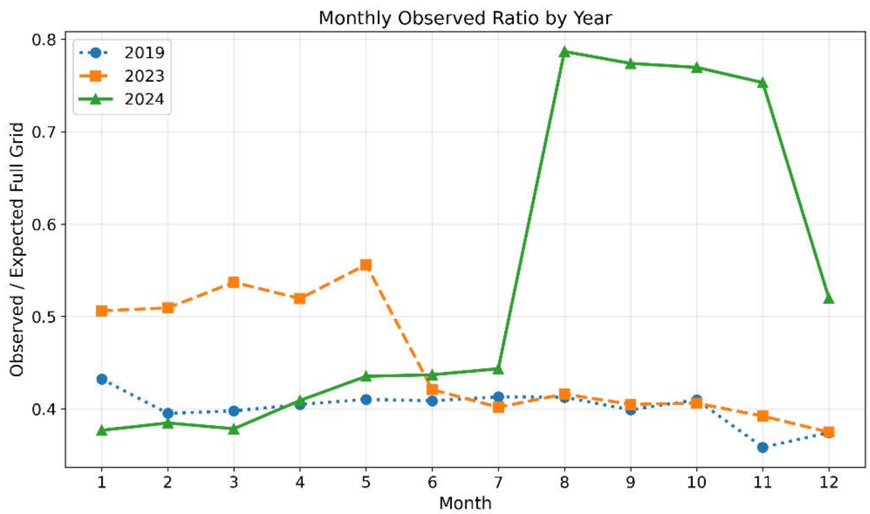

Figure 5-1: Monthly NPMRDS Observation Ratio by Year.

Figure 5-2 shows monthly total VHD aggregated statewide. In 2019 and 2023, delay generally increases from spring into summer, reaches peak levels during late summer, and then declines toward the end of the year. This pattern suggests a seasonal increase in delay during warmer months, likely reflecting higher travel demand and seasonal roadway construction. The 2024 trend follows a similar increase through early summer but drops sharply from August through November. This deviation may be related to abnormal changes in NPMRDS observation coverage during this period, which may have affected the delay estimates.

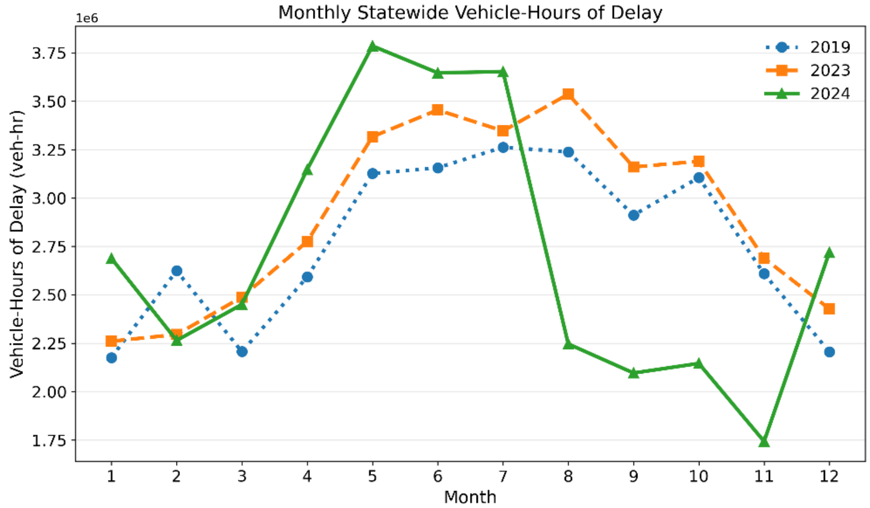

Figure 5-2: Monthly Statewide Vehicle-Hours of Delay.

Figure 5-3 decomposes monthly statewide VHD into recurrent and non-recurrent components. Non-recurrent delay accounts for the larger share of delay in all three years, while recurrent delay remains relatively stable across months. The seasonal increase in total delay during late spring and summer is mainly driven by increases in non-recurrent delay, indicating that event-related delay above the recurrent baseline plays a major role in monthly variation.

(a) 2019 (b) 2023 (c) 2024

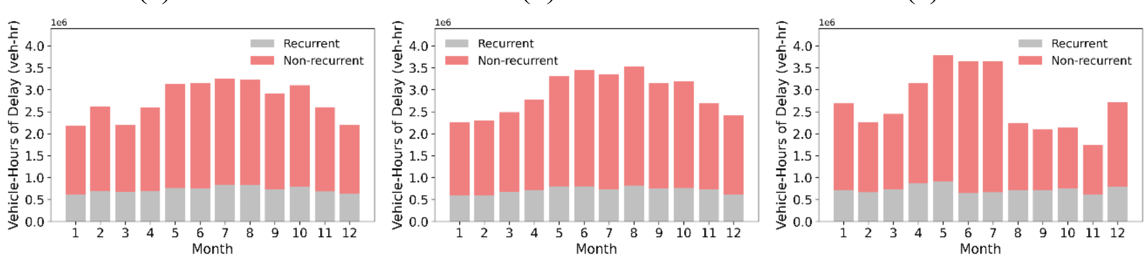

Figure 5-3: Monthly Statewide Recurrent and Non-Recurrent Delay.

Figure 5-4 maps annual TMC-level VHD in 2024 by direction. The map highlights the spatial concentration of delay along the highest-demand freeway and arterial facilities, particularly in urbanized areas. Direction-specific mapping helps identify whether high-delay locations are concentrated in one travel direction or appear in both directions, which is useful for distinguishing recurring bottlenecks and corridor-wide congestion.

(a) Eastbound and Southbound

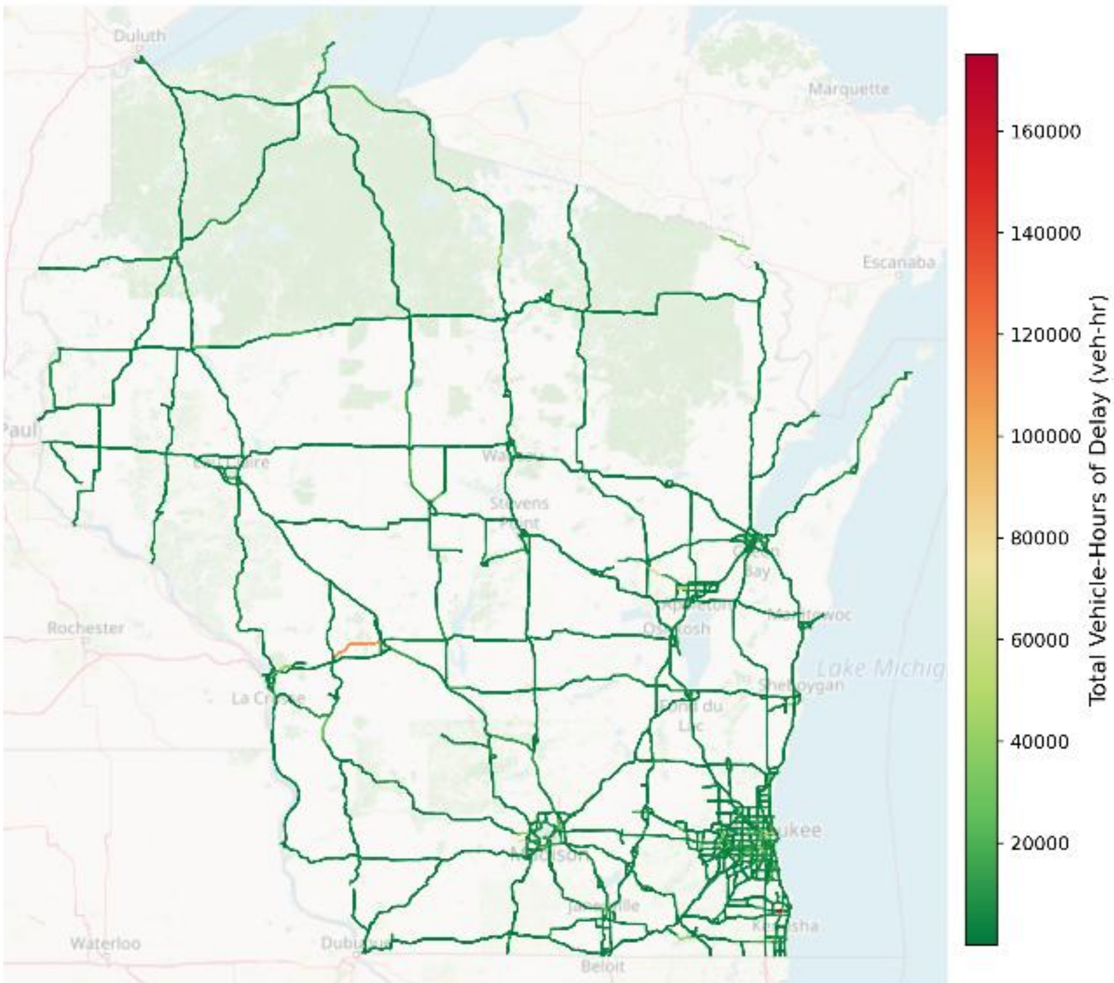

(b) Westbound and Northbound

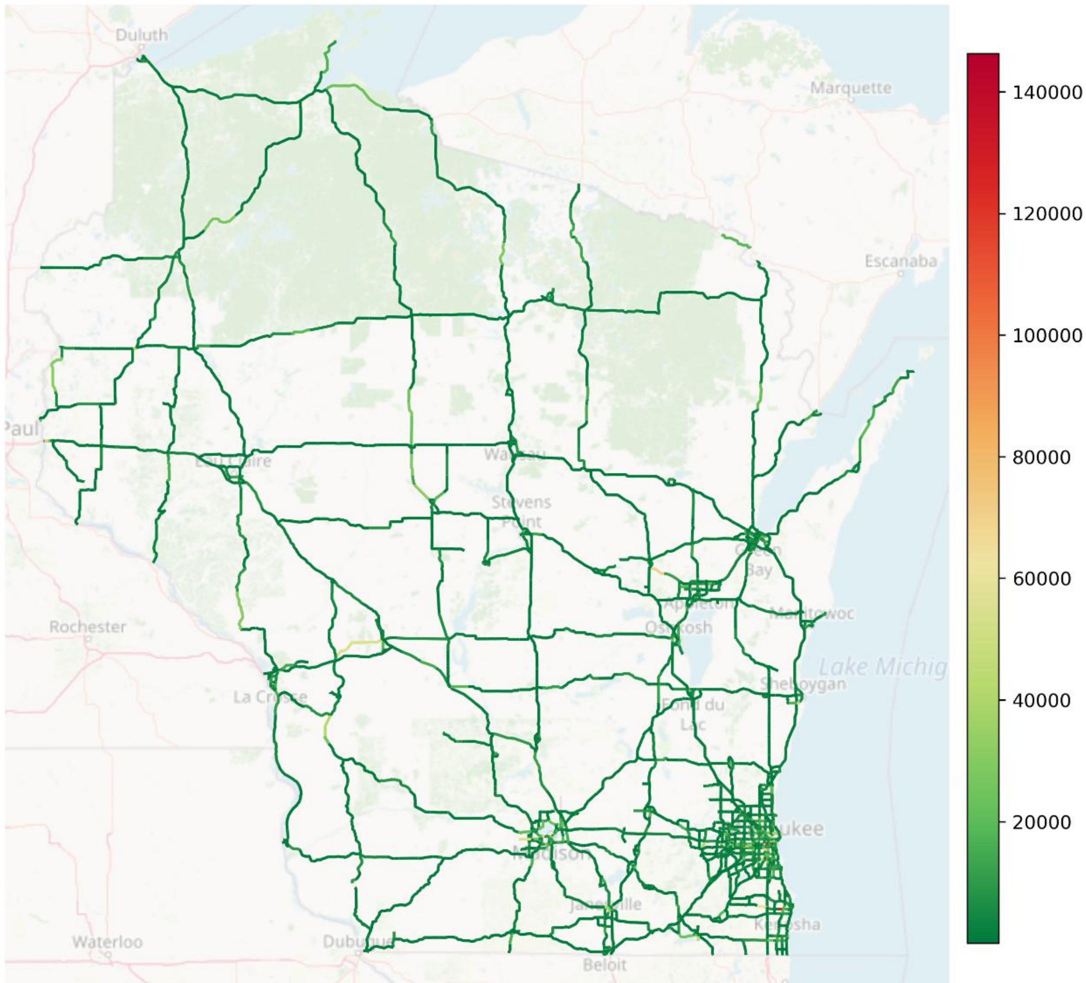

Figure 5-4: Statewide Annual TMC Delay (2024).

Regional Level

Figure 5-5 presents monthly VHD by WisDOT region for 2024. The Southeast region, which includes the Milwaukee area, consistently exhibits the highest delay levels throughout the year, with noticeable increases during late spring and summer months. The Southwest and Northeast regions show moderate delay levels, while the Northwest and North Central regions contribute comparatively smaller shares of statewide delay.

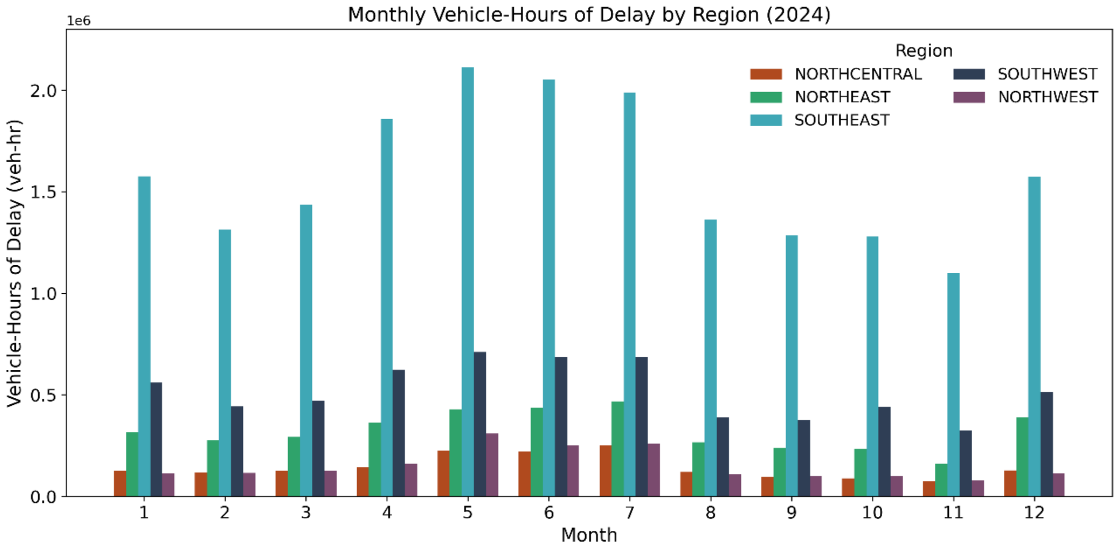

Figure 5-5: Monthly Vehicle-Hours of Delay by Region (2024).

Figure 5-6 presents the distribution of total VHD across WisDOT regions in 2024. The Southeast region accounts for the largest share of statewide delay, followed by the Southwest and Northeast regions.

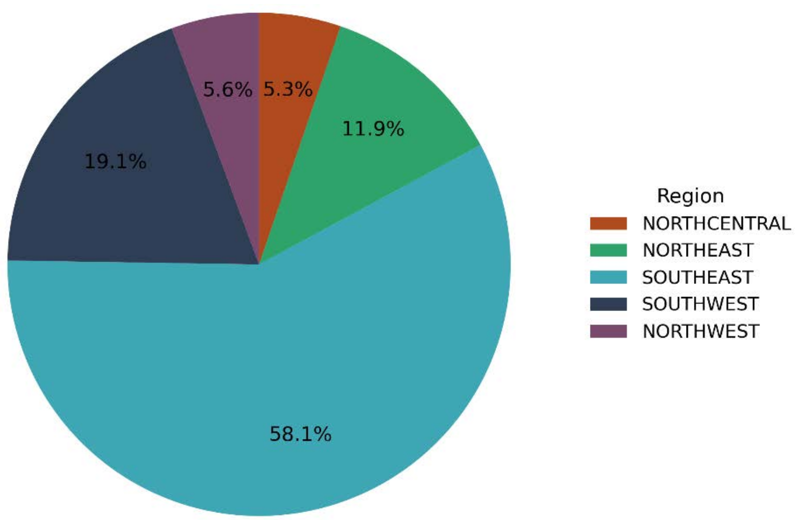

Figure 5-6: Annual Vehicle-Hours of Delay by Region (2024).

As shown in Figure 5-7, although the relative shares vary across years, the overall regional ranking remains generally consistent, highlighting the persistent concentration of delay in urbanized and high-demand areas.

(a) (b)

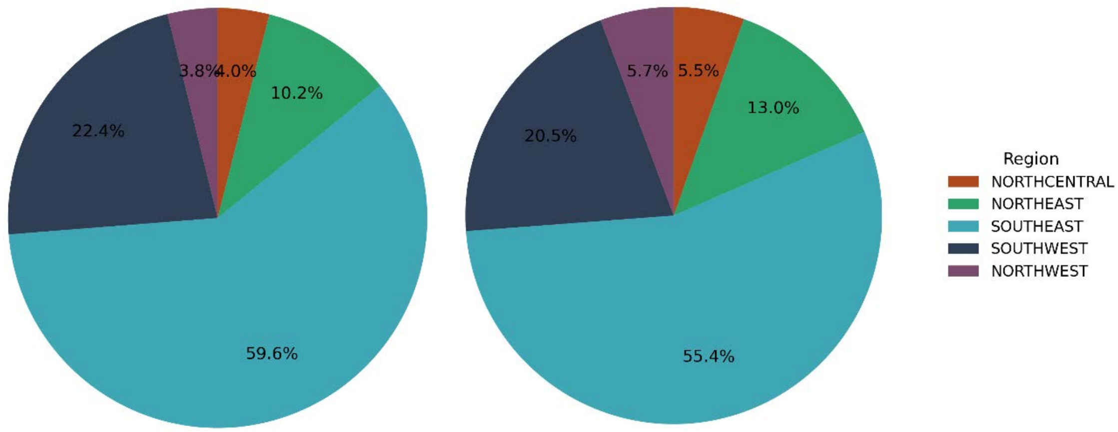

Figure 5-7: Annual Vehicle-Hours of Delay by Region in (a) 2019 and (b) 2023.

Table 5-2 further summarizes total VHD and the recurrent/non-recurrent delay shares by WisDOT region. The Southeast region has the highest recurrent delay share among the regions in all three analysis years. In contrast, the Northwest and North Central regions show relatively high non-recurrent shares, indicating that delay in these regions is more strongly associated with events rather than persistent recurring congestion.

Table 5-2: Total VHD and Recurrent/Non-Recurrent Delay Shares by Region.

Region	Year	Total VHD (veh-hr)	Recurrent Delay Share (%)	Non-Recurrent Delay Share (%)
North Central	2019	1,318,760	14.3	85.7
	2023	1,911,169	15.2	84.8
	2024	1,712,028	15.1	84.9
Northeast	2019	3,382,650	23.6	76.4
	2023	4,531,957	21.4	78.6
	2024	3,869,889	20.5	79.5
Southeast	2019	19,792,766	29.2	70.8
	2023	19,343,575	27.2	72.8
	2024	18,936,282	31.0	69.0
Southwest	2019	7,440,406	23.9	76.1
	2023	7,155,237	25.2	74.8
	2024	6,225,100	26.0	74.0
Northwest	2019	1,277,865	11.6	88.4
	2023	1,996,526	13.3	86.7
	2024	1,840,539	13.0	87.0

Figure 5-8 through Figure 5-17 provide region-specific monthly delay decomposition plots and 2024 TMC-level annual delay maps. These figures are intended to support more detailed review of regional delay patterns beyond the statewide summary.

North Central Region

(a) 2019 (b) 2023 (c) 2024

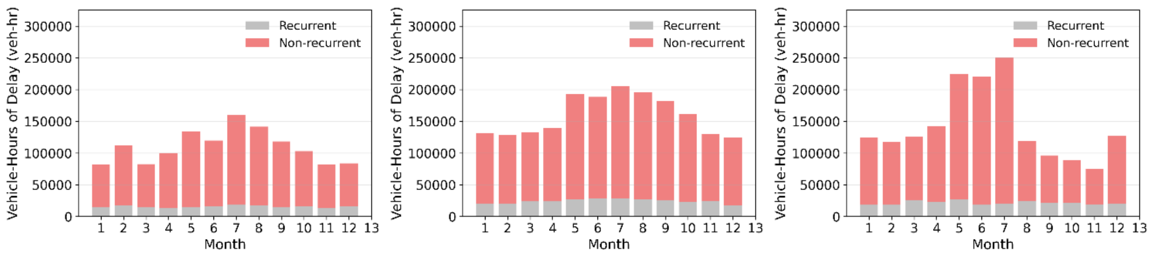

Figure 5-8: Monthly North Central Region Recurrent and Non-Recurrent Delay.

(a) Eastbound and Southbound (b) Westbound and Northbound

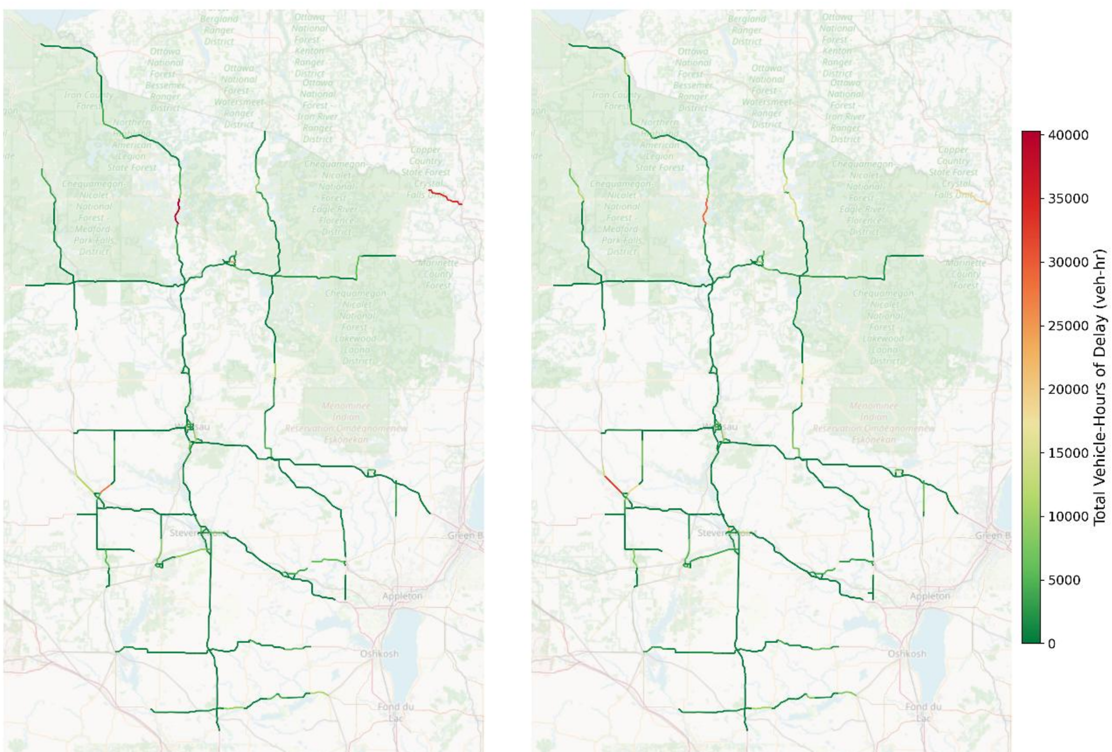

Figure 5-9: North Central Region Annual TMC Delay (2024).

Northeast Region

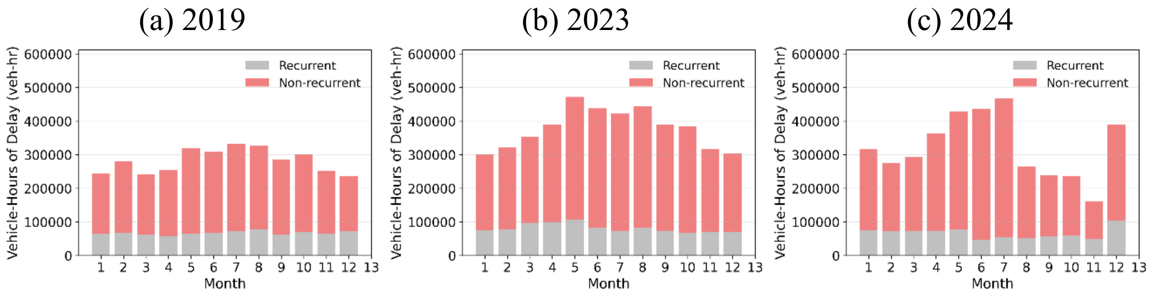

Figure 5-10: Monthly Northeast Region Recurrent and Non-Recurrent Delay.

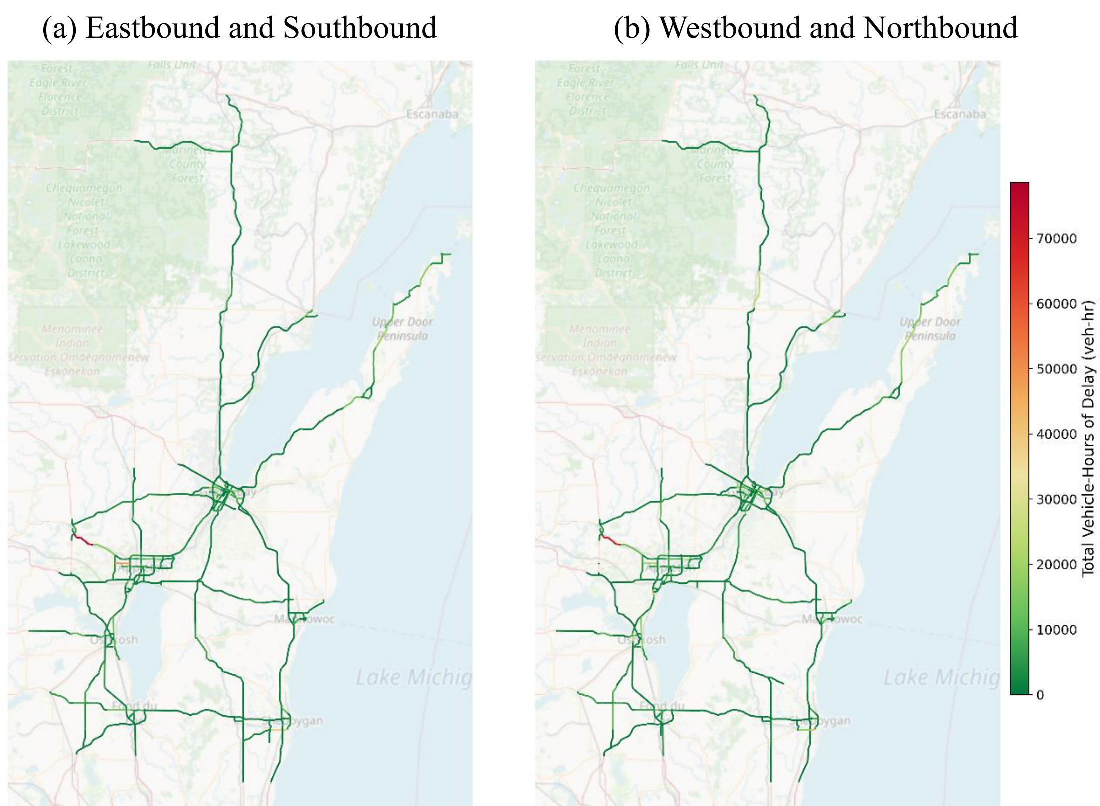

Figure 5-11: Northeast Region Annual TMC Delay (2024).

Southeast Region

(a) 2019 (b) 2023 (c) 2024

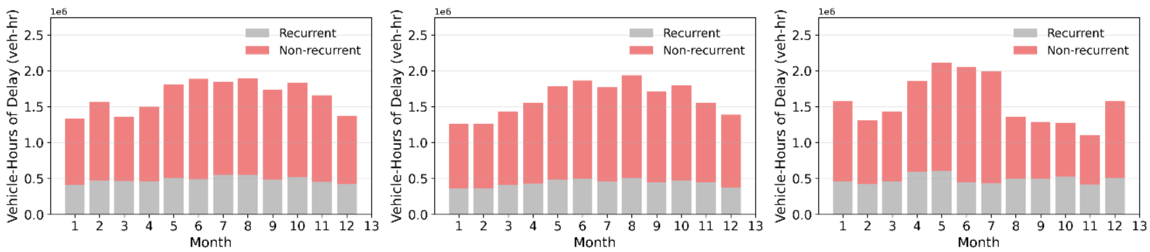

Figure 5-12: Monthly Southeast Region Recurrent and Non-Recurrent Delay.

(a) Eastbound and Southbound (b) Westbound and Northbound

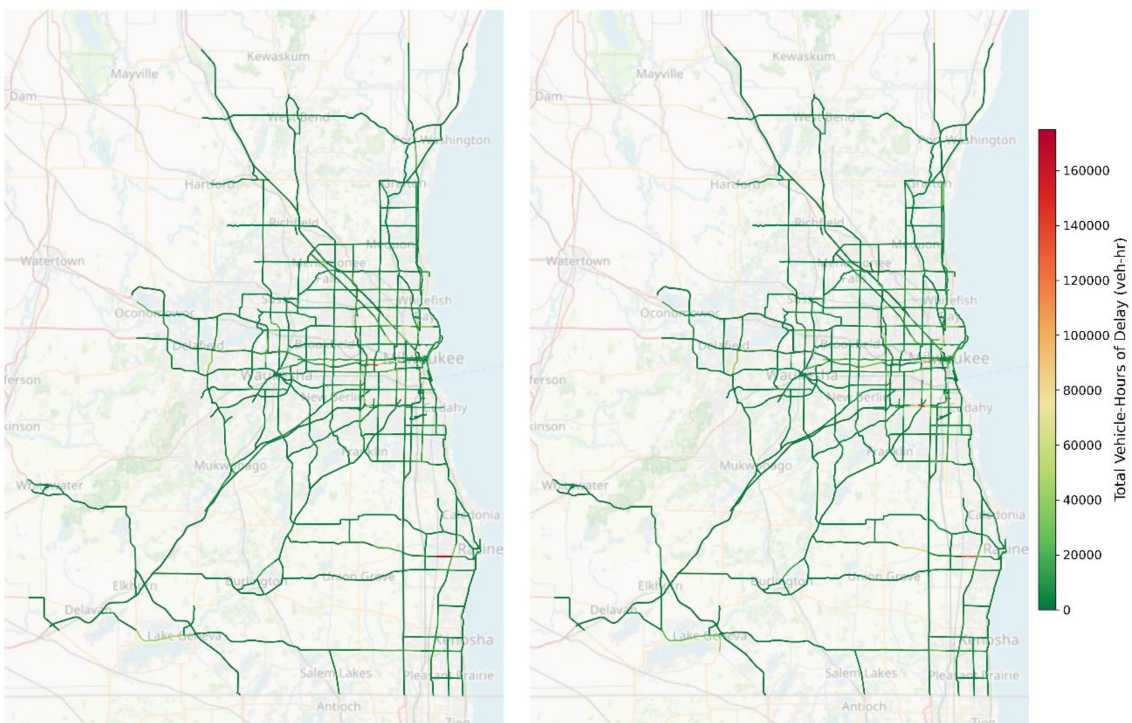

Figure 5-13: Southeast Region Annual TMC Delay (2024).

Southwest Region

(a) 2019 (b) 2023 (c) 2024

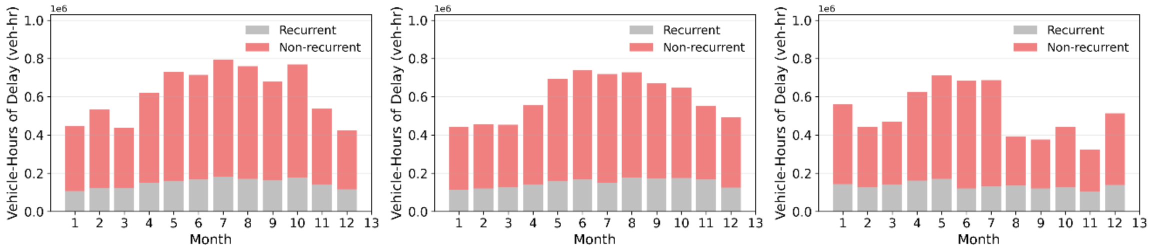

Figure 5-14: Monthly Southwest Region Recurrent and Non-Recurrent Delay.

(a) Eastbound and Southbound (b) Westbound and Northbound

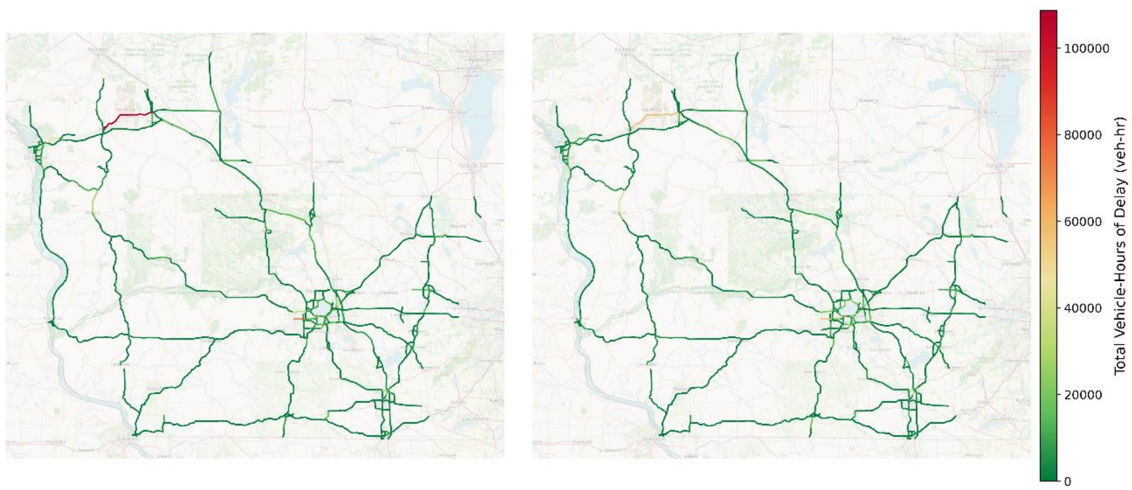

Figure 5-15: Southwest Region Annual TMC Delay (2024).

Northwest Region

(a) 2019 (b) 2023 (c) 2024

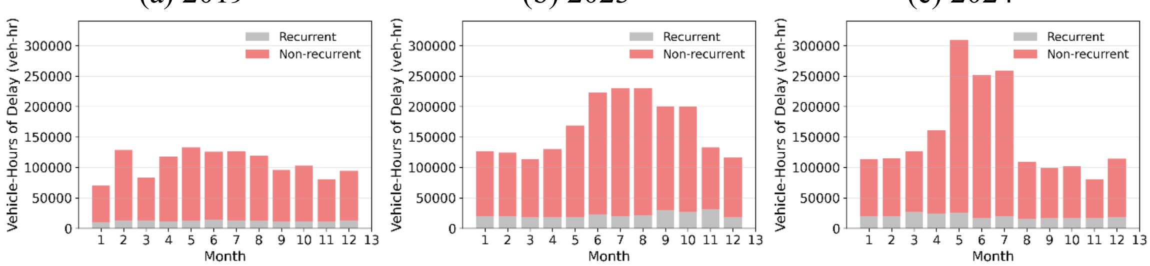

Figure 5-16: Monthly Northwest Region Recurrent and Non-Recurrent Delay.

(a) Eastbound and Southbound (b) Westbound and Northbound

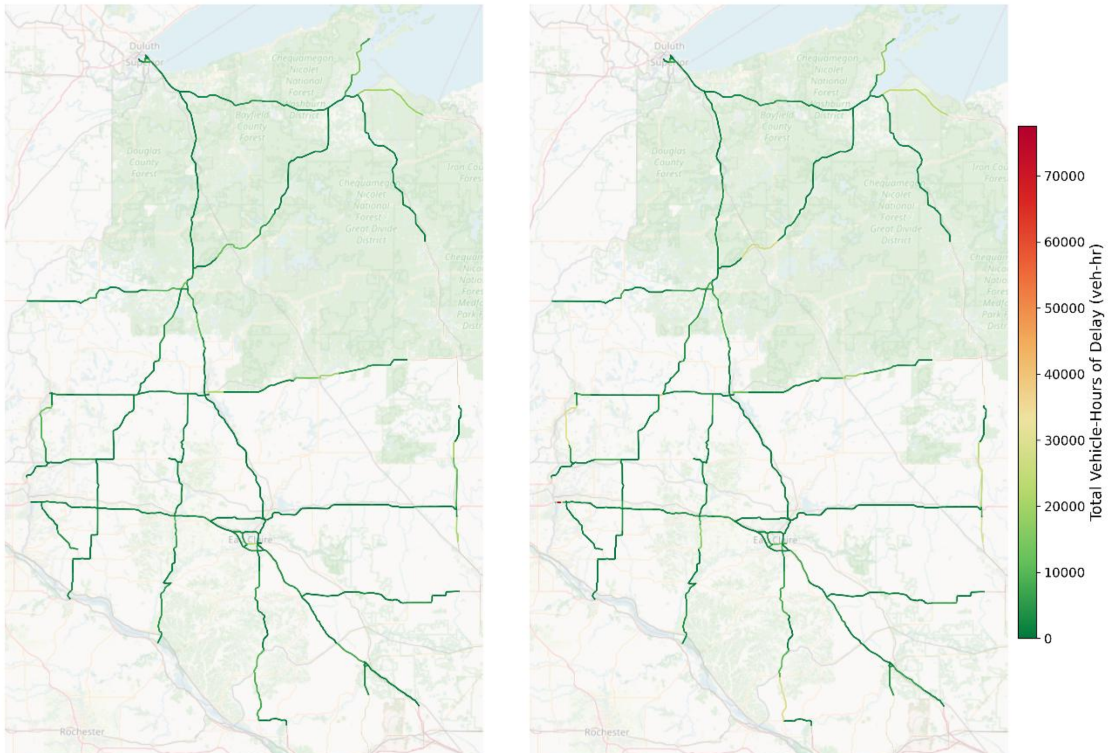

Figure 5-17: Northwest Region Annual TMC Delay (2024).

MPA Level

Figure 5-18 illustrates the magnitude and seasonality of delay across MPAs in 2024. The Southeastern Wisconsin MPA consistently accounts for the highest total VHD throughout the year, with substantially higher delay than all other MPAs. This pattern reflects the concentration of population and traffic demand in the Milwaukee metropolitan area.

Among the remaining MPAs, Madison forms the next highest delay tier, followed by mid-sized areas such as the Fox Cities and Green Bay. Smaller MPAs contribute comparatively lower levels of delay.

Seasonally, most MPAs exhibit higher delay from late spring through early fall, with peaks during the late spring through summer months. This pattern is especially pronounced in larger MPAs, suggesting that increased travel demand, seasonal activity, and construction-related disruptions may contribute to elevated delay during these periods.

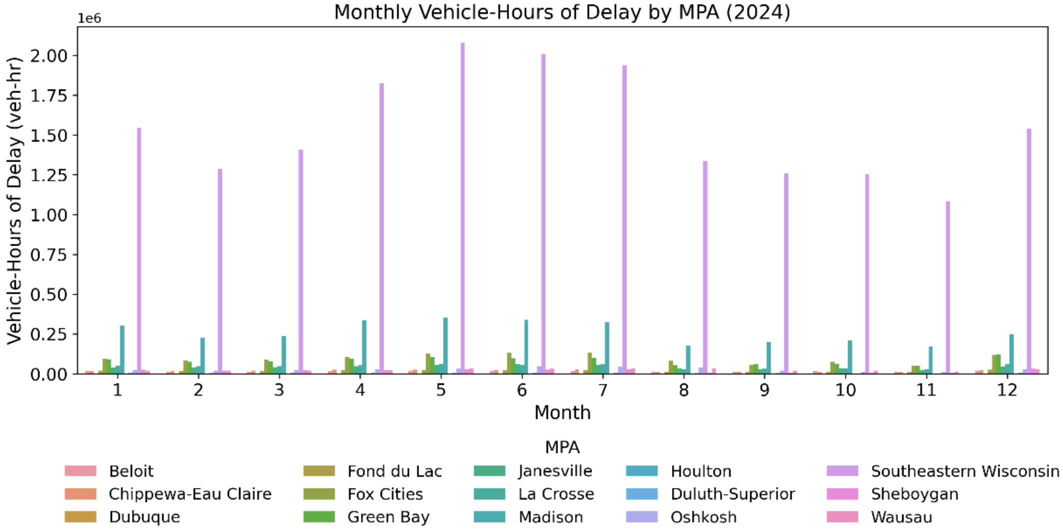

Figure 5-18: Monthly Distribution of Vehicle-Hours of Delay Across MPAs in 2024.

Table 5-3 summarizes total VHD and the recurrent/non-recurrent delay shares by MPA for the analysis years. Across most MPAs, non-recurrent delay accounts for the larger share of total delay. The Southeastern Wisconsin MPA (SEW) accounts for by far the largest total delay, followed by Madison (MAD), Fox Cities (FXC), and Green Bay (GBY). These MPAs also tend to show relatively higher recurrent delay shares than other MPAs, reflecting more persistent traffic demand and recurring congestion in urbanized areas. In contrast, several MPAs, such as Dubuque (DUB) and Duluth-Superior (MIC), show higher non-recurrent shares, indicating that a larger portion of their delay occurs above the recurrent baseline.

Table 5-3: Total VHD and Recurrent/Non-Recurrent Delay Shares by MPA.

MPA	Year	Total VHD (veh-hr)	Recurrent Delay Share (%)	Non-Recurrent Delay Share (%)
BEL	2019	199,727	12.1	87.9
	2023	268,681	25.1	74.9
	2024	187,349	21.3	78.7
CEC	2019	285,832	17.0	83.0
	2023	278,031	16.7	83.3
	2024	224,198	19.5	80.5
DUB	2019	8,173	7.7	92.3
	2023	5,468	7.5	92.5
	2024	5,897	8.8	91.2
FDL	2019	156,405	18.0	82.0
	2023	262,274	18.4	81.6

	2024	218,035	24.1	75.9
FXC	2019	1,179,170	25.3	74.7
	2023	1,369,290	24.0	76.0
	2024	1,149,452	21.4	78.6
GBY	2019	1,012,703	29.5	70.5
	2023	1,301,040	25.6	74.4
	2024	996,500	29.4	70.6
JAT	2019	543,503	28.3	71.7
	2023	579,936	42.7	57.3
	2024	512,228	37.6	62.4
LAC	2019	623,964	29.2	70.8
	2023	678,724	21.2	78.8
	2024	563,555	25.5	74.5
MAD	2019	4,254,290	26.5	73.5
	2023	3,502,816	29.2	70.8
	2024	3,122,646	31.7	68.3
MET	2019	92	0	100
	2023	6,568	53.6	46.4
	2024	11,138	83.1	16.9
MIC	2019	75,369	15.6	84.4
	2023	90,045	8.5	91.5
	2024	64,082	9.0	91.0
OSH	2019	190,499	19.2	80.8
	2023	299,589	19.0	81.0
	2024	320,379	18.7	81.3
SEW	2019	19,512,616	29.4	70.6
	2023	18,930,994	27.3	72.7
	2024	18,563,463	31.2	68.8
SHB	2019	240,712	28.8	71.2
	2023	306,151	29.9	70.1
	2024	236,552	26.8	73.2
WAU	2019	301,796	25.6	74.4
	2023	306,277	22.0	78.0
	2024	299,426	23.8	76.2
None (Rural)	2019	4,627,598	13.2	86.8
	2023	6,752,579	14.1	85.9
	2024	6,108,939	12.7	87.3

Figure 5-19 through Figure 5-22 provide additional detail for the two highest-delay MPAs: Southeastern Wisconsin and Madison. These figures show monthly recurrent and non-recurrent delay components across the three analysis years and 2024 TMC-level annual delay maps.

Southeastern Wisconsin

(a) 2019 (b) 2023 (c) 2024

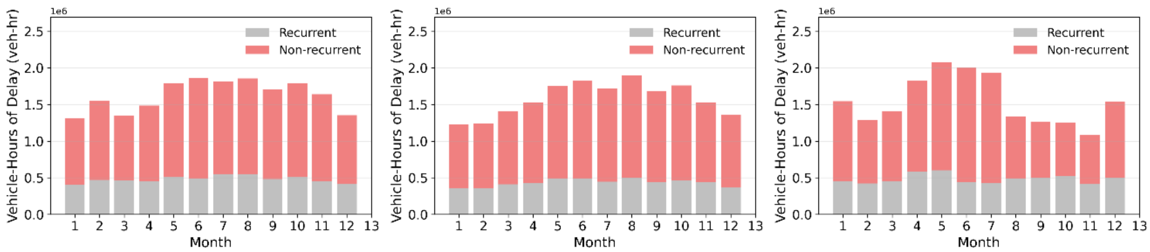

Figure 5-19: Monthly Southeastern Wisconsin MPA Recurrent and Non-Recurrent Delay.

(a) Eastbound and Southbound (b) Westbound and Northbound

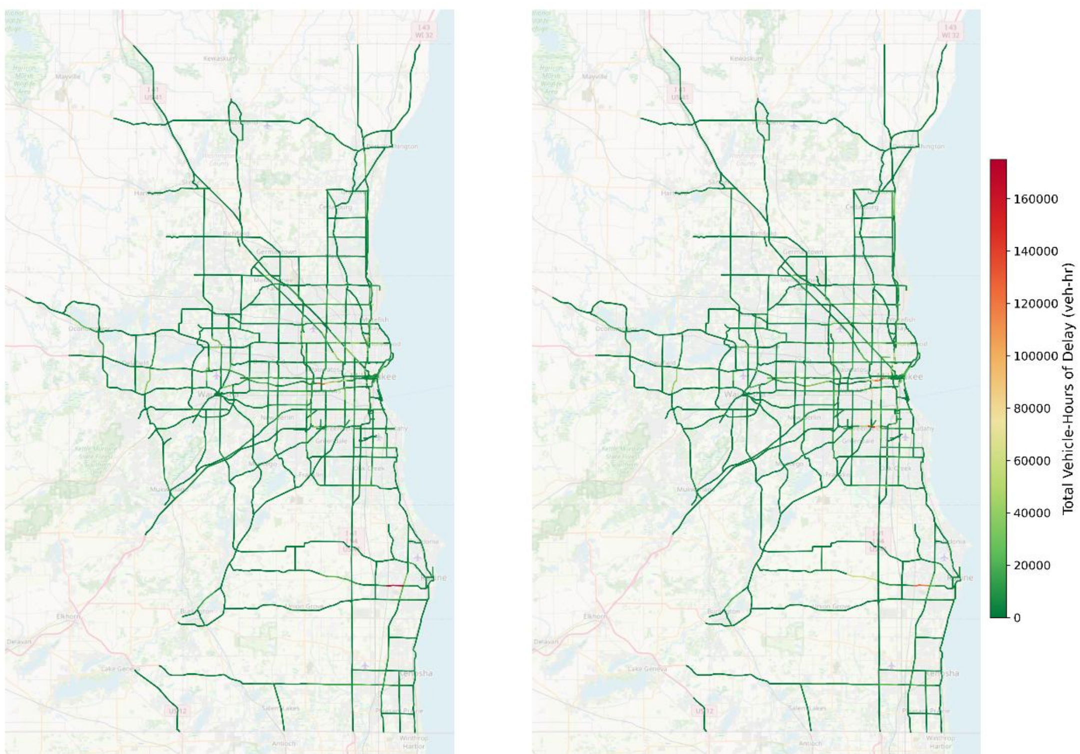

Figure 5-20: Southeastern Wisconsin MPA Annual TMC Delay (2024).

Madison

(a) 2019 (b) 2023 (c) 2024

Figure 5-21: Monthly Madison MPA Recurrent and Non-Recurrent Delay.

(a) Eastbound and Southbound (b) Westbound and Northbound

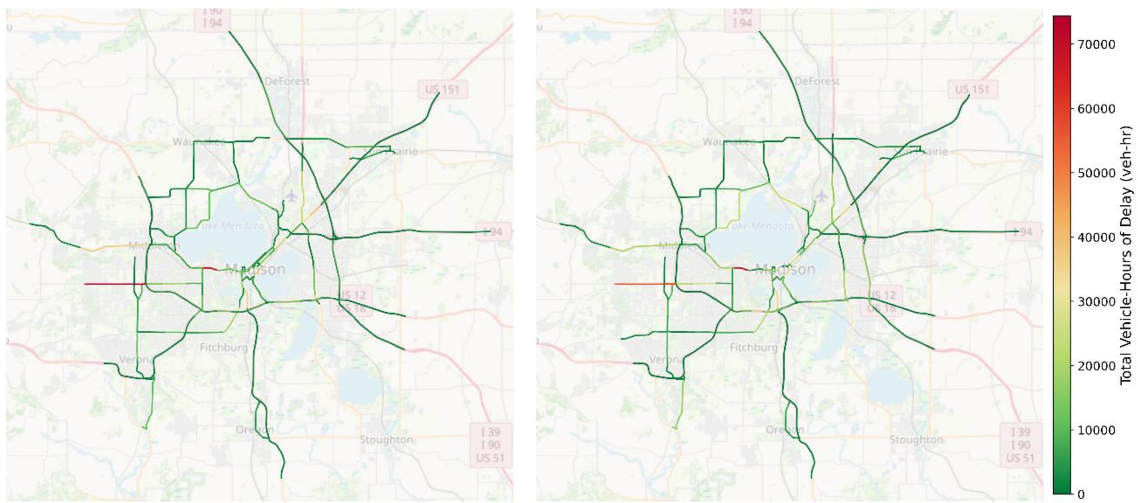

Figure 5-22: Madison MPA Annual TMC Delay (2024).

5.2. <u>Investigation of Delay Causation</u>

This section examines statewide delay composition using the causal factor assignment. While the previous section separates total delay into recurrent and non-recurrent components, this section further distinguishes recurrent delay by signalized and non-signalized TMCs and summarizes non-recurrent delay by matched event categories, multiple-cause cases, and unclassified delay.

<u>Statewide</u>

Figure 5-23 shows the statewide delay composition by cause in 2024. Unclassified delay with signal accounts for the largest single share of statewide delay, followed by work-zone delay and recurrent delay with signal. This indicates that a substantial portion of statewide delay occurs on signalized facilities, while work zones represent the largest identifiable event-based non-recurrent contributor.

Unclassified delay represents delay above the recurrent baseline that could not be matched to a recorded crash, non-crash incident, work zone, special event, holiday, or weather event using the available data and matching rules. This delay may reflect unreported events and event impacts extending beyond the spatial or temporal buffers. It may also include queue spillback or delay propagation from downstream signals that affects upstream TMCs without being matched to a signal indicator.

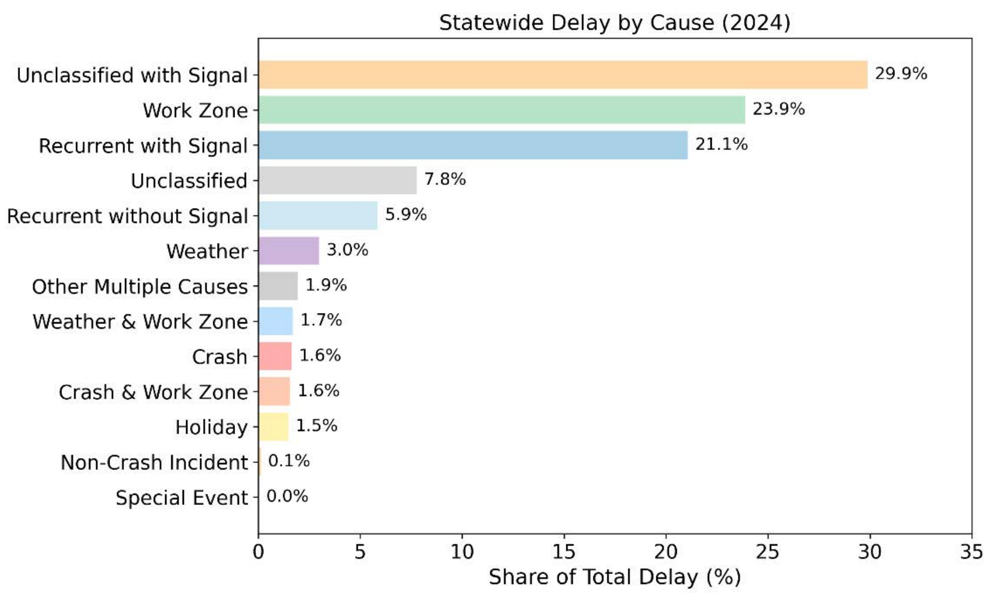

Figure 5-23: Statewide Delay Composition by Cause in 2024.

Figure 5-24 shows statewide delay composition by cause in 2024, distinguishing between delay on signalized and non-signalized TMCs. Delay on signalized TMCs accounts for approximately 70.3 percent of total statewide delay in 2024, corresponding to 22.9 million vehicle-hours, while delay on non-signalized TMCs account for the remaining 29.7 percent, or 9.7 million vehicle-hours.

The cause composition differs between signalized and non-signalized TMCs. On signalized TMCs, unclassified delay and recurrent delay account for the largest shares. On non-signalized TMCs, work zones represent the largest share, followed by unclassified delay. This indicates that work-zone activity is a more prominent identifiable contributor to delay on non-signalized facilities.

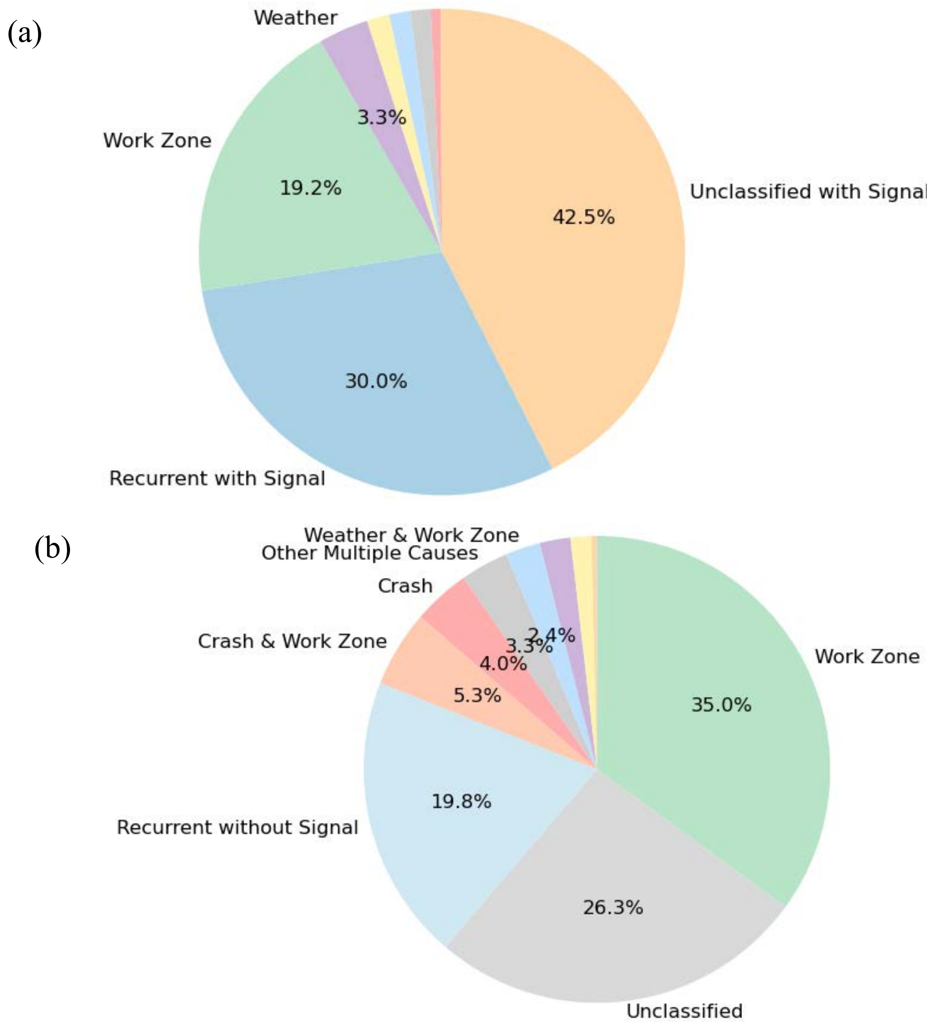

Figure 5-24: Statewide Delay by Cause in 2024:
Comparison of (a) Signalized and (b) Non-Signalized TMCs.

Across all three analysis years, unclassified delay with signal consistently represents the largest share of total delay. The share of work-zone-related delay increased from 2019 to 2023 and remained elevated in 2024, indicating that construction and lane-closure activities are important event-based contributors to statewide delay.

(a) In 2019 (b) In 2023

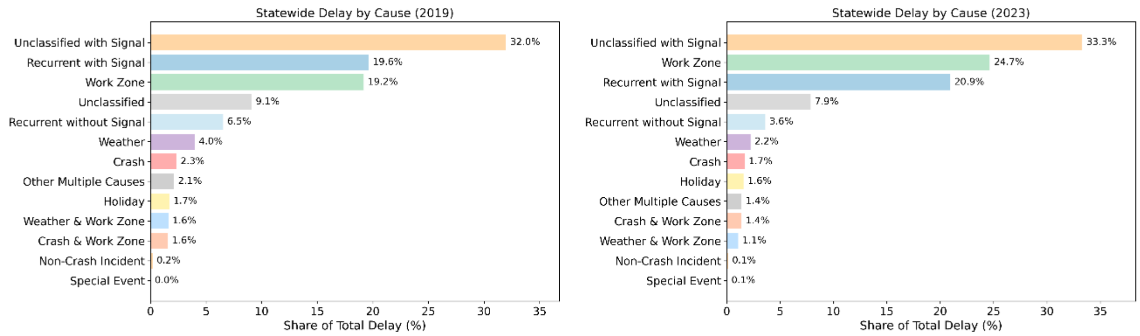

Figure 5-25: Statewide Delay Composition by Cause.

In 2024, recurrent delay with signal and unclassified delay with signal together account for a large share of delay throughout the year, indicating the importance of signalized facilities in statewide delay. Work-zone delay becomes more pronounced from late spring through fall and represents the largest category during several mid-year months. In contrast, crashes, weather, holidays, and other multiple-cause categories account for relatively small shares of total monthly delay.

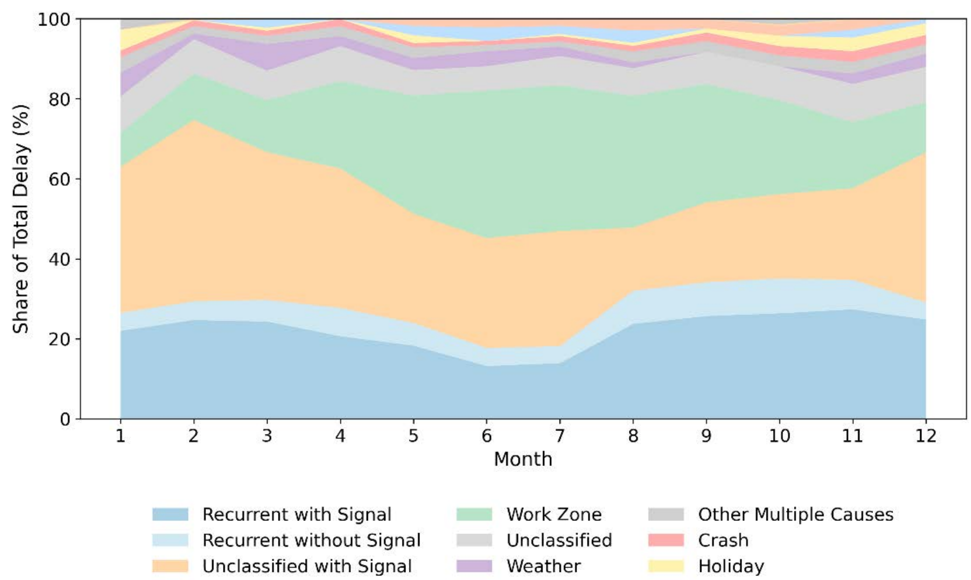

Figure 5-26: Monthly Statewide Delay Composition by Cause in 2024.

Regional Level

The following subsections summarize delay composition by cause for each WisDOT region. For each region, the 2024 delay composition is presented first, followed by the corresponding 2019 and 2023 compositions for comparison.

North Central Region

Figure 5-27 shows that delay in the North Central region is primarily concentrated in work-zone delay and unclassified delay.

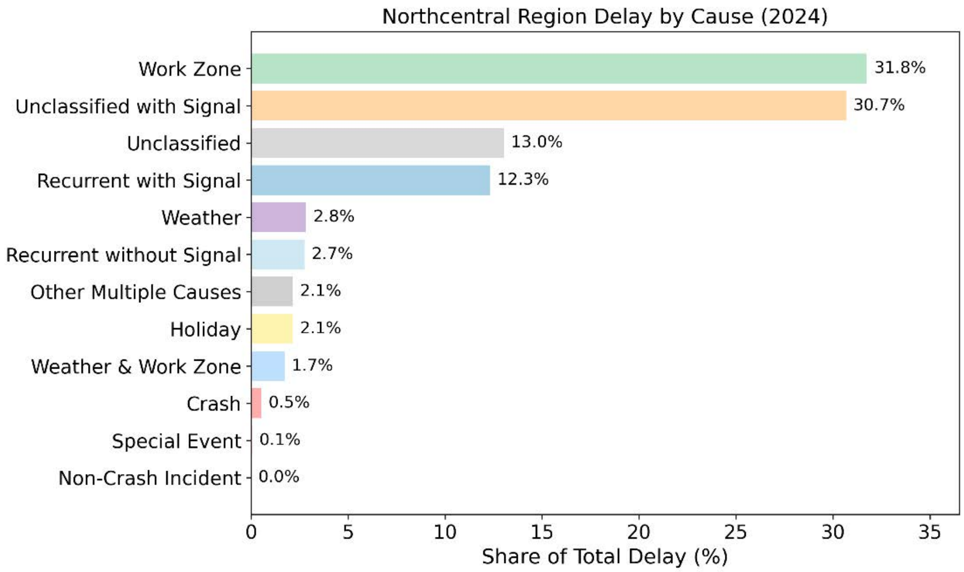

Figure 5-27: Delay Composition by Cause – North Central Region (2024).

The North Central region shows a relatively stable delay composition in 2019 and 2023. The share of unclassified delay with signal increased from 2019 to 2023 and then decreased in 2024. In contrast, the share of work zone-related delay declined in 2023 but increased in 2024, becoming the largest delay category. Weather, special events, and crashes account for relatively small shares of total delay.

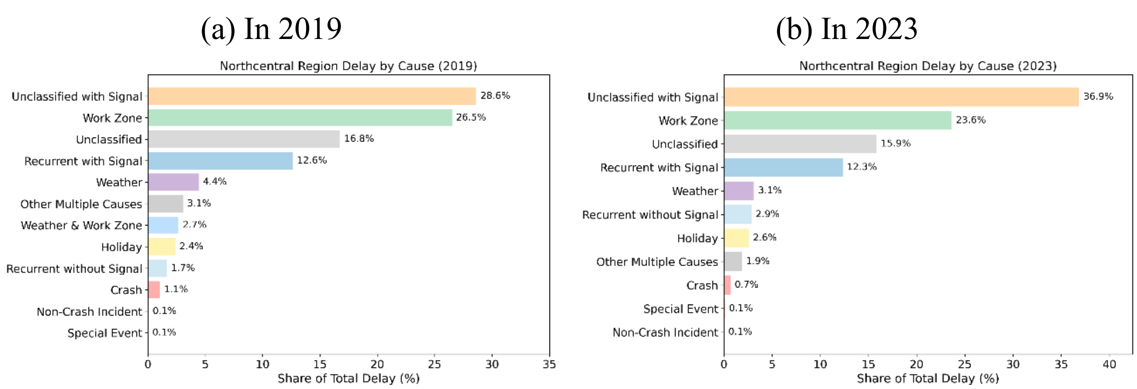

Figure 5-28: Delay Composition by Cause – North Central Region.

Northeast Region

In 2024, delay in the Northeast region is primarily concentrated in unclassified delay with signal, indicating that signalized facilities account for a substantial share of regional delay. Work-zone delay and recurrent delay with signal represent the next largest categories.

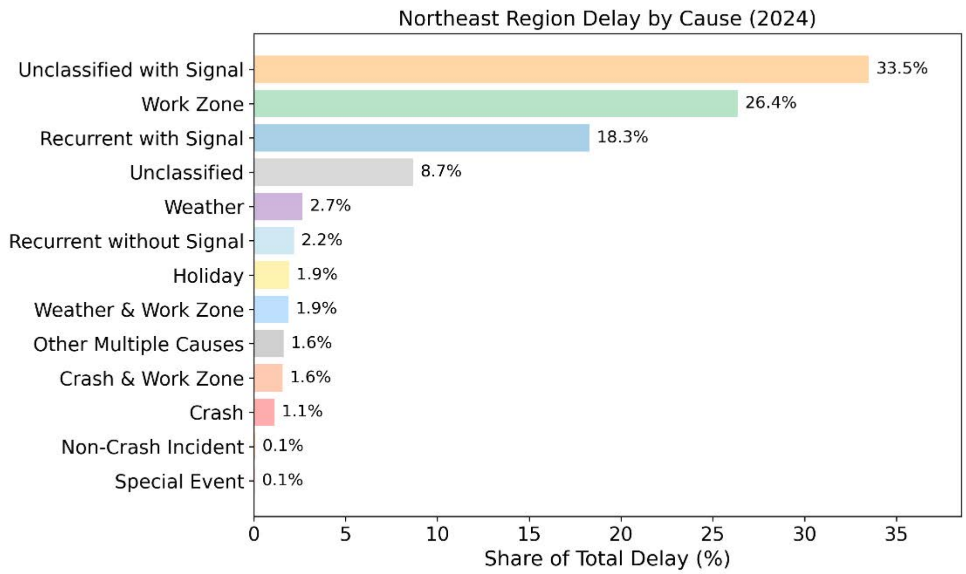

Figure 5-29: Delay Composition by Cause – Northeast Region (2024).

The overall delay composition remains broadly consistent across the three analysis years. The share of work-zone-related delay increased from 2019 to 2023 and remained elevated in 2024, suggesting a continued contribution from construction and lane-closure activity. Meanwhile, recurrent delay with signal declined compared with 2019.

(a) In 2019

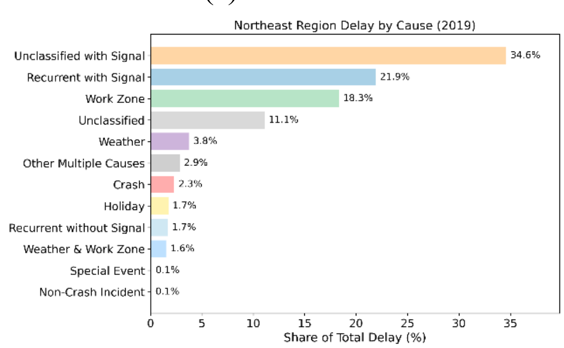

(b) In 2023

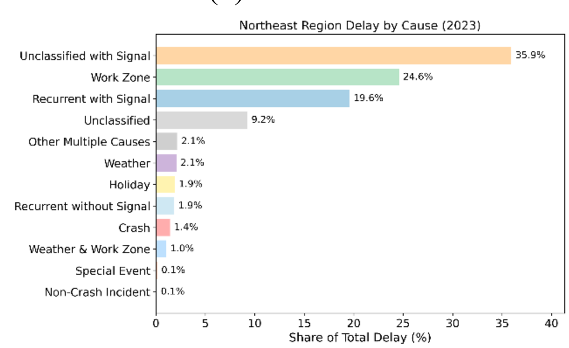

Figure 5-30: Delay Composition by Cause – Northeast Region.

Southeast Region

In the Southeast region, unclassified delay with signal represents the largest category in 2024. Work-zone delay represents the second-largest category. Recurrent delay with signal also accounts for a substantial share.

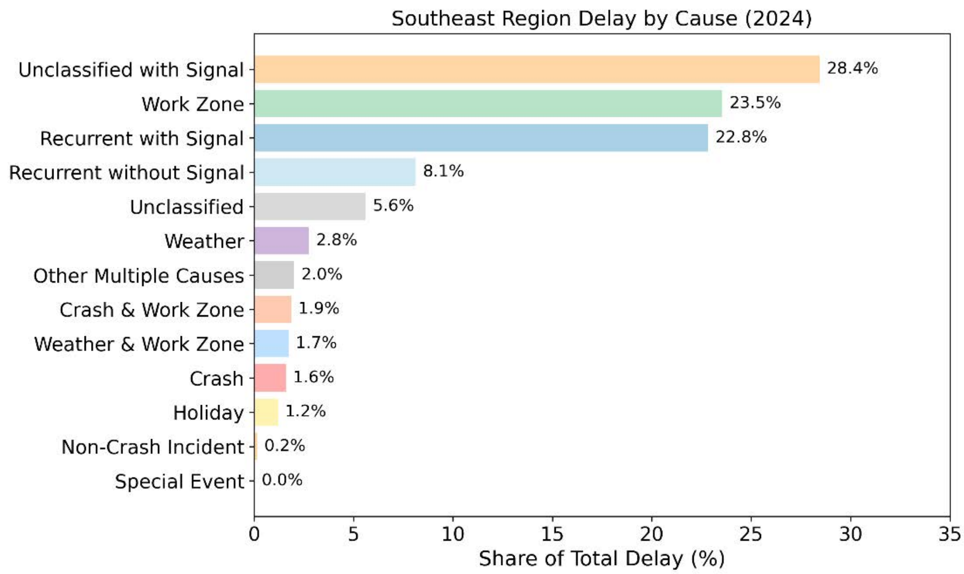

Figure 5-31: Delay Composition by Cause – Southeast Region (2024).

Work-zone-related delay shows a higher share in recent years (2023 and 2024), suggesting sustained construction and lane-closure impacts.

(a) In 2019 (b) In 2023

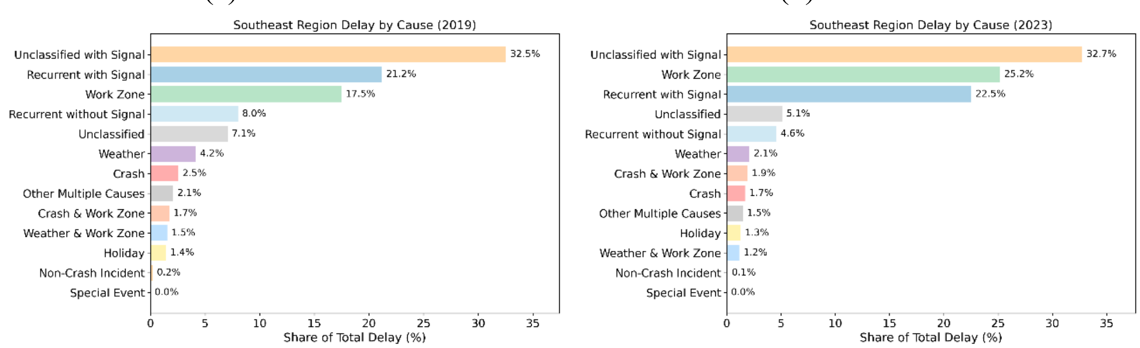

Figure 5-32: Delay Composition by Cause – Southeast Region.

In 2024, recurrent delay with signal and unclassified delay with signal represent a large and persistent share of monthly delay throughout the year. Work-zone delay becomes more pronounced during late spring and summer months. Recurrent delay without signal and unclassified categories account for smaller but relatively stable shares across months.

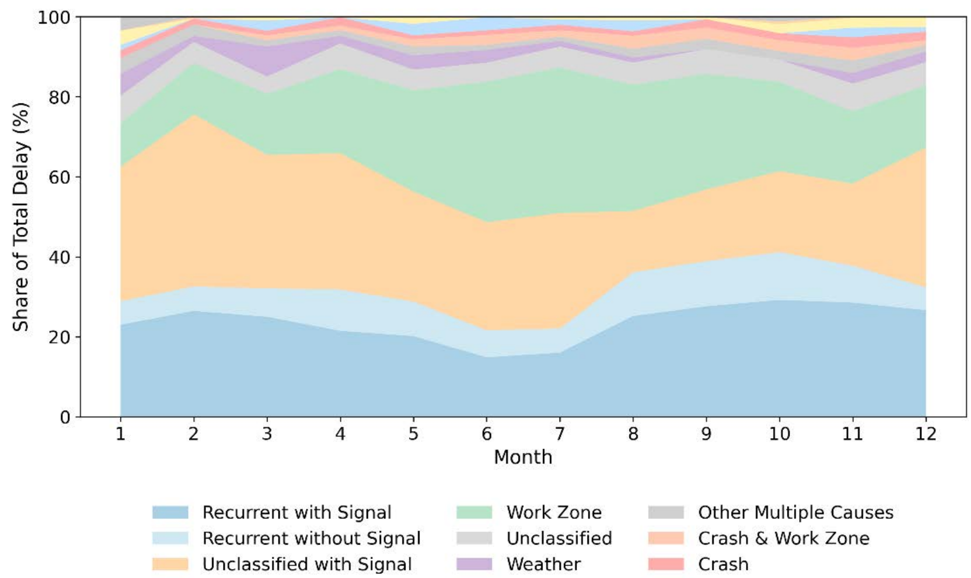

Figure 5-33: Monthly Delay Composition by Cause – Southeast Region (2024).

Southwest Region

The Southwest region's delay composition is strongly concentrated in unclassified delay with signal. Recurrent delay with signal represents the second-largest category, while work-zone delay accounts for a comparatively smaller share.

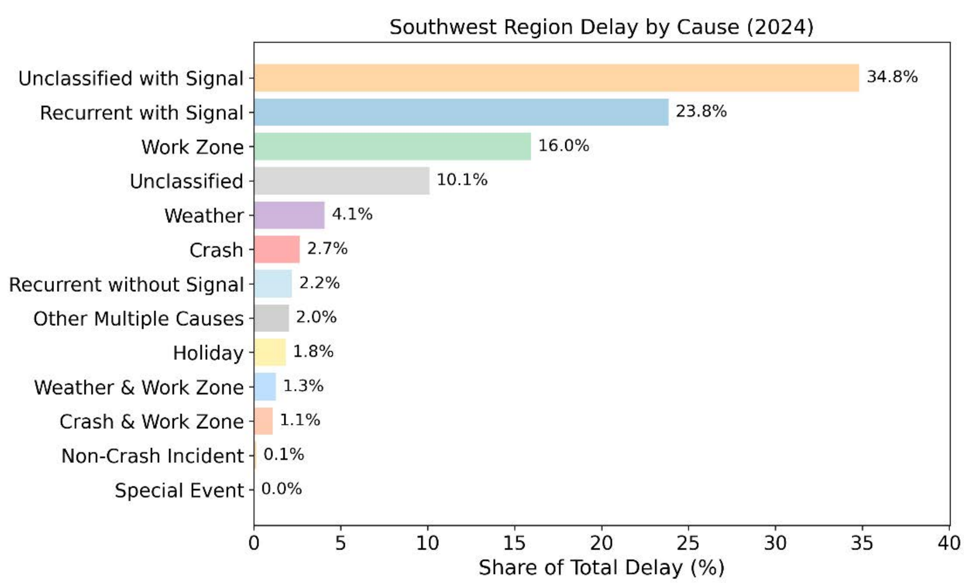

Figure 5-34: Delay Composition by Cause – Southwest Region (2024).

The share of recurrent delay with signal increased substantially after 2019 and remains the second largest category in 2023 and 2024. In contrast to the Southeast region, the share of work-zone delay in the Southwest region declined compared with 2019 and remains relatively low in 2024.

(a) In 2019 (b) In 2023

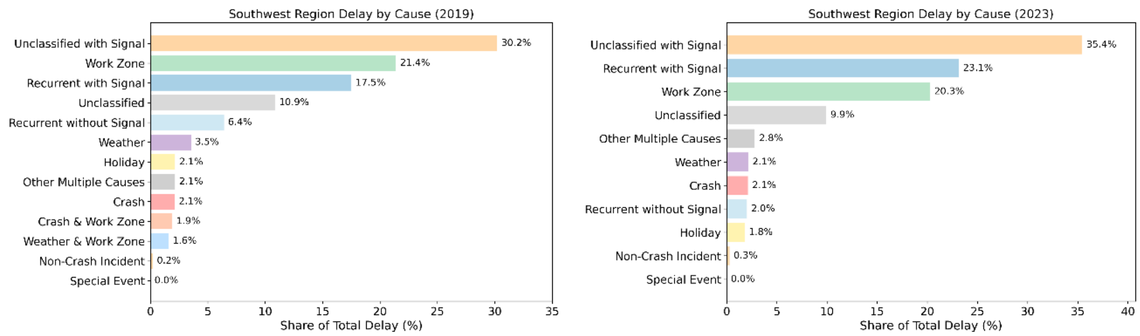

Figure 5-35: Delay Composition by Cause – Southwest Region.

In 2024, recurrent delay with signal and unclassified delay with signal account for the largest share of monthly delay in the Southwest region across most months. Work-zone-related delay becomes more visible during late spring and summer, although it remains smaller than the signalized delay categories.

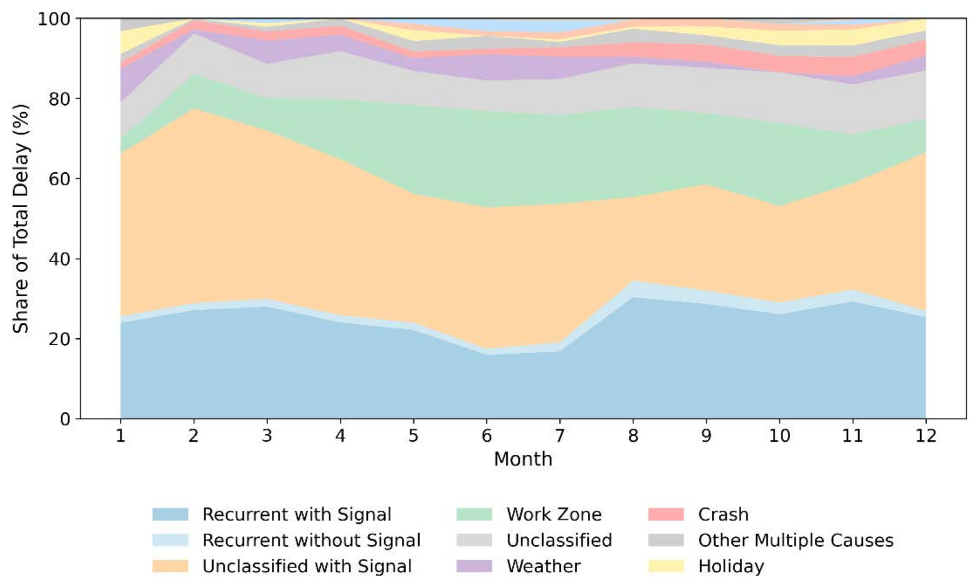

Figure 5-36: Monthly Delay Composition by Cause – Southwest Region (2024).

Northwest Region

In the Northwest region, 2024 delay is primarily concentrated in work-zone-related delay. Unclassified delay with signal and unclassified delay also account for meaningful shares.

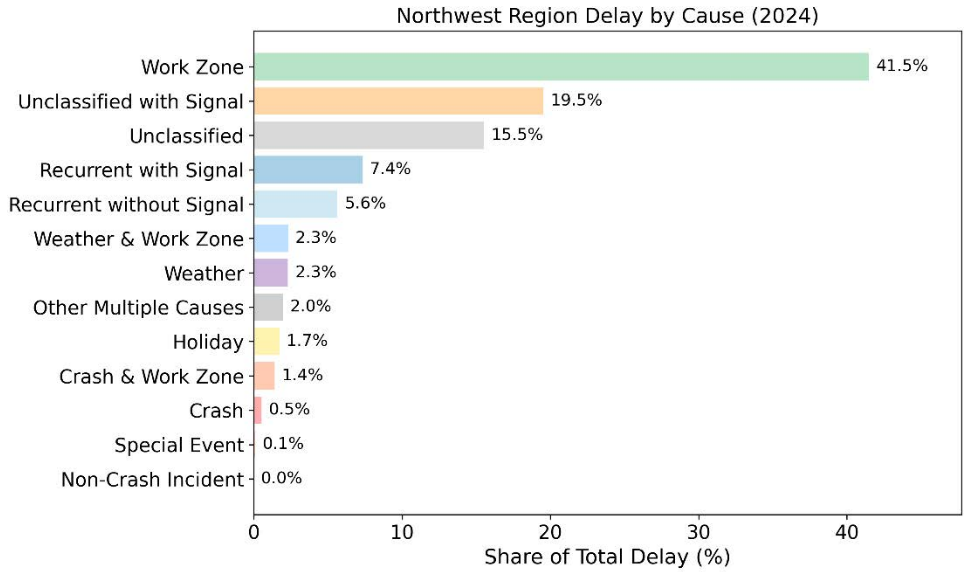

Figure 5-37: Delay Composition by Cause – Northwest Region (2024).

Work-zone-related delay accounts for a larger share in 2023 and 2024 than in 2019.

(a) In 2019

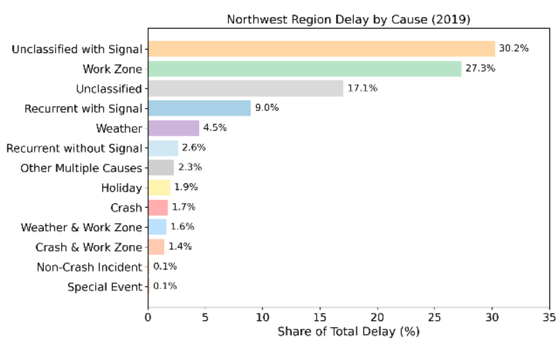

(b) In 2023

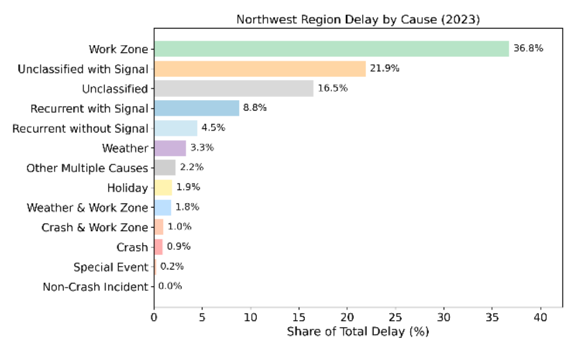

Figure 5-38: Delay Composition by Cause – Northwest Region.

MPA Level

The MPA-level analysis provides a more detailed view of delay composition in metropolitan areas. Because delay is highly concentrated in the largest MPAs, this section focuses on Southeastern Wisconsin and Madison. Results for the remaining MPAs are provided in the accompanying output files.

Southeastern Wisconsin

In 2024, delay in the Southeastern Wisconsin MPA is primarily concentrated in unclassified delay with signal. Work-zone delay and recurrent delay with signal form the next tier of categories.

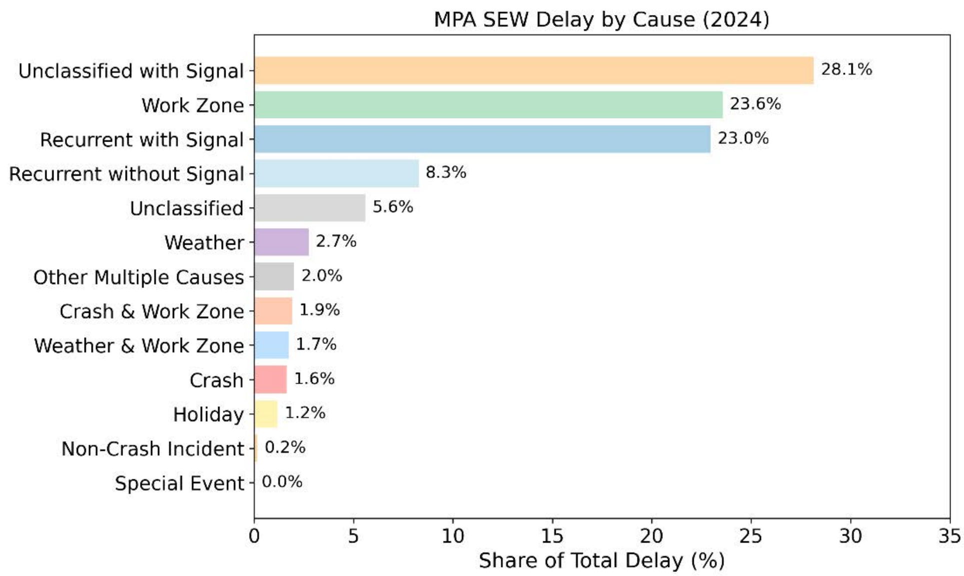

Figure 5-39: Delay Composition by Cause – Southeastern Wisconsin MPA (2024).

In 2019, the overall composition remains centered on delay on signalized TMCs, while work-zone delay remains prominent in 2023 and 2024. Compared with 2023, the 2024 distribution shows a lower share of unclassified delay with signal.

(a) In 2019

(b) In 2023

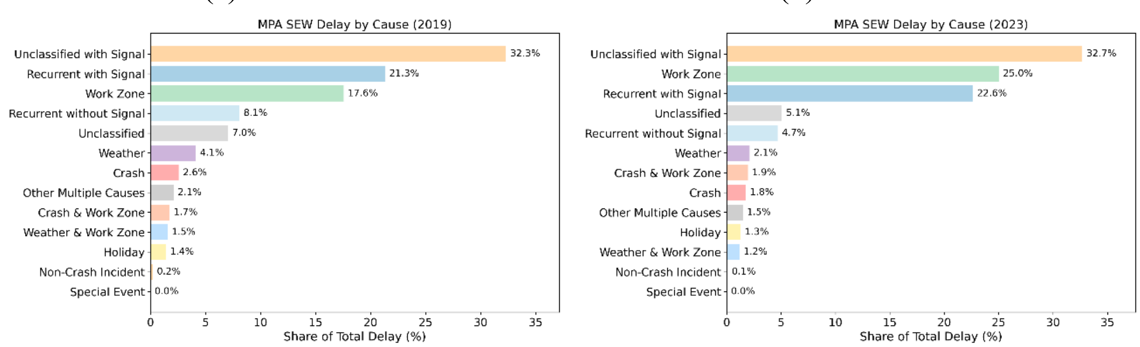

Figure 5-40: Delay Composition by Cause – Southeastern Wisconsin MPA.

In 2024, the Southeastern Wisconsin MPA shows clear seasonal variation in delay composition. The share of unclassified delay with signal decreases during late spring and summer as work-zone delay increases and peaks around mid-summer. Recurrent delay with signal remains moderate and relatively steady, while unclassified delay and other cause categories account for smaller shares.

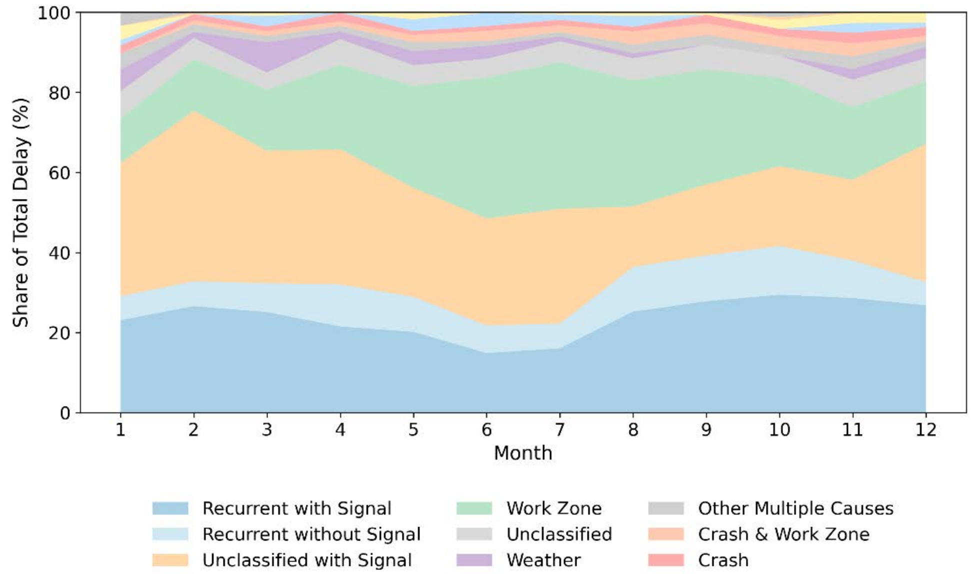

Figure 5-41: Monthly Delay Composition by Cause – Southeastern Wisconsin MPA (2024).

Madison

In 2024, delay in the Madison MPA is strongly concentrated in unclassified delay with signal. Recurrent delay with signal represents the second-largest category, while work-zone delay accounts for a comparatively smaller share.

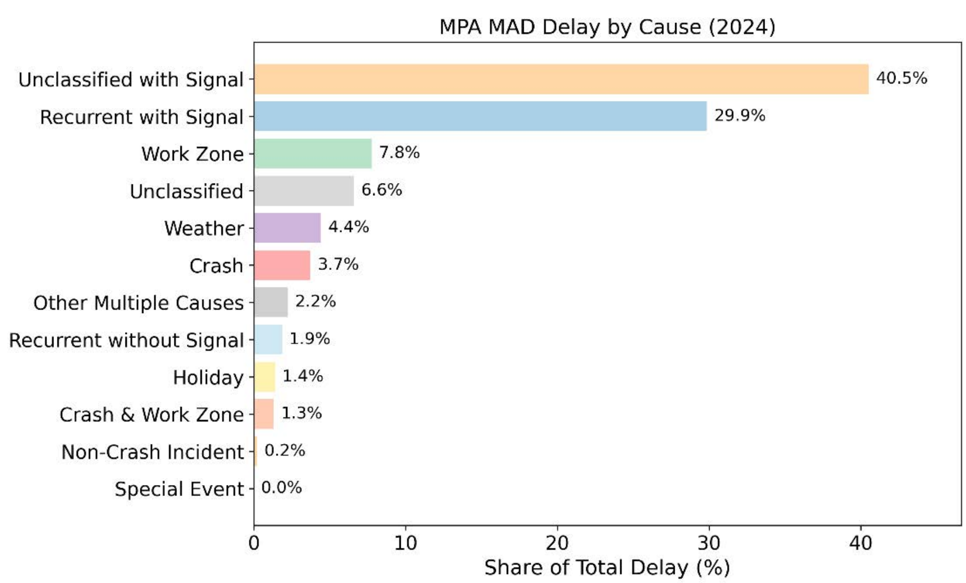

Figure 5-42: Delay Composition by Cause – Madison MPA (2024).

Compared with 2019, the 2024 distribution shows a stronger concentration in delay on signalized TMCs and a smaller share of work-zone delay. Compared with 2023, the 2024 pattern remains similar, with a reduction in work-zone delay and only modest variation in the other categories.

(a) In 2019 (b) In 2023

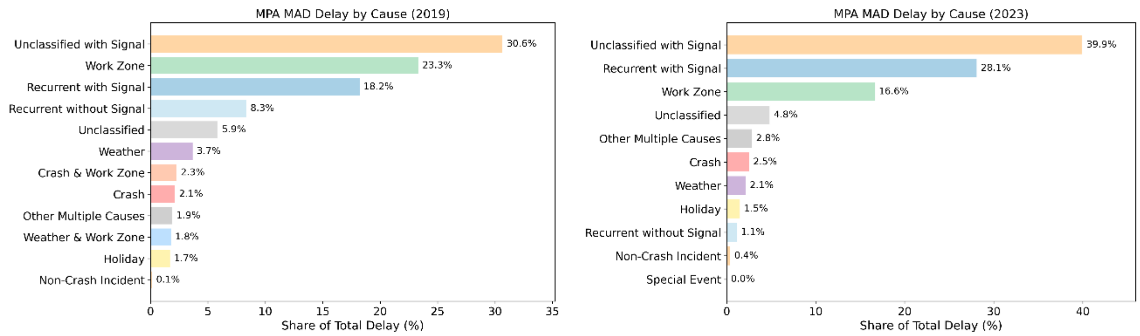

Figure 5-43: Delay Composition by Cause – Madison MPA.

In 2024, delay on signalized TMCs accounts for the largest share of monthly delay in the Madison MPA throughout the year. Work-zone delay increases slightly during the middle of the year, while other categories remain modest.

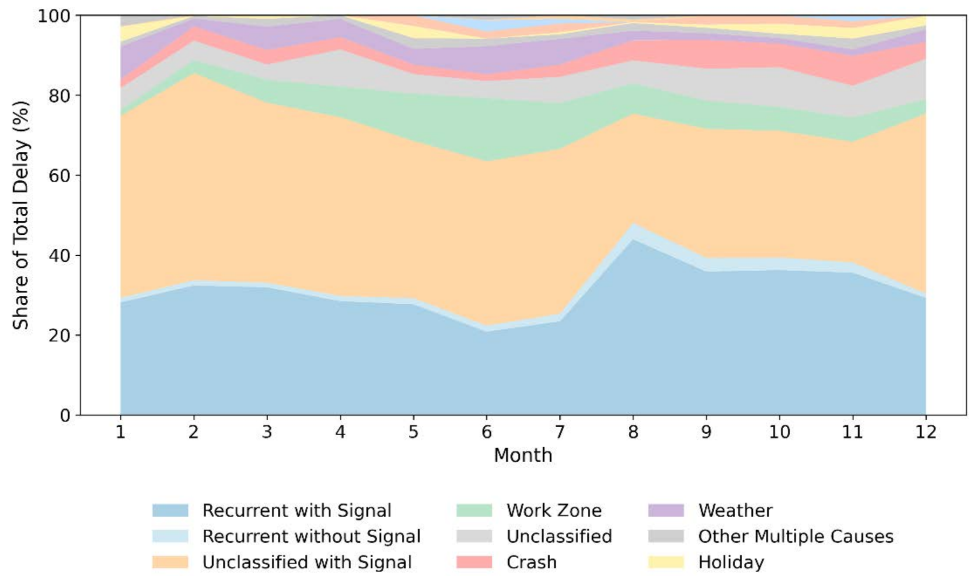

Figure 5-44: Monthly Delay Composition by Cause – Madison MPA (2024).

5.3. <u>Statewide Delay Causation Modeling</u>

This section presents regression and machine-learning analyses used to examine associations between delay and selected explanatory variables at the statewide level.

<u>Overall Modeling Conclusion</u>

The regression and machine-learning results consistently indicate that traffic demand and operational characteristics are strongly associated with short-term delay. While discrete events such as crashes can generate substantial local impacts, their modeled statewide contribution is relatively small compared with the contributions of hourly volume and signal presence.

Baseline Regression Modeling

To improve computational efficiency while preserving event information, 10 percent of event observations and 1 percent of non-event observations were randomly sampled for model estimation. This sampling approach retains sufficient event observations for estimating event-related associations while reducing data imbalance and computational burden.

Table 5-4 summarizes the severity-based regression results for total delay. Because the dependent variable is log-transformed, coefficients should be interpreted as associations with log-transformed delay rather than direct changes in vehicle-hours of delay. The signs and relative magnitudes are therefore used to compare directional associations across variables. Crash indicators, full work-zone closures, special events, heavy weather, signal presence, and hourly volume are positively associated with total delay. Partial work-zone closures, holiday indicators, and heavy vehicle ratio show negative coefficients in the total-delay model, suggesting that their marginal associations may be affected by correlations with traffic demand, facility type, and other operating conditions.

Table 5-4: Severity-Based Regression Results for Total Delay.

Variable	Coefficient	Robust SE	p-value	Interpretation
Intercept	-0.1254	0.0053	<0.001	Baseline log-delay close to zero under the reference condition
Minor crash	0.1207	0.0049	<0.001	Strong positive association
Major crash	0.2004	0.0193	<0.001	Strong positive association
Non-crash incident	0.0092	0.0030	0.003	Small positive association
Partial work-zone closure	-0.0033	0.0011	0.004	Small negative association
Full work-zone closure	0.0147	0.0031	<0.001	Small positive association
Special event	0.0106	0.0033	0.001	Small positive association
Holiday	-0.0050	0.0004	<0.001	Small negative association
Heavy weather	0.0061	0.0004	<0.001	Small positive association
Signal	0.0843	0.0022	<0.001	Modest positive association
Hourly volume	0.0259	0.0009	<0.001	Positive association with traffic demand
Heavy vehicle ratio	-0.0527	0.0132	<0.001	Negative association

Model R^2=0.045; Adjusted R^2=0.045

N=13 million observations

Figure 5-45 compares standardized regression coefficients across WisDOT regions. Standardized coefficients were obtained by re-estimating the regression after scaling both the dependent variable and explanatory variables to have mean zero and unit variance. Thus, they represent relative associations on a standard-deviation scale. Overall, the signs and relative magnitudes are generally consistent across regions, with signal presence and hourly volume showing the largest positive associations with total delay. Minor crashes and full work-zone closures also show positive associations in most regions, while heavy vehicle ratio and holiday indicators tend to show negative associations. A few variables, such as partial work-zone closure and non-crash incident, show sign differences in one region, and non-crash incident and special event indicators are not statistically significant in all regional models. Therefore, these variables should be interpreted more cautiously than the consistently significant variables.

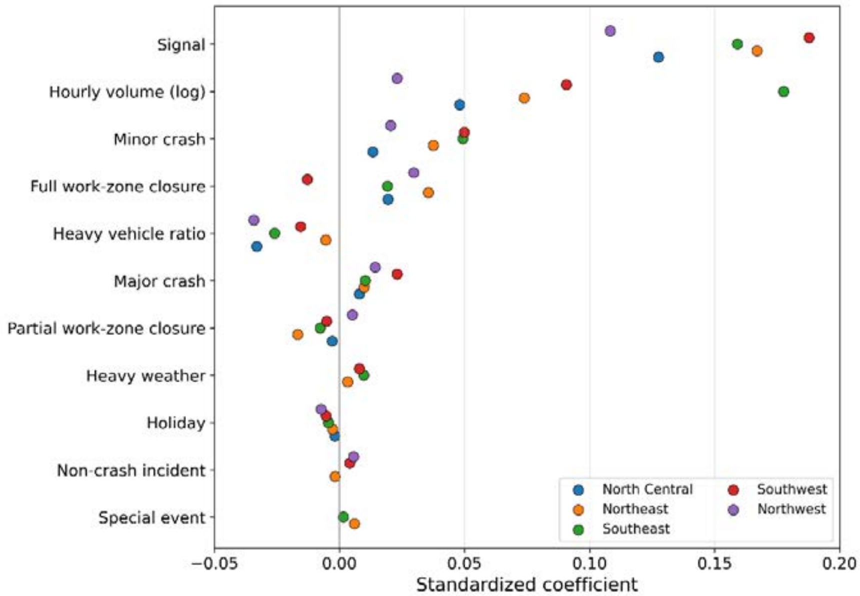

Figure 5-45: Standardized Coefficients from Regional Regression Models for Total Delay.

Table 5-5 summarizes the regression results for non-recurrent delay. Minor crashes exhibit a larger marginal association with non-recurrent delay than major crashes. This pattern may reflect the higher frequency of minor crashes and potential limitations in severe-crash records, including lower occurrence rates and greater missing-data concerns. Non-crash incidents are positively associated with non-recurrent delay, although their coefficient magnitude is smaller than those of crash indicators. For work zones, full closures show a substantially larger positive association with non-recurrent delay than partial closures, supporting the importance of distinguishing closure severity in the modeling framework. Heavy weather is statistically significant but has a small coefficient, suggesting that its incremental association with non-recurrent delay is limited after controlling for other factors. Signal presence and hourly volume remain positively associated with non-recurrent delay, although their standardized coefficients are smaller than in the total-delay model.

Table 5-5: Severity-Based Regression Results for Non-Recurrent Delay.

Variable	Coefficient	Robust SE	p-value	Interpretation
Intercept	-0.0818	0.0039	<0.001	Baseline log non-recurrent delay close to zero under the reference condition
Minor crash	0.1029	0.0040	<0.001	Strong positive association
Major crash	0.1991	0.0192	<0.001	Strong positive association
Non-crash incident	0.0106	0.0021	<0.001	Small positive association
Partial work-zone closure	0.0039	0.0009	<0.001	Small positive association
Full work-zone closure	0.0258	0.0028	<0.001	Small positive association
Special event	0.0106	0.0027	<0.001	Small positive association
Holiday	-0.0030	0.0003	<0.001	Small negative association
Heavy weather	0.0061	0.0003	<0.001	Small positive association
Signal	0.0576	0.0015	<0.001	Modest positive association
Hourly volume	0.0167	0.0006	<0.001	Positive association with traffic demand
Heavy vehicle ratio	-0.0309	0.0082	<0.001	Negative association

Model R^2=0.028; Adjusted R^2=0.028

N=13 million observations

Figure 5-46 compares standardized coefficients from the regional non-recurrent delay models. Overall, the signs and relative magnitudes are generally consistent across regions. Signal presence and hourly volume remain important positive predictors, but their standardized coefficients are smaller than in the total-delay models. In contrast, event-related variables, especially full and partial work-zone closures, become prominent positive factors in the non-recurrent delay models.

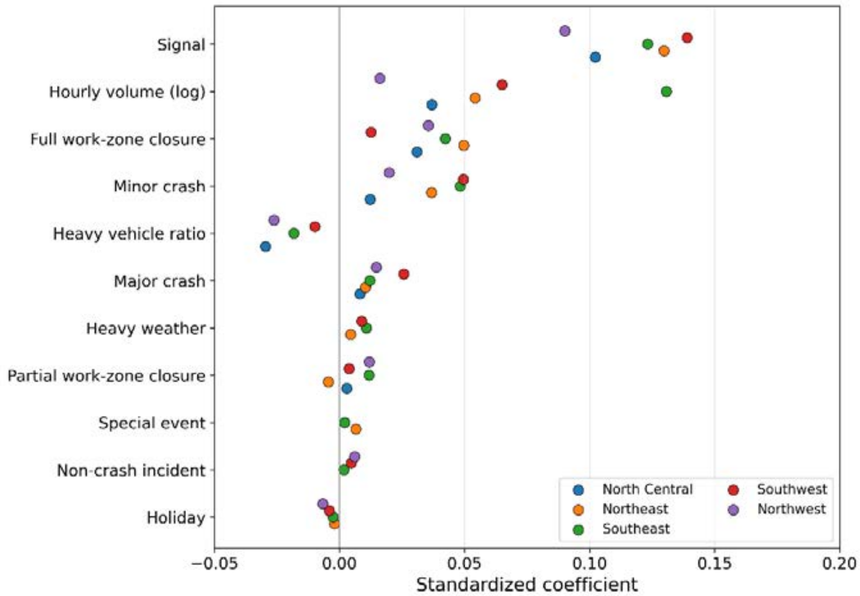

Figure 5-46: Standardized Coefficients from Regional Regression Models for Non-Recurrent Delay.

Table 5-6 summarizes the explanatory performance of the baseline regression models by dependent variable. Across all regions, the adjusted R^2 and test R^2 values are relatively low, indicating that the linear model captures only a limited portion of the 15-minute delay variability. This is expected because short-term delay is affected by nonlinear traffic dynamics, localized bottlenecks, and spatial propagation effects that are not fully represented in the baseline regression specification. The Southeast and Southwest regions show the highest model performance, while the Northwest and North Central regions show lower values. In all regions, the total-delay models have higher R^2 values than the non-recurrent delay models.

Table 5-6: Baseline Statewide and Regional Regression Specifications.

Location	Dependent Variable	Adjusted R^2	Test R^2
Statewide	Total delay	0.045	0.045
	Non-recurrent delay	0.028	0.028
North Central	Total delay	0.027	0.026
	Non-recurrent delay	0.018	0.018
Northeast	Total delay	0.038	0.037
	Non-recurrent delay	0.024	0.024
Southeast	Total delay	0.052	0.052
	Non-recurrent delay	0.032	0.032
Southwest	Total delay	0.049	0.048
	Non-recurrent delay	0.029	0.028
Northwest	Total delay	0.018	0.018
	Non-recurrent delay	0.013	0.013

Impact Size Interpretation

As shown in Table 5-7, hourly volume has the largest average log-scale contribution on non-recurrent delay because it is a continuous variable present across all observations. Among event-based variables, work-zone closures have larger average log-scale contributions than crashes because they occur more frequently and often persist over longer durations. Crash coefficients are relatively large, but their low occurrence rates result in smaller average statewide log-scale contributions.

Table 5-7: Statewide Average Log-Scale Contribution by Causal Factor.

Variable	Coefficient	Mean Frequency	Average Marginal Impact
Minor crash	0.1040	0.0096	0.0010
Major crash	0.1896	0.0003	0.0001
Partial work-zone closure	0.0038	0.3128	0.0012
Full work-zone closure	0.0259	0.1328	0.0034
Non-crash incident	0.0106	0.0035	0
Special event	0.0103	0.0024	0
Holiday	-0.0031	0.0771	-0.0002
Heavy weather	0.0059	0.0991	0.0006
Signal	0.0574	0.3838	0.0220
Hourly volume	0.0167	5.8062	0.0970
Heavy vehicle ratio	-0.0313	0.1061	-0.0033

Note: The dependent variable is $\ln(\text{Non-Recurrent Delay}+1)$. Therefore, the reported values represent average contributions on the log-delay scale and should not be interpreted as vehicle-hours of delay.

Table 5-8 reports regional average marginal impacts using the same definition shown above, computed as the estimated regression coefficient multiplied by the regional mean of each variable or regional occurrence rate for binary indicators. Hourly volume exhibits the largest average marginal impact across all regions, with the largest magnitude observed in the Southeast region. Signal presence and work zone closures also show higher average impacts in urbanized regions, reflecting stronger interactions between demand and capacity-reducing disruptions. Crash- and incident-related variables have very small average impacts due to their low occurrence rates.

Table 5-8: Regional Average Log-Scale Contribution by Causal Factor.

Variable	North Central	Northeast	Southeast	Southwest	Northwest
Minor crash	0.0001	0.0006	0.0015	0.0009	0.0003
Major crash	0	0	0.0001	0.0001	0
Partial work-zone closure	0.0003	-0.0006	0.0021	0.0004	0.0023
Full work-zone closure	0.0023	0.0040	0.0045	0.0010	0.0021
Non-crash incident	0	0	0	0.0001	0
Special event	0	0.0001	0	0	0
Holiday	-0.0001	-0.0001	-0.0002	-0.0003	-0.0004
Heavy weather	0	0.0003	0.0009	0.0007	0.0001
Signal	0.0100	0.0174	0.0344	0.0195	0.0079
Hourly volume	0.0291	0.0527	0.1692	0.0669	0.0144
Heavy vehicle ratio	-0.0129	-0.0004	-0.0081	-0.0026	-0.0098

Contribution Decomposition

Table 5-9 indicates that most modeled contribution on the log-delay scale is associated with hourly volume and signal presence. Negative contributions indicate inverse associations in the linear model and are reported for completeness; the "Positive Share" column summarizes the composition of positive modeled contributions only. Work-zone closures account for the largest positive modeled contribution among the event types. Crash-related variables contribute a relatively small modeled share at the statewide scale due to their lower occurrence rates, despite larger per-event coefficients.

Table 5-9: Statewide Modeled Contribution Shares for Non-Recurrent Delay.

Variable	Modeled Contribution	Share (%)	Positive Share (%)
Minor crash	13034.38	0.82	0.80
Major crash	745.30	0.05	0.05
Partial work-zone closure	15345.69	0.97	0.94
Full work-zone closure	44727.63	2.83	2.75
Non-crash incident	486.05	0.03	0.03
Special event	328.09	0.02	0.02
Holiday	-3103.86	-0.20	0
Heavy weather	7640.14	0.48	0.47
Signal	286539.96	18.10	17.59
Hourly volume (log)	1260517.36	79.63	77.36
Heavy vehicle ratio	-43220.89	-2.73	0

Note: The dependent variable is $\ln(\text{Non-Recurrent Delay}+1)$. Therefore, the reported contributions are computed on the log-delay scale and should not be interpreted as direct vehicle-hours of delay. Positive shares are calculated after excluding factors with negative modeled contributions.

Table 5-10 summarizes the regional composition of positive modeled contributions. Shares are computed relative to the total positive modeled contribution within each region; factors with negative or negligible implied shares are shown as zero, consistent with the definition provided in the table note. Across regions, hourly volume represents the largest positive modeled contribution, followed by signal presence. Work-zone variables account for a moderate share in several regions, while crash- and incident-related variables contribute very small shares in all regions due to their low occurrence rates.

Table 5-10: Regional Modeled Contribution Shares for Non-Recurrent Delay.

Variable	North Central	Northeast	Southeast	Southwest	Northwest
Minor crash	0.33	0.86	0.70	1.05	0.95
Major crash	0.04	0.04	0.03	0.10	0.13
Partial work-zone closure	0.76	0	1.01	0.50	8.46
Full work-zone closure	5.50	5.33	2.10	1.12	7.61
Non-crash incident	0.01	0	0.02	0.08	0.08
Special event	0	0.07	0.01	0	0.10
Holiday	0	0	0	0	0
Heavy weather	0	0.37	0.44	0.77	0.27
Signal	23.90	23.18	16.16	21.70	29.30
Hourly volume (log)	69.46	70.15	79.54	74.67	53.10
Heavy vehicle ratio	0	0	0	0	0

Note: This table reports positive shares only. A zero indicates that the factor's implied share is negative or negligible under the regional decomposition and is therefore not shown as a positive share.

Machine Learning Model

The machine-learning model was developed to improve the explanatory power for total delay by capturing nonlinear relationships and interaction effects. Total delay was used as the dependent variable in the LightGBM model. LightGBM achieved R^2=0.124, representing a substantial improvement over the linear regression model (R^2=0.045). This higher explanatory power indicates that nonlinear effects and interaction patterns play an important role in explaining 15-minute delay variation.

Feature Importance Analysis

Gain-based feature importance indicates the relative contribution of each variable to LightGBM prediction performance. As shown in Figure 5-47, the highest-ranked variables are:

1. Hourly volume
2. Heavy vehicle ratio
3. Signal
4. Full work-zone closure
5. Minor crash

Partial work-zone closures, major crashes, and other events show smaller relative importance in the machine-learning model.

Traffic state variables, including hourly volume and heavy vehicle ratio, are the highest-ranked factors in the LightGBM model, suggesting that traffic demand and composition are closely related to short-term delay variation. Signal presence is also highly ranked, reinforcing the importance of distinguishing signalized and non-signalized facilities. Work-zone severity, especially full closures, has greater predictive importance than minor crash in the statewide LightGBM model. While crash indicators have relatively large regression coefficients, their lower occurrence rates relative to traffic-state variability result in lower relative importance in the machine-learning model. Non-crash incidents and special events show modest importance, consistent with earlier findings.

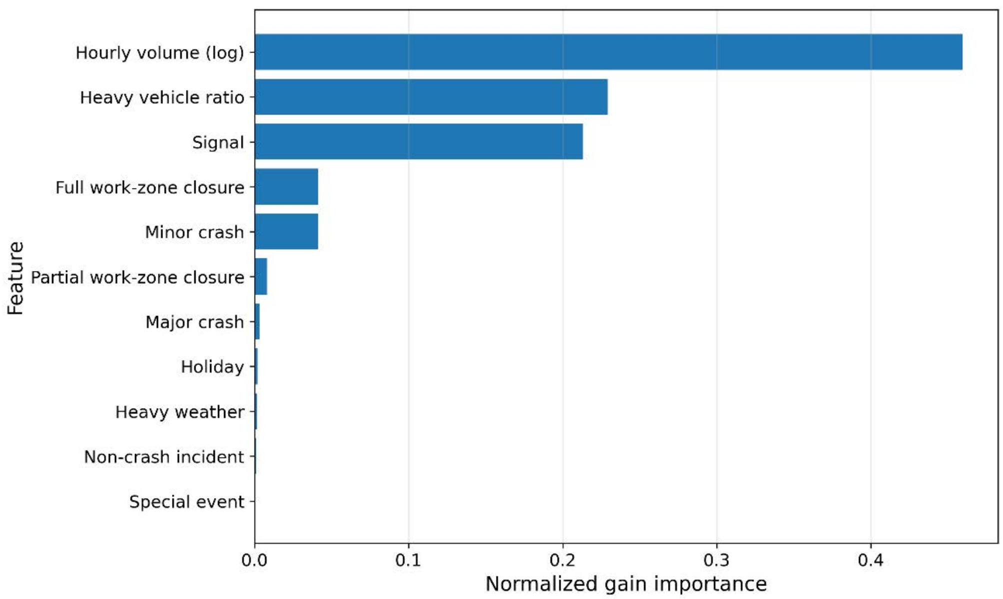

Figure 5-47: Statewide LightGBM Feature Importance.

Figure 5-48 compares LightGBM gain-based feature importance across WisDOT regions. Traffic state variables, particularly heavy vehicle ratio and hourly volume, account for the largest share of feature importance in most regions. Signal presence is also consistently important across regions. Among event-related variables, full work-zone closure shows the highest importance, while major crash, weather, special event, and non-crash incident variables contribute relatively little to overall predictive performance.

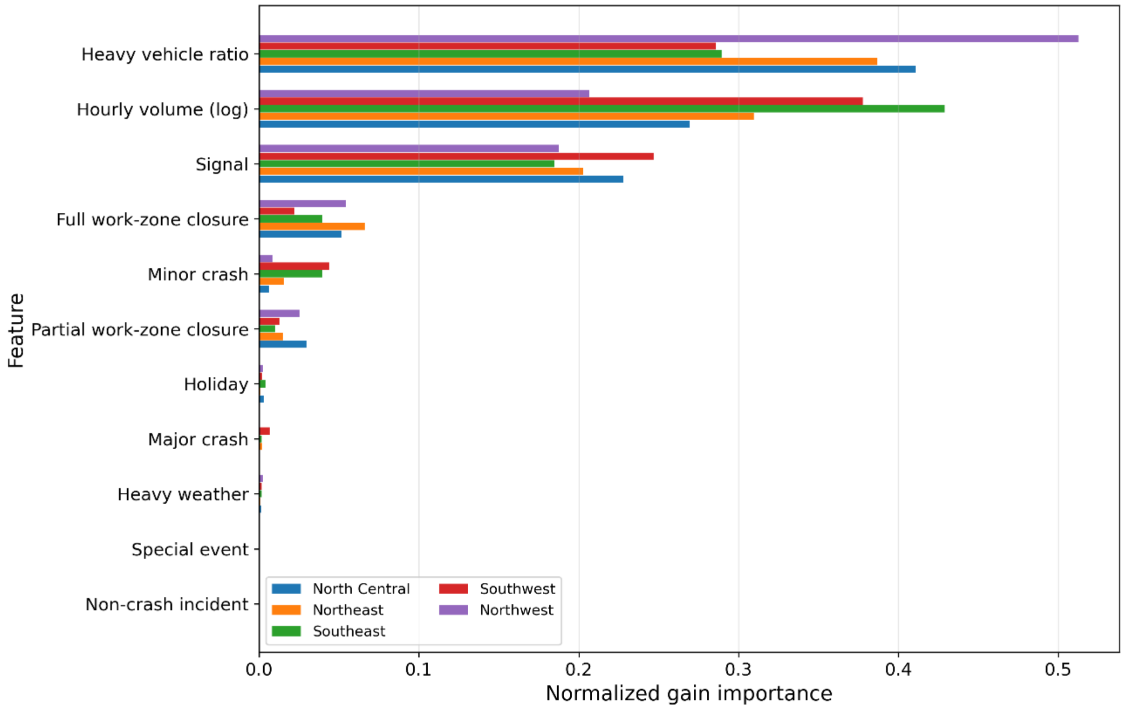

Figure 5-48: LightGBM Feature Importance by Region.

Shapley Additive Explanations (SHAP)

To interpret the LightGBM model, SHAP values were computed to decompose model predictions into additive feature contributions.

In the SHAP summary plot, the color scale indicates whether each feature value is relatively high or low for each observation. As shown in Figure 5-49, signal presence, hourly volume, and heavy vehicle ratio are the most influential predictors of 15-minute total delay in the statewide LightGBM model. Higher hourly volume is generally associated with positive SHAP values, indicating higher predicted delay, while low-volume observations tend to reduce predicted delay. Signal presence also shows a consistent positive contribution when active. Heavy vehicle ratio exhibits a more nonlinear pattern, with both positive and negative SHAP values depending on the broader traffic context. Among event-related variables, full work-zone closures and minor crashes show the clearest positive contributions, while heavy weather, partial closures, holidays, non-crash incidents, and special events have smaller effects centered closer to zero.

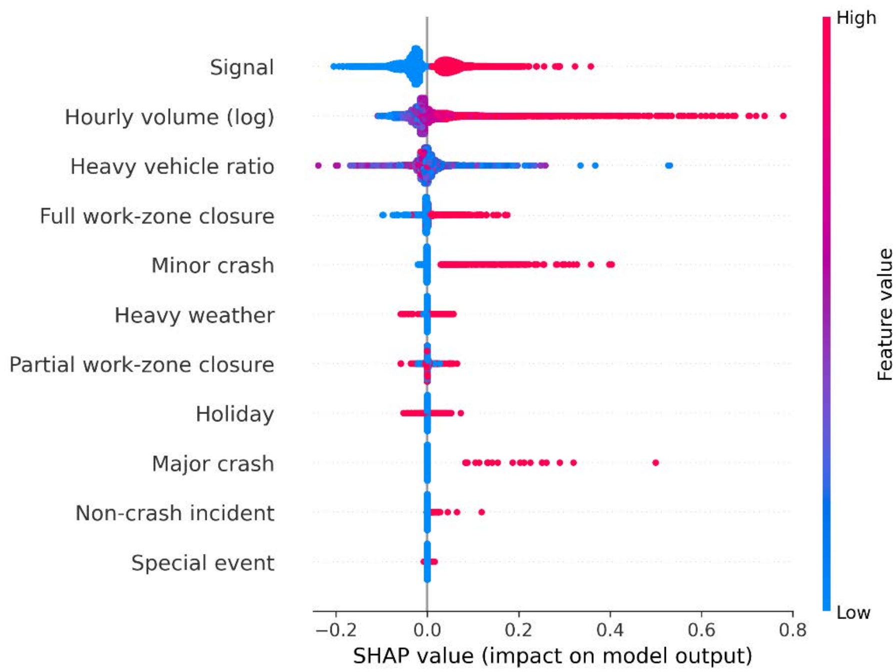

Figure 5-49: Statewide SHAP Summary Plot.

The SHAP analysis suggests that:

- Traffic state variables, including hourly volume and heavy vehicle ratio, are among the primary predictors of 15-minute total delay in the LightGBM model.
- Full work-zone closure has stronger predictive importance than crash in the statewide LightGBM model.
- Signal presence contributes positively to predicted total delay.
- Some effects are nonlinear and context-dependent, which helps explain the performance gap between LightGBM and linear regression.

Figure 5-50 presents SHAP summary plots by WisDOT region. Across regions, hourly volume, heavy vehicle ratio, and signal presence remain the most important predictors, but their relative importance varies by region. In the Southeast and Southwest regions, hourly volume shows a strong positive contribution to delay, reflecting the importance of demand-related variation in more urbanized regions. In the North Central and Northeast regions, signal presence and hourly volume remain important, while event-related variables generally have smaller and more dispersed effects. In the Northwest region, heavy vehicle ratio appears more influential relative to other variables, suggesting stronger regional heterogeneity in the relationship between traffic composition and delay. Full work-zone closures and minor crashes generally show positive SHAP contributions across regions, while other event variables have more limited and localized predictive effects.

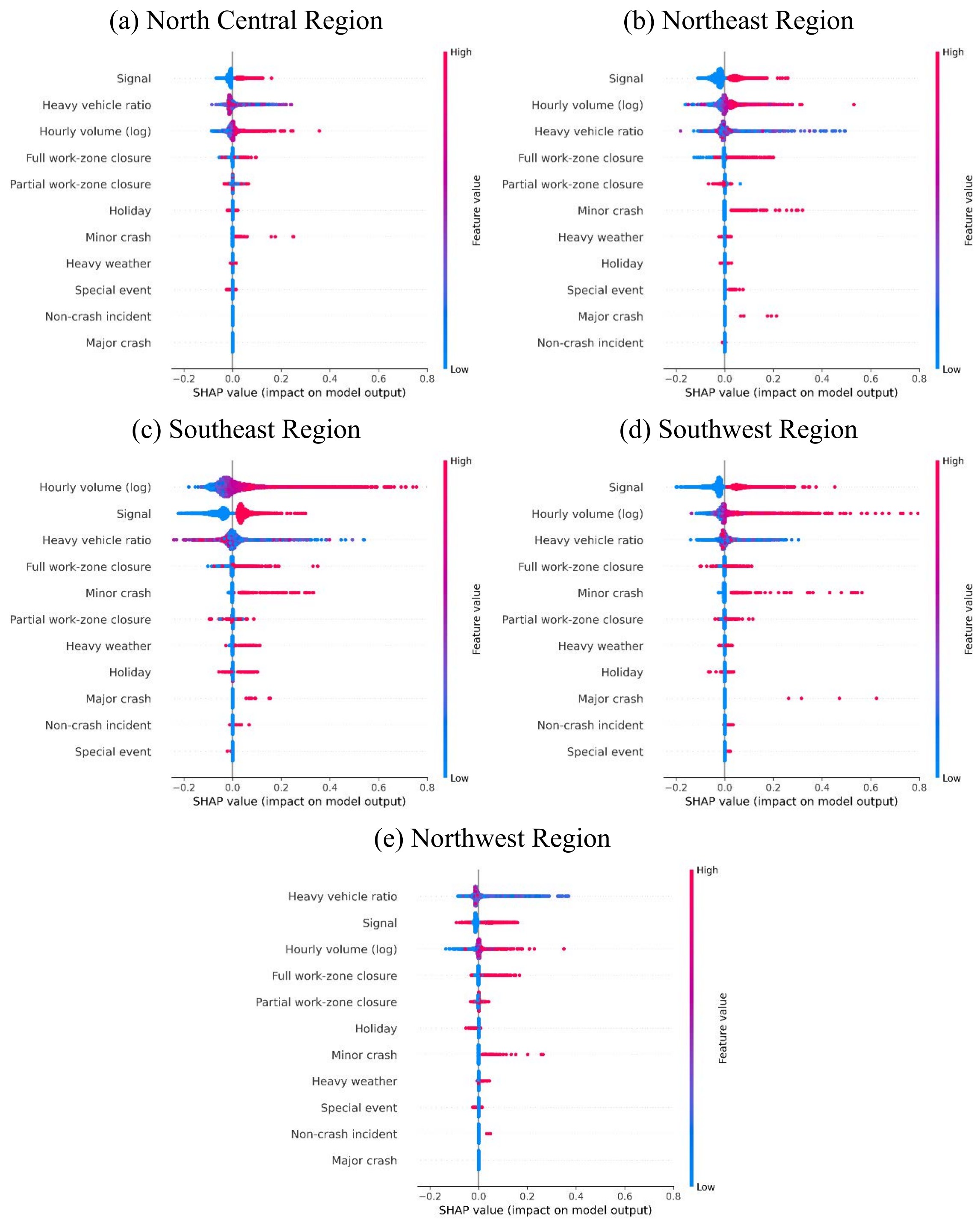

Figure 5-50: SHAP Summary Plots by Region.

5.4. Statewide Application Summary

This chapter applied a statewide, reproducible framework for measuring and analyzing traffic delay causation using 15-minute TMC-level NPMRDS data integrated with crash, non-crash incident, lane closure, weather, signal, and holiday datasets. Across all study years, non-recurrent delay accounts for the larger share of statewide delay, while the recurrent/non-recurrent split remains relatively stable despite fluctuations in total delay magnitude.

Modeling results consistently show that hourly volume and signal presence are strongly associated with delay. Among events, work-zone indicators show a stronger statewide modeled contribution than crash indicators, while crash-related effects are more localized and less influential in aggregate. Crash-related delay may also be underestimated because of limitations in the available crash data and spatial/temporal buffer rules. Heavy weather and special event indicators show comparatively limited incremental associations in the statewide models.

Machine-learning results indicate nonlinear effects and improve predictive performance relative to linear regression, while reinforcing the same overall insight: statewide delay is strongly related to traffic demand and operational characteristics, with event-related effects being more localized.

6. Corridor-Level Application

This chapter applies the delay causation methodology to selected Wisconsin corridors. Building on the statewide framework, this chapter examines corridor-level delay patterns and associated causal factors with finer spatial and temporal detail. The objective is to provide a more detailed understanding of delay causation within individual corridors.

The corridor-level application includes four components: corridor selection, recurrent and non-recurrent delay classification, investigation of delay causation, and corridor-level delay causation modeling. In coordination with WisDOT and HNTB experts, this study selected major corridors for analysis and evaluated delay patterns in relation to the causal factors considered in this report. The analysis emphasizes temporal profiles, spatial distributions, space-time contour diagnostics, and delay causation modeling to identify where, when, and how delay is concentrated within each corridor.

6.1. Corridor Selection

This section describes how corridors were selected. The selection combined data-driven screening based on 2024 delay with WisDOT input on operationally important corridors. The final study set was defined as the union of these two groups and includes 12 corridors.

Screening of Candidate Corridors

Candidate corridors were screened based on total annual VHD in 2024. Interstate facilities accounted for the highest delay, followed by several 'principal arterials' and 'other principal arterials'. In defining candidate corridors, the screening was conducted so that each TMC was assigned to only one corridor, thereby maintaining mutually exclusive corridor groupings. Based on this screening, seven corridors were identified for more detailed analysis:

- Interstate: I-94, I-43, I-41
- Principal arterial: US-18, US-151
- Other principal arterial: WI-190, WI-100

Figure 6-1 shows the top 10 corridors by total VHD in 2024. The screened corridors also differ in their recurrent and non-recurrent delay shares, indicating that total delay alone is not sufficient to characterize corridor performance. This supports a corridor-level analysis of temporal, spatial, and causal delay patterns.

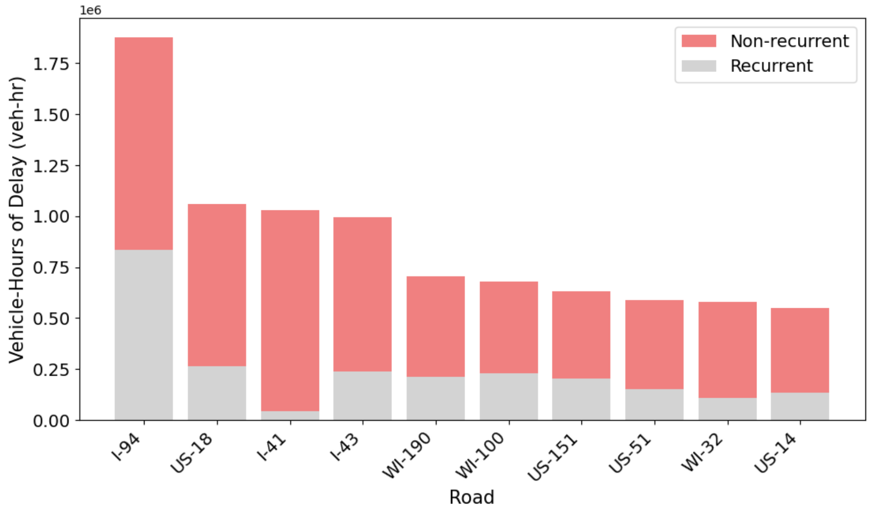

Figure 6-1: Top 10 Corridors by Total Vehicle-Hours of Delay in 2024.

WisDOT Input

WisDOT provided additional corridor suggestions based on operational priorities. These recommendations included locations with known congestion, work-zone activity, and corridor management interest. Some recommendations overlapped with the screened corridors, while others identified corridors that were operationally important but were not among the top statewide corridors by total delay.

Table 6-1 summarizes the corridor sections suggested by WisDOT.

Table 6-1: Corridor Sections Suggested by WisDOT.

Corridor	Suggested Section	County
I-94	Zoo Interchange to Willow Glen Rd	Waukesha
	Zoo Interchange to Marquette Interchange	Milwaukee
I-43	Marquette Interchange to County Line Rd	Milwaukee
I-41	Zoo Interchange to Good Hope Rd	Milwaukee
I-41/I-94	County Line to County Line	Racine
US-18/US-151	County PD to US-18	Dane, Iowa
US-151	Columbus (WIS 73) to Waupun (WI-49)	Dodge
US-51	US 8 to Minocqua (WI-47)	Lincoln, Oneida
	Beltline (US-12) to I-39/90/94 Interchange	Dane
US-53	I-94 to WI-29	Chippewa, Eau Claire
WI-19	Waunakee (WI-113 RAB) to Sun Prairie (US-151)	Dane
WI-125/County CE	I-41 to WI-55	Outagamie
WI-172	County EB (west of I-41) to US-141 (east of I-43)	Brown

Selected Corridors

The final corridor set was defined as the union of the seven screened corridors and the corridors suggested by WisDOT. Because several corridors appeared in both groups, the final set includes 12 unique corridors spanning interstate, principal arterial, and other principal arterial facilities.

Table 6-2 lists the final selected corridors. Together, they cover a range of functional classes, regions, and delay profiles, including corridors with relatively high recurrent delay and corridors with larger non-recurrent delay components.

Table 6-2: Final Selected Corridors.

Corridor	Functional Class	WisDOT Region	Selection Basis
I-41	Interstate	Northeast, Southeast, Southwest	Screening and WisDOT input
I-43	Interstate	Northeast, Southeast, Southwest	Screening and WisDOT input
I-94	Interstate	Northwest, Southeast, Southwest	Screening and WisDOT input
US-18	Principal arterial	Southeast, Southwest	Screening and WisDOT input
US-51	Principal arterial	North Central, Southwest	WisDOT input
US-53	Principal arterial	Northwest, Southwest	WisDOT input
US-151	Principal arterial	Northeast, Southwest	Screening and WisDOT input
WI-172	Principal arterial	Northeast	WisDOT input
WI-19	Other principal arterial	Southwest	WisDOT input
WI-100	Other principal arterial	Southeast	Screening
WI-125	Other principal arterial	Northeast	WisDOT input
WI-190	Other principal arterial	Southeast	Screening

Figure 6-2 shows the selected corridors across Wisconsin. The map was generated using the ROAD field in the TMC lookup table. Accordingly, some corridors may appear segmented where the roadway name changes.

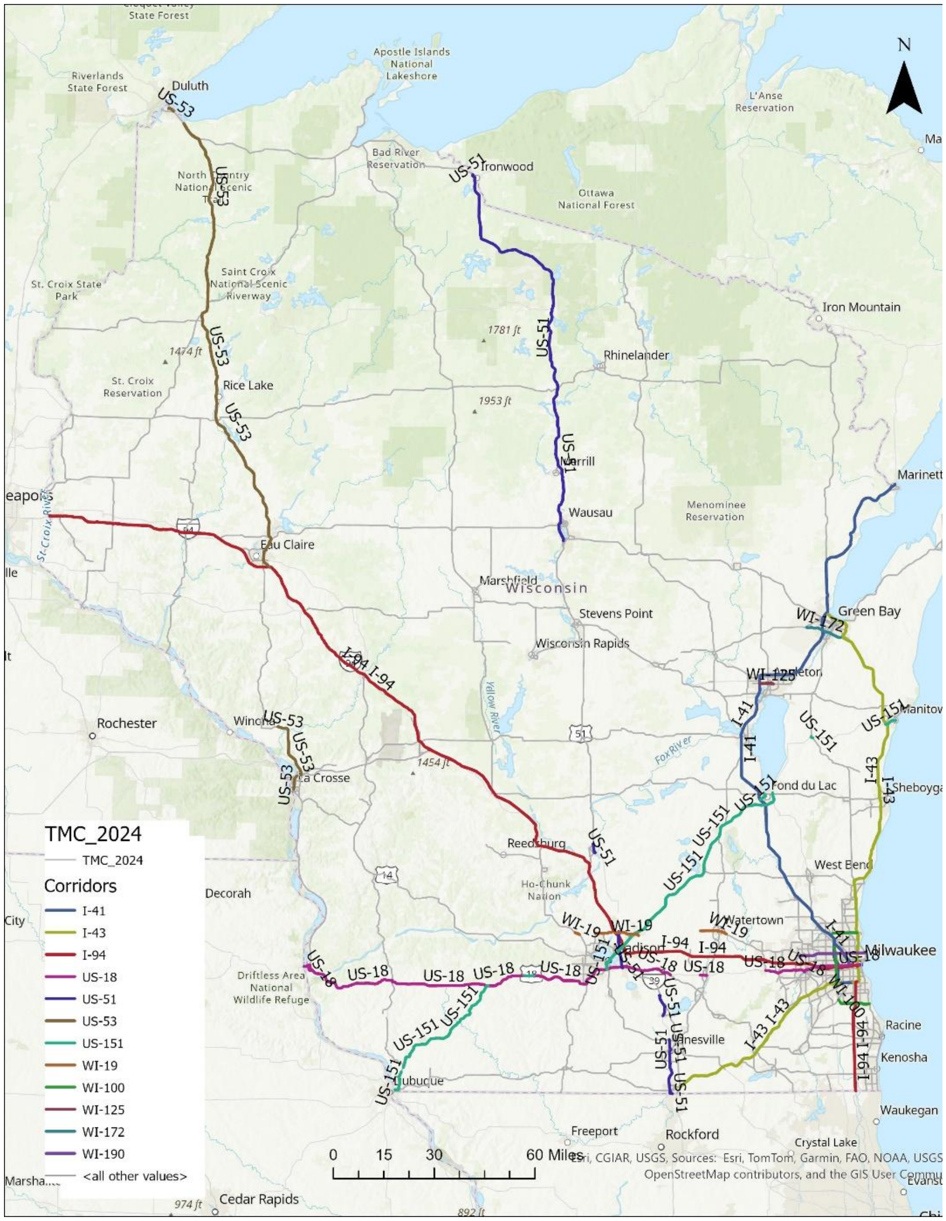

Figure 6-2: Selected Corridors in Wisconsin.

6.2. **Delay Classification and Corridor Diagnostics**

This section presents the delay classification results and corridor diagnostics for the selected corridors. Recurrent and non-recurrent delay shares are first summarized for each corridor to provide a comparative overview of corridor delay composition. The section then examines temporal profiles, spatial distributions, and space-time contour patterns to identify where and when delay is concentrated within each corridor. The spatial diagnostics consider the full corridor extent, while the space-time contour analysis focuses more closely on selected delay hotspot sections.

Recurrent and Non-recurrent Delay Classification

This section summarizes the recurrent and non-recurrent components of corridor delay for the selected corridors. For each corridor, annual total delay was decomposed into recurrent and non-recurrent components using the classification framework. The resulting shares provide a concise summary of whether corridor delay is primarily associated with persistent congestion patterns or with delay above the recurrent baseline. Although the screening step used mutually exclusive corridor groupings, some TMCs are associated with multiple selected corridor definitions because of overlapping road names.

Summary

Overall, across the selected corridors, non-recurrent delay accounts for the larger share of total delay. The results show meaningful differences in delay composition across corridors, with some corridors exhibiting a larger recurrent component than others. These differences suggest that total delay alone is not sufficient to describe corridor performance, motivating the corridor diagnostics presented in the following sections.

Interstate Corridors

Table 6-3 summarizes the recurrent and non-recurrent delay shares for the interstate corridors. Non-recurrent delay accounts for the larger share of total delay across all three interstate corridors. I-41 shows a particularly high non-recurrent share, reaching nearly 90 percent in 2024. I-43 is also dominated by non-recurrent delay, although the recurrent share is somewhat higher in 2019 and 2024 than in 2023. Among the interstate corridors, I-94 has the largest recurrent share, but non-recurrent delay still accounts for more than 60% of total delay in each analysis year. Overall, the interstate corridors are characterized primarily by non-recurrent delay, with the magnitude of the recurrent component varying by corridor.

Table 6-3: Recurrent and Non-Recurrent Delay Shares for Interstate Corridors.

Corridor	Year	Total VHD (veh-hr)	Recurrent Delay Share (%)	Non-Recurrent Delay Share (%)
I-41	2019	1,908,595	15.5	84.5
	2023	1,106,531	16.8	83.2
	2024	1,539,649	10.1	89.9
I-43	2019	1,203,865	27.9	72.1
	2023	1,534,383	8.7	91.3
	2024	1,206,931	23.9	76.1
I-94	2019	3,085,632	29.2	70.8
	2023	1,864,397	27.4	72.6
	2024	2,412,456	37.4	62.6

Principal Arterial Corridors

Table 6-4 summarizes recurrent and non-recurrent delay shares for the ‘principal arterial’ corridors. Similar to the interstate corridors, most ‘principal arterial’ corridors are dominated by non-recurrent delay. US-18, US-51, and US-151 show relatively consistent delay compositions across years, with recurrent delay generally accounting for about one-quarter to one-third of total delay. US-53 and WI-172 stand out for their particularly high non-recurrent shares, with recurrent delay remaining comparatively limited across all years. Overall, the ‘principal arterial’ corridors exhibit substantial variation in total VHD, but their delay composition is generally weighted toward non-recurrent delay.

Table 6-4: Recurrent and Non-Recurrent Delay Shares for Principal Arterial Corridors.

Corridor	Year	Total VHD (veh-hr)	Recurrent Delay Share (%)	Non-Recurrent Delay Share (%)
US-18	2019	2,213,956	26.9	73.1
	2023	1,110,894	20.8	79.2
	2024	1,058,508	24.8	75.2
US-51	2019	852,256	20.9	79.1
	2023	885,040	22.2	77.8
	2024	771,201	22.8	77.2
US-53	2019	165,451	21.2	78.8
	2023	193,215	9.2	90.8
	2024	175,268	7.8	92.2
US-151	2019	1,108,227	20.9	79.1
	2023	893,904	26.4	73.6
	2024	698,016	30.3	69.7
WI-172	2019	45,365	5.3	94.7
	2023	58,260	5.6	94.4
	2024	27,612	10.8	89.2

Other Principal Arterial Corridors

Table 6-5 summarizes recurrent and non-recurrent delay shares for the ‘other principal arterial’ corridors. These corridors also show a greater contribution from non-recurrent delay than from recurrent delay in most cases. WI-19 is notable for its particularly high non-recurrent share in 2024, while WI-100 and WI-190 have larger recurrent components than the other corridors in this group. WI-125 exhibits a relatively high recurrent share in 2023, although non-recurrent delay remains the larger component in 2024. Overall, the ‘other principal arterial’ corridors show corridor-specific variation, but non-recurrent delay remains the dominant component in most cases.

Table 6-5: Recurrent and Non-Recurrent Delay Shares for Other Principal Arterial Corridors.

Corridor	Year	Total VHD (veh-hr)	Recurrent Delay Share (%)	Non-Recurrent Delay Share (%)
WI-19	2019	134,004	22.9	77.1
	2023	138,510	25.3	74.7
	2024	136,839	5.2	94.8
WI-100	2019	1,036,333	24.4	75.6
	2023	876,638	32.2	67.8
	2024	677,709	33.9	66.1
WI-125	2019	No data	No data	No data
	2023	141,700	36.4	63.6
	2024	107,654	25.5	74.5
WI-190	2019	1,070,804	32.1	67.9
	2023	704,040	28.6	71.4
	2024	706,765	29.9	70.1

Temporal Profiles of Corridor Delay

This section presents temporal diagnostics of corridor delay using monthly recurrent and non-recurrent delay amounts and hour-of-day delay profiles. The monthly results show how delay magnitude and composition vary over the year, while the hourly profiles indicate when delay is most concentrated within the day. Together, these diagnostics provide a concise view of corridor-level temporal delay patterns.

Summary

Overall, the monthly results show that delay is generally higher from late spring through summer or early fall, depending on the corridor. The hour-of-day profiles indicate that delay is concentrated primarily during daytime periods, with most corridors showing a stronger afternoon peak and, in some cases, a smaller morning peak.

Interstate: I-41

Monthly delay exhibits a sustained increase from late spring through summer, with the monthly total peaking in June 2019, October 2023, and June 2024. Across all three years, non-recurrent delay accounts for the dominant share of monthly delay, while the recurrent component remains comparatively small, although it is more identifiable in several months.

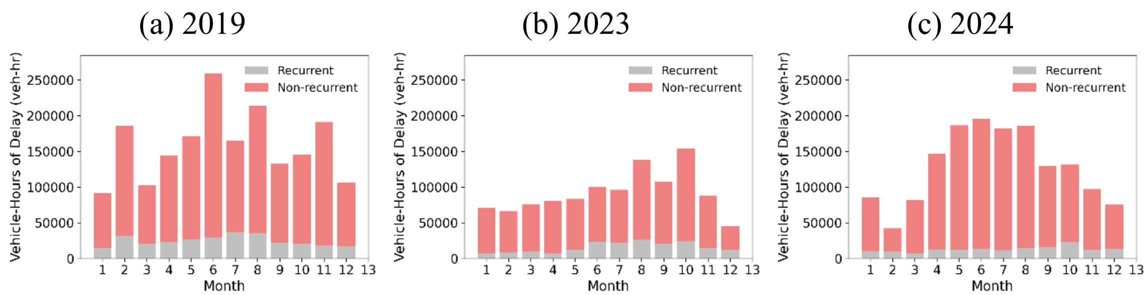

Figure 6-3: Monthly Recurrent and Non-Recurrent Delay for I-41.

The hour-of-day profile shows that delay is concentrated primarily during the afternoon period, with the highest levels occurring in the late afternoon (3–5 PM). A smaller secondary peak is also visible in the morning, while overnight delay remains limited.

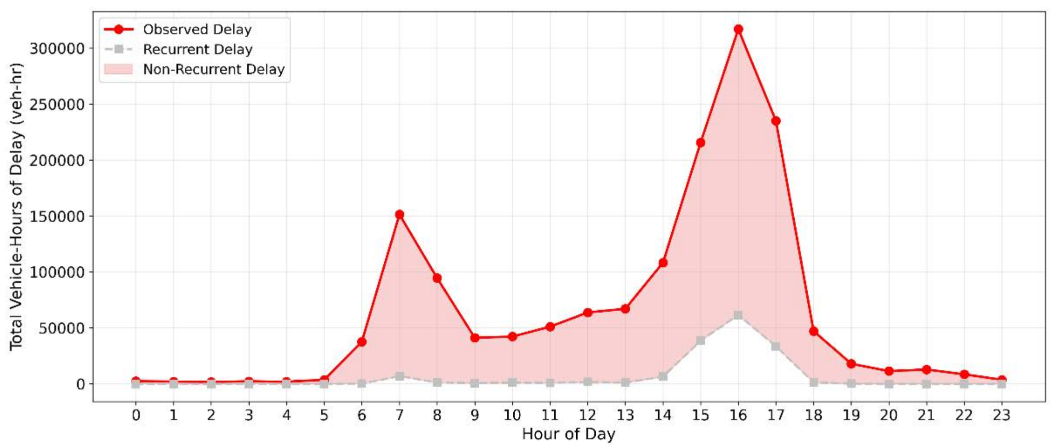

Figure 6-4: Hour-of-Day Delay Profile for I-41 in 2024.

Interstate: I-43

Monthly delay is generally highest from late spring through fall, with the largest totals occurring in October 2019 and 2023 and in June 2024. Non-recurrent delay accounts for the dominant share in all three years, although the recurrent component is more noticeable in several months of 2019 and in April–May 2024 than in 2023.

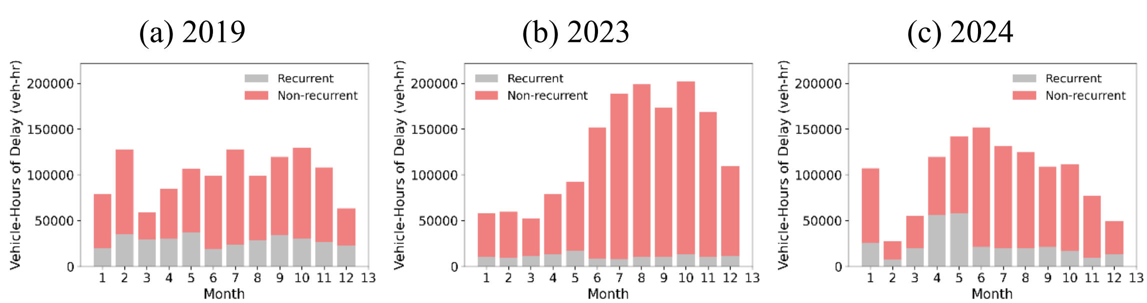

Figure 6-5: Monthly Recurrent and Non-Recurrent Delay for I-43.

The hour-of-day profile shows two distinct peaks, with a smaller morning peak around 7-8 AM and a stronger afternoon peak centered in the late afternoon, around 3–5 PM. Delay remains limited during overnight hours and drops sharply after the afternoon peak.

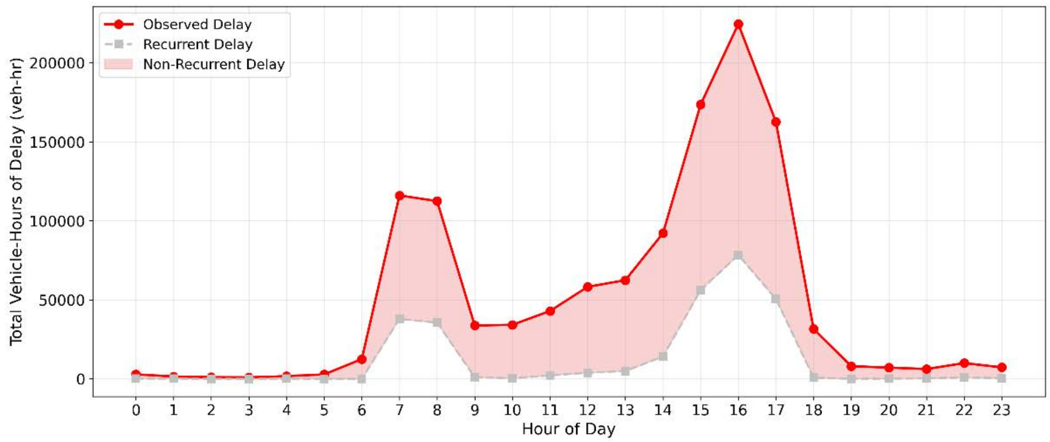

Figure 6-6: Hour-of-Day Delay Profile for I-43 in 2024.

Interstate: I-94

Monthly delay is highest from late spring through early fall across all three years, with the monthly total peaking in June in both 2019 and 2023 and in May 2024. Compared with I-41 and I-43, I-94 shows a larger recurrent component throughout the year, although non-recurrent delay still accounts for a substantial share of the monthly total in each year.

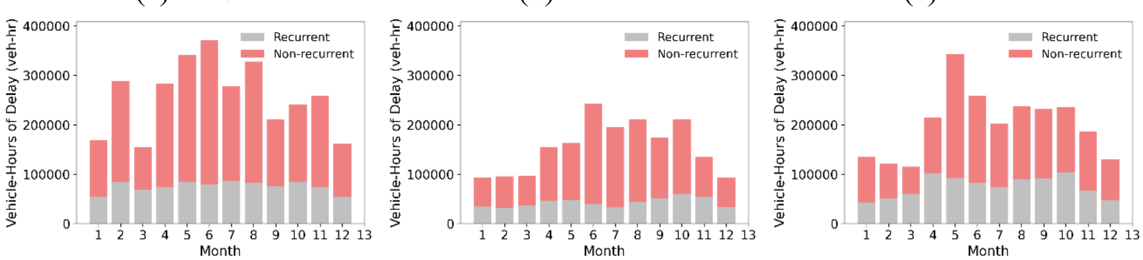

Figure 6-7: Monthly Recurrent and Non-Recurrent Delay for I-94.

The hour-of-day profile shows a distinct morning peak around 7–8 AM and a stronger afternoon peak centered in the late afternoon (3–5 PM). Delay remains elevated through much of the daytime period between these peaks, while overnight levels remain low.

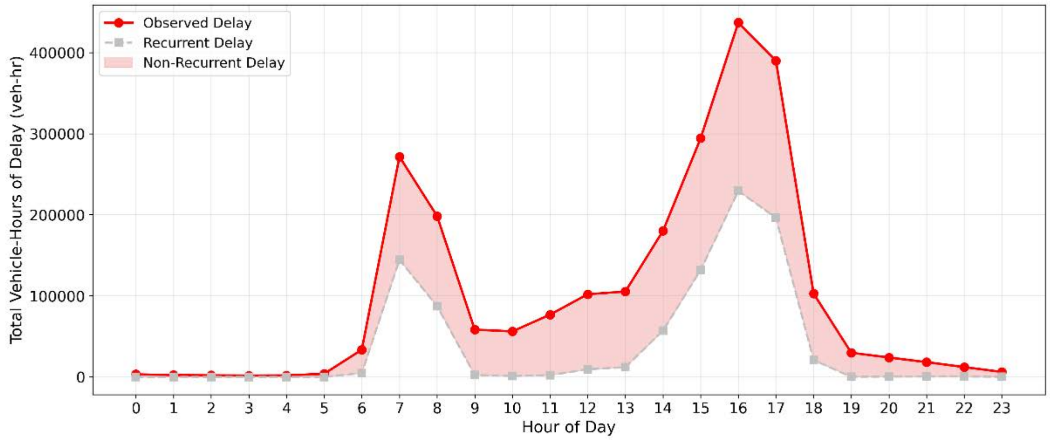

Figure 6-8: Hour-of-Day Delay Profile for I-94 in 2024.

Principal Arterials: US-18

Monthly delay is highest in late spring and early summer in both 2023 and 2024, while 2019 shows elevated delay over a broader range of months extending into fall. Unlike the interstate corridors, this arterial corridor shows the abnormal NPMRDS coverage pattern during August–November more clearly in the 2024 monthly results. In all three years, non-recurrent delay accounts for the larger share of monthly delay, while the recurrent component remains comparatively stable.

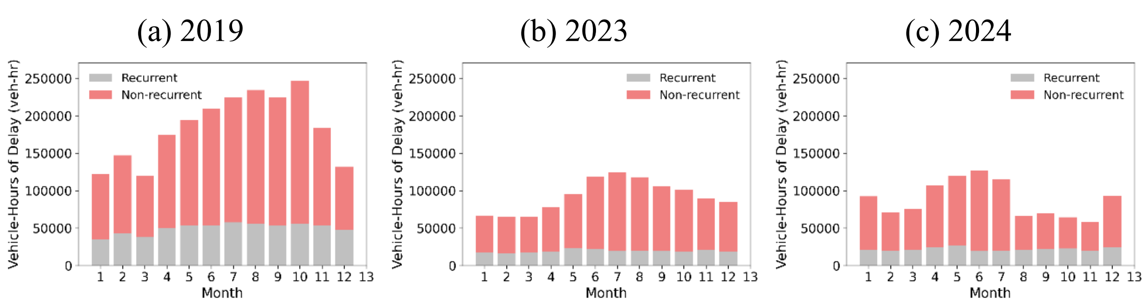

Figure 6-9: Monthly Recurrent and Non-Recurrent Delay for US-18.

The hour-of-day profile shows a morning peak around 7–8 AM, followed by elevated delay through the midday and afternoon periods. The highest delay occurs in the late afternoon (3–5 PM), while overnight delay is limited.

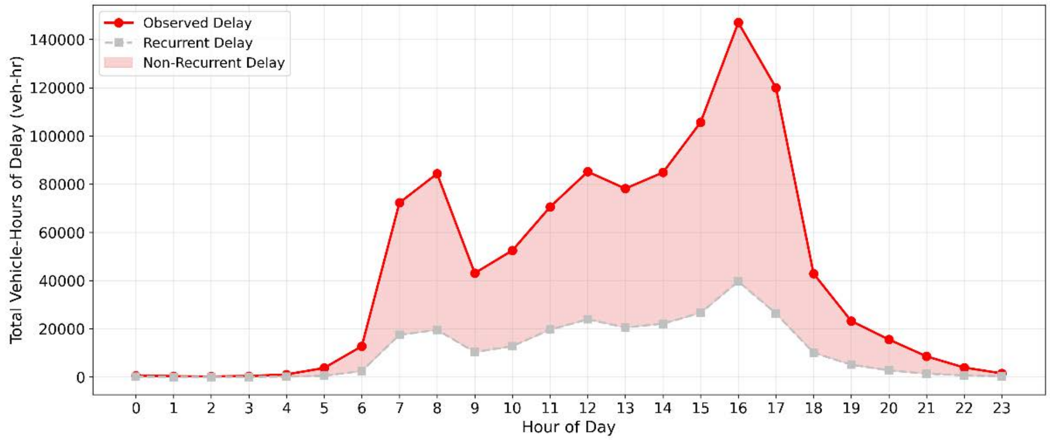

Figure 6-10: Hour-of-Day Delay Profile for US-18 in 2024.

Principal Arterials: US-51

Monthly delay is generally highest from late spring through early fall, with the monthly total peaking in July 2019, May 2023, and July 2024. Across all three years, non-recurrent delay accounts for the dominant share of monthly delay, while the recurrent component remains modest and stable.

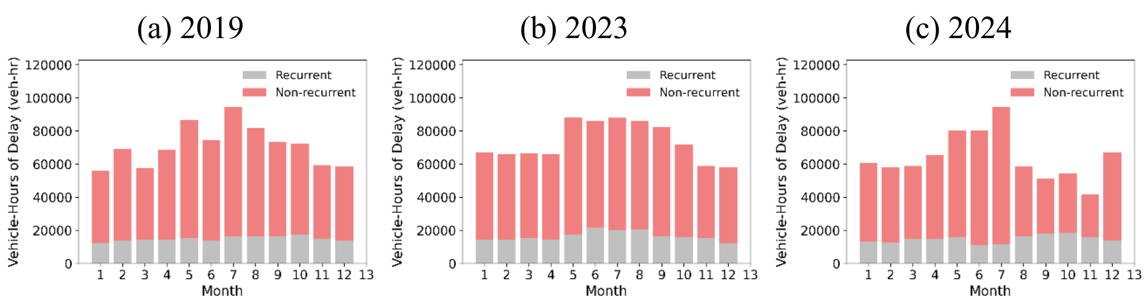

Figure 6-11: Monthly Recurrent and Non-Recurrent Delay for US-51.

The hour-of-day profile indicates that delay begins to increase in the early morning, remains elevated throughout the daytime period, and reaches its highest level in the late afternoon. Overnight delay remains low.

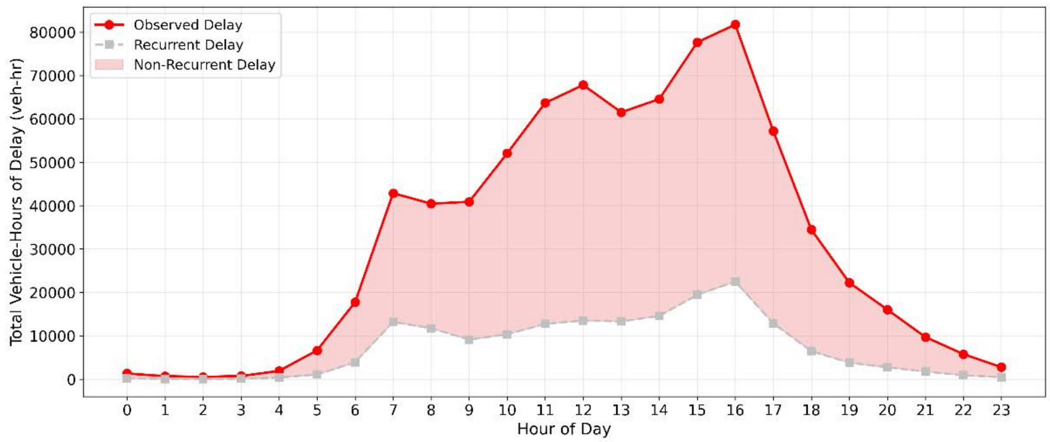

Figure 6-12: Hour-of-Day Delay Profile for US-51 in 2024.

Principal Arterials: US-53

Monthly delay is generally higher from late spring through summer, although the monthly total peaks in February 2019, June 2023, and June–July 2024. In each year, non-recurrent delay accounts for nearly all monthly delay, while the recurrent component remains minimal throughout the year.

(a) 2019 (b) 2023 (c) 2024

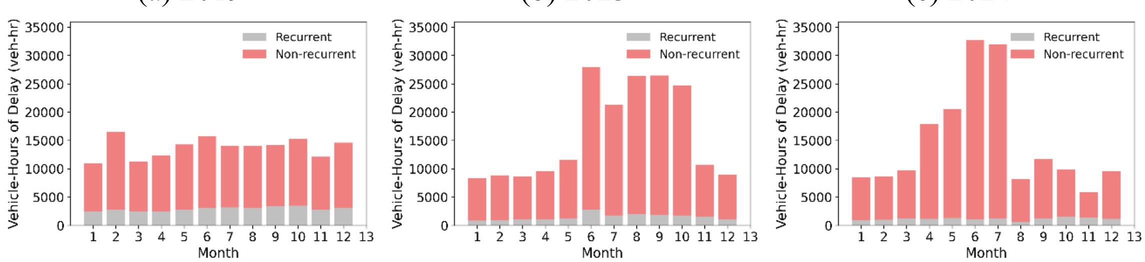

Figure 6-13: Monthly Recurrent and Non-Recurrent Delay for US-53.

The hour-of-day profile shows that delay begins to increase in the early morning, remains elevated throughout the daytime period, and reaches its highest level in the late afternoon. The recurrent component remains small throughout the day, while overnight delay remains low.

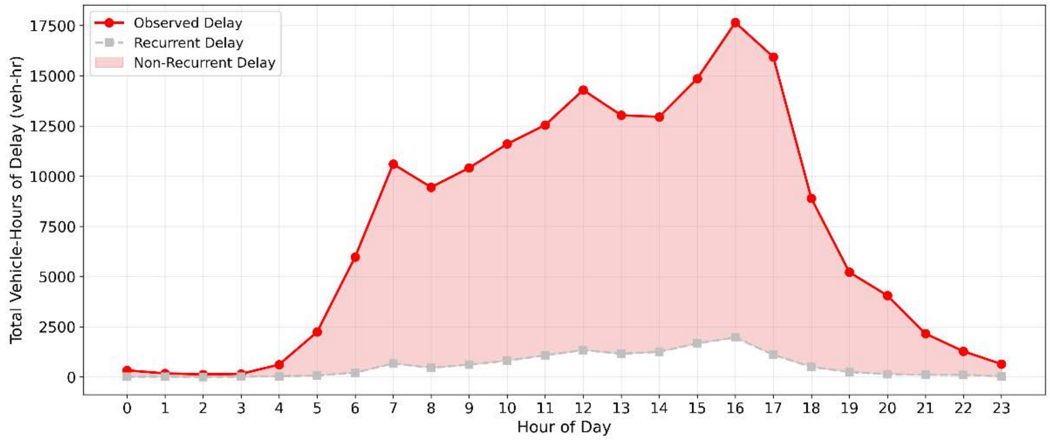

Figure 6-14: Hour-of-Day Delay Profile for US-53 in 2024.

Principal Arterials: US-151

Monthly delay is elevated from late spring through early fall in 2019 and 2023, while 2024 shows a declining pattern after early spring. Compared with US-53, US-151 shows a larger recurrent component, although non-recurrent delay remains the larger share in most months.

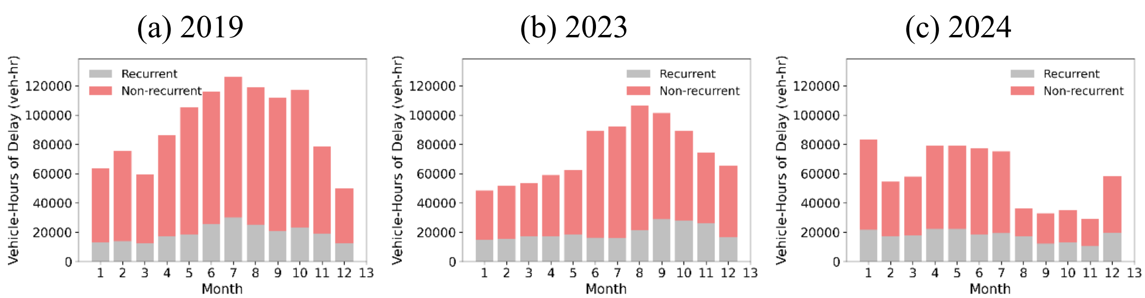

Figure 6-15: Monthly Recurrent and Non-Recurrent Delay for US-151.

The hour-of-day profile shows a morning peak around 7–8 AM and a stronger afternoon peak. Delay remains elevated through much of the daytime period, with a noticeable recurrent component from late morning through the afternoon, while overnight delay remains limited.

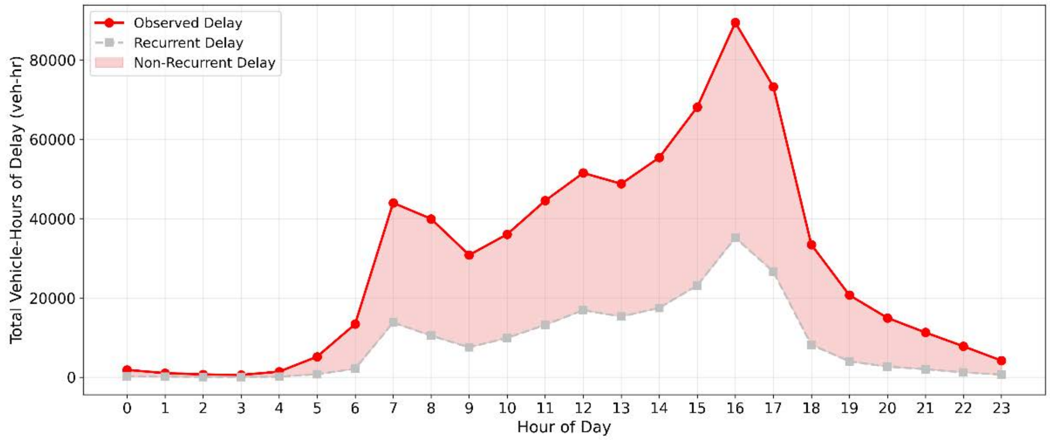

Figure 6-16: Hour-of-Day Delay Profile for US-151 in 2024.

Principal Arterials: WI-172

Monthly delay remains relatively low in magnitude across all three years, with no pronounced seasonal pattern. Non-recurrent delay accounts for nearly all monthly delay in most months, while the recurrent component is absent or minimal for much of the year, becoming more visible only in September–October 2024.

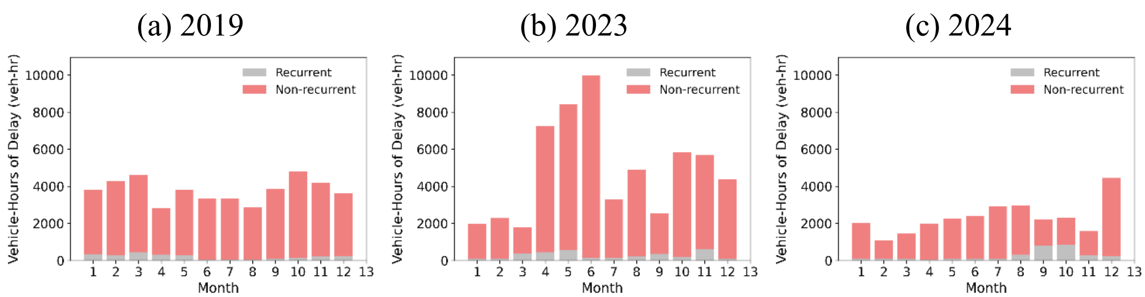

Figure 6-17: Monthly Recurrent and Non-Recurrent Delay for WI-172.

The hour-of-day profile indicates that delay is concentrated primarily in the afternoon, with the highest level occurring in the late afternoon (3–5 PM). A smaller rise around 10 AM is also visible, while early-morning and overnight delay remain limited.

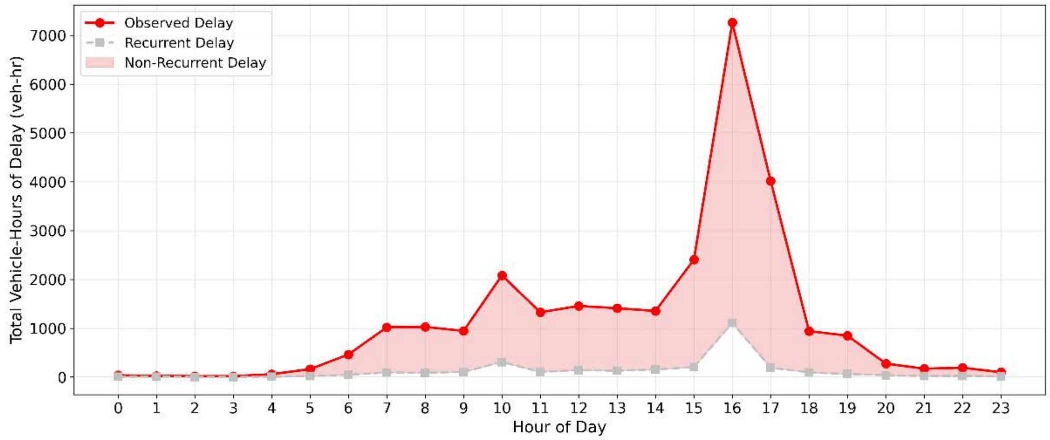

Figure 6-18: Hour-of-Day Delay Profile for WI-172 in 2024.

Other Principal Arterials: WI-19

Monthly delay is elevated in spring, with the highest monthly totals occurring in May. In each year, non-recurrent delay accounts for nearly all monthly delay, while the recurrent component is absent or minimal in many months, particularly in 2024.

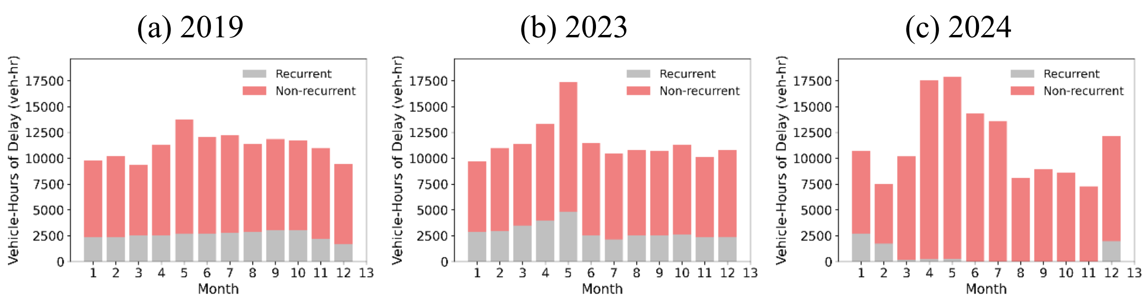

Figure 6-19: Monthly Recurrent and Non-Recurrent Delay for WI-19.

The hour-of-day profile shows that delay is concentrated primarily during the afternoon, with the highest level occurring in the late afternoon. A smaller morning peak is also visible, while overnight delay remains limited.

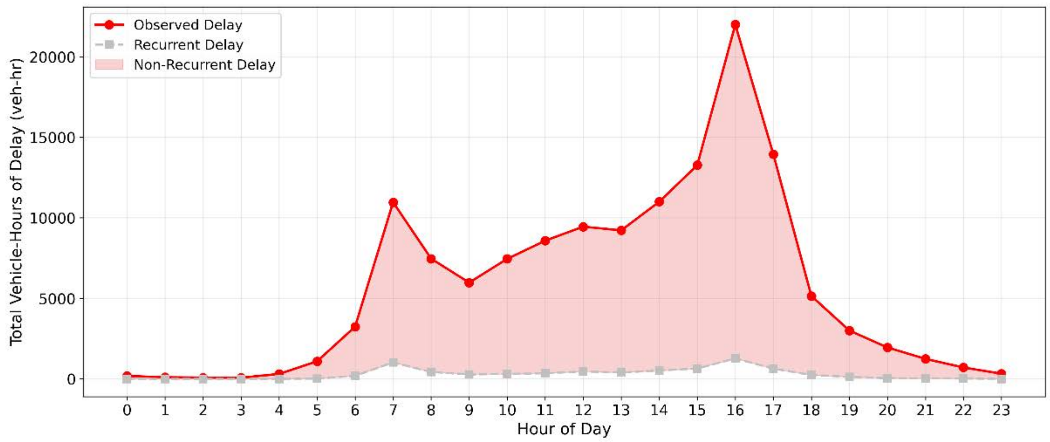

Figure 6-20: Hour-of-Day Delay Profile for WI-19 in 2024.

Other Principal Arterials: WI-100

Monthly delay is elevated from spring through summer in all three years. The recurrent component is more visible than in WI-19, although non-recurrent delay remains the dominant share in most months.

(a) 2019 (b) 2023 (c) 2024

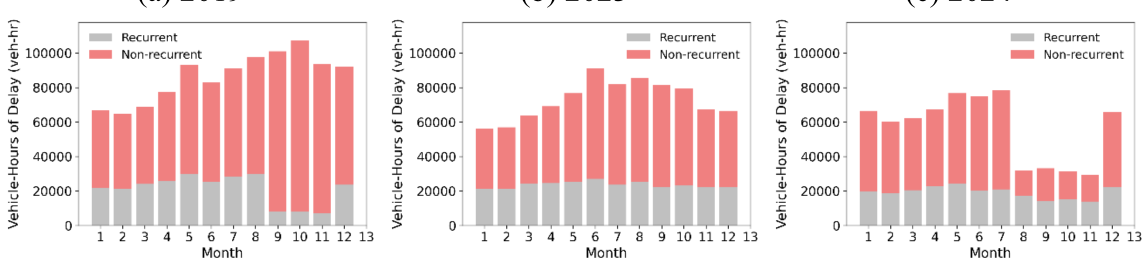

Figure 6-21: Monthly Recurrent and Non-Recurrent Delay for WI-100.

The hour-of-day profile indicates that delay begins to increase in the early morning, rises sharply around 7 AM, and remains elevated through the daytime period. A noticeable midday peak is observed around 12 PM, before delay reaches its highest level in the late afternoon. The recurrent component is clearly visible from late morning through the afternoon, and overnight delay remains low.

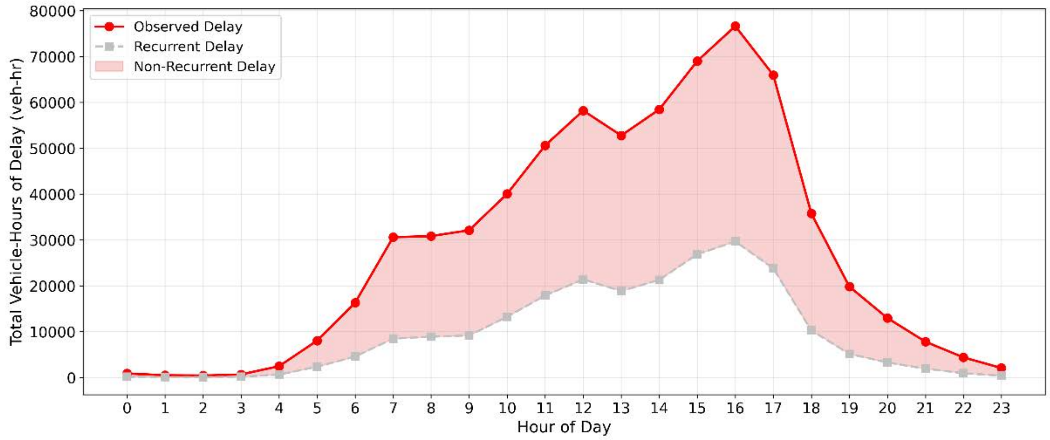

Figure 6-22: Hour-of-Day Delay Profile for WI-100 in 2024.

Other Principal Arterials: WI-125

Monthly delay is highest in spring and early summer in both 2023 and 2024. No 2019 data are available for WI-125. The recurrent component is clearly visible from January through May, while in 2024 the summer months are dominated almost entirely by non-recurrent delay.

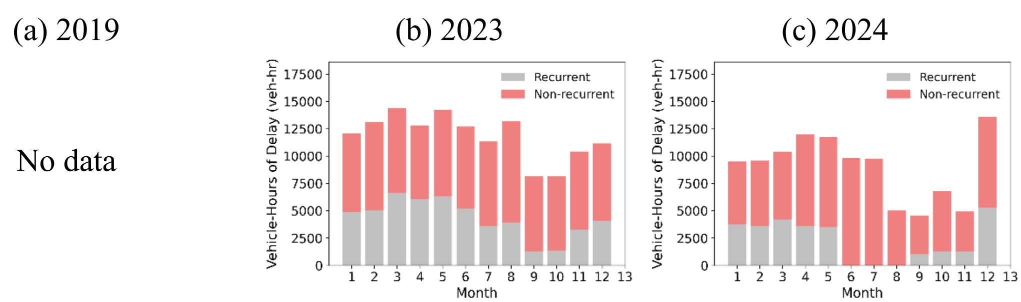

Figure 6-23: Monthly Recurrent and Non-Recurrent Delay for WI-125.

The hour-of-day profile indicates that delay rises sharply from late morning into midday, with a broad elevated period extending through the afternoon. A midday peak around noon is nearly as pronounced as the late-afternoon peak, while overnight delay remains low.

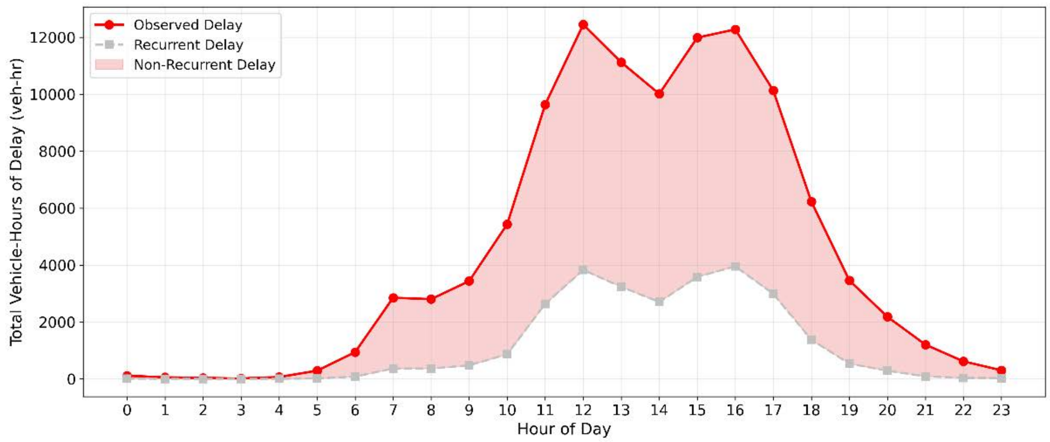

Figure 6-24: Hour-of-Day Delay Profile for WI-125 in 2024.

Other Principal Arterials: WI-190

Monthly delay is elevated over a broad range of months. In 2019 and 2023, delay remains sustained from spring through fall, while in 2024 it peaks in late spring and declines thereafter. The recurrent component is more visible than in WI-19, although non-recurrent delay remains the dominant share in most months.

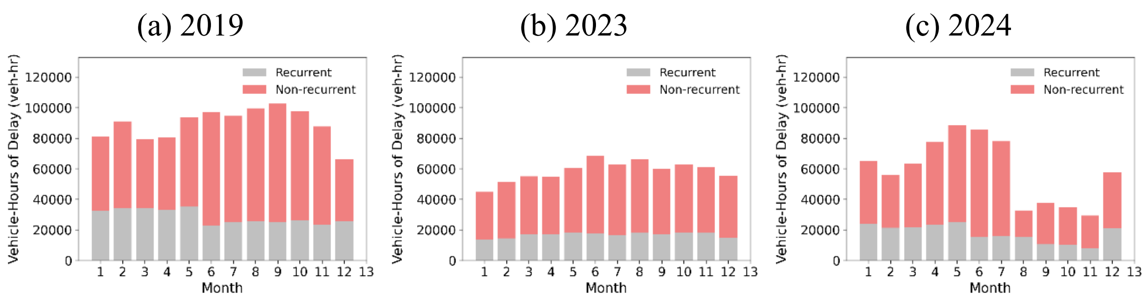

Figure 6-25: Monthly Recurrent and Non-Recurrent Delay for WI-190.

The hour-of-day profile shows a distinct morning peak, followed by a broad elevated daytime period with an additional midday rise. Delay reaches its highest level in the late afternoon, while overnight delay remains limited.

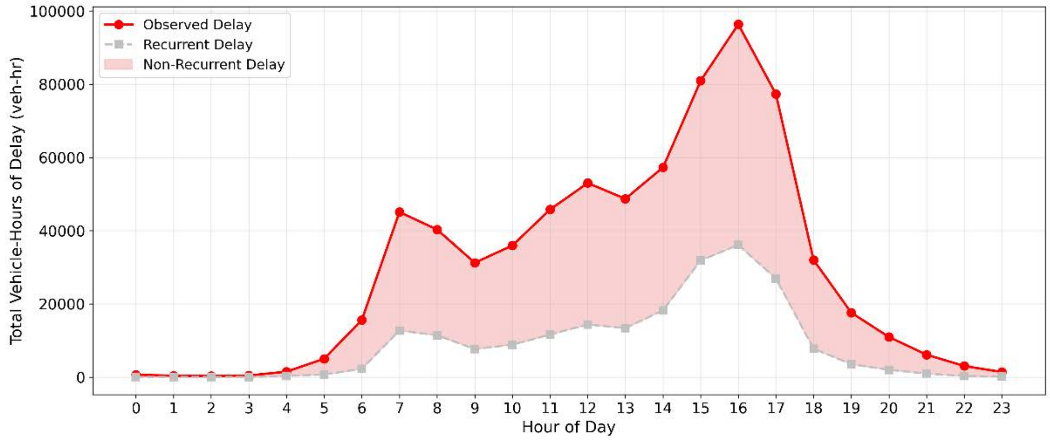

Figure 6-26: Hour-of-Day Delay Profile for WI-190 in 2024.

Spatial Distribution of Delay Along Corridors

This section presents spatial diagnostics of corridor delay using corridor-level total VHD maps and direction-specific profiles of recurrent and non-recurrent delay. The maps show how total delay is distributed across selected corridors statewide, while the direction-specific profiles indicate where recurrent and non-recurrent delay are concentrated within each corridor by travel direction. These diagnostics identify how delay is distributed within each corridor direction and locate major delay hotspot sections or segments. Accordingly, different color scales were applied to each corridor-direction map to make localized hotspots more visible, and direct comparison of color intensity across corridors is not recommended.

For the direction-specific profiles, delay was plotted by the road_order column using the TMC lookup data, including MPA information where available. When multiple TMCs shared the same road order, the TMC with the largest delay was selected as the representative segment. TMCs without road order information were excluded from the profiles. While these profiles provide useful TMC-level insights, they should be interpreted as supplemental to the maps because the road_order field may not fully reflect the exact spatial sequence or geographic continuity of the corridor.

Summary

Overall, the spatial diagnostics show that corridor delay is highly localized rather than evenly distributed along each corridor. For the interstate corridors, the largest delay concentrations generally occur near the Milwaukee area. For the 'principal arterials' and 'other principal arterials', hotspots are more corridor-specific, including Madison-area segments on US-18, US-51, and US-151; Spooner to Haugen on US-53; Watertown and Sun Prairie on WI-19; and interchange-related hotspots on WI-100 and WI-125. Across most corridors, non-recurrent delay accounts for the larger share of TMC-level delay, but several urban or interchange-area hotspots also show a noticeable recurrent component.

Table 6-6 summarizes the identified delay hotspots, integrating results from the spatial diagnostics with the corridor sections suggested by WisDOT.

Table 6-6: Summary of Major Delay Hotspots and WisDOT-Suggested Sections.

Corridor	Identified Hotspot and WisDOT-Suggested Section	Typical Temporal Pattern
I-41	• Zoo IC to Good Hope Rd • County Line to County Line • Appleton-area segments	Morning and afternoon peaks
I-43	• Marquette IC to County Line Rd	Morning and afternoon peaks
I-94	• Zoo IC to Willow Glen Rd • Zoo IC to Marquette IC	Morning and afternoon peaks
US-18	• County PD to US-18 • Milwaukee-area segments • Prairie du Chien-area segments	Morning and afternoon peaks
US-51	• US-8 to Minocqua (WI-47) • Beltline (US-12) to I-39/90/94 IC • Janesville-area segments	Afternoon-dominant daytime
US-53	• I-94 to WI-29 • Spooner-to-Haugen segments • Superior-area segments	Afternoon-dominant daytime
US-151	• Columbus (WI-73) to Waupun (WI-49) • Madison-area segments • Manitowoc-area segments	Morning and afternoon peaks
WI-172	• County EB (west of I-41) to US-141 (east of I-43) • WI-54 to I-41	Afternoon-dominant daytime
WI-19	• Waunakee (WI-113 RAB) to Sun Prairie (US-151) • Watertown-area segments	Morning and afternoon peaks
WI-100	• W Layton Ave to W Capitol Dr • WI-50 intersection area • W North Ave intersection area	Afternoon-dominant daytime
WI-125	• I-41 to WI-55	Afternoon-dominant daytime
WI-190	• I-41 to WI-32	Morning and afternoon peaks

Interstate: I-41

Delay is concentrated most strongly in the Milwaukee-area segments of I-41 in both directions, while much of the remaining corridor shows comparatively lower total delay. Outside the Milwaukee area, smaller localized higher-delay segments appear near the Appleton area in the southbound direction.

(a) Eastbound and Southbound (b) Westbound and Northbound

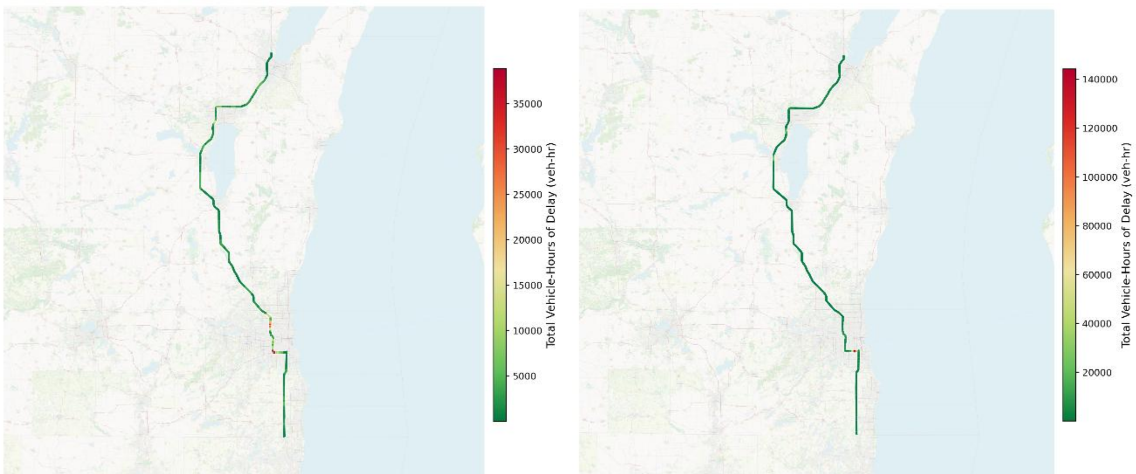

Figure 6-27: Spatial Distribution of Delay Across I-41 in 2024.

For I-41, delay is unevenly distributed across directions and segments, with the largest concentrations observed in the Milwaukee-area segments, particularly in the westbound direction. Non-recurrent delay accounts for most of the TMC-level total across directions, while the southbound profile also shows several segments with a substantial recurrent component, particularly near the Milwaukee area.

(a) Eastbound (b) Westbound

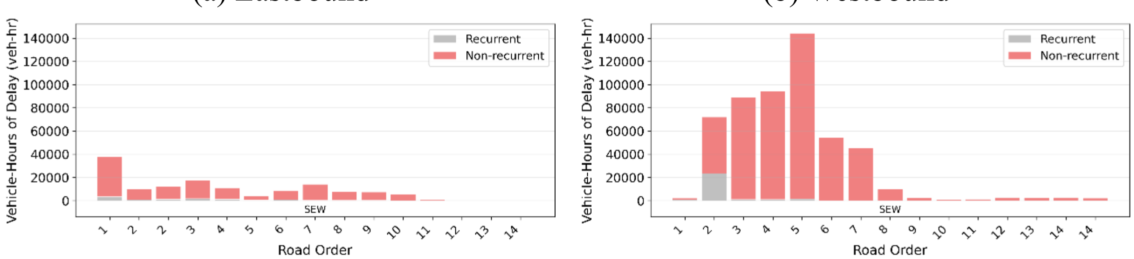

(c) Southbound (d) Northbound

Figure 6-28: Direction-Specific Recurrent and Non-Recurrent Delay for I-41 in 2024.

Interstate: I-43

Both directions show a localized delay concentration near the Milwaukee area, while the rest of the corridor has low total delay.

(a) Southbound (b) Northbound

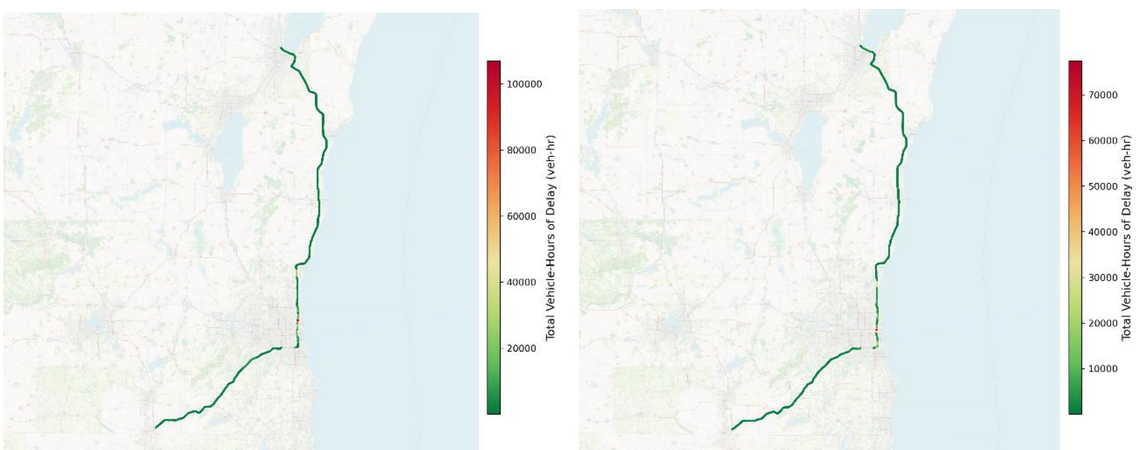

Figure 6-29: Spatial Distribution of Delay Across I-43 in 2024.

In the Milwaukee-area hotspots, the recurrent share is more pronounced in the northbound direction, whereas southbound delay is more strongly dominated by non-recurrent delay.

(a) Southbound (b) Northbound

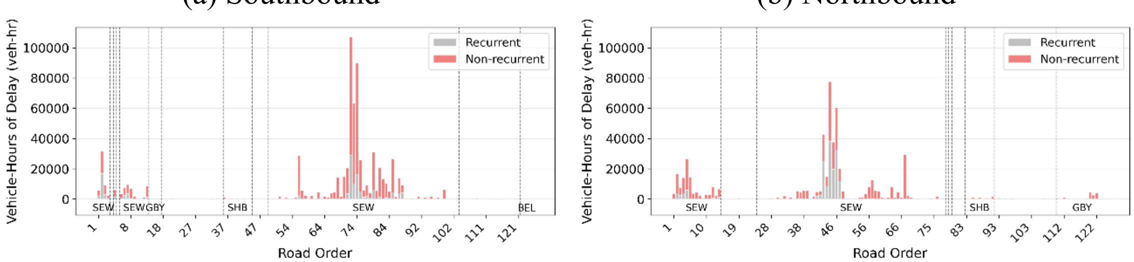

Figure 6-30: Direction-Specific Recurrent and Non-Recurrent Delay for I-43 in 2024.

Interstate: I-94

Delay is concentrated most strongly in the Milwaukee-area segments across travel directions, while much of the remaining corridor shows lower total delay.

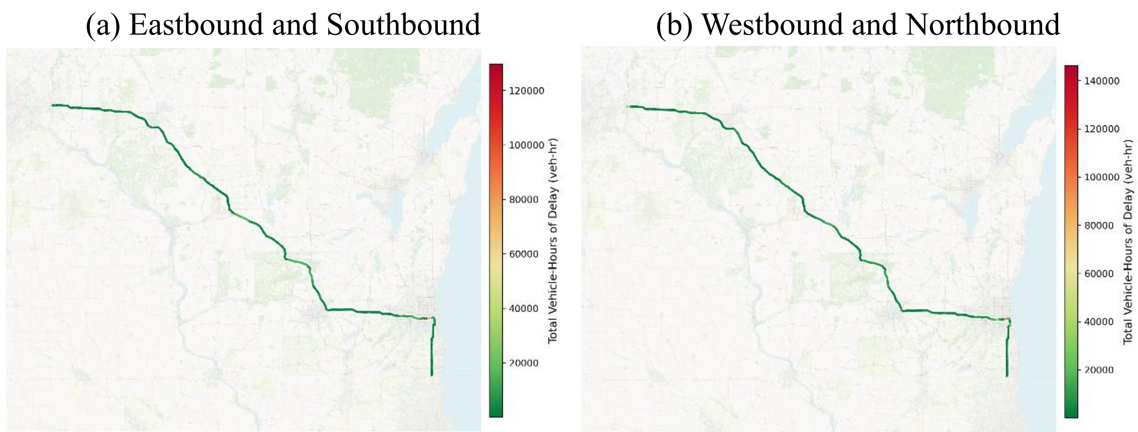

Figure 6-31: Spatial Distribution of Delay Across I-94 in 2024.

The direction-specific profiles also show a few localized hotspots outside Milwaukee, but the largest concentrations occur near Milwaukee and are composed of both recurrent and non-recurrent delay.

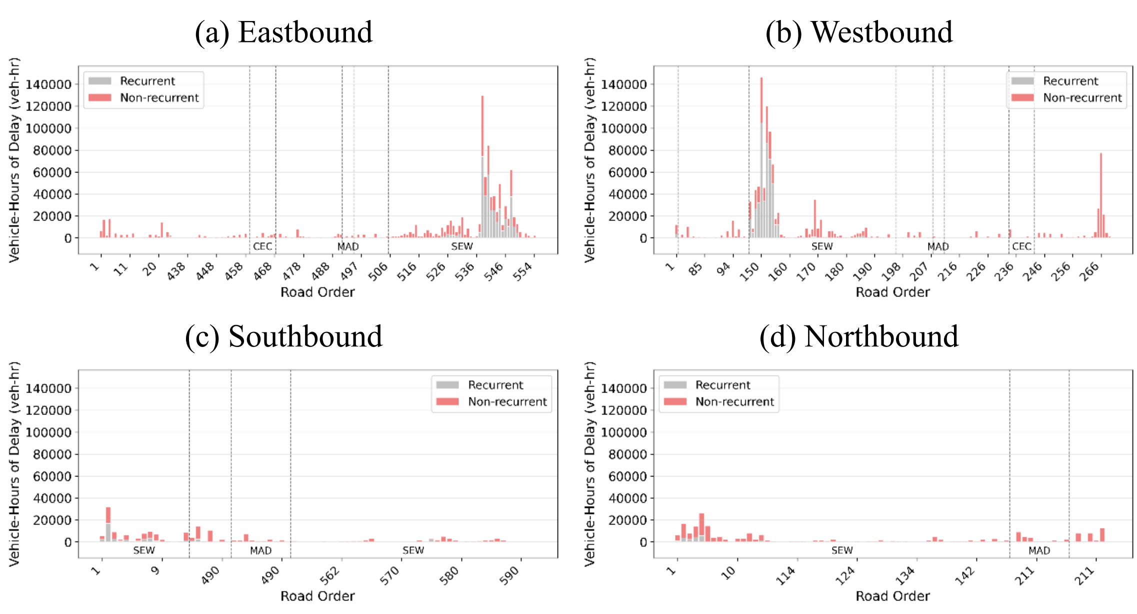

Figure 6-32: Direction-Specific Recurrent and Non-Recurrent Delay for I-94 in 2024.

Principal Arterials: US-18

Delay is concentrated mainly near the Milwaukee and Madison areas, with smaller localized delay concentrations also visible near Prairie du Chien.

(a) Eastbound (b) Westbound

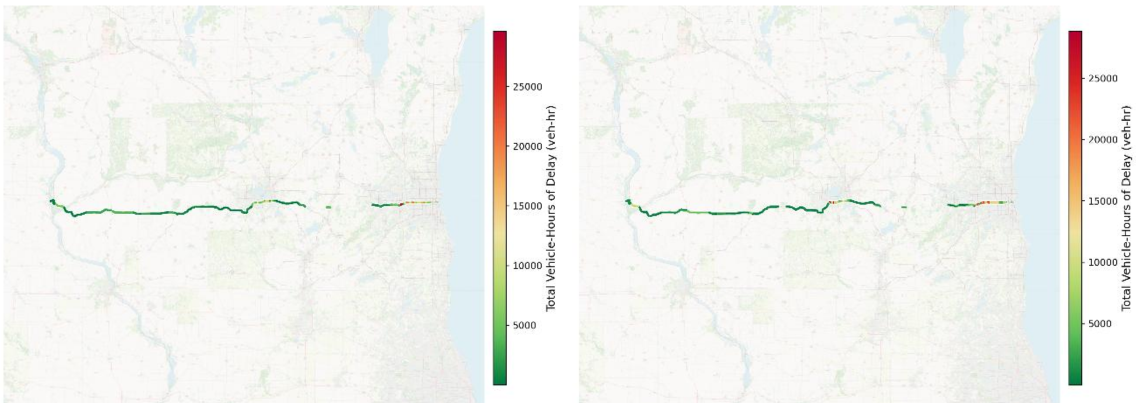

Figure 6-33: Spatial Distribution of Delay Across US-18 in 2024.

The direction-specific profiles indicate that the westbound delay near Madison is more spatially-concentrated than in the Milwaukee-area. Recurrent delay is noticeable at several major hotspot segments, but non-recurrent delay remains the dominant component overall.

(a) Eastbound (b) Westbound

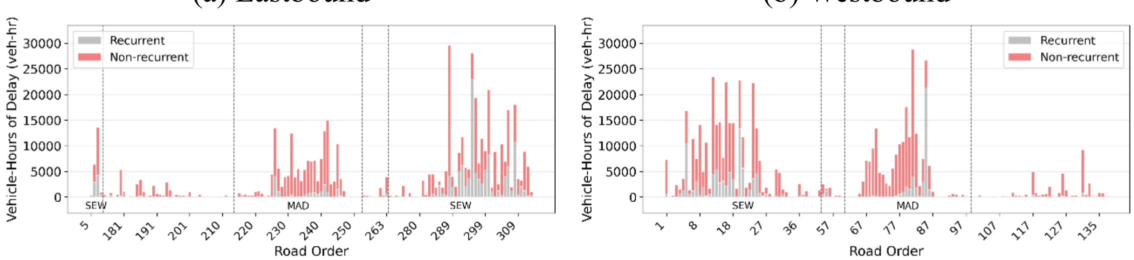

Figure 6-34: Direction-Specific Recurrent and Non-Recurrent Delay for US-18 in 2024.

Principal Arterials: US-51

Delay is concentrated at several localized areas rather than being continuously distributed along the corridor. In the northbound direction, higher-delay segments appear near Janesville, Madison, and Minocqua, while the southbound direction shows localized hotspots near Madison and Minocqua.

(a) Southbound (b) Northbound

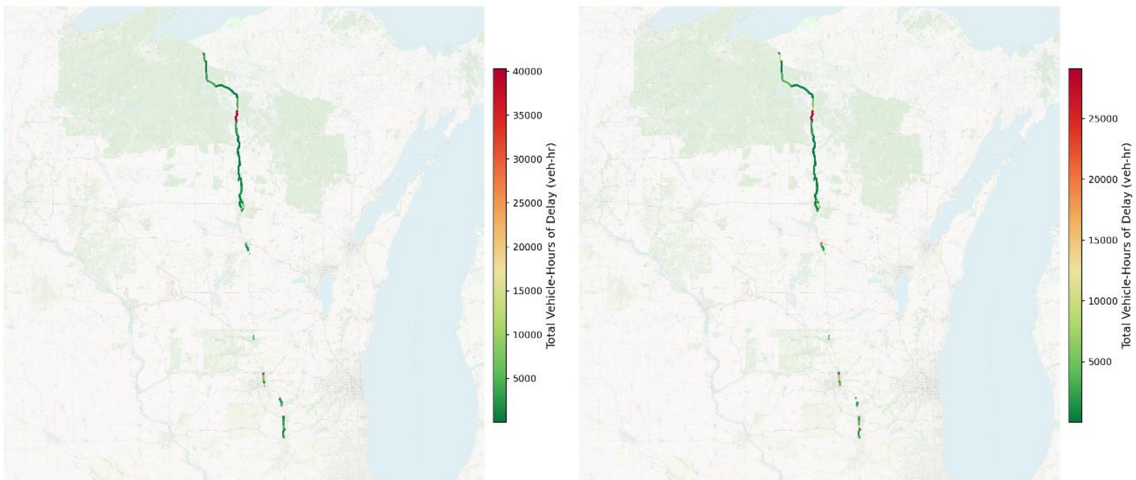

Figure 6-35: Spatial Distribution of Delay Across US-51 in 2024.

The direction-specific profiles indicate that the Madison-area hotspots include a substantial recurrent component, whereas delay at the other locations is dominated mainly by non-recurrent delay.

(a) Southbound (b) Northbound

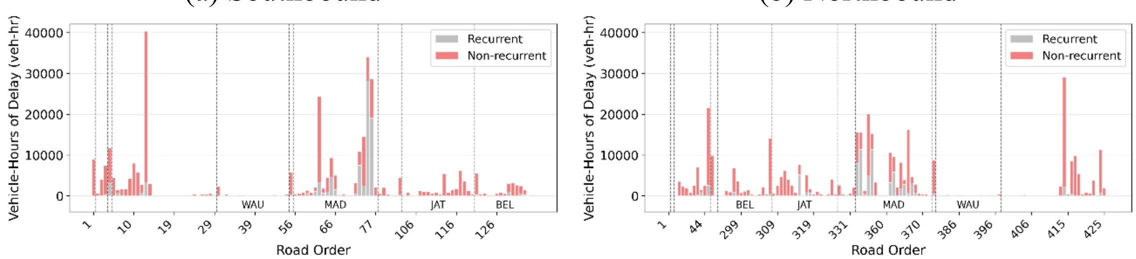

Figure 6-36: Direction-Specific Recurrent and Non-Recurrent Delay for US-51 in 2024.

Principal Arterials: US-53

Delay is concentrated at a few localized segments, with visible hotspots near Spooner and Superior. The Spooner-to-Haugen segments show a larger delay concentration, while the Superior-area delay is more limited.

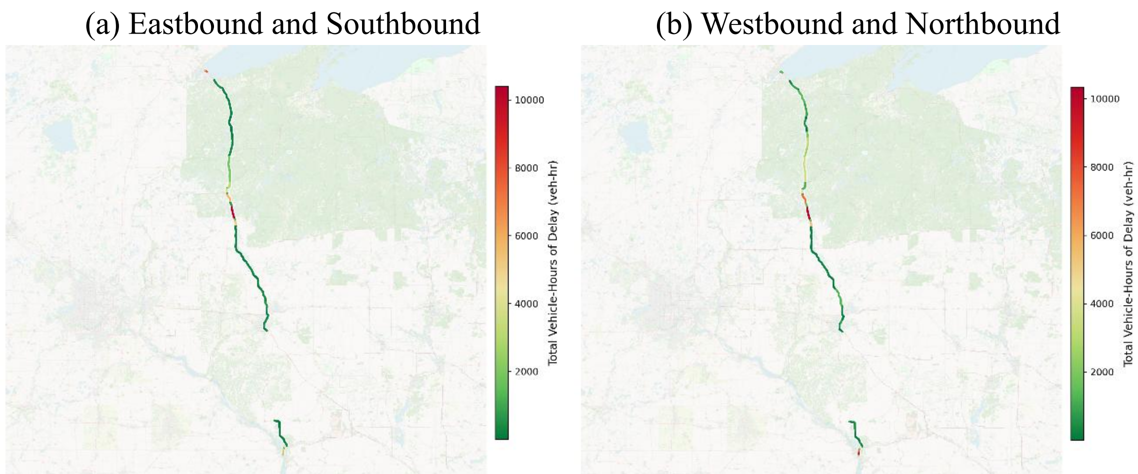

Figure 6-37: Spatial Distribution of Delay Across US-53 in 2024.

In the direction-specific profiles, the northbound and southbound directions account for most of the TMC-level delay. Across these hotspots, delay is dominated by the non-recurrent component, with only a limited recurrent share.

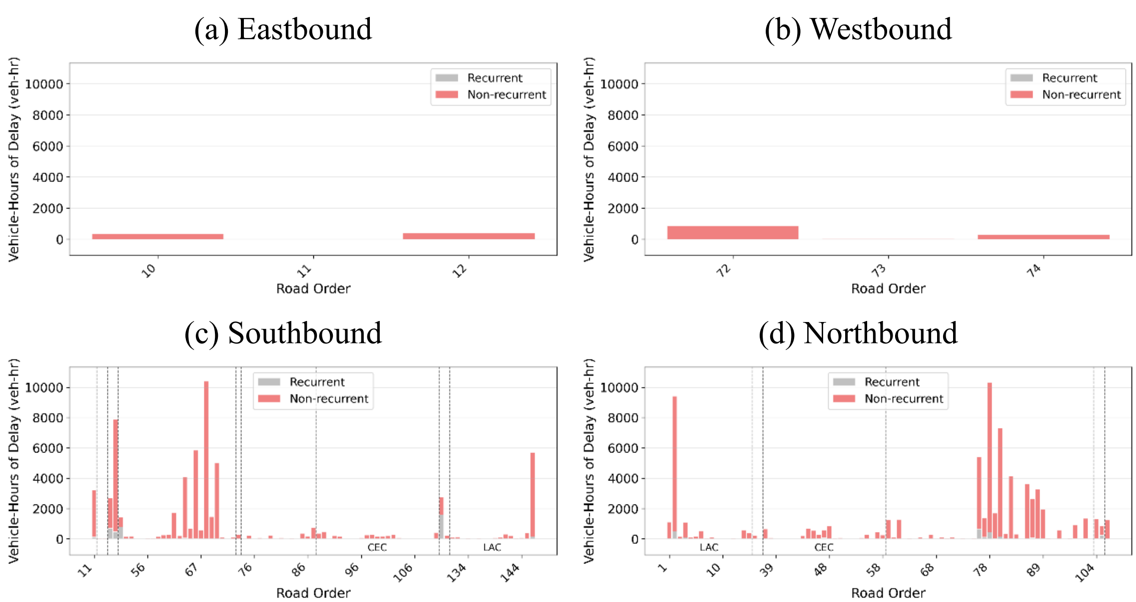

Figure 6-38: Direction-Specific Recurrent and Non-Recurrent Delay for US-53 in 2024.

Principal Arterials: US-151

Delay is concentrated primarily near the Madison area, with additional localized delay concentrations near the eastern end of the corridor around Manitowoc.

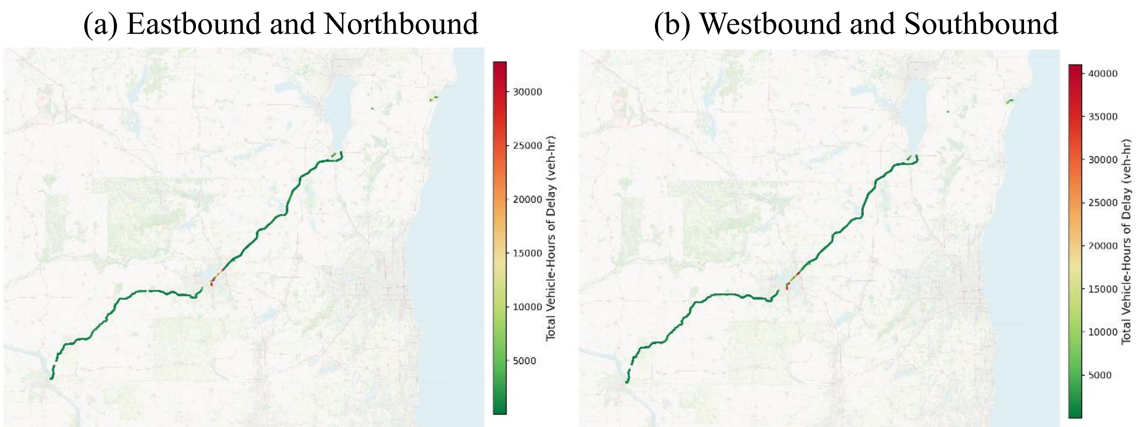

Figure 6-39: Spatial Distribution of Delay Across US-151 in 2024.

The direction-specific profiles indicate that the Madison-area hotspots are visible across multiple directions and include a noticeable recurrent component, while the Manitowoc-area delay is more localized and largely non-recurrent.

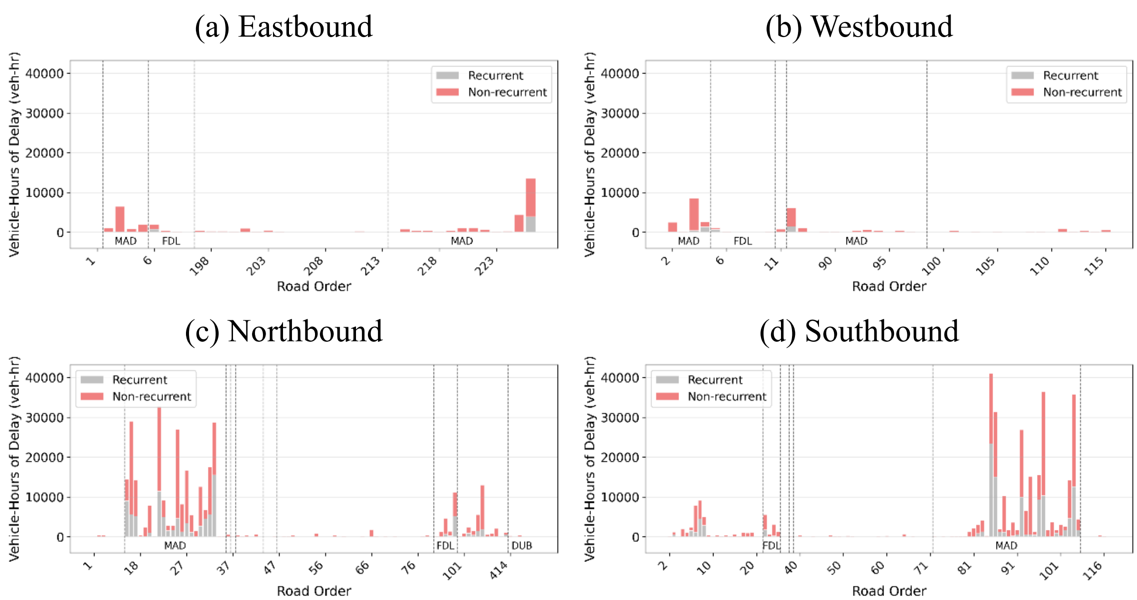

Figure 6-40: Direction-Specific Recurrent and Non-Recurrent Delay for US-151 in 2024.

Principal Arterials: WI-172

Delay is concentrated in a small number of segments near the WI-54 interchange area.

(a) Eastbound (b) Westbound

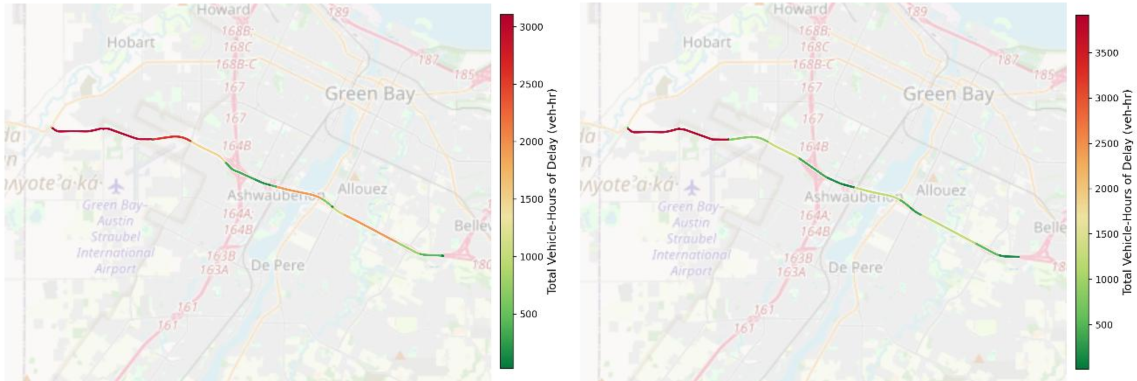

Figure 6-41: Spatial Distribution of Delay Across WI-172 in 2024.

The direction-specific profiles show that these hotspots are composed mostly of non-recurrent delay, with only limited recurrent delay at a few segments.

(a) Eastbound (b) Westbound

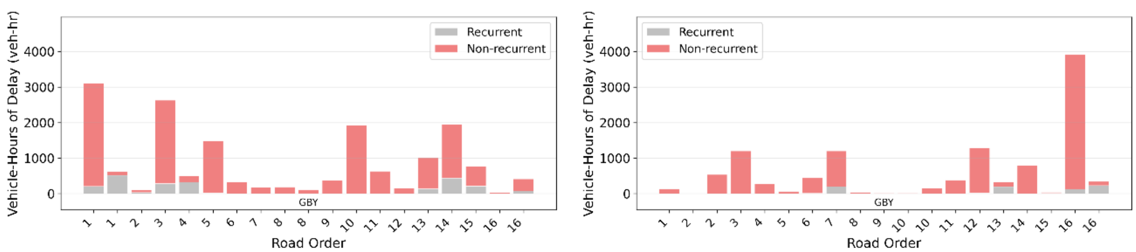

Figure 6-42: Direction-Specific Recurrent and Non-Recurrent Delay for WI-172 in 2024.

Other Principal Arterials: WI-19

Delay is concentrated at localized hotspots near Watertown and Sun Prairie.

(a) Eastbound (b) Westbound

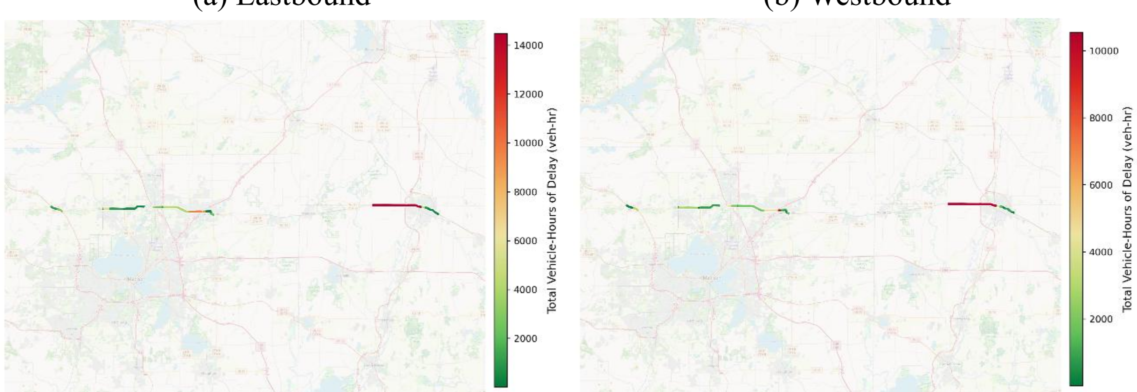

Figure 6-43: Spatial Distribution of Delay Across WI-19 in 2024.

The direction-specific profiles show that most of these TMC-level hotspots are dominated by non-recurrent delay, with only a small recurrent component at a few locations.

(a) Eastbound (b) Westbound

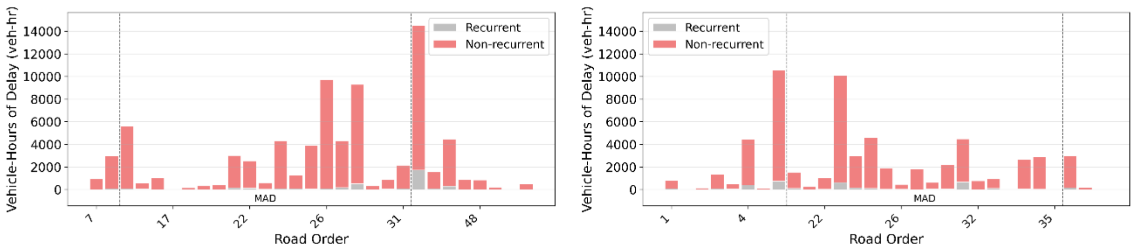

Figure 6-44: Direction-Specific Recurrent and Non-Recurrent Delay for WI-19 in 2024.

Other Principal Arterials: WI-100

Delay is more pronounced in the southbound and northbound directions than in the eastbound and westbound directions. The largest hotspots appear near the WI-50 intersection and the W. North Ave intersection, with additional delay distributed across the north-south portion of the corridor.

(a) Eastbound and Southbound (b) Westbound and Northbound

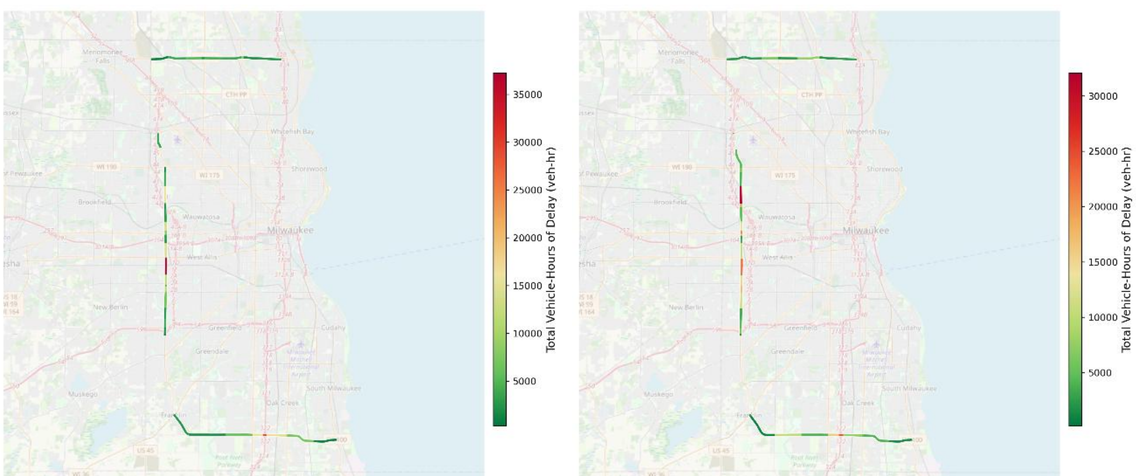

Figure 6-45: Spatial Distribution of Delay Across WI-100 in 2024.

The direction-specific profiles also show that delay is not limited to a single isolated segment; rather, several adjacent segments contribute to the corridor total, although one or two segments form the dominant peaks. Non-recurrent delay remains the larger component overall, but the profiles also show a noticeable recurrent share.

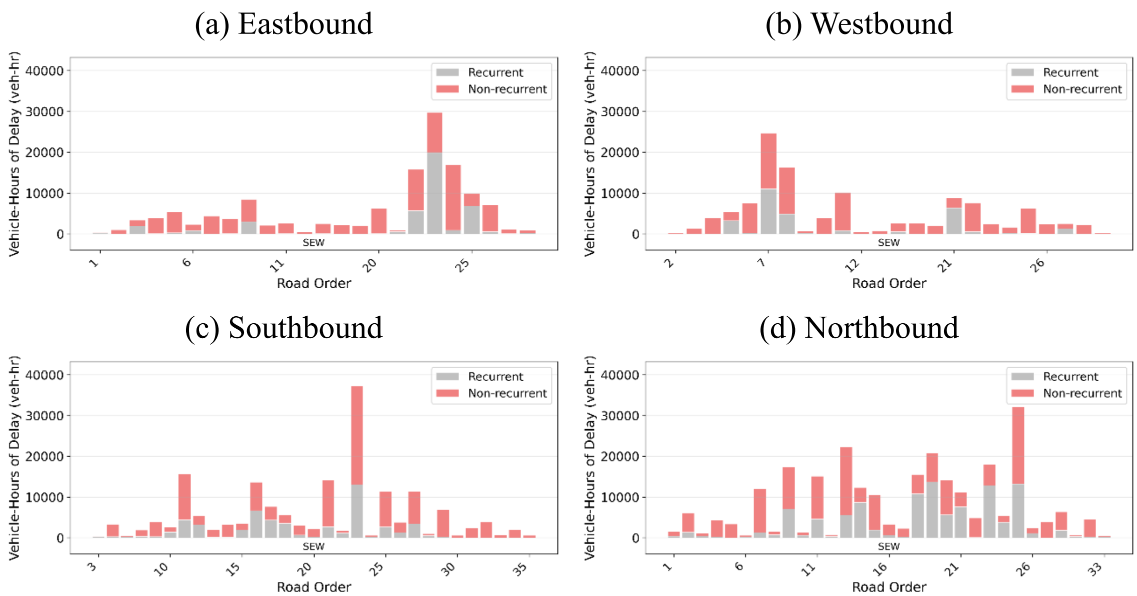

Figure 6-46: Direction-Specific Recurrent and Non-Recurrent Delay for WI-100 in 2024.

Other Principal Arterials: WI-125

Delay is concentrated near the interchange with I-41, while the rest of the corridor shows lower total delay. Because the road-order sequence was not sufficiently reliable for this corridor, direction-specific segment profiles were not generated.

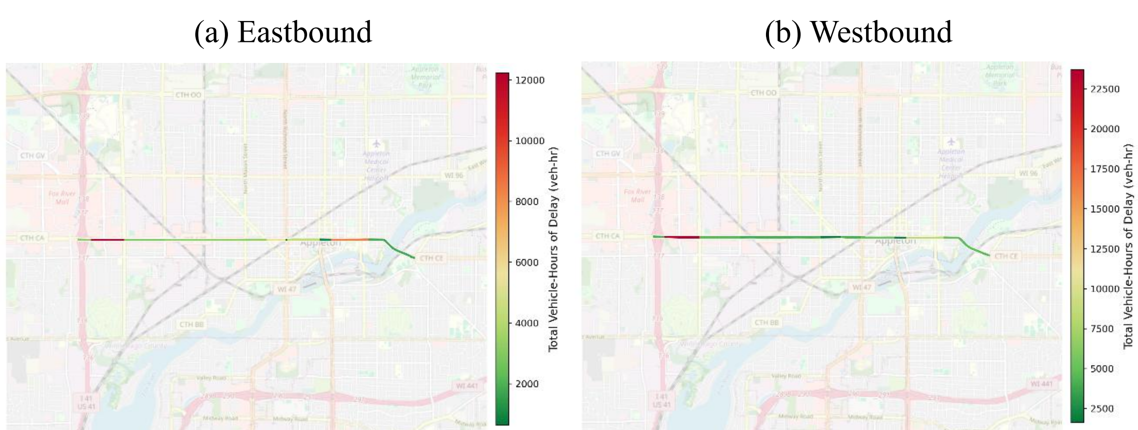

Figure 6-47: Spatial Distribution of Delay Across WI-125 in 2024.

Other Principal Arterials: WI-190

The highest-delay segments appear in similar locations in both directions, indicating that the main delay hotspots are shared across eastbound and westbound travel.

(a) Eastbound (b) Westbound

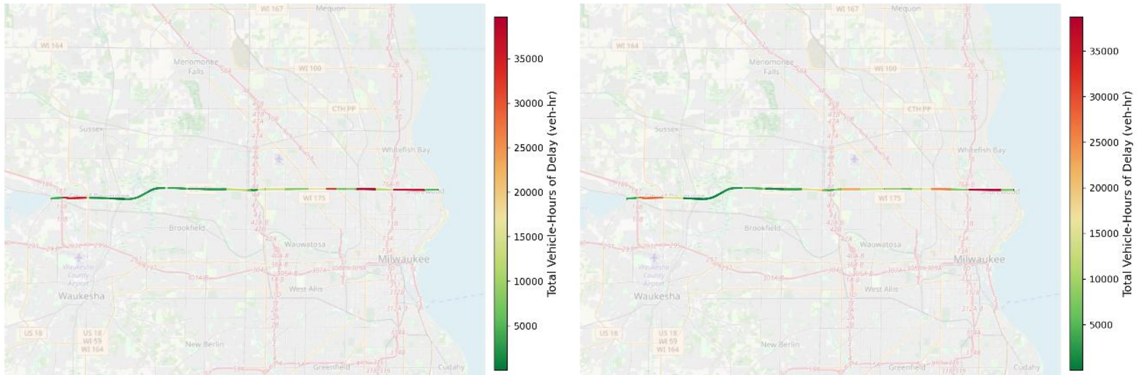

Figure 6-48: Spatial Distribution of Delay Across WI-190 in 2024.

The direction-specific profiles show that delay is spread across multiple segments, with several pronounced peaks rather than one dominant location. Non-recurrent delay accounts for much of the TMC-level total, although recurrent delay is also noticeable at some of the higher-delay segments.

(a) Eastbound (b) Westbound

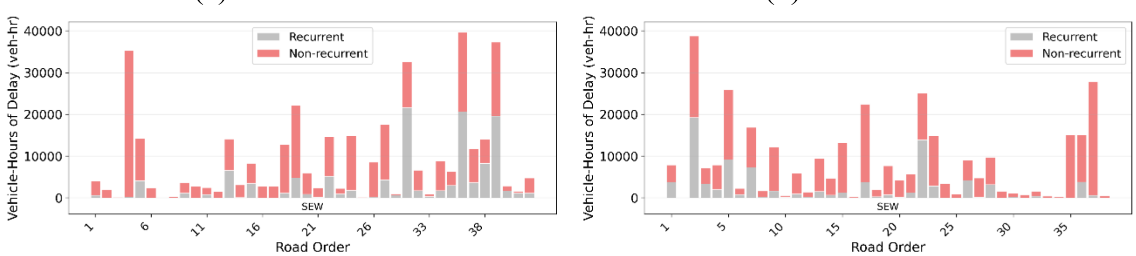

Figure 6-49: Direction-Specific Recurrent and Non-Recurrent Delay for WI-190 in 2024.

<u>Space-Time Contour Analysis</u>

This section provides detailed space-time diagnostics for the corridor sections selected by WisDOT. To facilitate spatial identification, each diagnostic case is presented alongside a corridor-section map illustrating total annual VHD. For these sections, the road-order sequence was manually adjusted based on the corridor maps to ensure that the space-time contours accurately reflect the actual spatial progression of each study area.

The analysis periods were selected to best capture the unique delay characteristics of each section. For locations where recurrent congestion is the primary concern, a typical midweek day (Tuesday through Thursday) was selected from a non-holiday during the school session to represent stable weekday travel patterns. However, for sections where delay is driven by specific events or weekend-peak congestion, the visualization focuses on the specific dates when those significant delays occurred. This approach allows the diagnostics to illustrate operationally relevant congestion patterns for each selected corridor. Because each contour is based on section-specific delay observed on a single date, color scales were set individually for each case; therefore, direct comparison of color intensity across sections is not recommended.

Table 6-7 summarizes the representative dates selected for the space-time contour analysis and the reasons each date was chosen.

Table 6-7: Representative Dates and Selection Reasons for Space-Time Contour Analysis.

Corridor	Section	Direction	Date	Day type	Selection Reason
I-41	Zoo IC to Good Hope Rd	NB/SB	2024-10-03	Thu	Typical weekday peak
	County Line to County Line	NB	2024-02-22	Thu	Crash-related
		SB	2024-10-18	Fri	Incident-related
I-43	Marquette IC to County Line Rd	NB/SB	2024-09-25/ 2024-09-18	Wed/ Wed	Typical weekday peak
I-94	Zoo IC to Willow Glen Rd	EB/WB	2024-09-17/ 2024-09-18	Tue/ Wed	Typical weekday peak
	Zoo IC to Marquette IC	EB/WB	2024-10-03/ 2024-09-26	Thu/ Thu	Typical weekday peak
US-18	County PD to US-18	EB	2024-06-17	Mon	Unusual pattern
		WB	2024-04-09	Tue	Unusual pattern
US-51	US-8 to Minocqua	NB/SB	2024-09-28	Sat	Special event-related
	Beltline to I-39/90/94 IC	NB/SB	2024-10-03	Thu	Typical signal-related
US-53	I-94 to WI-29	NB	2024-08-28	Wed	Unusual pattern
		SB	2024-07-07	Sun	Crash-related
US-151	Columbus to Waupun	NB/SB	2024-07-13/ 2024-03-27	Sat/ Wed	Unusual pattern
WI-172	County EB to US-141	EB/WB	2024-10-13 2024-09-29	Sun/ Sun	Game day-related

WI-19	Waunakee to Sun Prairie	EB/WB	2024-10-09	Wed	Typical signal-related
WI-125	I-41 to WI-55	EB/WB	2024-10-09	Wed	Typical signal-related

Summary

Overall, the space-time contours show that delay patterns vary substantially across the selected sections. Interstate corridors generally exhibit clearer peak-period bottlenecks, with congestion often forming near merge segments and, in some cases, propagating upstream during the morning or afternoon peak. In contrast, many 'principal arterial' corridor sections show more localized and intermittent delay, often associated with signalized segments, short-duration disturbances, special events, and crashes. Several sections, such as US-151, show isolated delay patterns that should be interpreted cautiously because they may reflect unclassified events or NPMRDS noise rather than stable recurrent congestion. These findings indicate that section-level delay is not driven by a single mechanism. Rather, it reflects a mix of recurring bottlenecks, localized intersection effects, and event-specific disturbances.

Interstate: I-41

- Zoo IC to Good Hope Rd

Northbound delay shows a dominant afternoon peak from 3 to 6 PM, with delay concentrated near merge segments 4 through 10. This localized delay overlaps with the active work zone (indicated by blue dots), although the total VHD level is lower than in the southbound direction. A short-duration morning bottleneck appears around 8 AM, but it remains localized and does not trigger substantial upstream propagation.

Southbound delay is concentrated during the afternoon peak, mainly from 3 to 6 PM, with the highest delay occurring near merge segments 4 through 9. The space-time contour indicates that congestion forms at these locations and propagates upstream during the peak period. A smaller delay is also observed around 8 AM, but its magnitude and duration are limited compared to the afternoon peak.

(a) Northbound (2024-10-03, Thursday)

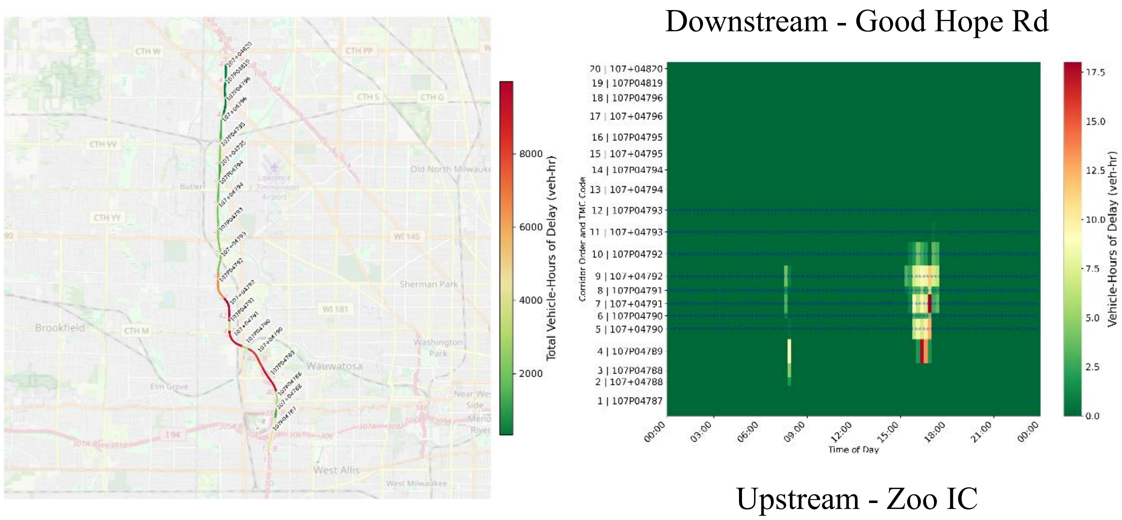

(b) Southbound (2024-10-03, Thursday)

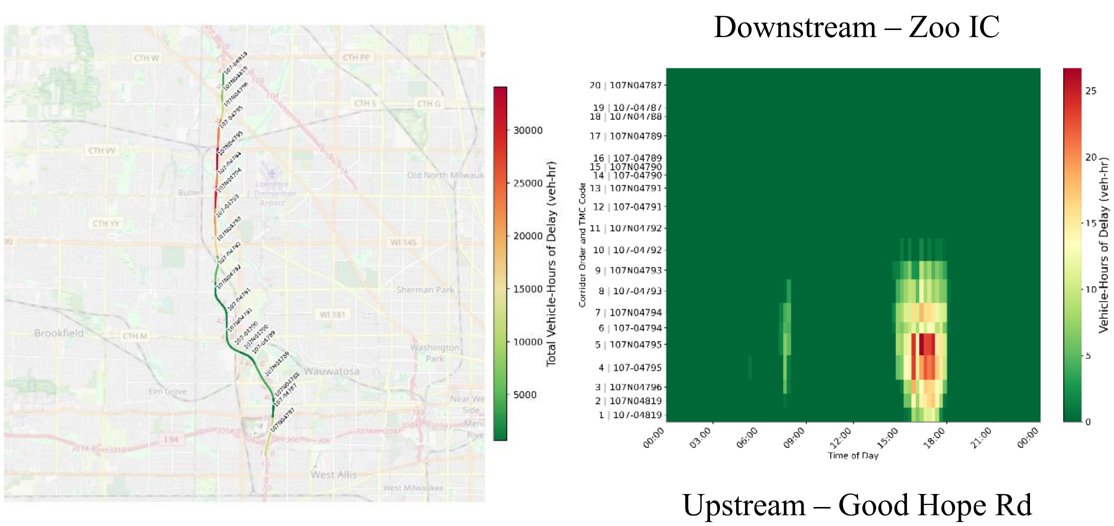

Figure 6-50: Representative Space-Time Contours from Zoo IC to Good Hope Rd.

- County Line to County Line

For the northbound direction, a significant localized delay is observed on February 22, 2024, near segment 6, downstream of the work zone and near the reported crash location (indicated by a black star). Although the delay persists for more than one hour, the contour indicates that congestion remains localized and does not propagate extensively upstream.

Southbound delay is more pronounced than northbound delay in this section. The main delay pattern occurs during the afternoon peak around 3 PM, near merge segments 10 and 12. The contour shows upstream propagation from these locations. On October 18, 2024, the delay duration appears to be extended near the reported crash location, suggesting that the crash may have contributed to the persistence of congestion during the peak period.

(a) Northbound (2024-02-22, Thursday)

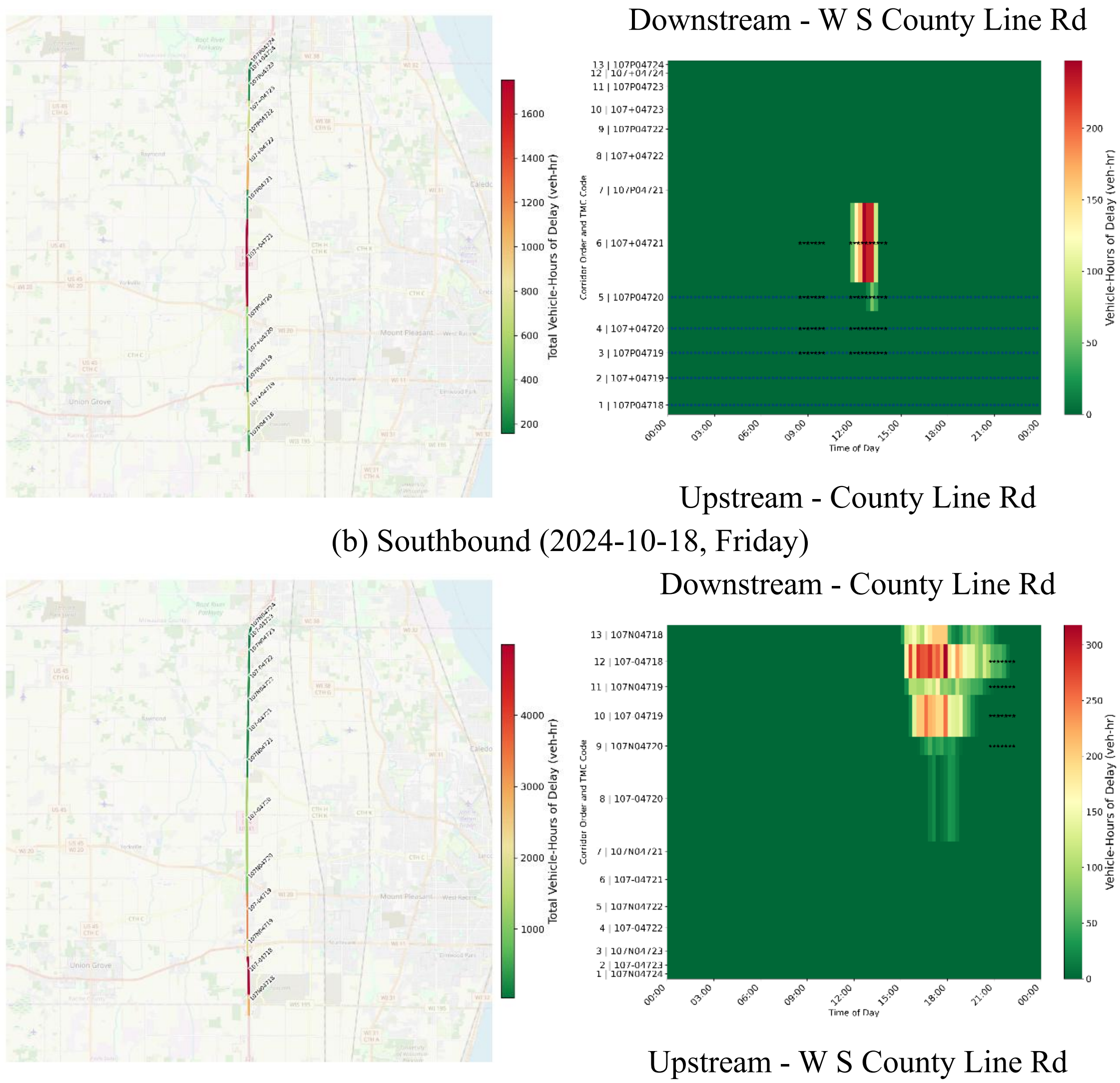

Figure 6-51: Representative Space-Time Contours from County Line to County Line.

Interstate: I-43

- Marquette IC to County Line Rd

Northbound delay is concentrated primarily during the afternoon peak, with the highest delay occurring near merge segment 6 from around 3 to 6 PM. The contour indicates that this delay remains spatially localized, with only limited upstream propagation. A few minor delay spots also appear at downstream segments, but their magnitude and duration are small compared with the main afternoon bottleneck.

Southbound delay shows a clearer combination of morning and afternoon peak-period congestion. A morning bottleneck forms near segments 8 through 10 around 8 AM, while afternoon delay appears around the same segments and near the downstream end of the section. Compared with the northbound direction, southbound delay is distributed across more segments and shows stronger peak-period recurrence, although the most severe delay remains confined to short sections.

(a) Northbound (2024-09-25, Wednesday)

Downstream - County Line Rd

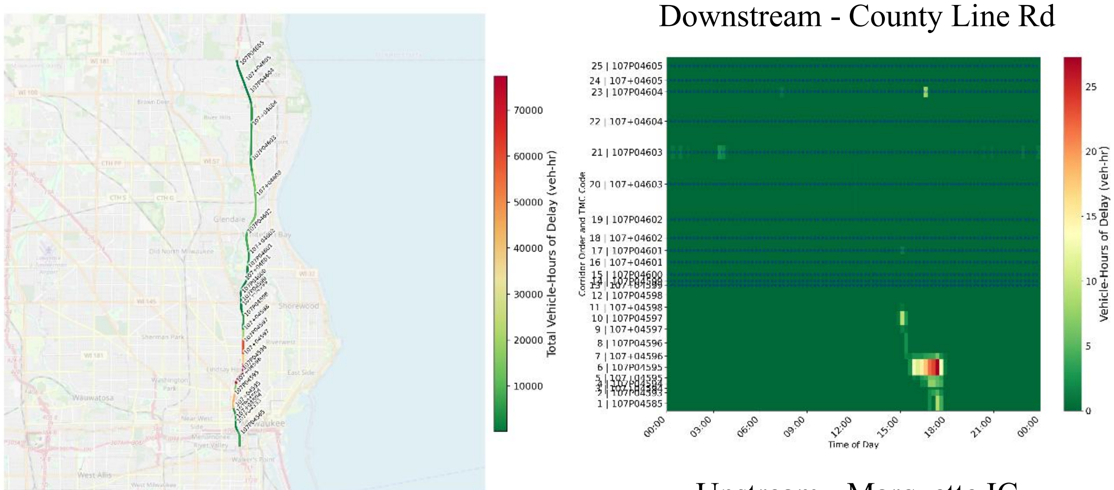

Upstream - Marquette IC

(b) Southbound (2024-09-18, Wednesday)

Downstream - Marquette IC

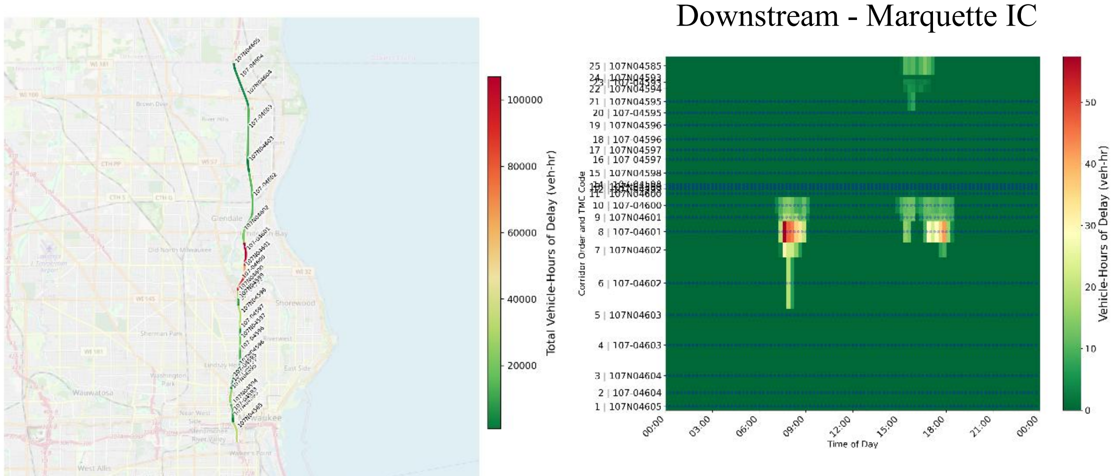

Upstream - County Line Rd

Figure 6-52: Representative Space-Time Contours from Marquette IC to County Line Rd.

Interstate: I-94

- Zoo IC to Willow Glen Rd

Eastbound delay is concentrated near the downstream portion of the section, with the highest delay occurring near segments 13 through 26. The contour shows two distinct peak-period patterns. Morning delay occurs around 7 AM and is localized, while afternoon delay extends across a relatively broad set of segments from around 3 to 5 PM. Both patterns remain mostly confined within the hotspot and do not show extensive upstream propagation.

Westbound delay is larger than eastbound delay and is concentrated near the upstream portion of the corridor, closer to the Zoo IC. The contour shows a strong afternoon delay pattern from around 4 to 5 PM, with delay concentrated across segments 3 through 9.

(a) Eastbound (2024-09-17, Tuesday)

Downstream - Zoo IC

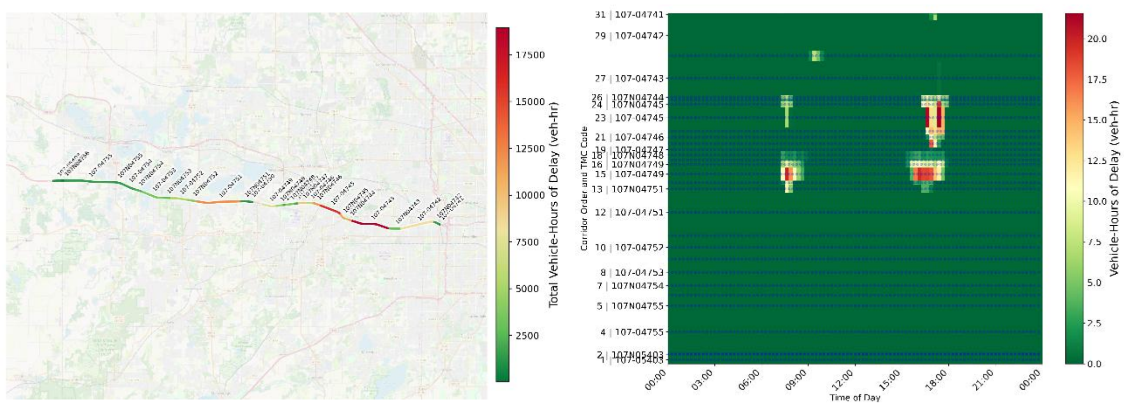

Upstream - Willow Glen Rd

(b) Westbound (2024-09-18, Wednesday)

Downstream - Willow Glen Rd

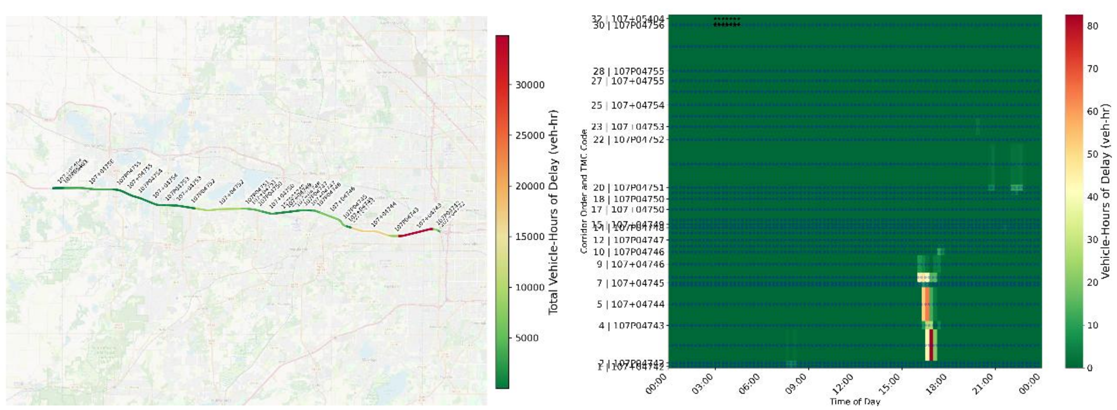

Upstream - Zoo IC

Figure 6-53: Representative Space-Time Contours from Zoo IC to Willow Glen Rd.

- Zoo IC to Marquette IC

Eastbound delay shows both morning and afternoon peak-period patterns. Morning delay occurs from 7 to 9 AM and is broadly distributed across segments 1 through 15. The afternoon delay is more severe and occurs mainly from 3 to 6 PM, with the highest delay concentrated near segments 1 through 5.

Westbound delay also shows a clear morning peak from 6 to 8 AM, followed by a broader and more sustained afternoon peak from about 2 to 7 PM. Compared with the eastbound direction, the westbound afternoon delay persists for a longer duration. The highest delay is concentrated near segments 3 through 7, while the downstream segments show limited delay despite the presence of work-zone and crash markers.

(a) Eastbound (2024-10-03, Thursday)

Downstream - Marquette IC

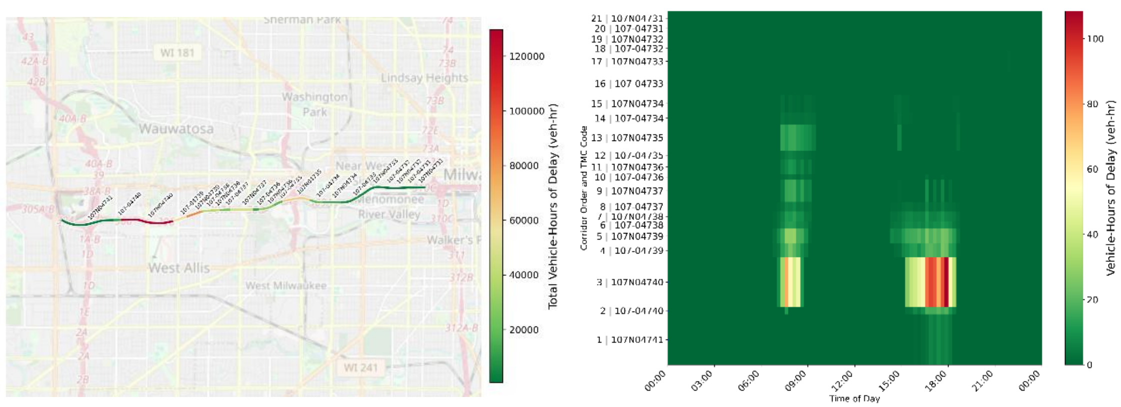

Upstream - Zoo IC

(b) Westbound (2024-09-26, Thursday)

Downstream - Zoo IC

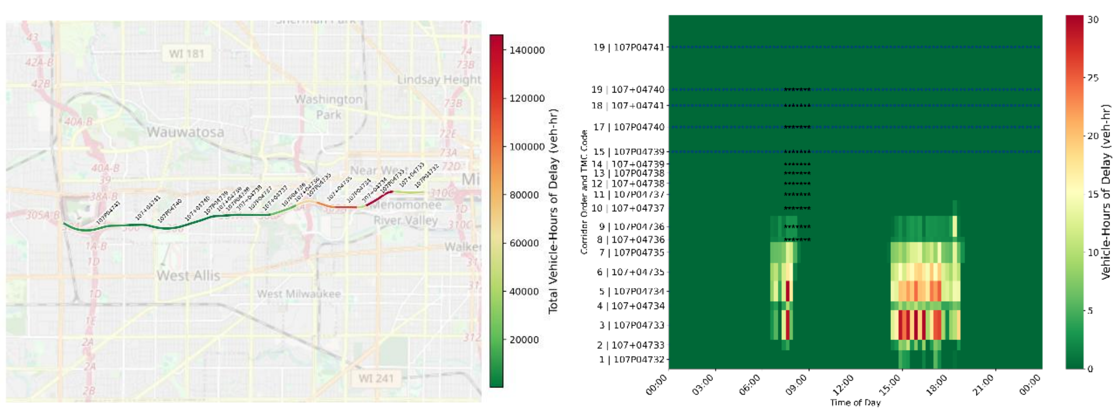

Upstream - Marquette IC

Figure 6-54: Representative Space-Time Contours from Zoo IC to Marquette IC.

Principal Arterials: US-18

- County PD to US-18

For each direction, the space-time contour was prepared using the day with the largest observed delay. Eastbound and westbound delays are observed near the Ridgeway area. This section does not typically exhibit peak-period delay, and no reported event was associated with either of the observed delay cases.

(a) Eastbound (2024-06-17, Monday)

Downstream - County PD

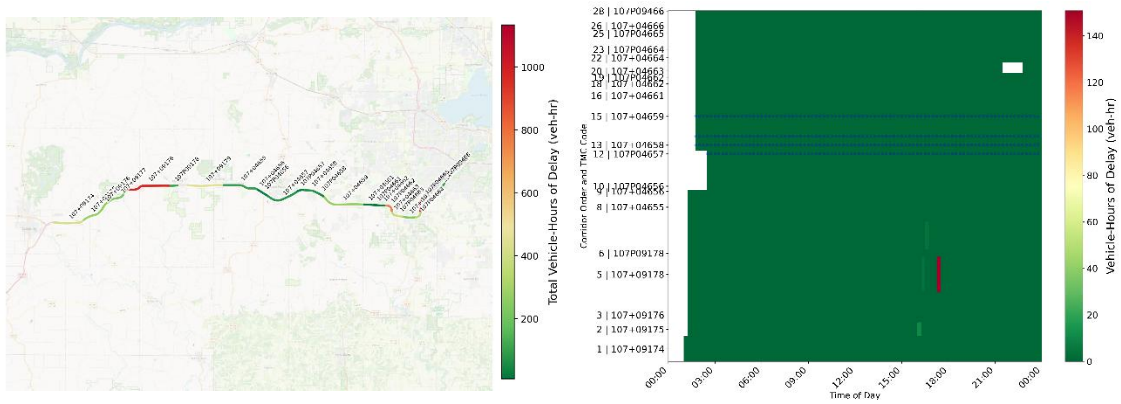

Upstream - US-18

(b) Westbound (2024-04-09, Tuesday)

Downstream - US-18

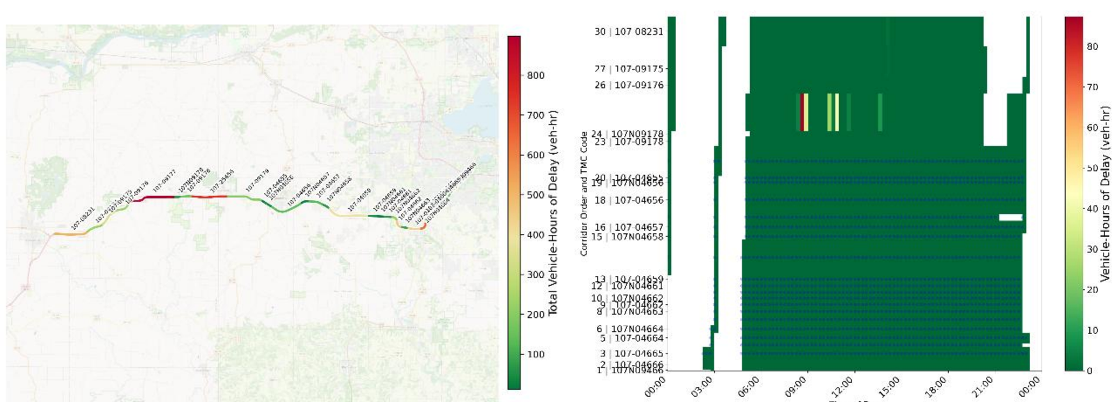

Upstream - County PD

Figure 6-55: Representative Space-Time Contours from County PD to US-18.

Principal Arterials: US-51

- US-8 to Minocqua (WI-47)

On September 28, a special-event-related full closure was reported within this segment. In the northbound direction, delay is concentrated mainly during the midday to early afternoon period. The strongest delay appears near segment 4 and persists for several hours from approximately 11 AM to 3 PM. A short delay also appears near the beginning of the day, but the main pattern is sustained midday delay rather than a typical commuter peak.

Southbound delay also appears during the midday period, mainly near segment 3 from approximately 9 AM to 2 PM. Compared with the northbound direction, the southbound delay remains shorter in duration. Overall, the contours indicate an event-related delay pattern associated with the full closure rather than a typical commuter peak-period bottleneck.

(a) Northbound (2024-09-28, Saturday)

Downstream - Minocqua

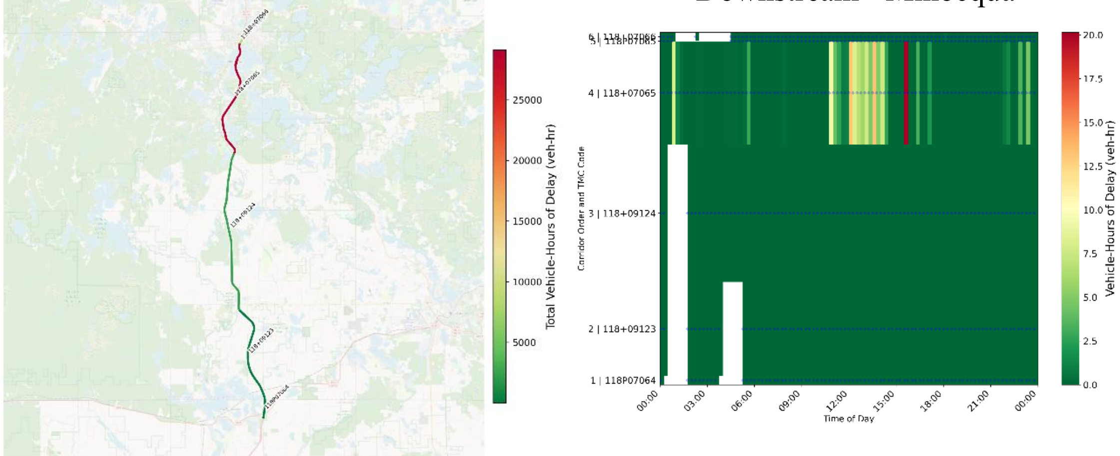

Upstream - US-8

(b) Southbound (2024-09-28, Saturday)

Downstream - US-8

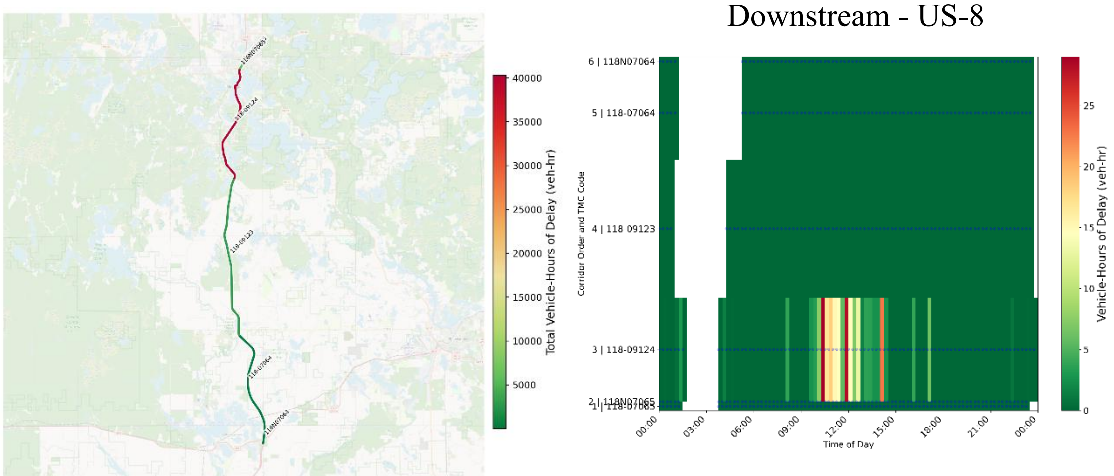

Upstream - Minocqua

Figure 6-56: Representative Space-Time Contours from US-8 to Minocqua.

- Beltline (US-12) to I-39/90/94 IC

Northbound delay is concentrated mainly near signalized segments, especially around segments 1 through 4. Delay is visible throughout much of the daytime period and becomes most pronounced from around 4 to 5 PM. The contour shows intermittent delay across segments, but the main pattern remains tied to signalized locations rather than propagating continuously through the full section.

Southbound delay is more sustained through the day, particularly near segments 9 and 10, which are also signalized. Delay begins in the morning and remains visible through the afternoon, with several short-duration vertical bands appearing across upstream segments. Compared with the northbound direction, the southbound pattern is less concentrated at a single peak time and instead reflects a more persistent daytime delay pattern near the signalized segments.

(a) Northbound (2024-10-03, Thursday)

Downstream - I-39/90/94 IC

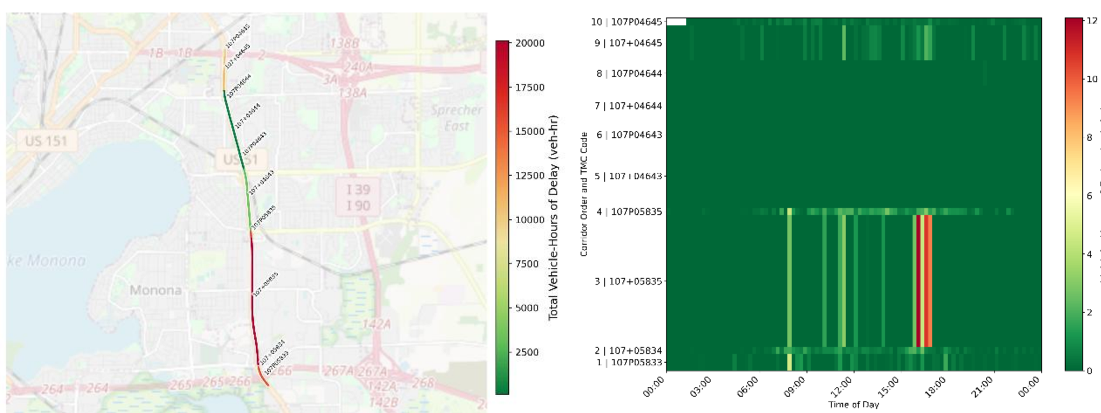

Upstream - Beltline

(b) Southbound (2024-10-03, Thursday)

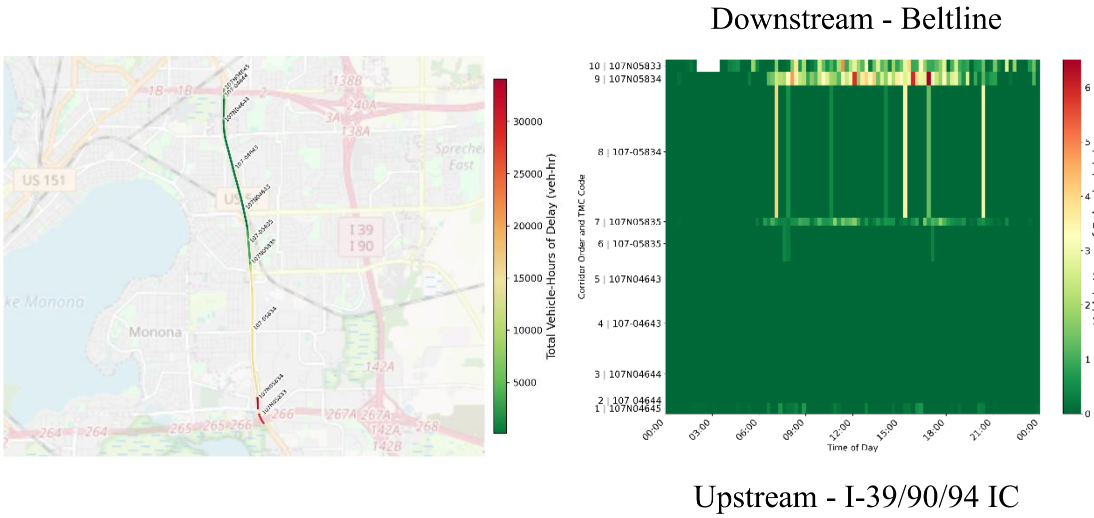

Figure 6-57: Representative Space-Time Contours from Beltline to I-39/90/94 IC.

Principal Arterials: US-53

- I-94 to WI-29

Northbound delay is limited on the representative day and does not show a recurring peak-period pattern. The main delay appears as a short duration, localized disturbance near segments 12 and 13 in the late afternoon. Because no event was reported during this period, this delay remains unclassified in the current framework.

Southbound delay is more pronounced and is associated with a reported crash on July 7. The contour shows a strong but localized delay near segments 3 through 6 during the early afternoon. The delay persists for a short period but does not propagate across the full section. Overall, this corridor shows episodic, event-specific delay rather than a stable commuter peak pattern.

(a) Northbound (2024-08-28, Wednesday)

Downstream - WI-29

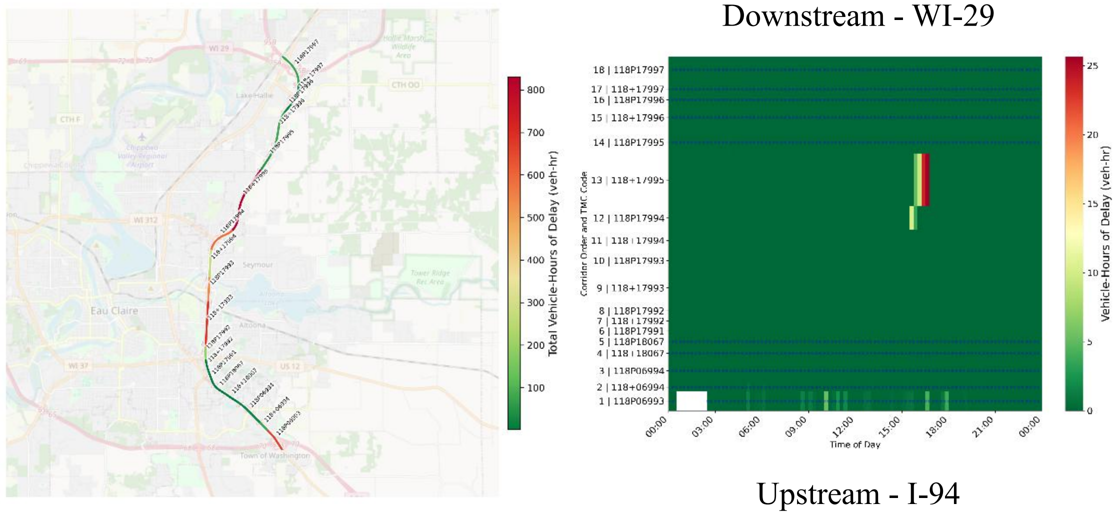

Upstream - I-94

(b) Southbound (2024-07-07, Sunday)

Downstream - I-94

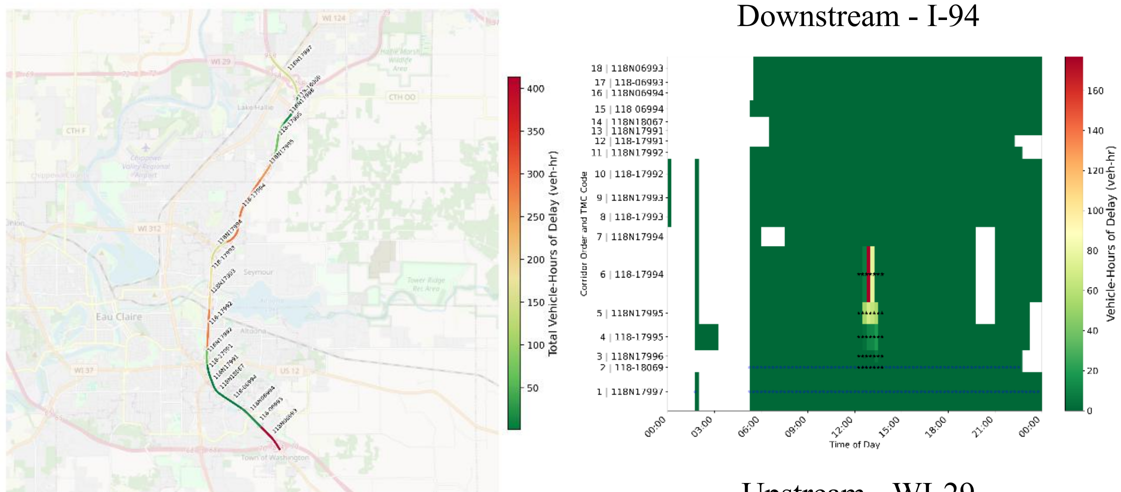

Upstream - WI-29

Figure 6-58: Representative Space-Time Contours from I-94 to WI-29.

Principal Arterials: US-151

- Columbus (WI-73) to Waupun (WI-49)

Northbound delay is limited to a single short-duration disturbance on July 13, 2024. The contour shows a brief delay near segment 14 around 3 PM, with no clear upstream propagation or sustained congestion pattern. Although no event was reported on the representative day, this segment includes an at-grade rail crossing, and the observed disturbance may have been influenced by a train crossing. Therefore, the pattern should be interpreted cautiously, as it may reflect a train-crossing event, another unclassified delay, or NPMRDS noise rather than a recurring bottleneck.

Southbound delay is also highly localized, with a short-duration delay appearing near segment 19 around 6 PM. Rain was recorded on March 27, 2024, so the delay may be related to a localized weather condition; however, given its isolated spatial extent and brief duration, it may also reflect NPMRDS noise. Overall, the contours do not indicate a stable recurrent congestion pattern in this section, and the observed delays appear to be isolated, short-lived disturbances.

(a) Northbound (2024-07-13, Saturday)

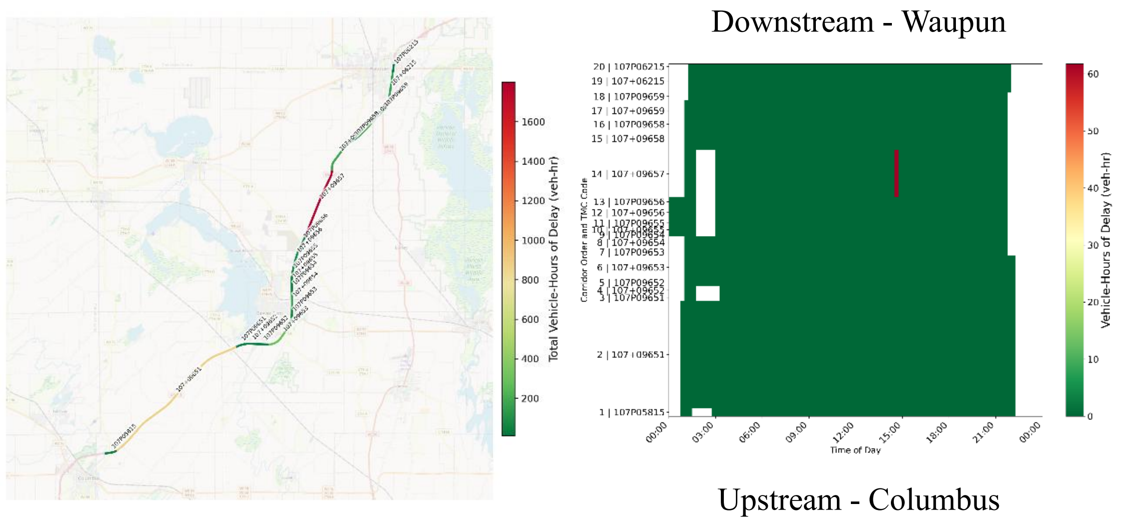

(b) Southbound (2024-03-27, Wednesday)

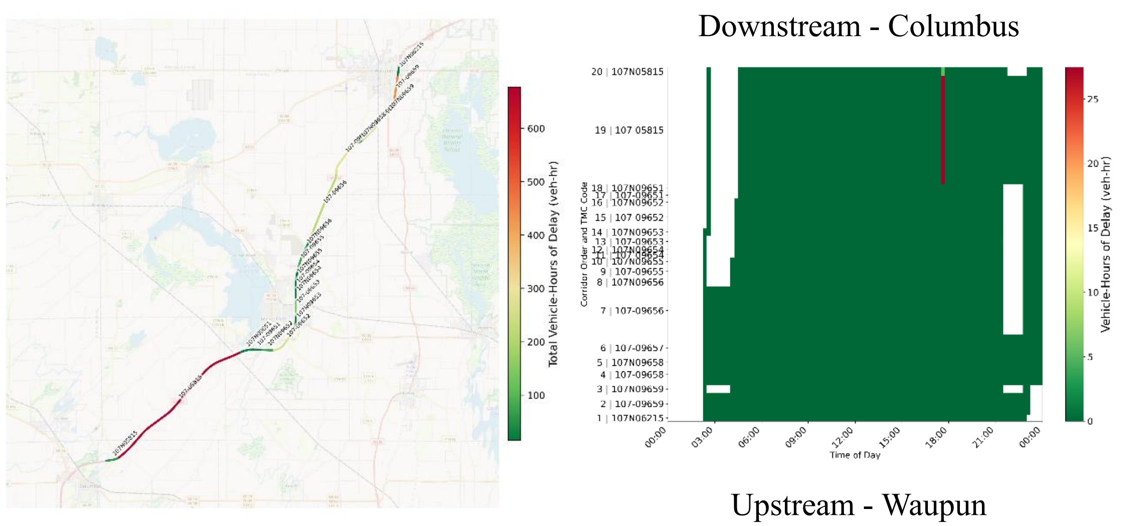

Figure 6-59: Representative Space-Time Contours from Columbus to Waupun.

Principal Arterials: WI-172

- County EB (west of I-41) to US-141 (east of I-43)

Eastbound delay is concentrated during the late afternoon, mainly from about 3 to 5 PM.

The strongest delay occurs near segments 4 through 6, with weaker delay propagating to adjacent segments. Although no roadway event was reported, the representative day coincided with a Green Bay Packers game. Therefore, the observed pattern is likely associated with game-day traffic rather than a typical peak.

Westbound delay occurs earlier in the day, from late morning to midday, and is concentrated near segment 7. This direction also corresponds to a Packers game day with no reported roadway event, suggesting that the delay may reflect event-related travel demand rather than a recurring bottleneck. Overall, both contours show localized game-day delay patterns, with eastbound delay concentrated in the late afternoon and westbound delay appearing in the late morning.

(a) Eastbound (2024-10-13, Sunday)

Downstream - US-141

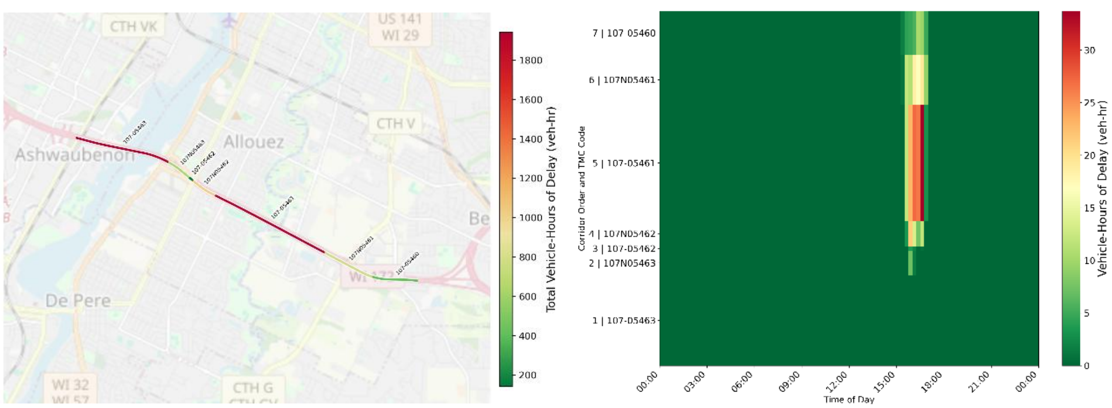

Upstream - County EB

(b) Westbound (2024-09-29, Sunday)

Downstream - County EB

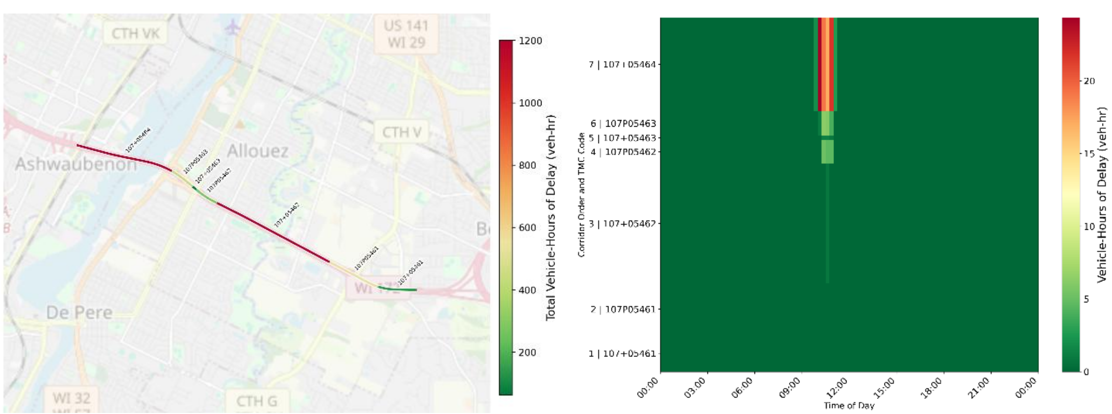

Upstream - US-141

Figure 6-60: Representative Space-Time Contours from County EB to US-141.

Other Principal Arterials: WI-19

- Waunakee (WI-113 RAB) to Sun Prairie (US-151)

Eastbound delay is scattered across the day and does not show a single continuous congestion band. Several short-duration delays appear near the signalized segments, with small peaks around midday and during the afternoon period. Work zone activity is also present along the corridor, but the contour does not indicate strong upstream propagation.

Westbound delay shows a similarly intermittent pattern, with short delay spikes appearing at multiple times of day. The most visible delays occur near the signalized segments, including isolated spikes in the morning, afternoon, and evening periods. Although work zone activity is present, the observed delay remains localized and discontinuous.

(a) Eastbound (2024-10-09, Wednesday)

Downstream - Sun Prairie

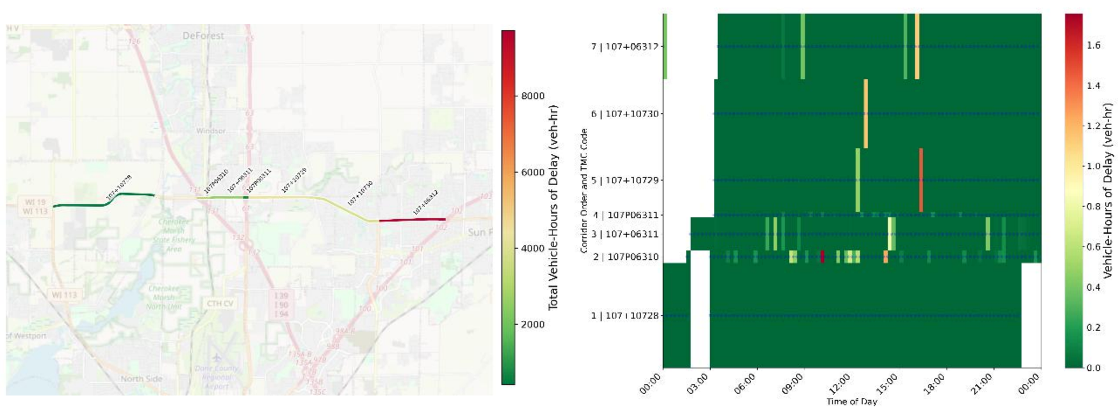

Upstream - Waunakee

(b) Westbound (2024-10-09, Wednesday)

Downstream - Waunakee

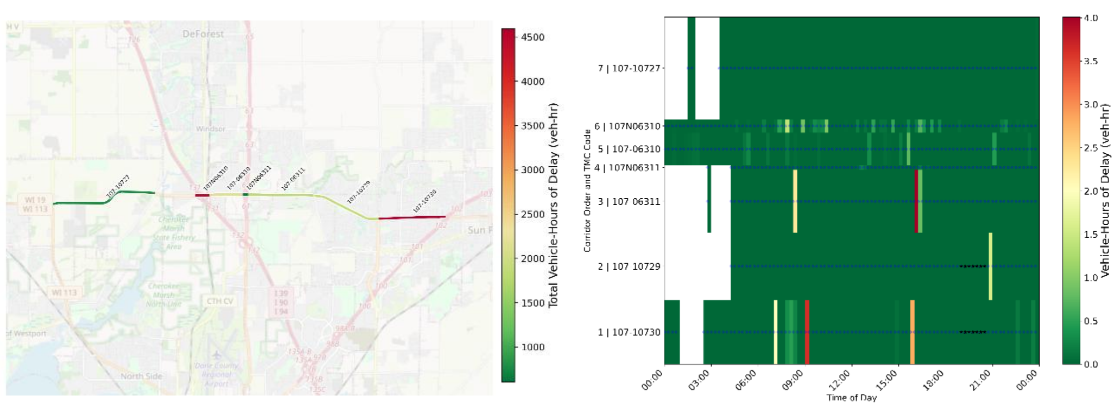

Upstream - Sun Prairie

Figure 6-61: Representative Space-Time Contours from Waunakee to Sun Prairie.

Other Principal Arterials: WI-125

- I-41 to WI-55

Eastbound delay is intermittent and distributed across several signalized segments rather than forming a continuous queue. The most visible delay occurs in the afternoon near segment 12, with additional lower-magnitude delay appearing near segments 2, 10, and 18. This pattern suggests localized intersection-related delay, with no clear evidence of sustained upstream propagation across the section.

Westbound delay also appears to be largely associated with signalized segments, especially around segments 6 through 11 and the downstream segments near 20 through 21. Delay is visible across both the midday and afternoon periods, but it remains spatially discontinuous. Segment 12 shows a distinct isolated delay that does not align clearly with the signalized locations, so it may reflect a localized disturbance or unclassified delay rather than the same signal-related pattern observed elsewhere.

(a) Eastbound (2024-10-09, Wednesday)

Downstream - WI-55

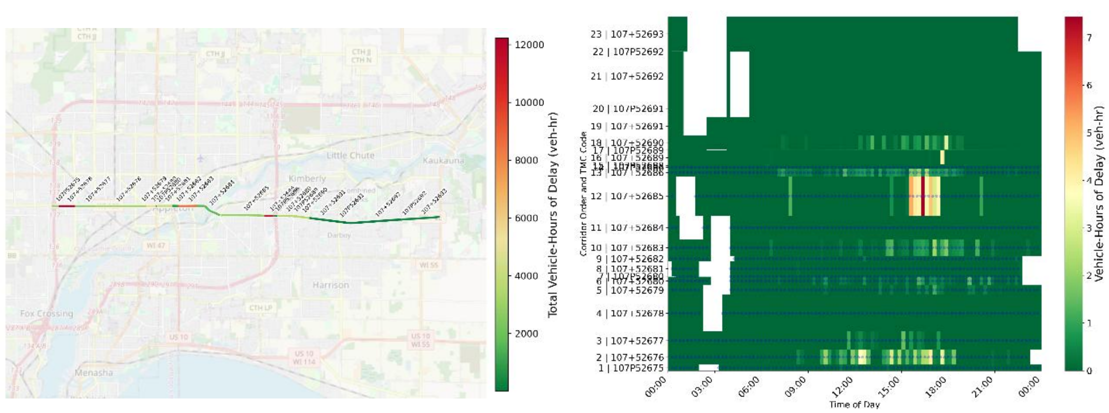

Upstream - I-41

(b) Westbound (2024-10-09, Wednesday)

Downstream - I-41

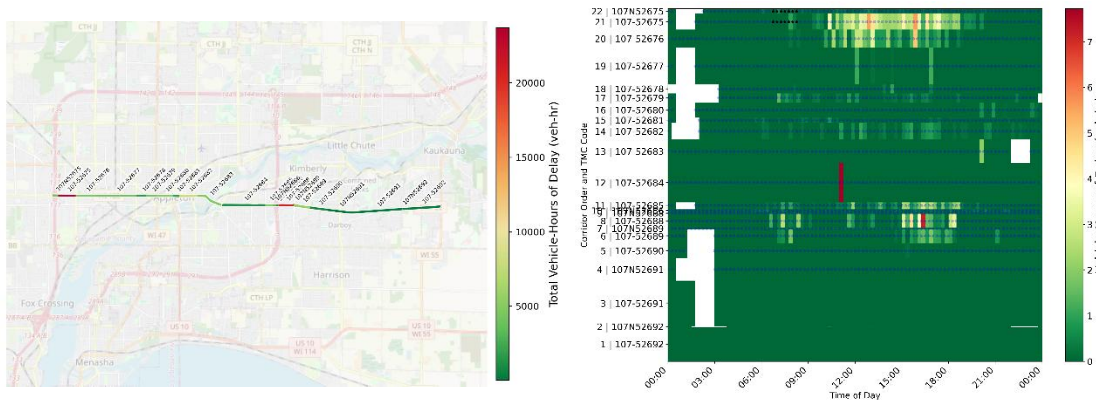

Upstream - WI-55

Figure 6-62: Representative Space-Time Contours from I-41 to WI-55.

6.3. <u>**Investigation of Delay Causation**</u>

This section investigates delay causation in the selected corridors using two complementary analyses: corridor-level delay attribution by cause and representative case studies. The section first identifies the dominant delay categories across the 12 selected corridors and the WisDOT-suggested sections, then uses representative cases to illustrate how specific events and operating conditions are reflected in observed delay.

<u>***Corridor-Level Delay Attribution by Cause***</u>

This section applies the delay attribution framework described earlier to the selected corridors. Delay composition by cause is first summarized for each of the 12 selected corridors and then presented for the WisDOT-suggested sections. Together, these results identify the dominant causes of delay at the corridor and section levels and show how delay composition varies within corridors.

Summary

Table 6-8 summarizes the top two delay categories for each selected corridor. Overall, work-zone delay is the dominant corridor-level cause across the selected corridors. Among the 12 corridors, work-zone delay is the largest component in seven corridors and the second-largest component in two corridors. For ‘principal arterial’ and ‘other principal arterial’ corridors, signal-related delay also emerges as a major contributor, especially through unclassified and recurrent delay at signalized segments. Several corridors (US-53 and WI-172) show a substantial unclassified share, which may reflect queue spillback from downstream signalized intersections into upstream TMCs that are not coded as signalized segments. This suggests that corridor-level delay composition cannot be fully explained by the recorded causal factors and may require interpretation in the context of corridor characteristics, surrounding land uses, possible unreported events, and limitations of the spatial and temporal matching rules.

Table 6-8: Top Two Delay Causes by Selected Corridor (2024).

Functional Class	Corridor	Primary Cause	Secondary Cause
Interstate	I-41	Work zone (51.2%)	Crash & Work zone (12.2%)
	I-43	Work zone (45.8%)	Recurrent without signal (23.9%)
	I-94	Recurrent without signal (37.3%)	Work zone (27.0%)
Principal arterial	US-18	Work zone (24.1%)	Recurrent with signal (21.3%)
	US-51	Unclassified with signal (40.0%)	Work zone (22.9%)
	US-53	Work zone (46.4%)	Unclassified (22.2%)
	US-151	Unclassified with signal (47.0%)	Recurrent with signal (29.8%)
	WI-172	Unclassified (43.0%)	Unclassified with signal (19.1%)
Other principal arterial	WI-19	Work zone (76.2%)	Other multiple causes (8.4%)
	WI-100	Unclassified with signal (35.0%)	Recurrent with signal (33.8%)
	WI-125	Work zone (43.5%)	Recurrent with signal (25.5%)
	WI-190	Work zone (35.4%)	Recurrent with signal (29.0%)

Interstate: I-41

For I-41, work-zone delay accounts for the largest share of corridor-level delay, reflecting the corridor-wide presence of work zones in 2024. Crash-and-work-zone delay is the second-largest component, followed by recurrent delay without signal.

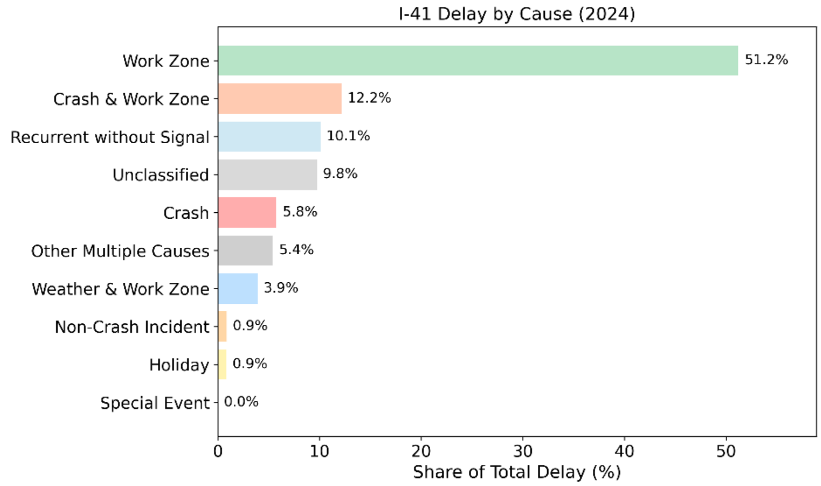

Figure 6-63: Delay Composition by Cause – I-41 (2024) (Total VHD: 1.54 million veh-hr).

In the Zoo IC to Good Hope Rd section, recurrent delay without signal is the largest component, followed by unclassified delay, consistent with delay concentrated at merge segments. In the County Line to County Line section, non-crash incidents account for the largest share, largely driven by the fire incident on October 18, 2024, which resulted in substantial non-recurrent delay.

(a) Zoo IC to Good Hope Rd
Total VHD: 0.278 million veh-hr

(b) County Line to County Line
Total VHD: 0.023 million veh-hr

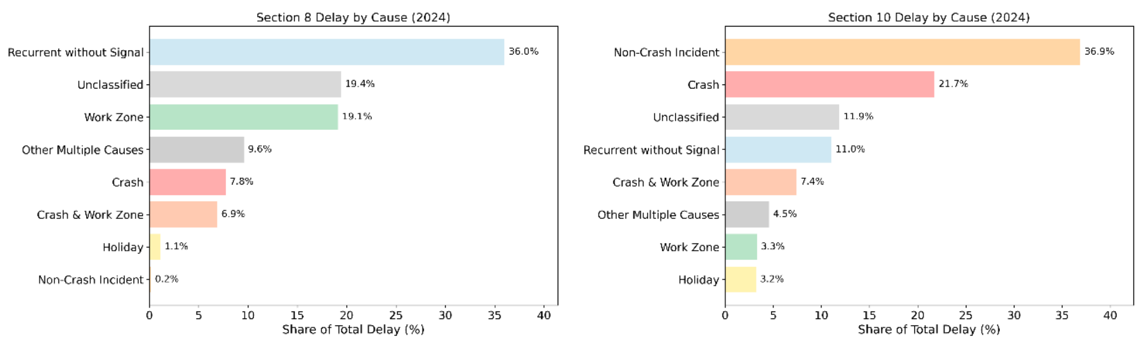

Figure 6-64: Delay Composition by Cause – I-41 WisDOT-Suggested Sections (2024).

Interstate: I-43

For I-43, work-zone delay accounts for the largest share of corridor-level delay, followed by recurrent delay without signal. This reflects both work-zone exposure and the concentration of delay during morning and afternoon peak periods.

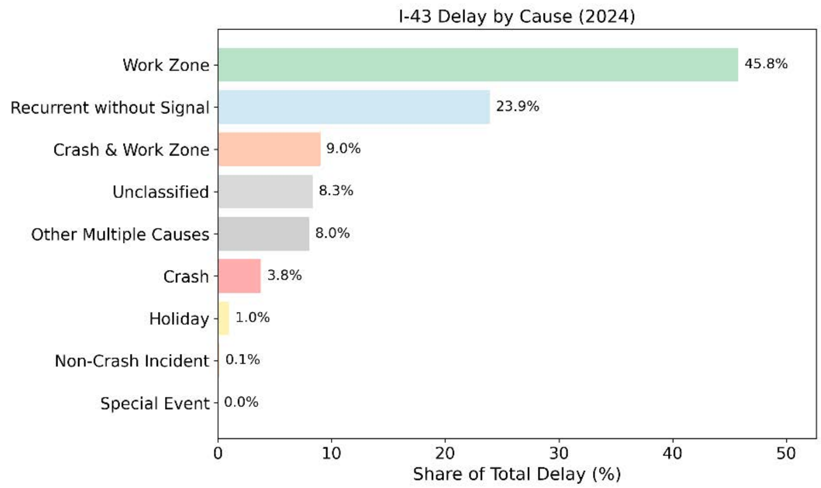

Figure 6-65: Delay Composition by Cause – I-43 (2024) (Total VHD: 1.21 million veh-hr).

In the Marquette IC to County Line Rd section, the delay composition is similar to that of the full corridor, although the share of recurrent delay without signal is slightly higher.

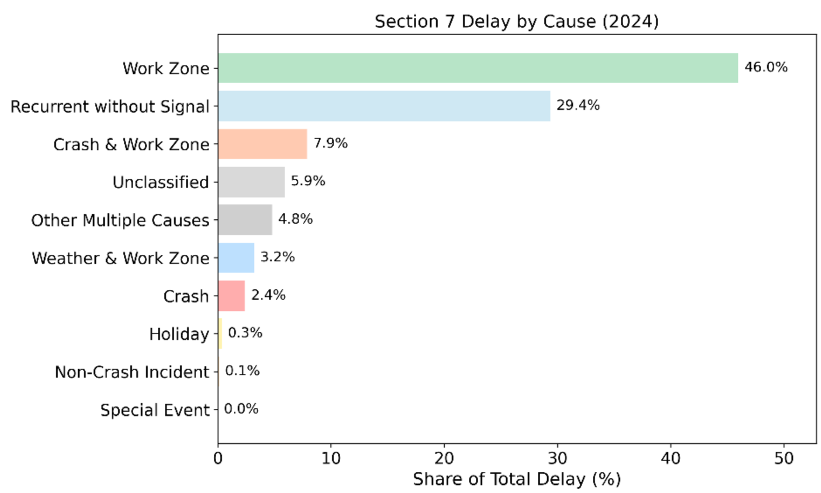

Figure 6-66: Delay Composition by Cause – I-43 Marquette IC to County Line Rd (2024) (Total VHD: 0.852 million veh-hr).

Interstate: I-94

For I-94, recurrent delay without signal and work-zone delay are the dominant causes, while the sizable unclassified share suggests additional variability associated with demand conditions.

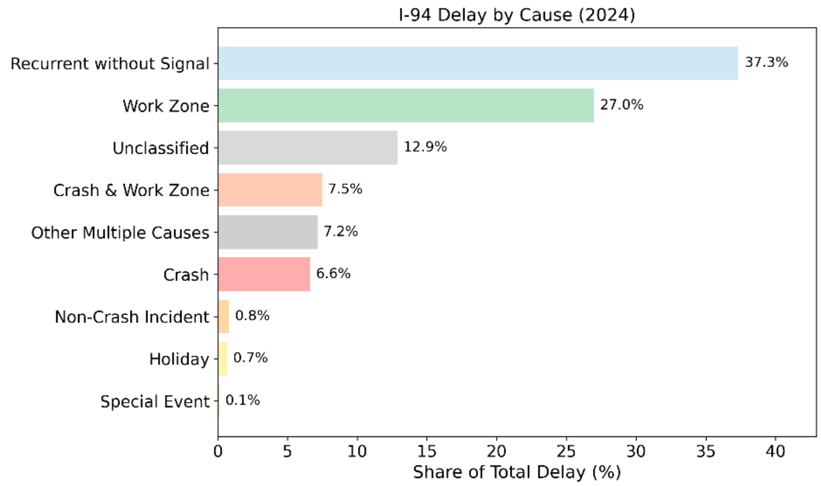

Figure 6-67: Delay Composition by Cause – I-94 (2024) (Total VHD: 2.41 million veh-hr).

In the Zoo IC to Willow Glen Rd section, work-zone delay accounts for the largest share because most of the section was within an active work zone, and crash-and-work-zone category also represents a notable portion. In the Zoo IC to Marquette IC section, recurrent delay without signal is the dominant component, indicating that delay in this section is concentrated primarily during peak periods.

(a) Zoo IC to Willow Glen Rd
Total VHD: 0.29 million veh-hr

(b) Zoo IC to Marquette IC
Total VHD: 1.23 million veh-hr

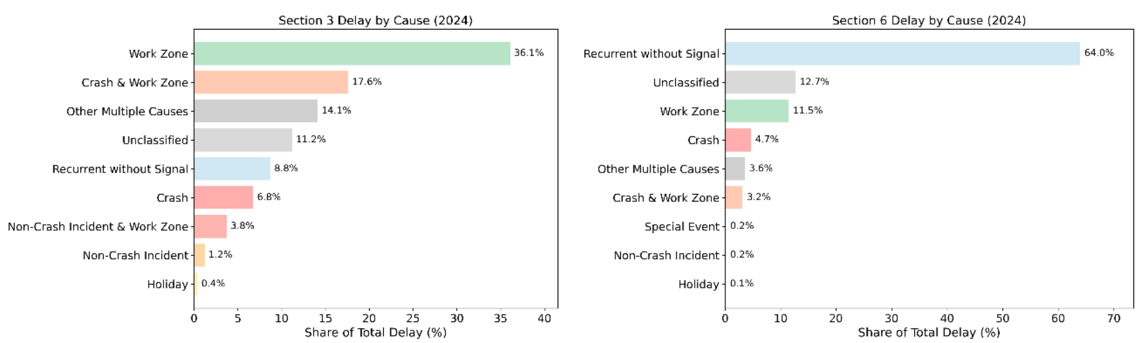

Figure 6-68: Delay Composition by Cause – I-94 WisDOT-Suggested Sections (2024).

Principal Arterials: US-18

For US-18, delay is distributed across several causes. Work-zone delay accounts for the largest share, reflecting the corridor-wide work-zone presence, while recurrent delay with signal and unclassified delay with signal are also substantial. The sizable unclassified share suggests additional delay variability associated with demand conditions.

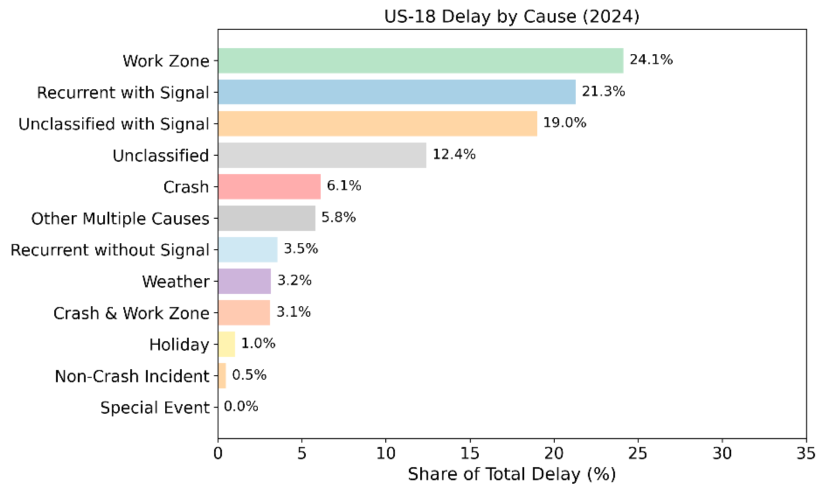

Figure 6-69: Delay Composition by Cause – US-18 (2024) (Total VHD: 1.06 million veh-hr).

In the County PD to US-18 section, unclassified delay is the largest component in 2024, followed by work-zone-related delay. However, annual delay in this section was substantially higher in 2023, reaching 0.109 million vehicle-hours, approximately seven times the 2024 level. In 2023, work-zone-related delay accounted for about 80 percent of total section delay, making it the dominant delay category.

(a) In 2023
Total VHD: 0.109 million veh-hr

(b) In 2024
Total VHD: 0.016 million veh-hr

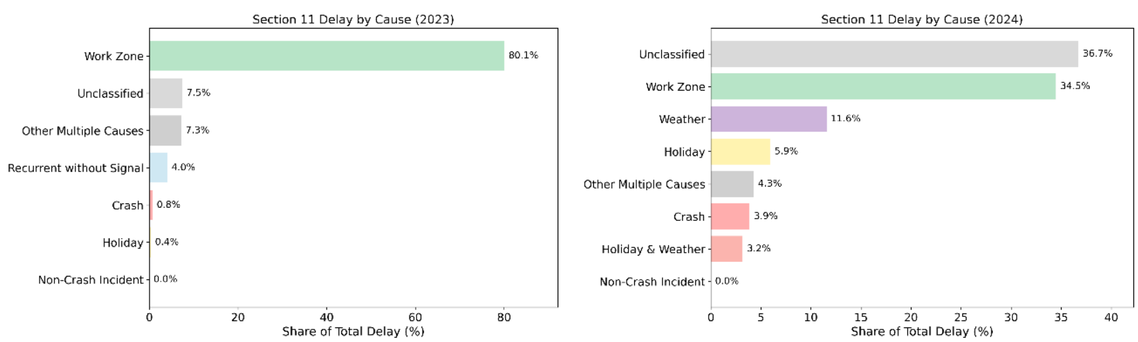

Figure 6-70: Delay Composition by Cause – US-18 County PD to US-18.

Principal Arterials: US-51

For US-51, unclassified delay with signal accounts for the largest share, indicating that a large portion of delay occurs on signalized TMCs but is not matched to a recorded event.

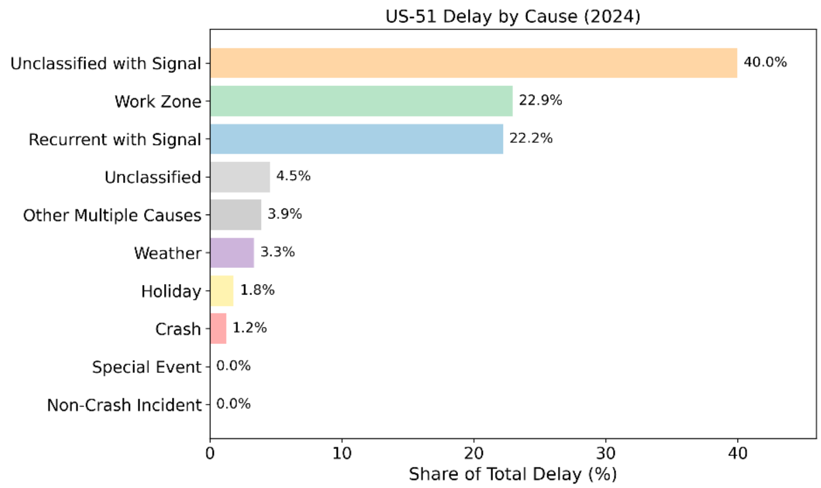

Figure 6-71: Delay Composition by Cause – US-51 (2024) (Total VHD: 0.77 million veh-hr).

In the US-8 to Minocqua section, the presence of a work zone results in nearly 57% of total delay being attributed to work-zone delay. In the Beltline to I-39/90/94 section, recurrent delay with signal and unclassified delay with signal are the dominant components, again showing that delay is concentrated at signalized segments.

(a) US-8 to Minocqua (WI-47)
Total VHD: 0.092 million veh-hr

(b) Beltline (US-12) to I-39/90/94 IC
Total VHD: 0.187 million veh-hr

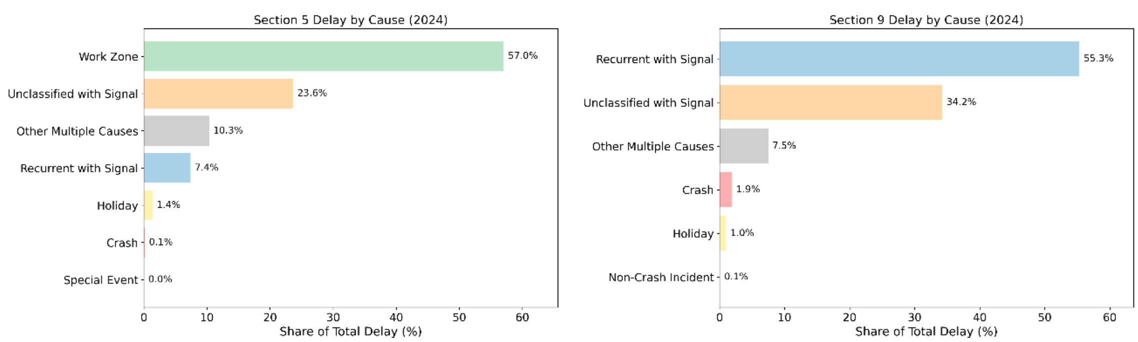

Figure 6-72: Delay Composition by Cause – US-51 WisDOT-Suggested Sections (2024).

Principal Arterials: US-53

For US-53, work-zone delay accounts for the largest share, consistent with the presence of work zones across much of the corridor, followed by unclassified delay.

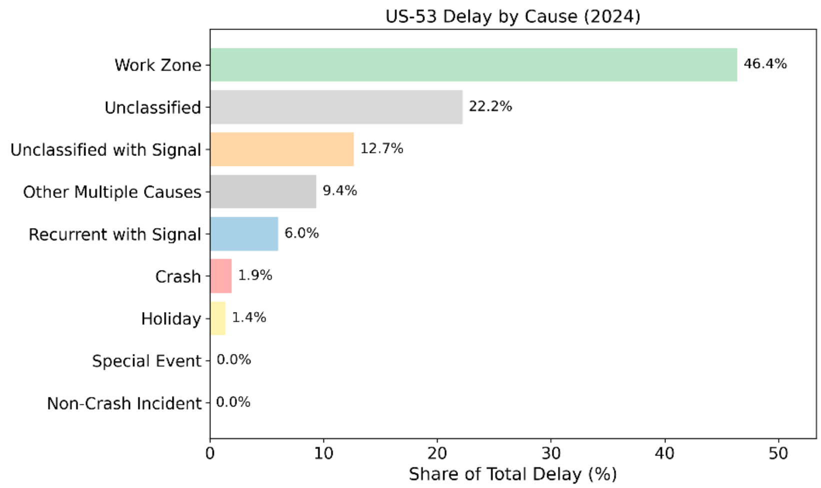

Figure 6-73: Delay Composition by Cause – US-53 (2024) (Total VHD: 0.18 million veh-hr).

In the I-94 to WI-29 section, unclassified delay is the largest component, and crash-related delay is also notable, accounting for 22% of total delay. Accordingly, further review of unreported events may be needed to better understand the source of the unclassified delay, and segments with frequent crash-related delay may warrant additional attention.

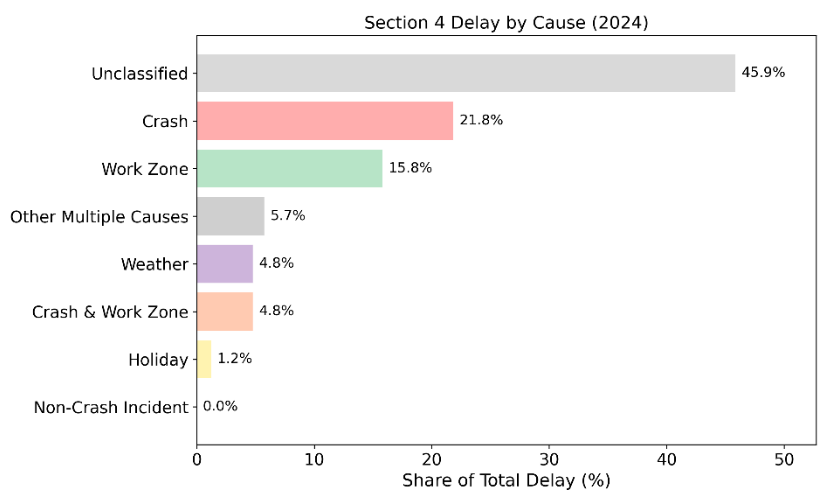

Figure 6-74: Delay Composition by Cause – US-53 I-94 to WI-29 (2024) (Total VHD: 0.006 million veh-hr).

Principal Arterials: US-151

For US-151, unclassified delay with signal and recurrent delay with signal account for the largest shares.

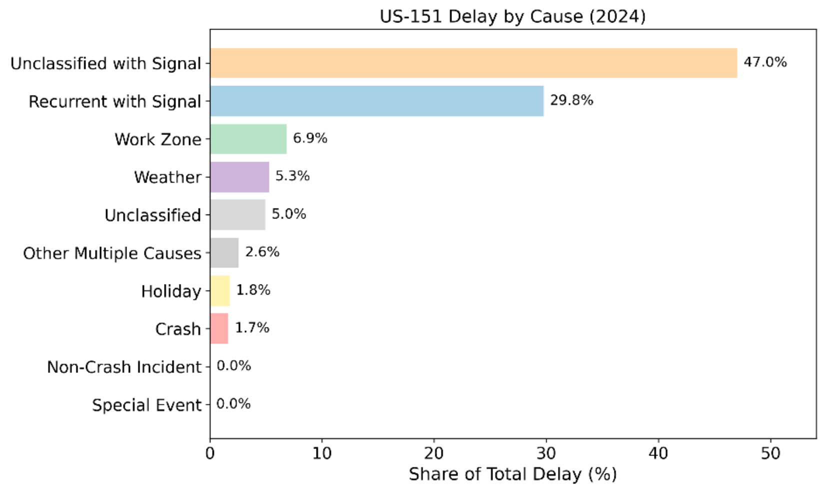

Figure 6-75: Delay Composition by Cause – US-151 (2024) (Total VHD: 0.70 million veh-hr).

In the Columbus to Waupun section, unclassified delay represents about 56% of total delay. Given the isolated, short-duration delay patterns observed earlier, this section may warrant additional review of NPMRDS data quality and possible unreported events on the representative dates. Some of this unclassified delay may also reflect queue spillback from signalized intersections to upstream non-signalized TMCs.

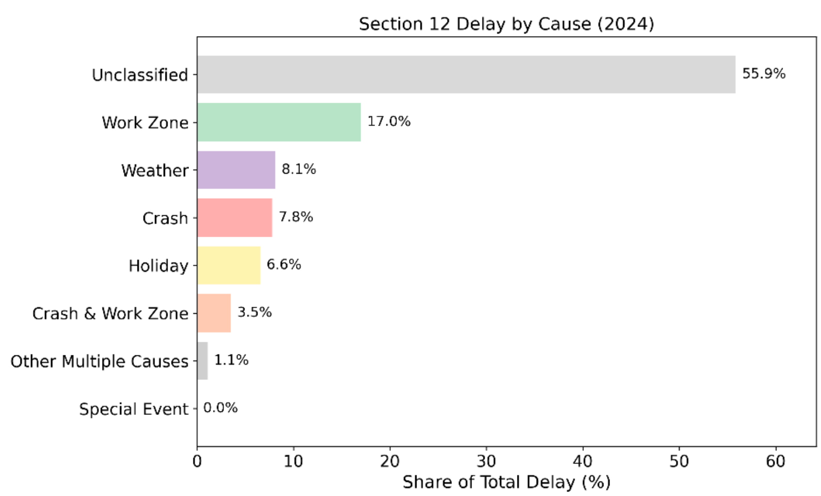

Figure 6-76: Delay Composition by Cause – US-151 Columbus to Waupun (2024) (Total VHD: 0.007 million veh-hr).

Principal Arterials: WI-172

For WI-172, unclassified delay accounts for the largest share. Delay is concentrated near localized hotspots and may be influenced by event-related travel demand, including

Packers game-day traffic.

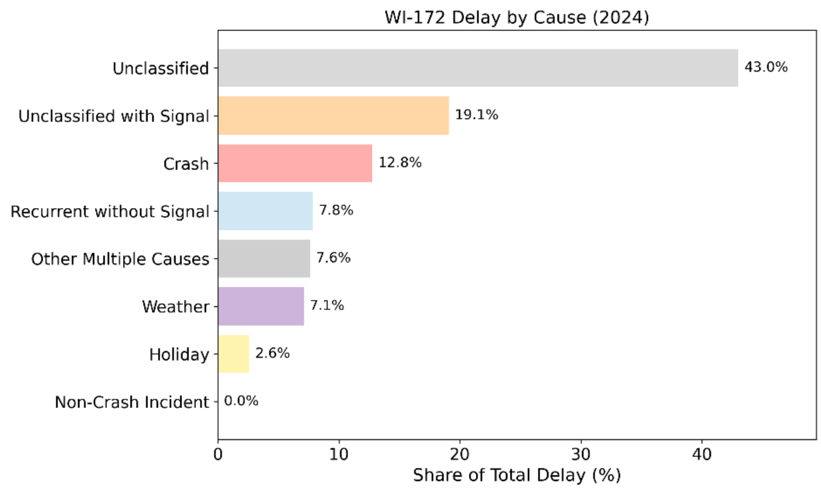

Figure 6-77: Delay Composition by Cause – WI-172 (2024) (Total VHD: 0.03 million veh-hr).

In the County EB to US-141 section, unclassified delay remains the largest component, and crash-related delay accounts for about 25% of total delay. However, delay in this section coincided with Packers game days and was not accompanied by a lane closure or other matched event, so much of the event-related delay remains classified as unclassified non-recurrent delay.

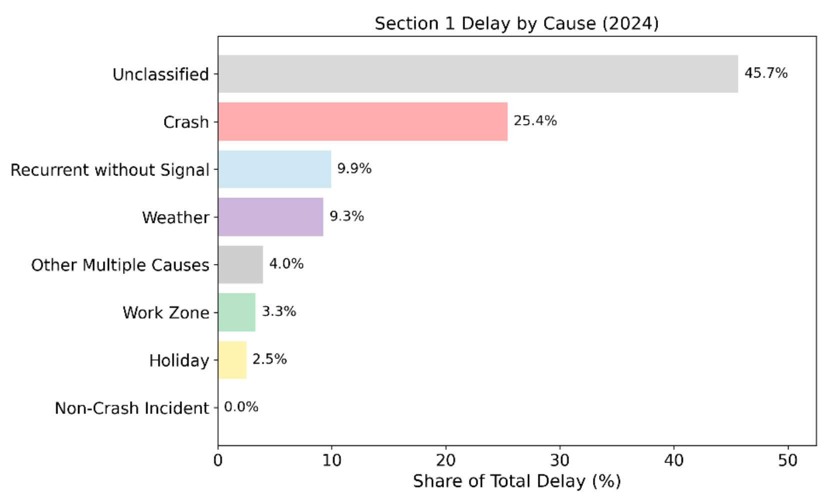

Figure 6-78: Delay Composition by Cause – WI-172 County EB to US-141 (2024) (Total VHD: 0.011 million veh-hr).

Other Principal Arterials: WI-19

For WI-19, work-zone delay accounts for more than 76% of total corridor delay, consistent with the corridor-wide presence of work zones.

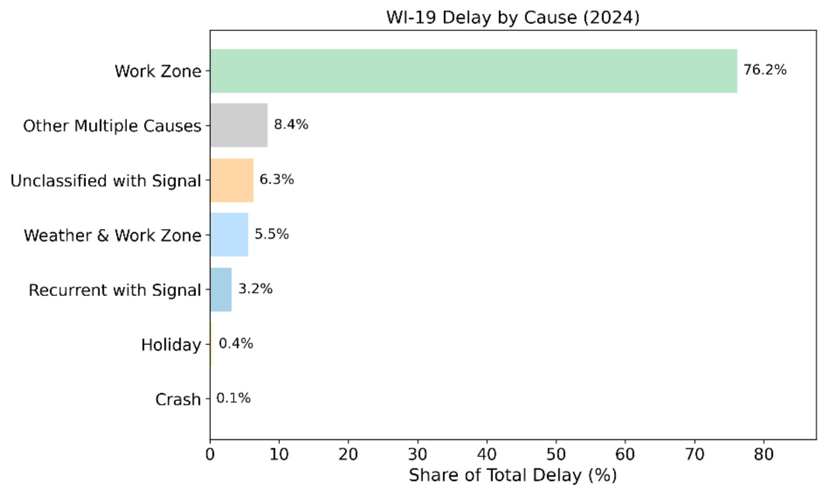

Figure 6-79: Delay Composition by Cause – WI-19 (2024) (Total VHD: 0.14 million veh-hr).

The Waunakee to Sun Prairie section shows a similar delay composition, with unclassified delay with signal accounting for about 8%, indicating that part of the delay is associated with the signalized segments.

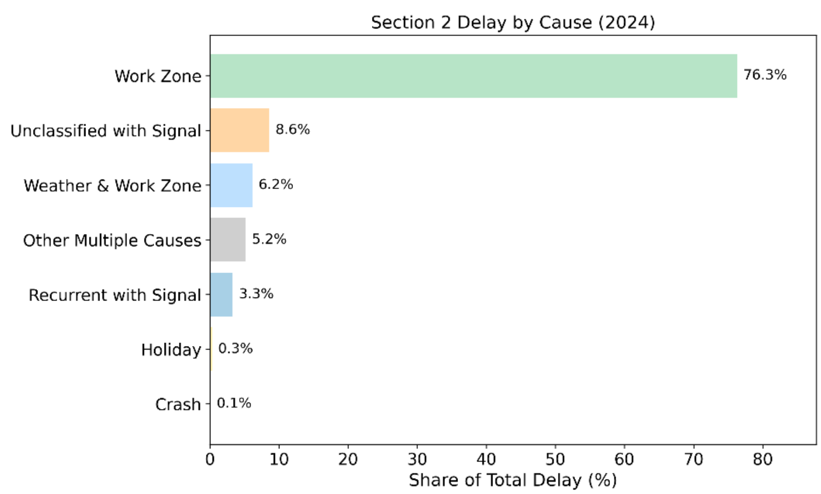

Figure 6-80: Delay Composition by Cause – WI-19 Waunakee to Sun Prairie (2024) (Total VHD: 0.041 million veh-hr).

Other Principal Arterials: WI-100

For WI-100, signal-related delay accounts for about 70% of total delay, with recurrent delay with signal and unclassified delay with signal forming the largest individual components. Work-zone delay is also present but smaller than the two signal-related categories.

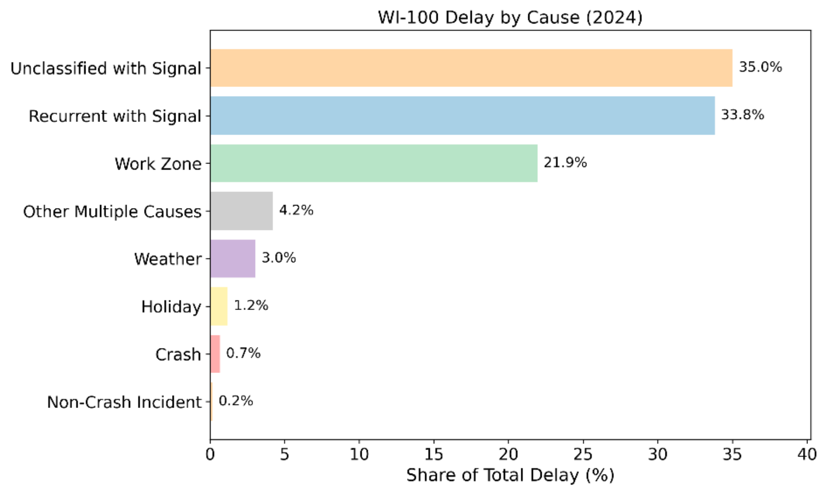

Figure 6-81: Delay Composition by Cause – WI-100 (2024) (Total VHD: 0.68 million veh-hr).

Other Principal Arterials: WI-125

For WI-125, work-zone delay accounts for the largest share, followed by recurrent delay with signal.

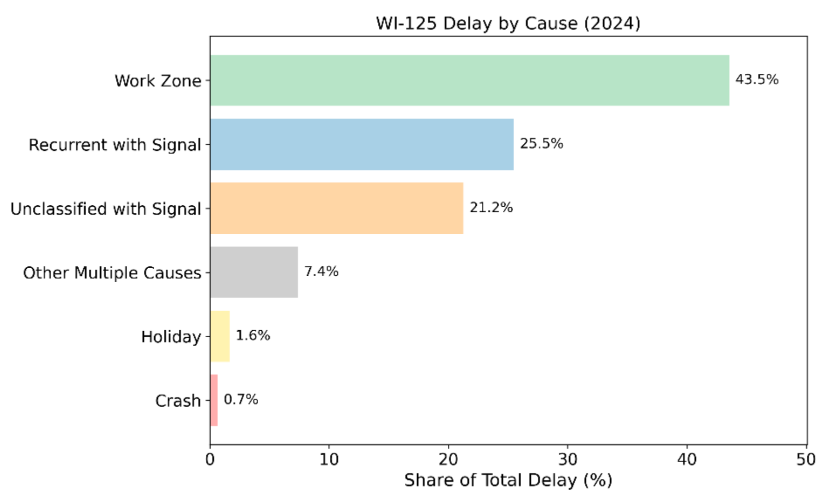

Figure 6-82: Delay Composition by Cause – WI-125 (2024) (Total VHD: 0.11 million veh-hr).

The I-41 to WI-55 section shows a similar composition, with work-zone delay remaining dominant and signal-related delay forming the next largest component, indicating that delay in this section reflects both work-zone conditions and signalized-segment effects.

The section-level total VHD exceeds the WI-125 corridor total because the section was selected spatially regardless of road name, while the corridor summary was based only on TMCs coded as WI-125 in the TMC lookup table.

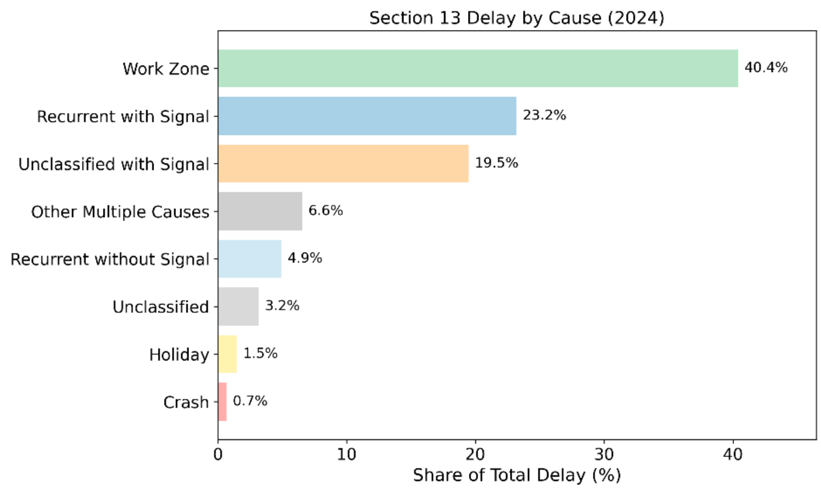

Figure 6-83: Delay Composition by Cause – WI-125 I-41 to WI-55 (2024) (Total VHD: 0.18 million veh-hr).

Other Principal Arterials: WI-190

For WI-190, work-zone delay accounts for the largest share, followed by recurrent delay with signal.

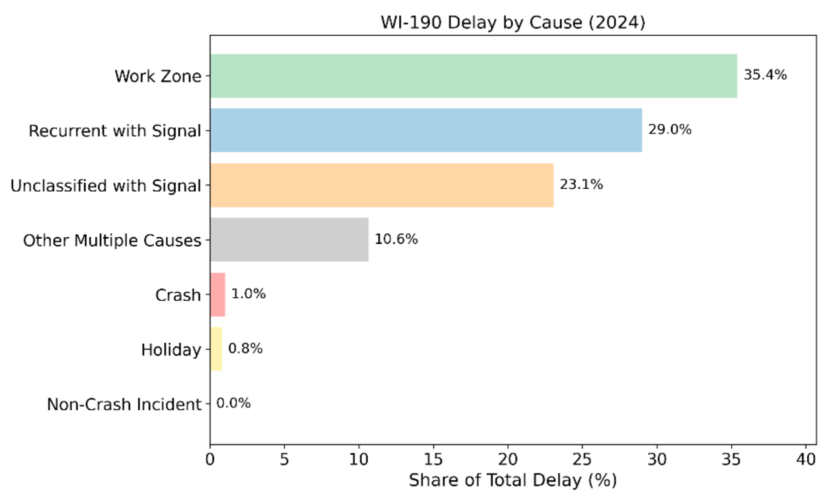

Figure 6-84: Delay Composition by Cause – WI-190 (2024) (Total VHD: 0.71 million veh-hr).

Representative Cause-Specific Case Studies

This section presents representative case studies to illustrate how specific causal factors are reflected in corridor-level delay. Selected examples focus on work zones, crashes, non-crash incidents, special events, and signal-related delay using WisDOT-suggested sections. For each case, the analysis combines a brief case summary, a space-time contour, and a case-specific overlay to describe the timing, location, and propagation of delay.

Work Zone Example

This case presents the northbound I-43 section from Marquette IC to County Line Rd, where work-zone delay accounted for a large share of total delay. Although queue formation immediately upstream of the work-zone start is not clearly visible in the contour, under the current framework, non-recurrent delay in the section is attributed to work-zone delay when an active work zone is present.

Table 6-9: Case Study Dashboard – Work Zone.

<table>
<tr><td>Overview</td><td>Section: I-43 Marquette IC to County Line Rd Northbound
Date: 2024-10-16 (Wednesday)
Observed delay: Recurrent 155.6 veh-hr | Non-recurrent 3174.0 veh-hr</td></tr>
<tr><td>Space-Time Contour</td><td>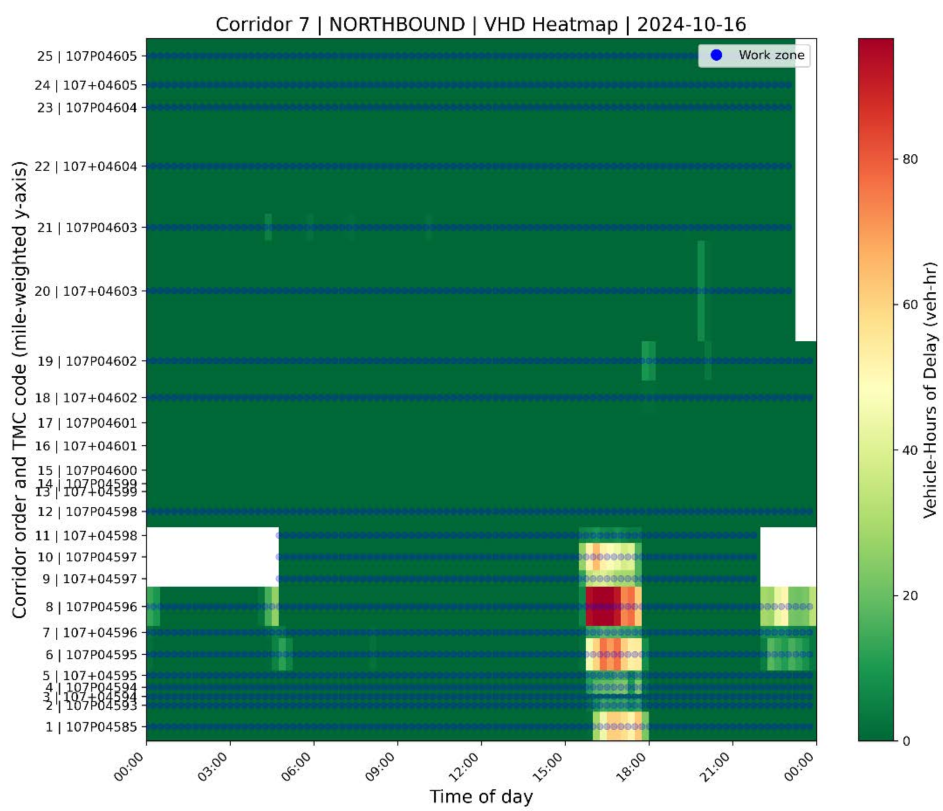
</td></tr>
</table>

Case Overlay	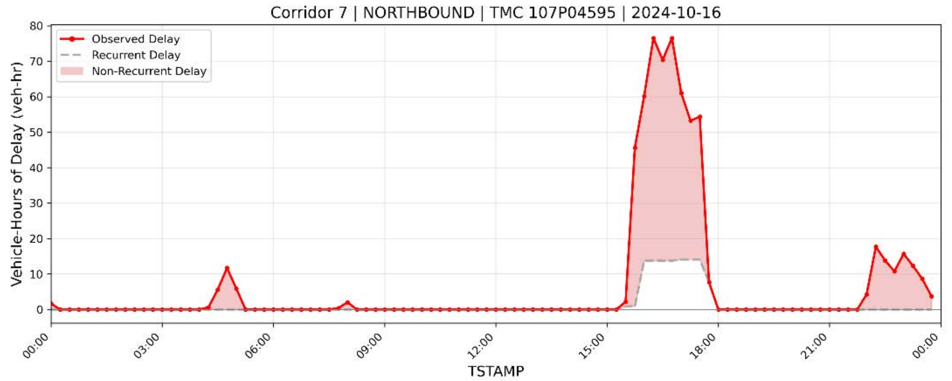
Baseline Overlay	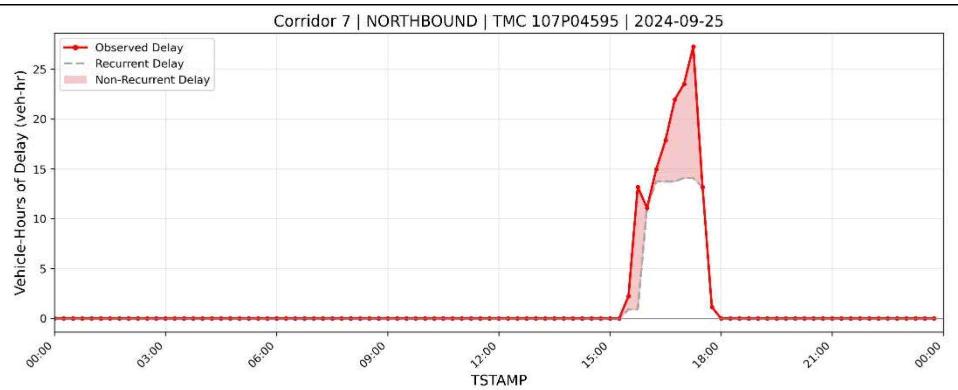
Note	Delay is observed in the upstream segments during the afternoon peak and persists from 3:30 to 5:45 PM. Under the current attribution framework, when a work zone is present, the resulting non-recurrent delay is assigned entirely to work-zone delay. Compared with the baseline case, in which no upstream work zone was present, the case day shows larger non-recurrent delay, indicating that the work zone intensified the delay.

Crash Example

These cases illustrate crash-related delay in two sections where the crash-related share is relatively high: US-53 from I-94 to WI-29 and WI-172 from County EB to US-141. The examples show how crash-related delay can remain localized or propagate upstream depending on the location and duration of the disruption.

Table 6-10: Case Study Dashboard – Crash 1.

Overview	Section: US-53 I-94 to WI-29 Southbound Date: 2024-07-07 (Sunday) Observed delay: Recurrent 0 veh-hr | Non-recurrent 549.7 veh-hr

Space-Time Contour	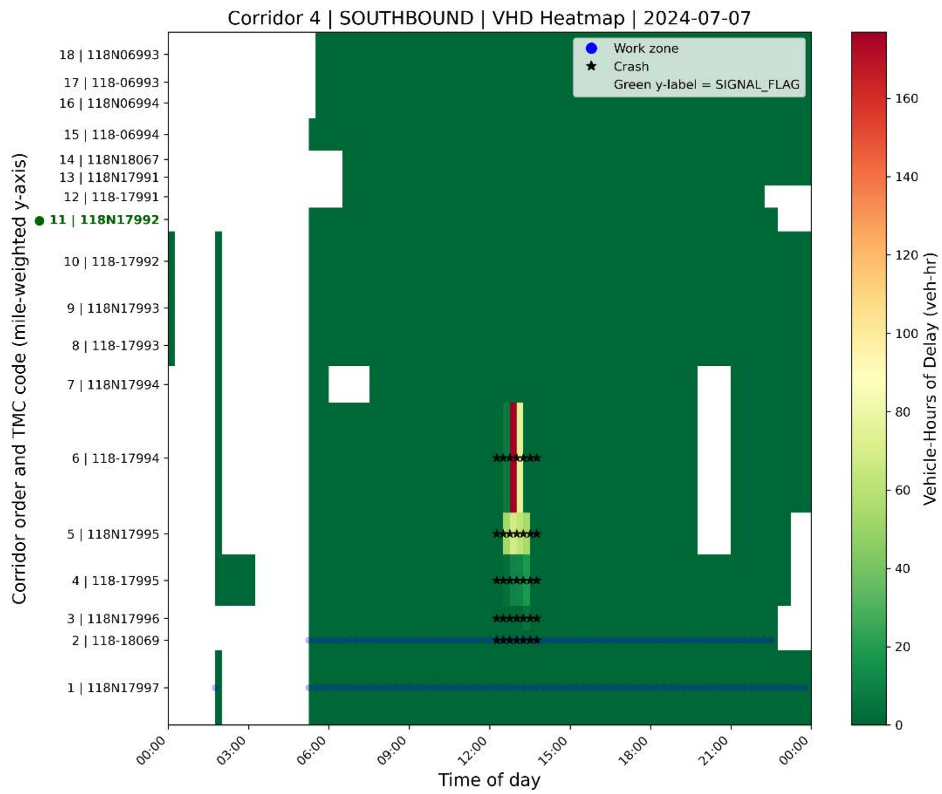
Case Overlay	Crash: severity O from 12:15 to 1 PM 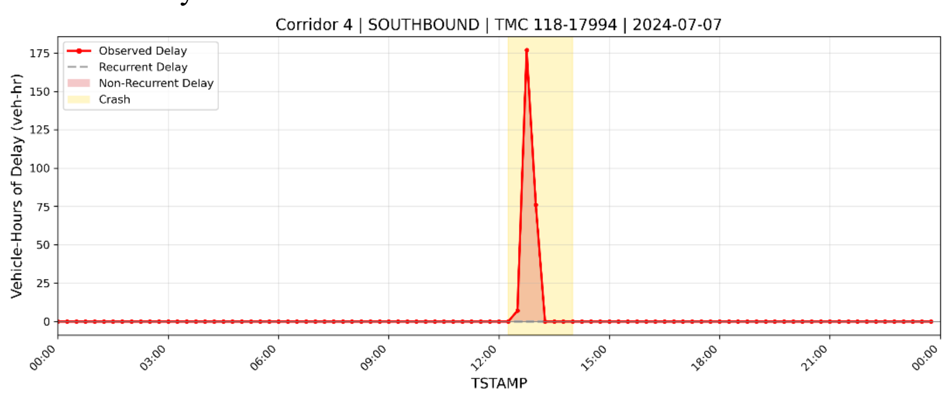
Note	A crash was reported on TMC 118-17994 at 12:15 PM. Delay was observed on the crash TMC until 1 PM, while delay on the upstream segments persisted until 1:15 PM. The resulting delay propagated upstream as far as TMC 118N17996, corresponding to an upstream distance of more than 3.5 miles.

Table 6-11: Case Study Dashboard – Crash 2.

Overview	Section: WI-172 County EB to US-141 Westbound Date: 2024-10-07 (Monday) Observed delay: Recurrent 0 veh-hr | Non-recurrent 468.7 veh-hr
Space-Time Contour	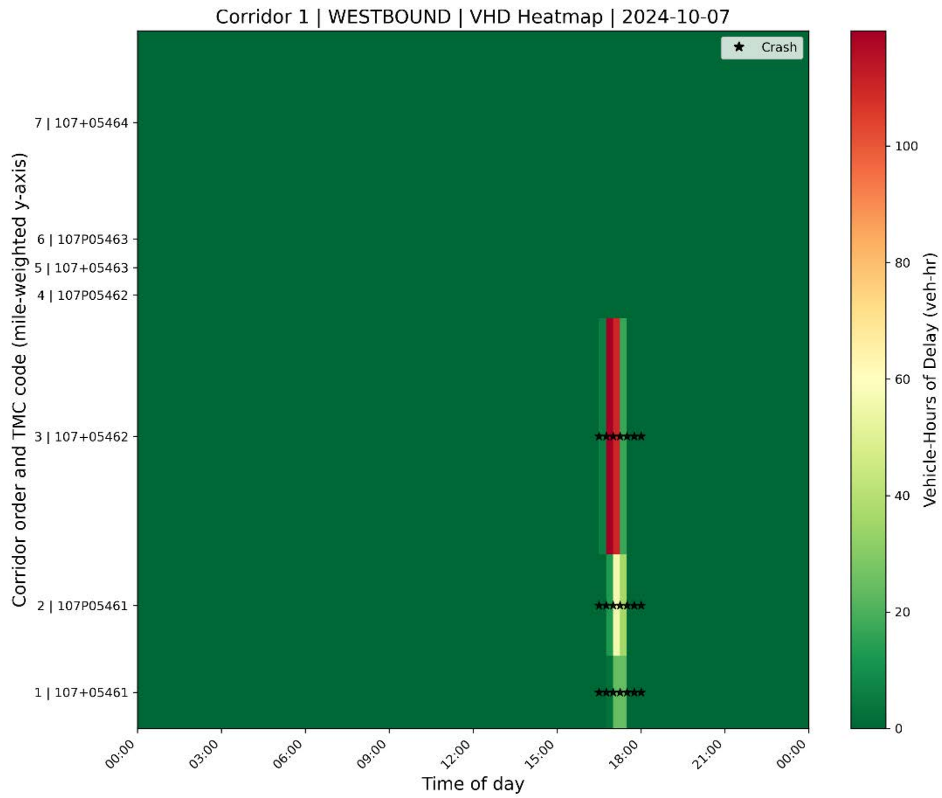
Case Overlay	Crash: severity B from 4:30 to 5:30 PM 
Note	A crash was reported on TMC 107+05462 at 4:30 PM, and delay was observed for approximately 60 minutes. The resulting delay propagated more than 2.6 miles upstream.

Non-Crash Incident Example

This case presents the southbound County Line to County Line section of I-41, where non-crash incident-related delay accounts for a large share of total delay. The example shows a prolonged incident that generated substantial non-recurrent delay and extended upstream congestion.

Table 6-12: Case Study Dashboard – Non-Crash Incident.

Overview	Section: I-41 County Line to County Line Southbound Date: 2024-10-18 (Friday) Observed delay: Recurrent 2541.5 veh-hr | Non-recurrent 9296.4 veh-hr
Space-Time Contour	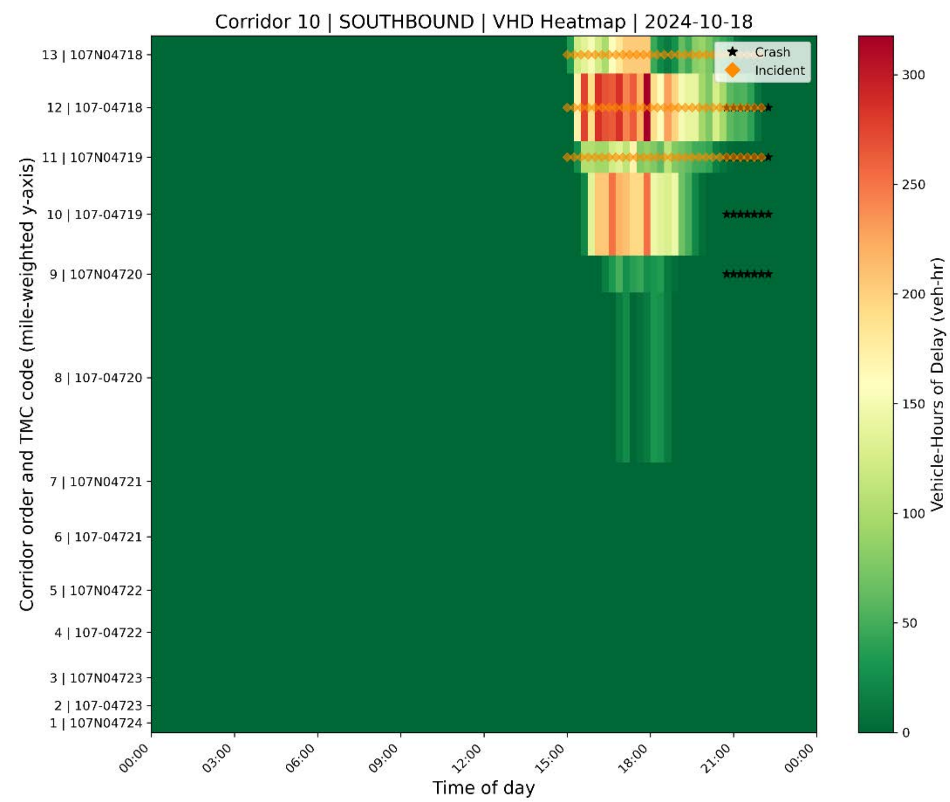
Case Overlay	Non-crash incident: fire (code 70) from 3 to 10 PM Crash: severity O from 8:45 to 9:30 PM

	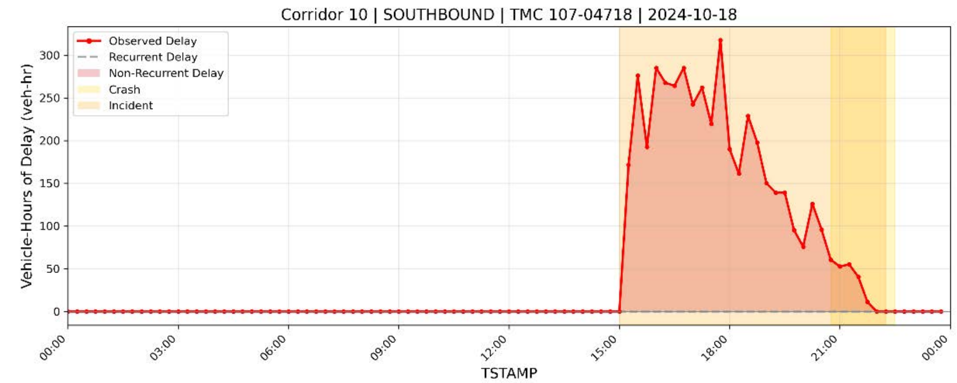
Note	A non-crash incident was reported at 3 PM on downstream TMC 107-04717, after which congestion developed along the corridor section. The largest delay occurred on upstream TMC 107-04718, and delay persisted until the incident was cleared at 10 PM. The delay propagated upstream as far as TMC 107-04720, corresponding to more than 7.5 miles. A crash was then reported at 8:45 PM, overlapping with the incident-related congestion. During this overlap, non-recurrent delay associated with the crash continued until 10 PM, lasting approximately 75 minutes, and its impact extended up to 1.76 miles upstream.

Special Event Example

This case presents the County EB to US-141 section of WI-172, where delay associated with game-day travel demand is clearly observed. The example highlights directional differences in delay before and after the game and shows how special-event travel demand can overlap with other reported events.

Table 6-13: Case Study Dashboard – Special Event (Game).

Overview	Section: WI-172 County EB to US-141 Date: 2024-09-15 (Sunday) Observed delay Westbound: Recurrent 49.4 veh-hr | Non-recurrent 48.3 veh-hr Eastbound: Recurrent 179.5 veh-hr | Non-recurrent 416.4 veh-hr

Space-Time Contour	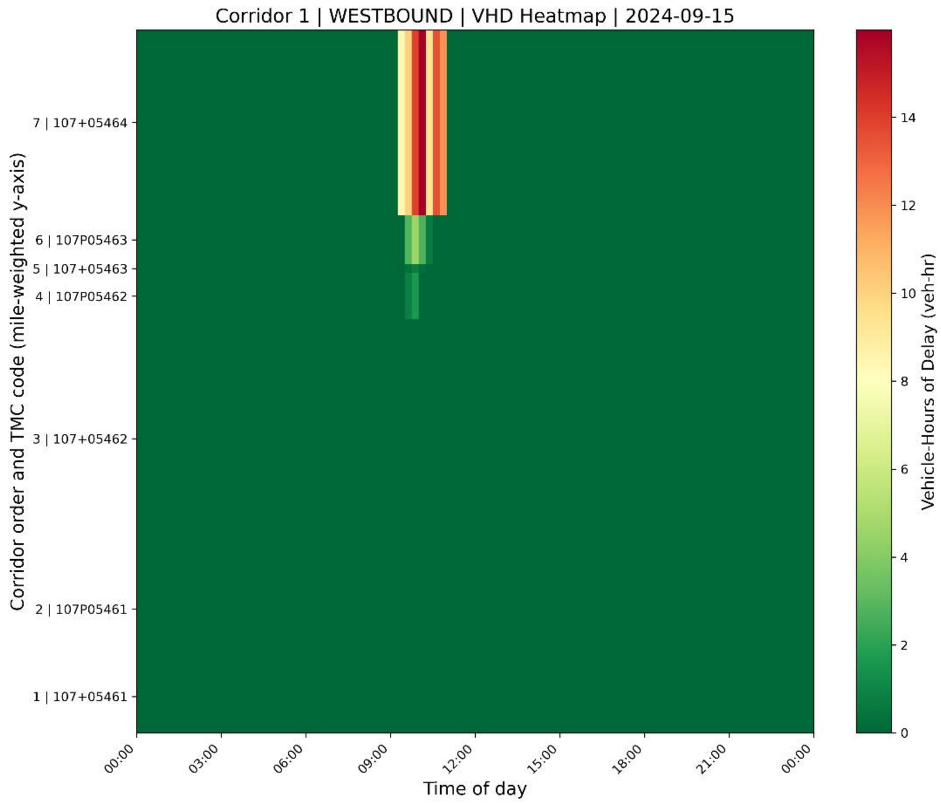 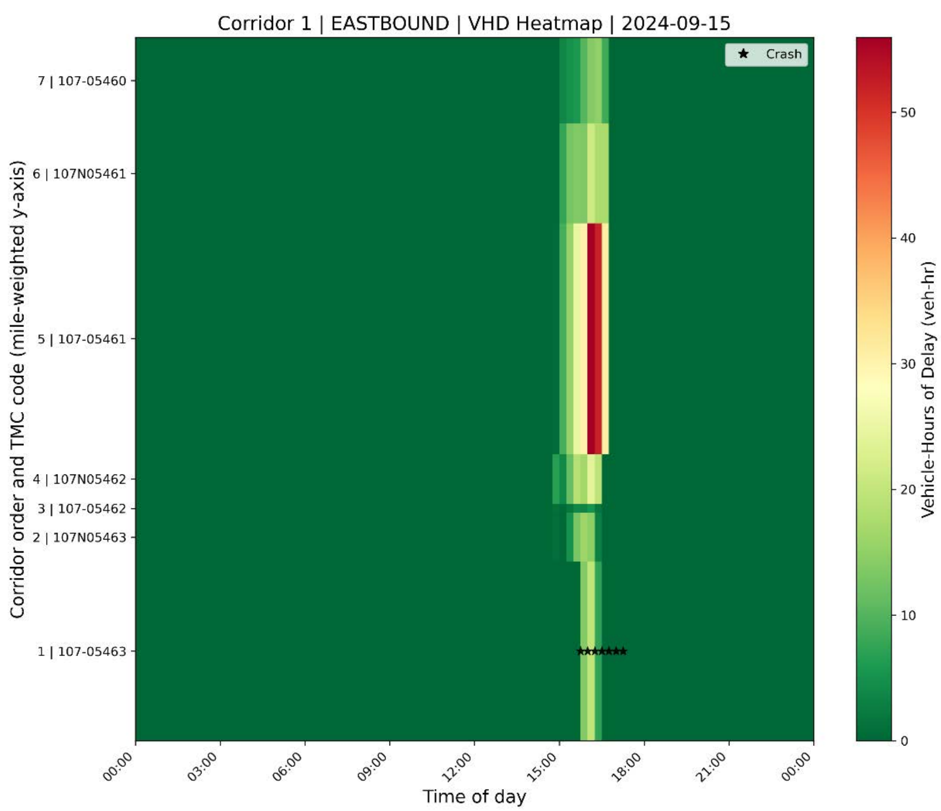

<table>
<tr><td>Case Overlay</td><td>Green Bay Packers game: started at 1 PM
Crash: severity O from 3:45 to 4:30 PM in the eastbound direction
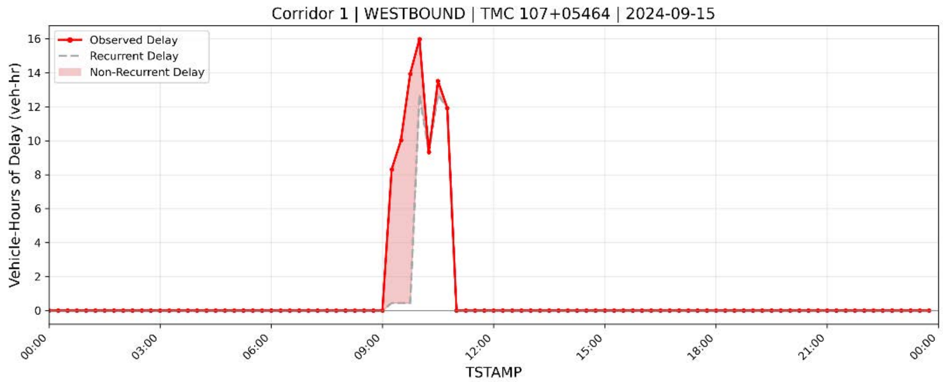

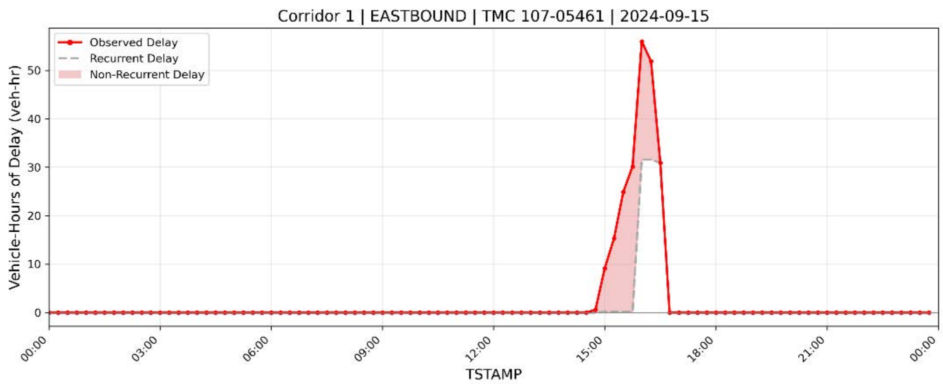

</td></tr>
<tr><td>Note</td><td>On the Packers game day, delay is observed in the westbound direction during the morning as traffic approaches the stadium and in the eastbound direction after 3 PM as traffic departs the area. The eastbound delay is larger than the westbound delay and persists for about two hours. A crash was also reported in the eastbound direction at 3:45 PM and appears to overlap with the existing game-related delay.</td></tr>
</table>

Signal-Related Example

This case presents the southbound Beltline to I-39/90/94 interchange section of US-51, where recurrent delay with signal and unclassified delay account for substantial shares of total delay. The example illustrates how delay concentrated at a signalized segment can extend to an adjacent upstream TMC as queue spillback, while much of the resulting spillback remains classified as unclassified under the current framework.

Table 6-14: Case Study Dashboard – Signal-Related Delay.

Overview	Section: US-51 Beltline to I-39/90/94 interchange Southbound Date: 2024-10-03 (Thursday) Observed delay: Recurrent 251.2 veh-hr | Non-recurrent 47.0 veh-hr

Space-Time Contour	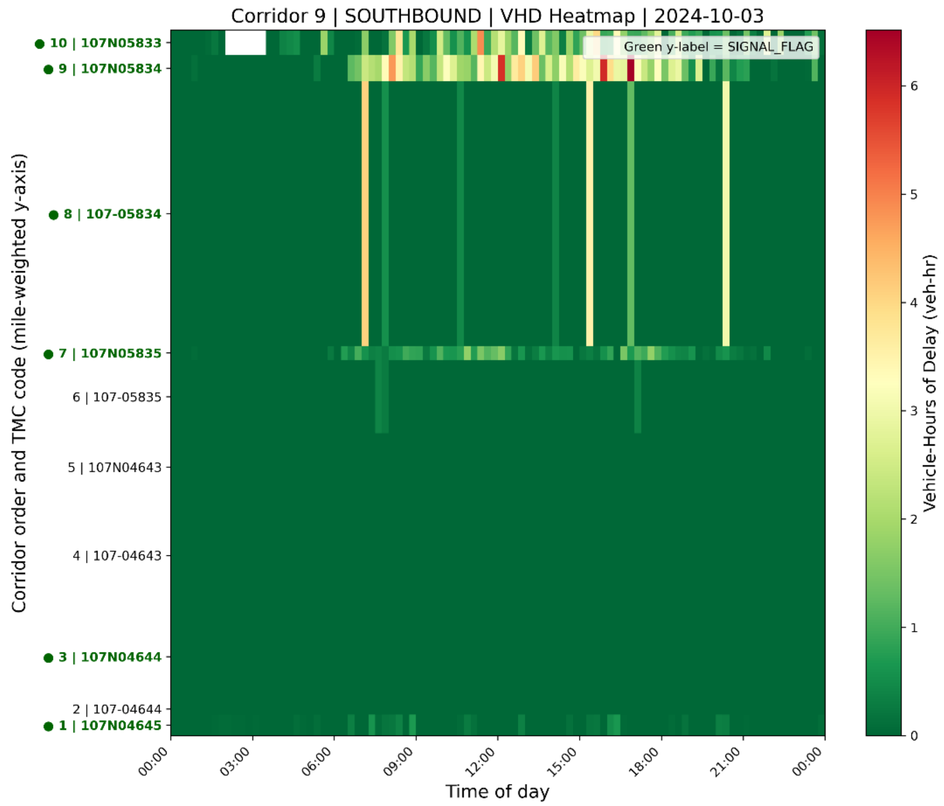
Case Overlay	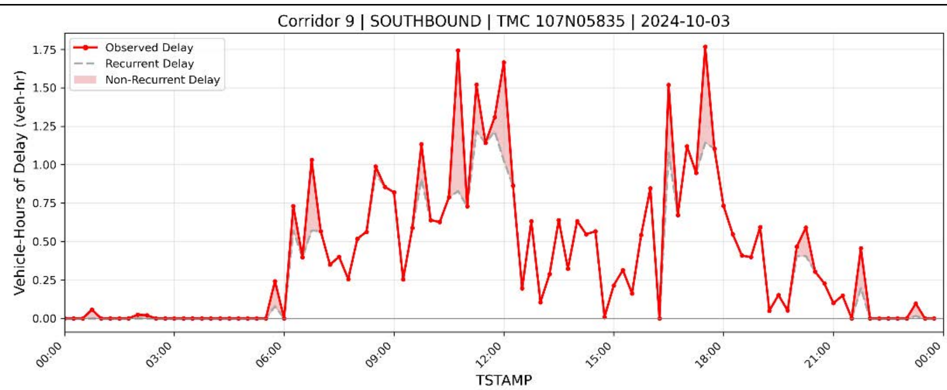 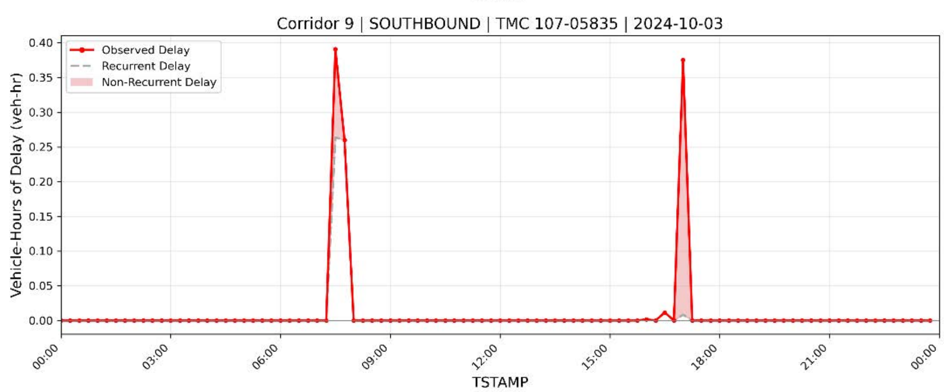

Note	Delay is observed near signalized segments throughout the daytime period. The delay observed on the upstream TMC 107-05835 appears to reflect queue spillback from this signalized intersection. However, because this upstream TMC is not coded as a signalized segment, the resulting non-recurrent delay is classified as unclassified.

6.4. Corridor-Level Delay Causation Modeling

This section presents corridor-level delay causation modeling for the selected corridors. These models are developed primarily to examine how delay is associated with corridor characteristics, traffic demand, and event conditions, rather than to provide operational forecasts for the next time step. The analysis uses TMC-level 15-minute observations to examine how delay is associated with traffic demand, event indicators, and corridor characteristics. Baseline, extended, machine-learning, and probabilistic models are compared to evaluate how the major factors associated with delay differ across functional classes. The tabulated modeling results focus on the three representative corridors (I-41, US-18, and WI-125), while selected figures include all 12 selected corridors to provide a broader comparison of corridor-level patterns.

Summary

The modeling results indicate that corridor delay is shaped by traffic demand, event conditions, corridor structure, and especially short-term delay correlation. Baseline OLS models provided interpretable signs and significance patterns. Geometry terms added only limited improvement, whereas lagged variables substantially improved model fit. The LightGBM models were broadly consistent with these findings and captured additional nonlinear variation in the arterial corridors. The probabilistic extension further showed that the likelihood of observing non-recurrent delay varies across corridors.

The previous sections show that corridor delay is shaped by a combination of recurring traffic conditions, work zones, signalized operations, and event-related disruptions, with the dominant cause varying by functional class and corridor. Work-zone delay is the most common major cause across the selected corridors, while signal-related and unclassified delay are especially important in arterial and other principal corridors. The case studies show that non-recurrent delay can remain localized or propagate upstream depending on the event type, event location, and corridor setting. The modeling results indicate that short-term delay correlation, traffic demand, and corridor structure are key factors associated with delay. Together, these findings provide a corridor-level interpretation of delay causation that complements the broader statewide analysis.

Table 6-15 summarizes the main comparative findings for each selected corridor, highlighting the dominant delay causes, representative characteristics, and key implications from the attribution, case study, and modeling analyses.

Table 6-15: Comparative Findings by Selected Corridor.

Functional Class	Corridor	Dominant Delay Cause	Representative Finding	Modeling Note
Interstate	I-41	Work zone and unclassified delay	Delay varies by section	Strong temporal delay correlation; Heavy vehicle ratio has a negative impact on delay
	I-43	Work zone and recurrent delay without signal	Peak-period bottlenecks dominate	
	I-94	Recurrent delay without signal and work zone	Peak-period bottlenecks dominate	
Principal arterial	US-18	Work zone and recurrent delay with signal	Peak-period signal-related bottlenecks dominate	Signal effects are important in the corridor-level models
	US-51	Unclassified with signal and work zone	Delay is concentrated at signalized segments	
	US-53	Work zone and unclassified delay	Work zone delay dominates	
	US-151	Unclassified with signal and recurrent with signal	Delay is concentrated at signalized segments	
	WI-172	Unclassified delay dominates	Game-day demand and localized hotspots are important	
Other principal	WI-19	Work zone dominates	Work zone delay dominates	Greater heterogeneity and

arterial	WI-100	Signal-related delay dominates	Delay is concentrated at signalized segments	lower model fit; hourly volume effects are important
	WI-125	Work zone and recurrent with signal	Work zone delay dominates	
	WI-190	Work zone and recurrent with signal	Work zone delay dominates	

Modeling Framework

To reflect different facility contexts, three representative corridors were selected by functional class: I-41 for interstate facilities, US-18 for 'principal arterials', and WI-125 for 'other principal arterials'. These corridors were used to compare how the relationships between delay and its contributing factors vary across facility types.

Table 6-16 summarizes the dependent and explanatory variables used in the corridor-level delay causation models. In addition to traffic-related and severity-based event variables, geometry-related variables were added to account for TMC-specific structural differences that may condition how delay forms and accumulates. Lagged variables were then introduced to represent temporal dependence common in time-series data and adjacent-segment correlation in delay. Delay evolves over time and space and may exhibit serial correlation beyond what is captured by the baseline event-and-demand specification. Geometry features may affect delay differently across corridors and even across segments within the same corridor. For example, the effect of the number of through lanes may be positively associated with delay where additional lanes coincide with higher traffic volumes, but it may also be negatively associated with delay where added lane capacity reduces vulnerability to breakdown. A similar ambiguity applies to free-flow speed. Higher free-flow speed may make it less likely that speeds fall below the delay threshold, but when delay does occur, the associated VHD may still be large because such segments often carry higher volumes. Functional class and facility type were treated as categorical variables, so no single directional relationship was assumed.

Table 6-16: Modeling Variables Used in Corridor-Level Causation Models.

Variable Group	Variable	Temporal Resolution	Expected Relationship
Dependent variable	Total delay	15-minute	-
	Non-recurrent delay	15-minute	-
Crash	Minor crash with severity O/C/B	15-minute	Positive
	Major crash with severity A/K	15-minute	Positive
Incident	Non-crash incident or emergency	15-minute	Positive
Work zone	Partial work-zone closure	15-minute	Positive
	Full work-zone closure	15-minute	Positive
Special event	Special event with lane closure	15-minute	Positive
Holiday	Holiday indicator	Daily	Negative
Heavy weather	Heavy rain/snow event	Daily	Positive
Signal	Signal indicator	Yearly	Positive
Traffic demand	Hourly volume	Hourly	Positive
	Heavy vehicle ratio	Yearly	Varies
Geometry	Length of TMC segment	Yearly	Unclear
	Number of through lanes	Yearly	Varies
	Free-flow speed of TMC segment	Monthly	Varies
	Functional class	Yearly	Unclear
	Facility type	Yearly	Unclear
Lagged variable	Previous 15-minute delay	15-minute	Positive
	Upstream TMC delay in the previous 15-minute interval	15-minute	Positive
	Downstream TMC delay in the previous 15-minute interval	15-minute	Positive

Baseline Interpretable Model

Across the three representative corridors, the baseline models showed that most explanatory variables were statistically significant, although the sign and magnitude of some variables differed by corridor. Table 6-17 summarizes the significant factors identified in the baseline regression models for total delay across the three representative corridors. The results indicate that some delay factors are broadly consistent across functional classes, whereas others are more corridor-specific. All baseline variables were carried forward to the subsequent modeling stages so that their effects could be re-evaluated in the extended specifications.

Table 6-17: Significant Factors in Baseline Regression Models for Total Delay.

Factor	Sign			Significance			Interpretation
	I	P	O	I	P	O	
Minor crash	+	+	+	***	***	***	Associated with higher delay
Major crash	+	+		***	***	.	Generally associated with higher delay when observed
Non-crash incident	+	-		***	***	.	Effects vary by corridor
Partial work-zone closure	+	+	+	***	***	***	Associated with higher delay
Full work-zone closure	+	+	-	***	*	***	Effects vary by corridor
Special event	-	+	-	***	*	***	Effects vary by corridor
Holiday	+	+	+	***	***	**	Associated with higher delay
Heavy weather	+	+	+	***	***	**	Associated with higher delay
Signal	-	+	+	***	***	***	Effects are more important outside interstate contexts
Hourly volume	+	+	+	***	***	***	Higher demand associated with higher delay
Heavy vehicle ratio	-	-	+	***	***	***	Effects vary by corridor

Functional class I: Interstate I-41; P: Principal arterial US-18; O: Other principal arterial WI-125

Sign +: positive; -: negative

Significance levels: ***p <0.001; **p <0.01; *p <0.05; . non-significant at 5% level

While Table 6-17 focuses on the three representative corridors, the following standardized coefficient figures include all 12 selected corridors to provide a broader comparison of corridor-level model patterns. Figure 6-85 compares the standardized coefficients from the baseline models for total delay across the selected corridors. Hourly volume has one of the largest positive coefficients in most corridors, indicating that traffic demand is one of the most consistent predictors of total delay. Signal presence is especially important in the ‘principal arterial’ and ‘other principal arterial’ corridors, whereas its coefficient is approximately zero in the interstate corridors. Both minor and major crash variables have positive coefficients across all corridors, confirming that crashes are generally associated with increased delay. The heavy vehicle ratio shows mixed patterns, with negative or near-zero coefficients in several interstate corridors and larger positive coefficients in several arterial corridors. The work-zone coefficients also vary across corridors, with full work-zone closures showing both positive and negative coefficients depending on the corridor. Heavy weather likewise has positive coefficients across all corridors, suggesting a consistent association with increased delay. By contrast, the estimated coefficients for holidays, non-crash incident indicators, and special events are smaller and clustered near zero, with limited variation compared with the larger demand, signal, and heavy vehicle ratio variables. Overall, the figure shows that corridor delay is influenced by a common set of factors, but both the magnitude and relative importance of these effects differ across functional classes, and corridor-specific interpretation remains necessary to reflect operating conditions and event contexts.

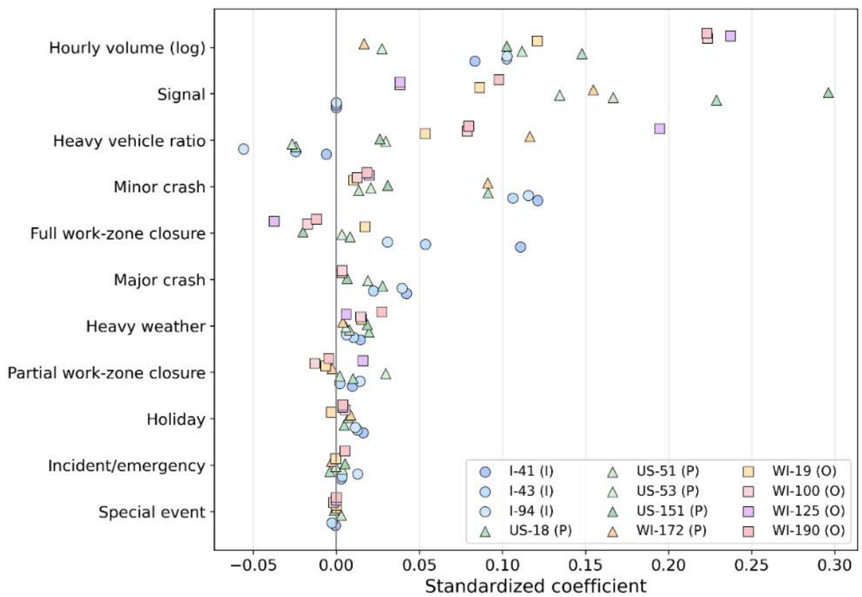

Figure 6-85: Standardized Coefficients from Regression Models for Total Delay.

Figure 6-86 compares standardized coefficients for non-recurrent delay. Compared with the total-delay models, hourly volume and signal remain important predictors, but event-related variables become relatively more prominent in the non-recurrent delay models. This pattern suggests that non-recurrent delay is more sensitive to event conditions, while still being influenced by broader demand and operating factors. Common patterns by functional class are also less pronounced, indicating that non-recurrent delay is more sensitive to corridor- and segment-specific conditions.

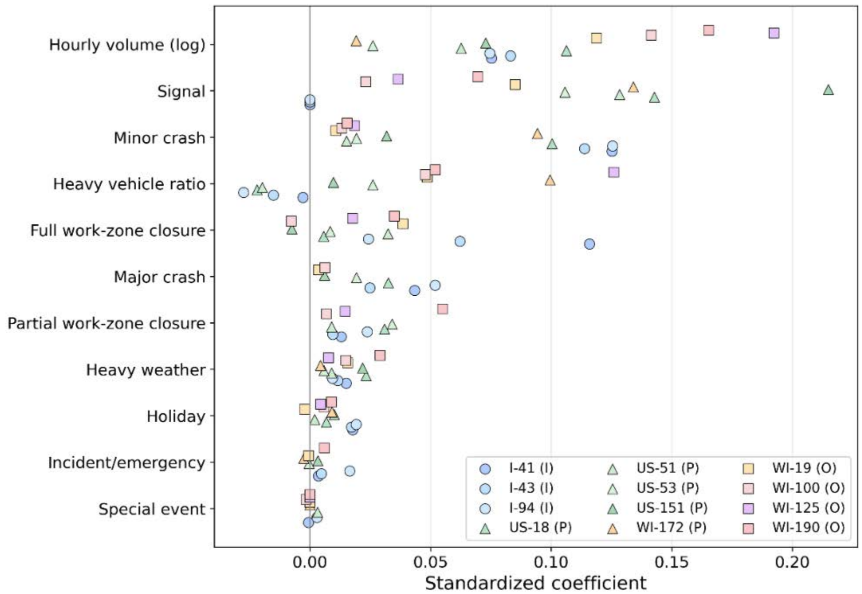

Figure 6-86: Standardized Coefficients from Regression Models for Non-Recurrent Delay.

Baseline regression model performance was generally low for both total and non-recurrent delay, with total-delay models performing better for US-18 and WI-125 but not for I-41. Non-recurrent delay is defined relative to the historical recurrent baseline, which can make it more difficult to explain using the baseline event-and-demand specification alone. Among the three corridors, I-41 shows the highest adjusted R^2, but its negative test R^2 indicates poor out-of-sample performance, meaning that the fitted model did not generalize well to unseen data.

Table 6-18: Baseline Regression Specifications.

Corridor	Dependent Variable	Adjusted R^2	Test R^2
I-41	Total delay	0.215	-0.025
	Non-recurrent delay	0.218	-0.021
US-18	Total delay	0.117	0.118
	Non-recurrent delay	0.095	0.083
WI-125	Total delay	0.085	0.086
	Non-recurrent delay	0.047	0.048

The low predictive performance of the baseline model is not unexpected. A linear model using only event and traffic-demand variables cannot fully capture the dynamic and spatial nature of corridor delay, especially when delay formation depends on persistence, spillback, and local operating conditions. In addition, no data were available on operational features such as signal timing that could more directly represent the dynamic delay formation. Positive delay (delay occurrence) also occupies only a small share of the full 15-minute

TMC-level sample, which makes model fitting more difficult. This is especially evident for I-41, where the positive shares of both total and non-recurrent delays are much lower than in the arterial corridors. These results motivate the extended model specifications that incorporate corridor- and TMC-specific geometry features.

Table 6-19: Sample Size and Positive Delay Share.

Corridor	Number of Rows	Positive Share of Total VHD	Positive Share of Non-Recurrent VHD
I-41	14,431,521	1.37 %	1.26 %
US-18	7,222,801	12.58 %	8.04 %
WI-125	547,030	23.42 %	18.21 %

<u>Extended Dynamic Models</u>

To improve explanatory power while retaining interpretability, significant geometry terms were added to the baseline event-and-demand model. These variables improved model fit modestly in all three representative corridors, indicating that TMC structure contributes to delay variation beyond event and demand conditions alone.

Table 6-20 shows that most segment and geometry terms are statistically significant across the representative corridors, although their signs differ by functional class. This suggests that structural corridor characteristics influence delay, but their effects are not uniform across interstate and arterial contexts.

Table 6-20: Significant Segment and Geometry Terms in the Extended Models.

Factor	Sign			Significance			Interpretation
	I	P	O	I	P	O	
Length of TMC segment	+	+	-	***	***	***	TMC segment length is associated with delay, but the sign varies by corridor; not interpreted as a direct geometry effect
Number of through lanes	-	+	-	***	***	***	Lane configuration affects delay differently across corridors
Free-flow speed of TMC segment	-	-	+	***	***	***	Effects vary by corridor
TMC functional class	+	-		***	***	.	Functional class helps explain delay in the interstate and principal arterial models
TMC facility type	+	-	+	***	***	***	Delay varies systematically across facility types

Functional class I: Interstate I-41; P: Principal arterial US-18; O: Other principal arterial WI-125

Sign +: positive; -: negative

Significance levels: ***p <0.001; **p <0.01; *p <0.05; . non-significant at 5% level

The extended models then added lagged delay variables to account for the temporal evolution of delay and the serial dependence remaining after the baseline specification. The purpose of these terms was not to treat past delay as a causal factor in itself, but to represent short-term temporal dependence and adjacent-segment correlation. The temporal lag term represents delay in the same TMC during the previous 15-minute interval, while the spatial lag terms represent delay in adjacent upstream and downstream TMCs during the previous 15-minute interval within the same corridor and direction. Only statistically significant lagged terms were retained.

Table 6-21 shows that all lagged delay variables were positive and highly significant across the three representative corridors. This indicates that corridor delay exhibits strong short-term temporal dependence as well as spatial correlation with adjacent segments. Relative to the geometry terms, the lagged variables explain a larger share of the remaining variation left unexplained by the baseline model.

Table 6-21: Significant Lagged Terms in the Extended Models.

Factor	Sign			Significance			Interpretation
	I	P	O	I	P	O	
Previous 15-minute delay	+	+	+	***	***	***	Current delay is strongly correlated with recent delay in the same TMC
Upstream delay in the previous 15-minute interval	+	+	+	***	***	***	Upstream conditions are associated with subsequent local delay
Downstream delay in the previous 15-minute interval	+	+	+	***	***	***	Downstream conditions are associated with subsequent local delay

Functional class I: Interstate I-41; P: Principal arterial US-18; O: Other principal arterial WI-125

Sign +: positive; -: negative

Significance levels: ***p <0.001; **p <0.01; *p <0.05; . non-significant at 5% level

Table 6-22 compares model fit for the three representative corridors after adding significant geometry terms and then lagged delay terms. Geometry variables improved fit only slightly, whereas lagged terms produced substantial gains in all three corridors. The improvement was largest for I-41, followed by US-18 and WI-125, indicating that delay dynamics are especially important for the interstate corridor. Based on these results, the machine-learning model was developed using the variables retained in the final extended specification.

Table 6-22: Extended Total-Delay Model Fit Comparison.

Corridor	Model	Added Terms	Adjusted R2	Change from Baseline
I-41	Geometry selected	Length, through-lanes, FFS, facility type, functional system	0.231	0.016
	Final selected	Geometry + lagged terms	0.779	0.564
US-18	Geometry selected	Length, through-lanes, FFS, facility type, functional system	0.133	0.016
	Final selected	Geometry + lagged terms	0.370	0.253
WI-125	Geometry selected	Length, through-lanes, FFS, facility type	0.094	0.008
	Final selected	Geometry + lagged terms	0.239	0.154

Figure 6-87 compares the adjusted R^2 values of the baseline, geometry-selected, and final selected models across all selected corridors. Overall, final model fit is generally higher for interstate corridors than for ‘principal arterial’ and ‘other principal arterial’ corridors. Adding geometry terms yields only modest improvement over the baseline model across most corridors, whereas the inclusion of lagged delay variables produces a substantial increase in explanatory power. This improvement is especially pronounced for the interstate corridors, indicating stronger short-term delay correlation and more stable spatiotemporal delay propagation. At the same time, the variation in adjusted R^2 across corridors within the same functional class shows that corridor-specific context remains important, and it also suggests that linear models are less able to represent delay in ‘principal arterial’ and ‘other principal arterial’ corridors, where signals and greater segment-to-segment heterogeneity play a larger role.

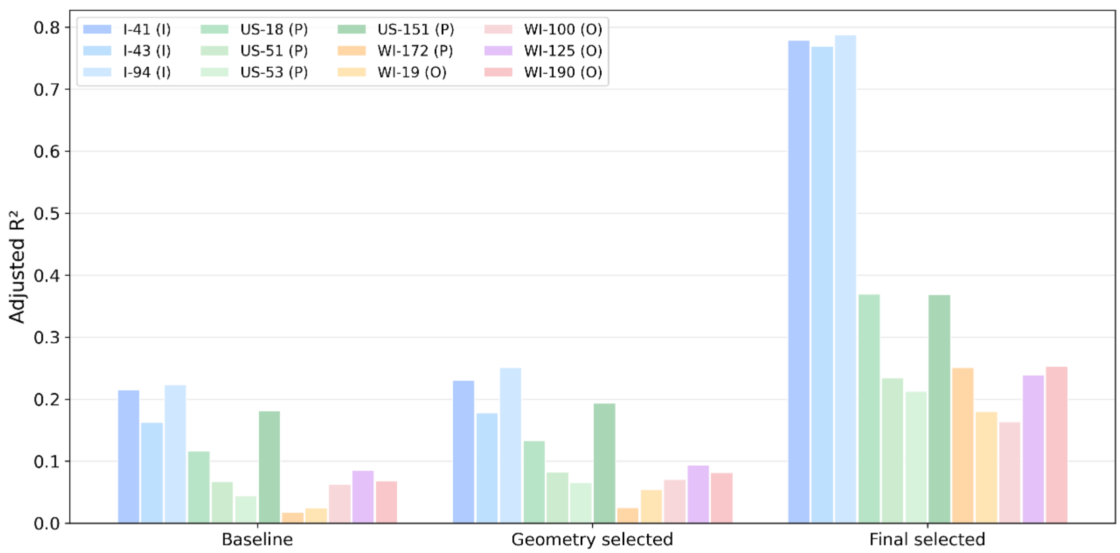

Figure 6-87: Model Fit Comparison Across Baseline and Extended Models.

Interaction Effects

Table 6-23 summarizes the selected interaction effects retained in the extended models. Only a limited number of interaction terms were statistically significant, and their signs were not consistent across corridors.

Table 6-23: Selected Interaction Effects in the Causation Model.

Interaction Term	Sign			Significance		
	I	P	O	I	P	O
Minor crash × Partial work-zone closure	+	-		**	*	.
Major crash × Partial work-zone closure		+		.	***	.
Minor crash × Full work-zone closure	-		-	***	.	***
Minor crash × Heavy weather	-		+	***	.	**
Major crash × Heavy weather		+		.	***	.
Full work-zone closure × Heavy weather	-		-	***	.	***

Functional class I: Interstate I-41; P: Principal arterial US-18; O: Other principal arterial WI-125

Sign +: positive; -: negative

Significance levels: ***p <0.001; **p <0.01; *p <0.05; . non-significant at 5% level

Figure 6-88 compares the estimated coefficients of significant interaction terms across the corridors. The interaction effects vary substantially in both sign and magnitude, making it difficult to identify a consistent pattern across functional classes or corridors. This suggests that compound effects involving crashes, work zones, and weather are highly corridor-specific and are likely influenced by local operating conditions, event overlap, and limited observations of these combined states. Overall, the figure suggests that these interaction terms are better interpreted as supplementary rather than dominant factors in corridor-level delay modeling.

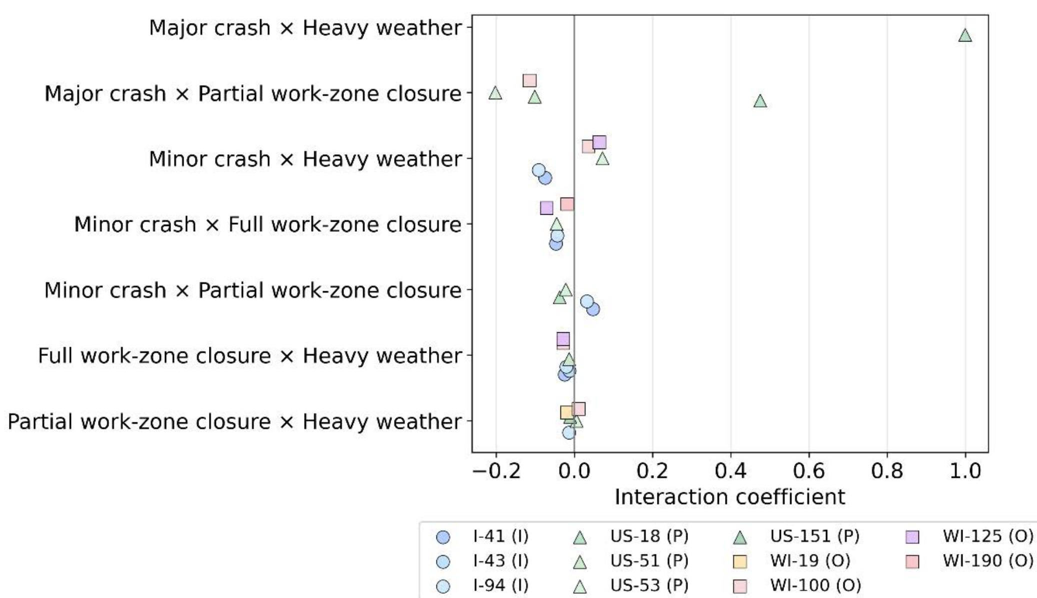

Figure 6-88: Selected Interaction Effects.

Machine Learning Model

As a supplementary nonlinear model, Light Gradient-Boosting Machine (LightGBM) was used to assess whether nonlinear associations in the corridor data could be captured more effectively than in the linear specifications. For each representative corridor, the model was trained using the variables retained as significant in the corridor-specific extended OLS specifications, excluding interaction terms. The data were split into training, validation, and test sets at a ratio of 6:2:2, and the model hyperparameters were tuned to minimize L2 loss.

Table 6-24 summarizes the predictive performance of the LightGBM models for the three representative corridors. Consistent with the OLS results, predictive performance was generally higher for total delay than for non-recurrent delay. Among the three representative corridors, model fit was highest for I-41, moderate for US-18, and lowest for WI-125. The relatively lower performance in WI-125 may reflect greater short-term variability and less stable traffic structure than in the interstate corridor. Although I-41 already showed relatively strong in-sample fit in the OLS models, the LightGBM models achieved higher R^2 values for US-18 and WI-125, suggesting that the machine-learning approach was better able to capture nonlinear and heterogeneous delay patterns in the arterial corridors that were not fully represented by the linear OLS specification.

Table 6-24: LightGBM Predictive Performance by Representative Corridor.

Corridor	Target	R^2	RMSE	MAE
I-41	Total delay	0.738	0.105	0.012
	Non-recurrent delay	0.711	0.103	0.012
US-18	Total delay	0.402	0.200	0.060
	Non-recurrent delay	0.308	0.186	0.051
WI-125	Total delay	0.300	0.252	0.120
	Non-recurrent delay	0.186	0.238	0.106

While Table 6-24 reports model performance for the three representative corridors, Figure 6-89 and Figure 6-90 summarize LightGBM feature importance and SHAP patterns for all 12 selected corridors to provide a broader diagnostic comparison.

Figure 6-89 compares LightGBM feature importance values across all selected corridors. For the interstate corridors, the previous 15-minute delay variable has higher importance than in most arterial corridors, indicating a stronger role of short-term delay correlation. By contrast, hourly volume and several TMC geometry variables tend to have greater importance in the arterial corridors than in the interstate corridors, suggesting that demand

and segment-level structure play a larger role there. The figure also highlights corridor-specific patterns, such as the relatively high importance of heavy vehicle ratio in WI-125 and signal in US-151, showing that important predictors can differ substantially by corridor.

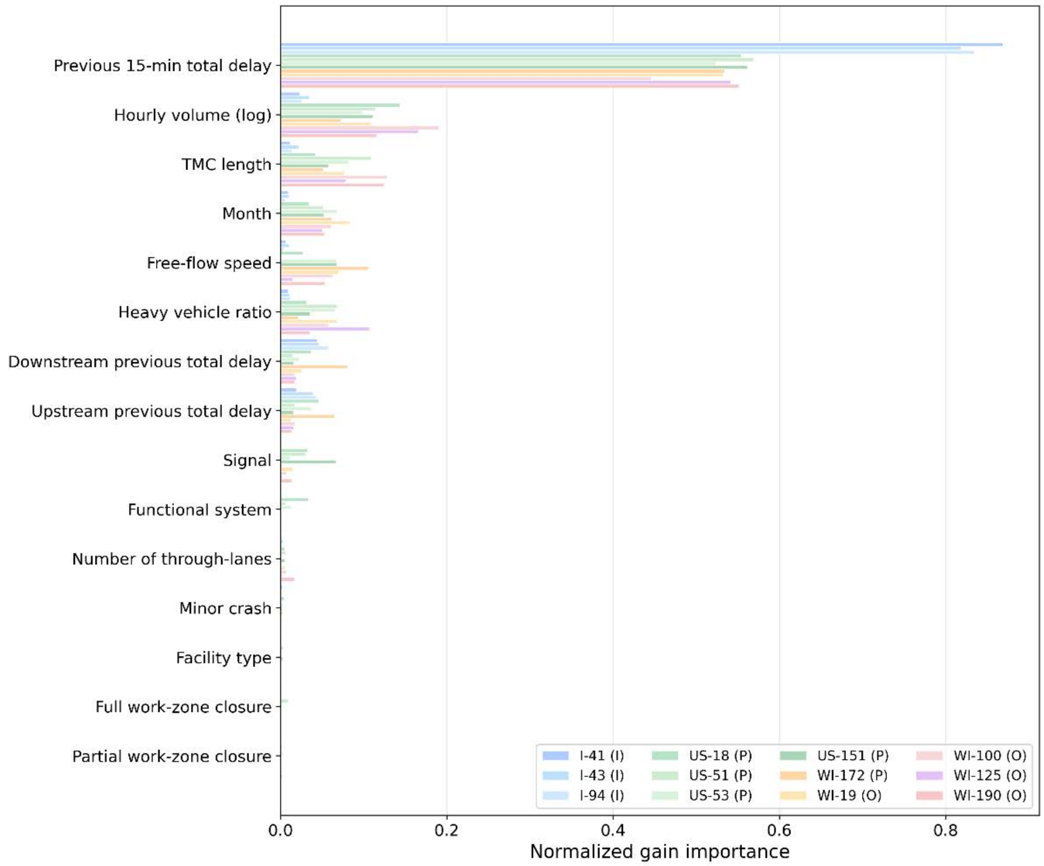

Figure 6-89: LightGBM Feature Importance by Corridor.

Figure 6-90 presents SHAP summary plots for all selected corridors. Compared with the interstate corridors, several ‘principal arterial’ and ‘other principal arterial’ corridors show broader variation in SHAP values across variables, indicating greater heterogeneity in how the predictors affect delay. This pattern is especially pronounced in the ‘other principal arterial’ corridors, where the effects of individual variables vary more widely across observations.

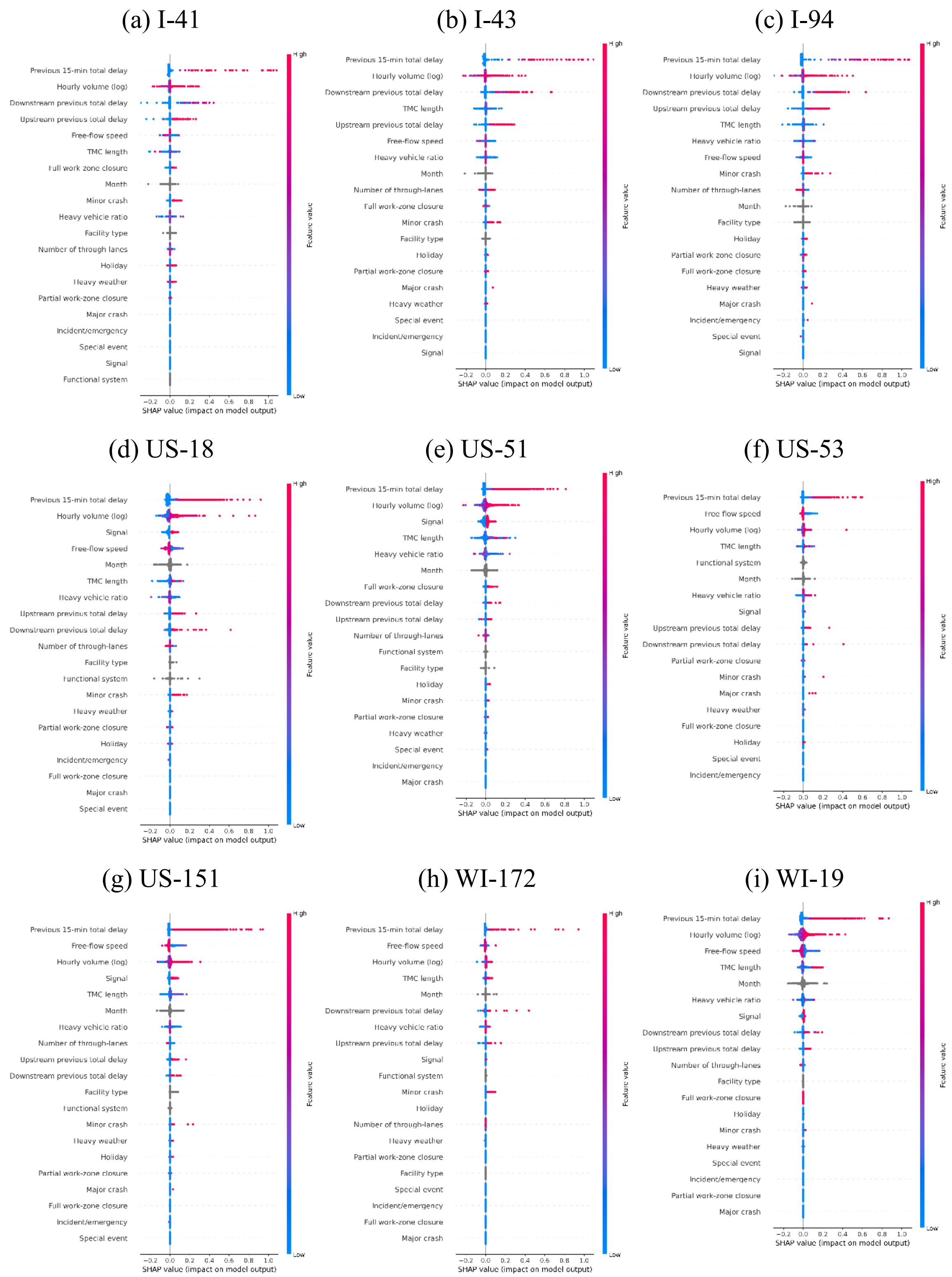
(a) I-41
Previous 15-min total delay
Hourly volume (log)
Downstream previous total delay
Upstream previous total delay
Free-flow speed
TMC length
Full work zone closure
Month
Minor crash
Heavy vehicle ratio
Facility type
Number of through lanes
Holiday
Heavy weather
Partial work-zone closure
Major crash
Incident/emergency
Special event
Signal
Functional system
SHAP value (impact on model output)
Feature value
High
Low
(b) I-43
Previous 15-min total delay
Hourly volume (log)
Downstream previous total delay
TMC length
Upstream previous total delay
Free-flow speed
Heavy vehicle ratio
Month
Number of through-lanes
Full work-zone closure
Minor crash
Facility type
Holiday
Partial work-zone closure
Major crash
Heavy weather
Special event
Incident/emergency
Signal
SHAP value (impact on model output)
(c) I-94
Previous 15-min total delay
Hourly volume (log)
Downstream previous total delay
Upstream previous total delay
TMC length
Heavy vehicle ratio
Free-flow speed
Minor crash
Number of through-lanes
Month
Facility type
Holiday
Partial work zone closure
Full work-zone closure
Heavy weather
Major crash
Incident/emergency
Special event
Signal
SHAP value (impact on model output)
(d) US-18
Previous 15-min total delay
Hourly volume (log)
Signal
Free-flow speed
Month
TMC length
Heavy vehicle ratio
Upstream previous total delay
Downstream previous total delay
Number of through-lanes
Facility type
Functional system
Minor crash
Heavy weather
Partial work-zone closure
Holiday
Incident/emergency
Full work-zone closure
Major crash
Special event
SHAP value (impact on model output)
(e) US-51
Previous 15-min total delay
Hourly volume (log)
Signal
TMC length
Heavy vehicle ratio
Month
Full work-zone closure
Downstream previous total delay
Upstream previous total delay
Number of through-lanes
Functional system
Facility type
Holiday
Minor crash
Partial work-zone closure
Heavy weather
Special event
Incident/emergency
Major crash
SHAP value (impact on model output)
(f) US-53
Previous 15-min total delay
Free flow speed
Hourly volume (log)
TMC length
Functional system
Month
Heavy vehicle ratio
Signal
Upstream previous total delay
Downstream previous total delay
Partial work-zone closure
Minor crash
Major crash
Heavy weather
Full work-zone closure
Holiday
Special event
Incident/emergency
SHAP value (impact on model output)
(g) US-151
Previous 15-min total delay
Free-flow speed
Hourly volume (log)
Signal
TMC length
Month
Heavy vehicle ratio
Number of through-lanes
Upstream previous total delay
Downstream previous total delay
Facility type
Functional system
Minor crash
Heavy weather
Holiday
Partial work-zone closure
Major crash
Full work-zone closure
Incident/emergency
Special event
SHAP value (impact on model output)
(h) WI-172
Previous 15-min total delay
Free-flow speed
Hourly volume (log)
TMC length
Month
Downstream previous total delay
Heavy vehicle ratio
Upstream previous total delay
Signal
Functional system
Minor crash
Holiday
Number of through-lanes
Heavy weather
Partial work-zone closure
Facility type
Special event
Incident/emergency
Full work-zone closure
Major crash
SHAP value (impact on model output)
(i) WI-19
Previous 15-min total delay
Hourly volume (log)
Free-flow speed
TMC length
Month
Heavy vehicle ratio
Signal
Downstream previous total delay
Upstream previous total delay
Number of through-lanes
Facility type
Full work-zone closure
Holiday
Minor crash
Heavy weather
Special event
Incident/emergency
Partial work-zone closure
Major crash
SHAP value (impact on model output)

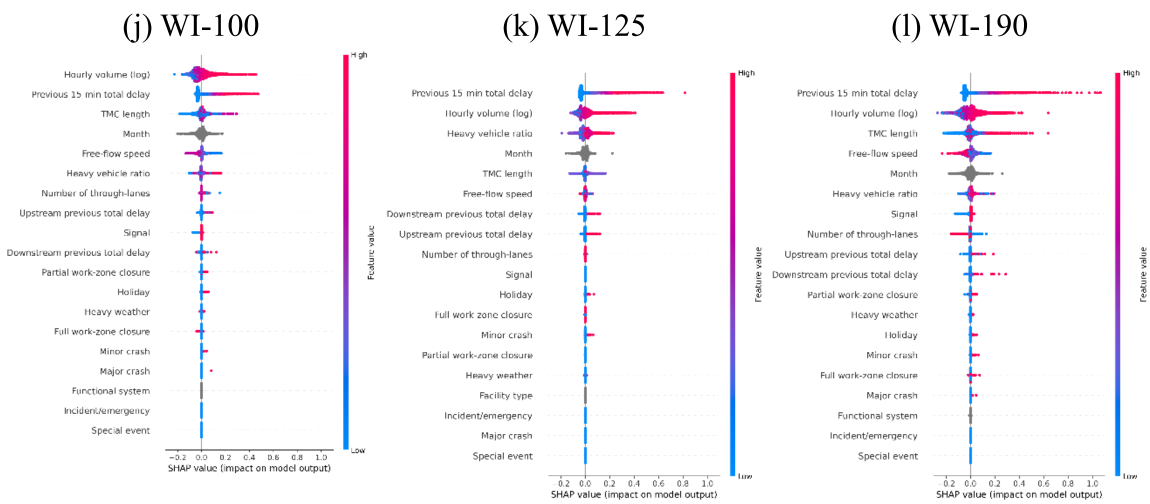

Figure 6-90: SHAP Summary Plots by Corridor.

Probabilistic Extension

A probabilistic extension was developed to estimate the probability of non-recurrent delay occurrence under selected event and operating conditions. From an operations perspective, non-recurrent delay that exceeds the typical recurrent delay baseline may warrant a response. This model therefore serves as a probability-based complement to the continuous delay models.

Table 6-25 summarizes the classification performance of the probabilistic models for non-recurrent delay occurrence in the three representative corridors, using a probability threshold of 0.5. Among the three representative corridors, the I-41 model shows the strongest overall performance, with the highest area under the curve (AUC) and balanced precision, recall, and F1-score. US-18 and WI-125 also achieve reasonably high AUC values and accuracy, indicating that the models can distinguish positive and negative cases to some extent. However, their lower recall and F1 scores should be interpreted in the context of class imbalance, because positive non-recurrent delay observations account for only a small share of the full sample. As a result, accuracy alone tends to appear favorable even when positive cases remain difficult to capture consistently.

Table 6-25: Probabilistic Model Performance for Non-Recurrent Delay Occurrence.

Corridor	AUC	Accuracy	Precision	Recall	F1-Score
I-41	0.945	0.994	0.699	0.698	0.698
US-18	0.906	0.929	0.622	0.203	0.306
WI-125	0.800	0.829	0.598	0.237	0.340

Similarly, while Table 6-25 reports classification performance for the three representative corridors, Figure 6-91 extends the probability comparison to all 12 selected corridors.

Figure 6-91 compares the predicted probability of non-recurrent delay occurrence under selected causal conditions across all selected corridors. In the interstate corridors, the probability increases most noticeably under the minor-crash condition, although the overall predicted values remain low. Among the ‘principal arterial’ corridors, US-51 shows the highest predicted probabilities across the tested conditions. In the ‘other principal arterial’ corridors, the predicted probability of non-recurrent delay occurrence is generally higher under all conditions, with WI-125 standing out as the highest. This pattern may reflect corridor-specific characteristics of WI-125 that make delays more likely to exceed the recurrent baseline and be classified as non-recurrent delay.

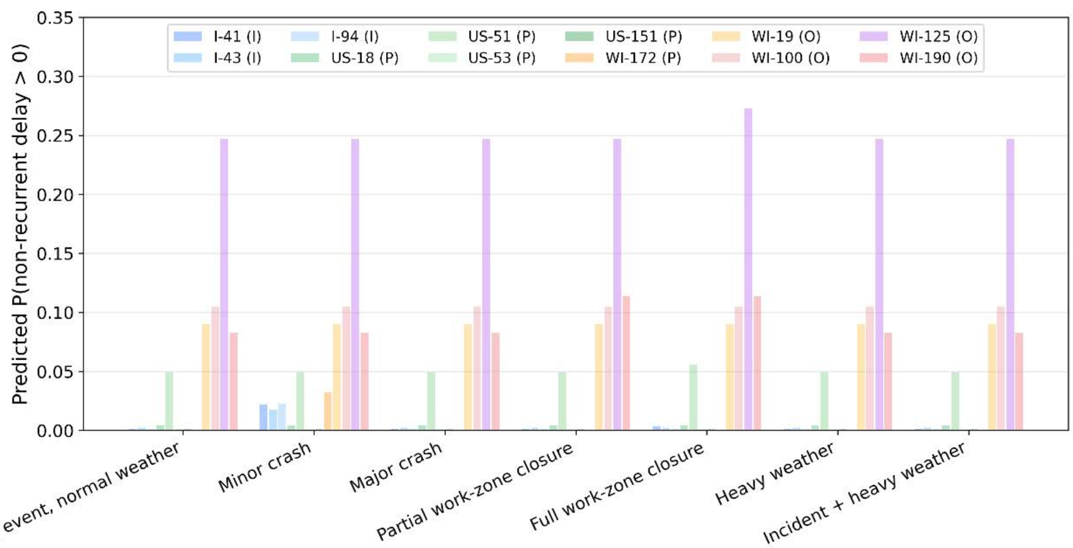

Figure 6-91: Predicted Probability of Non-Recurrent Delay by Causal Condition.

6.5. <u>Corridor-Level Application Summary</u>

This chapter applied the delay causation framework to 12 selected corridors. Across the selected corridors, non-recurrent delay generally accounted for the larger share of total delay, although the recurrent share varied by corridor. Delay was often concentrated in localized hotspot sections rather than evenly distributed along a corridor, and the dominant temporal pattern was typically a stronger afternoon peak, with some corridors also showing a smaller morning peak.

The causation analysis showed that work-zone delay was the most common major cause across the selected corridors, while signal-related delay was important in 'principal arterial' and 'other principal arterial' corridors. Several corridors also showed substantial unclassified delay, indicating that recorded event data alone do not fully explain corridor delay patterns and that corridor context, surrounding land use, and possible unreported events remain important considerations. The representative case studies further showed that delay can remain localized or propagate upstream depending on the event type, severity, corridor structure, and operating conditions.

The corridor-level modeling results showed that delay is associated with traffic demand, event conditions, corridor structure, and especially short-term delay correlation. Baseline linear models provided interpretable signs and significance patterns, but adding geometry and lagged delay terms produced substantial improvement. The LightGBM models captured additional nonlinear variation in the arterial corridors, while the probabilistic extension showed that the likelihood of non-recurrent delay differs by corridor. Overall, the results demonstrate that corridor delay causation is corridor-specific and that effective diagnosis requires the combined use of attribution analysis, hotspot diagnostics, and modeling.

7. Conclusion

This study developed and applied a reproducible framework for measuring and analyzing highway delay causation in Wisconsin, focusing on Interstate and non-Interstate highways and principal arterials. Through temporal and spatial matching, the framework integrates 15-minute TMC-level travel time data with traffic volume estimates, crash records, non-crash incident data, work-zone and lane closure records, special event information, weather data, holiday indicators, signal information, and roadway attributes. The resulting methodology provides a consistent process for calculating VHD, separating recurrent and non-recurrent delay, assigning non-recurrent delay to available causal factor categories, and identifying unclassified delay.

The statewide application showed that non-recurrent delay accounted for more than 70 percent of statewide delay across the three analysis years. Delay was spatially concentrated, with the Southeast region accounting for more than 55 percent of statewide delay and the Southwest region accounting for more than 19 percent. At the MPA level, delay was most concentrated in the Southeastern Wisconsin MPA, followed by the Madison MPA. Work-zone-related delay was the most prominent identifiable event-based contributor, representing approximately 24 percent of statewide annual VHD, while unclassified and recurrent delay on signalized TMCs also represented substantial components. Heavy weather, crash-related, and holiday-related delay each accounted for less than 5 percent of statewide delay. MPA-level results further showed that the Southeastern Wisconsin MPA had large shares of unclassified delay on signalized TMCs, work-zone-related delay, and recurrent delay on signalized TMCs, each exceeding 20 percent, while Madison MPA's work-zone delay share decreased after 2019 to approximately 8 percent in 2024. Year-to-year comparisons involving 2023 and 2024 should be interpreted with caution because changes in NPMRDS data supply and observation coverage may have affected delay estimates.

The corridor-level application showed that delay causation varies by corridor and facility type. Across the 12 selected corridors, delay was often concentrated in localized hotspots rather than evenly distributed along the full corridor. These hotspots were generally observed in urban or interchange areas. Work-zone-related delay was the most common major cause, while signal-related and unclassified delay were especially important in 'principal arterial' and 'other principal arterial' corridors. This observation is also consistent with statewide results. Case studies showed that event impacts can remain localized or propagate upstream depending on event type, severity, location, corridor structure, and operating conditions.

The modeling results provided supplementary evidence on factors associated with delay. Statewide models via linear regression identified traffic demand, signal presence, work-zone closure severity, crash indicators, and heavy vehicle ratio as important factors. Corridor-level models showed that short-term temporal delay correlation was especially important, as lagged delay variables substantially improved model fit. Geometry-related variables provided modest improvement. LightGBM machine-learning models captured additional nonlinear variation, and probabilistic models showed that the likelihood of non-recurrent delay differs by corridor.

Several limitations should be considered. First, delay estimates depend on NPMRDS data quality and coverage. The quantified delay was sensitive to changes in travel time data coverage, including the data provider issue likely affecting the period from June 2023 to July 2024 and the abnormal surge in observations from August to November 2024. During the latter period, delay estimates decreased sharply despite the abnormal increase in observations, indicating that changes in coverage may have affected the magnitude and temporal pattern of estimated VHD. In addition, the share of observed records relative to the expected full TMC-time grid remained limited, at approximately 40 percent in 2019, 45 percent in 2023, and 54 percent in 2024. While the current study uses NPMRDS 15-minute travel time data, the analysis can be significantly improved by complementing these data with commercial, higher resolution travel time datasets (such as 1-minute INRIX travel time data). This could improve both data accuracy and data completeness. Second, causal factor assignment depends on event data accuracy and completeness, as well as spatial-temporal matching rules. The share of unclassified delay may reflect unreported events, event impacts extending beyond the standardized buffers, queue spillback, or other conditions not captured in the available datasets. For instance, identification of crash-related delay is performed using data from the Crash Reporting System. Supplementing police-reported crash records with minor incidents information through commercial third-party data sources such as Waze could improve data quality. Third, some input variables are available only at coarser temporal or spatial resolutions, such as hourly traffic volume estimates, annual heavy vehicle ratios, daily weather indicators, and static signal information. Signal-related delay was identified using signal location information, not detailed signal timing or operations data. Finally, the regression and machine-learning models should be interpreted as diagnostic tools for identifying associations and relative importance rather than proof of direct causal effects.

Overall, the framework provides WisDOT with a practical, reproducible method for monitoring recurrent and non-recurrent delay, identifying causes of delay, and supporting future statewide and corridor-level diagnostics. Future implementation can build on this framework by updating the analysis with new years of data, refining event matching rules, incorporating more detailed operational data where available, and using the accompanying scripts and documentation to reproduce results in future reporting cycles.

8. References

[1] Federal Highway Administration, "Transportation Performance Management," [Online]. Available: https://www.fhwa.dot.gov/tpm/rule/pm3/phed.pdf..

[2] Cambridge Systematics, "Traffic Congestion and Reliability: Trends and Advanced Strategies for Congestion Mitigation (No. FHWA-HOP-05-064)," Federal Highway Administration, 2005.

[3] Texas Transportation Institute, "Urban Mobility Study," 2004.

[4] S. Chin, O. Franzese, D. Greene, H. Hwang and R. Gibson, "Temporary Losses of Highway Capacity and Impacts on Performance: Phase 2 (ORNL/TM-2004/209)," Oak Ridge National Lab, 2004.

[5] "Regional Integrated Transportation Information System (RITIS)," [Online]. Available: https://www.ritis.org/.

[6] RITIS, "RITIS: Causes of Congestion Tool Features and Navigation," [Online]. Available: https://congestion-causes.ritis.org/help.

[7] Oregon Department of Transportation, "2024 Statewide Congestion Overview," 2025.

[8] Pennsylvania Department of Transportation, "Transportation Systems Management and Operations Performance Report (TSMO)," 2024.

[9] Virginia Department of Transportation, "Freeway Operations and Special Facilities Performance," 2025.

[10] A. Soltani-Sobh, M. Ostojic, A. Stevanovic, J. Ma and D. K. Hale, "Development of Congestion Causal Pie Charts for Arterial Roadways," *International Journal for Traffic & Transport Engineering,* 2017.

[11] J. Kwon and P. Varaiya, "The congestion pie: delay from collisions, potential ramp metering gain, and excess demand.," in *Proceedings of 84th Transportation Research Board Annual Meeting*, 2005.

[12] Federal Highway Administration, "Empirical Studies on Traffic Flow in Inclement Weather (No. FHWA-HOP-07-073)," 2006.

[13] J. H. Friedman, "Greedy Function Approximation: A Gradient Boosting Machine," *The Annals of Statistics,* vol. 29, no. 5, pp. 1189-1232, 2001.

[14] G. Ke, Q. Meng, T. Finley, T. Wang, W. Chen, W. Ma, Q. Ye and T.-Y. Liu, "LightGBM: A Highly Efficient Gradient Boosting Decision Tree," in *Advances in Neural Information Processing Systems 30 (NIPS 2017)*, 2017.

9. Appendices

9.1. Required Input Data

This appendix summarizes the main input data categories needed to reproduce the methodology. These details are provided here rather than in the main text to keep the body focused on methodology.

Table 9-1: Required Input Data and Files.

Input Dataset	Example File or Source	Required Fields or Content	Use in Analysis
NPMRDS travel time	15min_NPMRDS_{YEAR}/15min_NPMRDS_{YEAR}_All.csv	TMC code; timestamp; travel time; travel speed; reference speed	Base travel time data for delay calculation
TMC identification	15min_NPMRDS_{YEAR}/TMC_Identification.csv	TMC code; road name; direction; road order; length; AADT; heavy vehicle ratio; lane count; functional class; facility type	Network inventory and TMC attributes
Region and MPA references	Input/WI_region.csv; Input/WI_MPA.csv	County/region and TMC/MPA assignment information	Spatial grouping for regional and MPA summaries
CCS hourly profiles	WisDOT CCS profile assignment and hourly profile tables	Hourly distribution factors by profile, day class, and month	Traffic volume estimation
Holiday calendar	Input/holiday_dates_2015_2035.csv	Holiday dates and labels	Day classification and holiday flag
Crash data	Crash factor files	Crash time, severity, matched TMCs	Crash flag and severity-based matching
Non-crash incident data	Incident factor files	Incident start/end time, type, matched TMCs	Incident delay assignment

Lane closure data	Lane closure factor files	Closure time, closure type, roadway status, matched TMCs	Work zone, emergency, and special-event lane-closure flags
Weather data	Weather files	Rain, snow, snow depth, weather station distance, matched TMCs	Weather event flags and intensity attributes
Signal data	Signal files	Signal flag, distance, matched TMC	Static signal flag
Candidate corridor table	Input/Wisconsin_Candidate_Corridors_2024.csv	Corridor/section ID, start/end limits	Selected corridor and section extraction
NPMRDS TMC shapefile	Zipped Wisconsin TMC shapefile; Input/tmc_list_{YEAR}.csv	TMC geometry and standardized direction	Mapping

9.2. <u>**Step-by-Step Processing Scripts**</u>

This appendix summarizes the data processing workflow used to construct the analysis-ready datasets and generate outputs. All Python scripts referenced below are provided separately. Rather than reproducing the full source code, this section documents the purpose, primary inputs, and outputs of each script to ensure transparency and reproducibility.

The processing workflow follows a sequential structure, beginning with event and TMC metadata preparation and ending with aggregation and visualization outputs. Each step produces intermediate files that are reused by later steps.

<u>Workflow Summary</u>

The complete processing pipeline proceeds as follows:

1. Process raw event data (crash, incident, lane closure, weather, and signal) into TMC-matched datasets
2. Generate annual TMC lookup tables and spatial grouping fields
3. Estimate hourly traffic volumes using TMC-level AADT and CCS hourly profiles
4. Compute total VHD from 15-minute NPMRDS travel time records
5. Match causal factors to the 15-minute VHD records

6. Decompose total VHD into recurrent and non-recurrent components
7. Assign non-recurrent delay to matched causal factors and aggregate delay records
8. Corridor data generation and analysis
9. Generate visualization outputs
10. Modeling analysis

This structured workflow ensures that all procedures are reproducible and traceable from raw NPMRDS data to final aggregated outputs.

Table 9-2: Primary Input and Output by Processing Step.

Step	Primary Input	Primary Output	Meaning of Output
0	NPMRDS TMC shapefile, raw event data	Matched event data	Each event was matched to one or more TMC segments.
1	NPMRDS TMC metadata; region, MPA, and TMC reference tables	Annual TMC lookup tables	Reference tables containing TMC attributes and region/MPA assignments.
2	TMC AADT; CCS hourly profile table; holiday calendar	Hourly volume estimates	Directional hourly volume by TMC, month, day class, and hour.
3	15-minute NPMRDS travel time; lookup and volume files	15-minute VHD files	TMC-level total VHD before causal factor matching.
4	VHD files; crash, incident, lane closure, weather, signal, special event, and holiday data	Matched VHD-factor files	15-minute TMC-level delay records with causal factor indicators.
5	Matched VHD-factor files	Decomposed delay files	Matched dataset with recurrent and non-recurrent delay components.
6	Decomposed delay files; lookup tables	Summary tables	Daily, monthly, annual, statewide, regional, MPA, corridor, and section summaries.
7	Decomposed delay files; lookup tables; corridor/section definitions	Corridor and section outputs	Datasets and summaries used for corridor diagnostics.
8	Summary tables; NPMRDS shapefile	Figures and maps	Reporting graphics and spatial diagnostics.
9	Decomposed delay files	Modeling results	Reporting modeling results.

Script 0. Event Data Processing

Purpose

This step converts raw event data (crashes, non-crash incidents, lane closures, weather, and traffic signals) into datasets matched to the NPMRDS TMC network. The matched event datasets provide the causal-factor records that are joined to 15-minute TMC delay in the

Delay-Cause Matching step.

Inputs

- Crash extract (WisTransPortal / DT4000): `Input/Crash_{YEAR}.csv`
- Non-crash incident extract (WisTransPortal / InterCAD): `Input/Incident_{YEAR}.csv`
- Lane closure extract (WisLCS): `Input/LCS_{YEAR}.csv`
- Weather station metadata and daily files (NOAA GHCNd): `Input/Weather/`
- WisDOT signal inventory and OSM signals: `Input/Signal/`
- Annual NPMRDS TMC network: `Input/TMC_{YEAR}.shp`

Main Steps

- Collect each event data into the Input folder
- Clean the crash data and match it to TMCs: automatically by scripts and manual review in ArcGIS Pro
- Clean the incident data and match it to TMCs: automatically by scripts and manual review in ArcGIS Pro
- Clean the lane-closure data and match it to TMCs: automatically by scripts and manual review in ArcGIS Pro
- Clean the weather data and match each TMC to its nearest three active stations per day
- Match the traffic-signal data to TMCs
- Save the matched event datasets to the Output folder

Output

- Matched crash data: `Output/Matched Crash Data_Upstream Included_{YEAR}.csv`
- Matched incident data: `Output/Matched Incident Data_Upstream Included_{YEAR}.csv`
- Matched lane closure data: `Output/Matched Lane Closure Data_Upstream Included_{YEAR}.csv`
- Matched weather data: `Output/Matched Weather Data_{YEAR}.csv`
- Matched traffic signal data: `Output/Matched Traffic Signal Data_{YEAR}.csv`

Each matched output links an event to one or more TMC segments, and where applicable to upstream segments and an opposite-direction flag. These datasets are the causal-factor inputs used in the Delay-Cause Matching step below.

Script 1. TMC Lookup File Generation

Purpose
This script generates cleaned annual TMC lookup tables used as the spatial reference for the delay analysis pipeline.

Inputs

- Annual NPMRDS TMC metadata: `15min_NPMRDS_{YEAR}/TMC_Identification.csv`
- County-to-region table: `Input/WI_region.csv`
- TMC-to-MPA table: `Input/WI_MPA.csv`
- TMC road name and direction reference: `Input/tmc_list_{YEAR}.csv`
- Analysis years: 2019, 2023, and 2024

Main Steps

- Load and standardize annual TMC metadata
- Remove TMCs with missing AADT
- Calculate heavy vehicle ratio
- Add region, MPA, road name, and standardized direction fields
- Save annual lookup tables

Outputs

- Raw lookup tables: `Input/tmc_lookup_{YEAR}.csv`
- Final lookup tables: `Input/tmc_lookup_{YEAR}_filled.csv`

The final lookup tables include key TMC attributes such as AADT, heavy vehicle ratio, facility type, lane count, region, MPA, road name, and direction.

Script 2. Hourly AADT Generation

Purpose
This script generates hourly AADT estimates for each primary TMC using CCS hourly flow profiles.

Inputs

- TMC lookup tables: `Input/tmc_lookup_{YEAR}_filled.csv`
- TMC-to-CCS profile assignment table
- CCS hourly flow profile table
- Holiday calendar: `Input/holiday_dates_2015_2035.csv`
- Analysis years: 2019, 2023, and 2024

Main Steps

- Load primary TMCs from the annual lookup table
- Match each TMC to a CCS profile
- Preprocess CCS hourly flow profiles and holiday information
- Expand each TMC to month, day-class, and hour records
- Calculate hourly AADT using CCS hourly fractions
- Apply a fallback value for unmatched TMCs
- Save annual hourly AADT files

Output

- Hourly AADT files: `Input/tmc_hourly_aadt_{YEAR}.parquet`

The output provides hourly traffic volume estimates used in subsequent delay calculation steps.

Script 3. VHD Calculation

Purpose

This script converts raw 15-minute NPMRDS speed data into delay and vehicle-hours of delay (VHD) files.

Inputs

- Raw NPMRDS files: `15min_NPMRDS_{YEAR}/15min_NPMRDS_{YEAR}_All.csv`
- TMC lookup tables: `Input/tmc_lookup_{YEAR}_filled.csv`
- Hourly AADT files: `tmc_hourly_aadt_{YEAR}.parquet`
- Holiday calendar: `Input/holiday_dates_2015_2035.csv`

Main Steps

- Read raw NPMRDS data and calculate 15-minute delay
- Save regional monthly delay files
- Interpolate short speed gaps only
- Merge delay records with hourly AADT
- Calculate VHD

Outputs

- Delay files: `delay_{region}_{year}_{month}.parquet`
- VHD files: `vhd_{region}_{year}_{month}.parquet`

The VHD files are used in later regional, statewide, and corridor-level delay analyses.

Script 4. Delay–Cause Matching

Purpose

This script merges non-recurrent causal factors with 15-minute TMC-level VHD data.

Inputs

- VHD files: `Delay/vhd_{REGION}_{YEAR}_{MONTH}.parquet`
- Preprocessed factor files in the `Factor` folder
- TMC lookup tables: `Input/tmc_lookup_{YEAR}_filled.csv`
- Analysis years: 2019, 2023, and 2024

Causal Factors

- Crash (severity-based temporal buffering)
- Non-crash incident (event duration expansion)
- Lane closure (monthly clipping and 15-minute expansion)
- Traffic signal (static TMC-level attribute)
- Weather (station-based daily assignment)

Main Steps

- Preprocess crash, incident, lane-closure, signal, and weather factors
- Expand time-based events into 15-minute bins
- Merge factor indicators with 15-minute VHD data
- Save matched outputs in weekly files for memory-safe processing

Output

- Matched VHD-factor files: `Delay/Matched/vhd_factor_{REGION}_{YEAR}_{MONTH}_{WEEK_START}.parquet`

These files are used in recurrent baseline construction and subsequent delay-cause analysis.

Script 5. Recurrent vs. Non-Recurrent Delay Classification

Purpose

This script decomposes observed VHD into recurrent and non-recurrent components.

Inputs

- Matched VHD-factor files: `Delay/Matched/vhd_factor_{REGION}_{YEAR}_{MONTH}_{WEEK_START}.par` `quet`

- Analysis years: 2019, 2023, and 2024

Main Steps

- Identify event-free 15-minute observations
- Group observations by TMC, season, day-of-week, and hour
- Use the 75th percentile of event-free VHD as the recurrent baseline
- Decompose observed VHD into recurrent and non-recurrent components

Outputs

- Recurrent lookup tables: `Delay/Matched/RecurrentLookup/recurrent_lookup_{REGION}_{YEAR}.parquet`

  Decomposed matched files: `Delay/Matched/recdef/vhd_factor_{REGION}_{YEAR}_{MONTH}_{WEEK_START}.parquet`

The output files include `REC_VHD` and `NONREC_VHD` and are used in subsequent delay-cause summaries and modeling.

<u>Script 6. Aggregation and Summary Output</u>

Purpose

This script aggregates decomposed delay data into daily, monthly, and yearly summary tables.

Inputs

- Decomposed recdef files: `Delay/Matched/recdef/vhd_factor_{REGION}_{YEAR}_{MONTH}_{WEEK_START}.parquet`
- TMC lookup tables: `Input/tmc_lookup_{YEAR}_filled.csv`
- Analysis years: 2019, 2023, and 2024

Main Steps

- Aggregate 15-minute records to daily TMC-level files
- Build raw monthly cause-combination tables by region and MPA
- Convert internal cause combinations into readable reporting labels
- Generate monthly and yearly summary tables

Outputs

- Daily TMC-level files: `Delay/Matched/recdef/vhd_factor_daily_{REGION}_{YEAR}_{MONTH}.parquet`
- Raw monthly tables: `Annual/raw_monthly_region_flag_{YEAR}.csv`, `Annual/raw_monthly_mpa_flag_{YEAR}.csv`
- Final summary tables: `Annual/monthly_*, Annual/yearly_*`

These tables are used for statewide, regional, MPA-level, and annual delay-cause reporting.

Script 7. Corridor-Level Analysis

Purpose
This script generates corridor-level and selected-section datasets and summary tables for corridor diagnostics and case-study analysis.

Inputs

- Decomposed recdef files: `Delay/Matched/recdef/vhd_factor_{REGION}_{YEAR}_{MONTH}_{WEEK_START}.parquet`
- TMC lookup tables: `Input/tmc_lookup_{YEAR}_filled.csv`
- Selected corridor/section table: `Input/Wisconsin_Candidate_Corridors_2024.csv`
- Analysis years: 2019, 2023, and 2024

Main Steps

- Aggregate annual delay totals by TMC
- Extract road-corridor datasets using ROAD and ROAD_NAME fields
- Extract selected section datasets using the candidate corridor table
- Aggregate corridor and section delay by month and cause combination
- Generate optional daily diagnostic heatmaps and TMC-level delay component plots

Outputs

- TMC-level annual summaries: `Annual/yearly_tmc_{YEAR}.csv`
- Corridor files: `Delay/Matched/Corridor/{ROAD}_{YEAR}.parquet`
- Section files: `Delay/Matched/Corridor/Section_{SECTION_ID}_{YEAR}.parquet`
- Corridor summary tables: `Annual/monthly_corridor_flag_{YEAR}.csv`, `Annual/yearly_corridor_flag_{YEAR}.csv`
- Section summary tables: `Annual/monthly_section_flag_{YEAR}.csv`, `Annual/yearly_section_flag_{YEAR}.csv`

- Optional diagnostic figures: `Figure/Daily_Diagnostic/`

These outputs support corridor-level delay summaries, selected-section diagnostics, and case-study visualizations.

Script 8. Visualization

Purpose

This script generates summary figures for statewide, regional, MPA-level, corridor-level, and selected-section delay reporting.

Inputs

- Monthly and yearly summary tables under `Annual/`
- TMC lookup tables: `Input/tmc_lookup_{YEAR}_filled.csv`
- NPMRDS Wisconsin TMC shapefile
- Selected corridor/section table: `Input/Wisconsin_Candidate_Corridors_2024.csv`
- Analysis years: 2019, 2023, and 2024

Main Steps

- Plot monthly total delay at statewide, region, and MPA levels
- Plot recurrent and non-recurrent delay components
- Plot annual event-based delay share
- Generate delay composition charts by geography level
- Generate statewide, regional, MPA-level, corridor-level, and section-level maps
- Save all figures under the `Figure/` folder

Outputs

- Statewide figures: `Figure/Statewide/`
- Region figures: `Figure/Region/`
- MPA figures: `Figure/MPA/`
- Corridor figures: `Figure/Corridor/`
- Section figures: `Figure/Section/`
- Maps: `Figure/Map/`

Script 9. Statewide and Regional Delay Modeling

Purpose

This script estimates statewide and regional relationships between causal factors and 15-minute delay outcomes using statistical regression and machine-learning models.

Inputs

- Decomposed recdef files: `Delay/Matched/recdef/vhd_factor_{REGION}_{YEAR}_{MONTH}_{WEEK_START}.parquet`
- Analysis regions, months, and modeling year specified in the configuration

Main Steps

- Build a memory-efficient sample of event and non-event observations
- Create event severity, traffic volume, signal, weather, and heavy vehicle variables
- Check whether each factor has sufficient observations and TMC support
- Fit statewide and regional regression models for total and non-recurrent delay
- Calculate standardized coefficients, effect sizes, and contribution shares
- Fit statewide and regional LightGBM models for total delay
- Generate feature-importance and optional SHAP results

Outputs

- Modeling tables: `Modeling/{YEAR}/Tables/`
- Modeling figures: `Modeling/{YEAR}/Figures/`

9.3. Data Dictionary

Road Data

NPMRDS TMC Network

- **tmc**: Unique Traffic Message Channel identifier defining a directional roadway segment
- **direction**: Direction of travel encoded in the TMC (NB, SB, EB, WB)
- **tmclinear**: Linear identifier grouping TMC segments within the same corridor
- **road_order**: Sequential ordering of TMCs within a corridor (upstream to downstream)
- **roadname, roadnumber**: Signed route or roadway name and route number
- **f_system**: Functional roadway class (1 interstate, 2 freeway/expressway, 3+ arterial/collector/local)
- **miles**: Segment length in miles
- **aadt**: Annual Average Daily Traffic associated with the segment
- **startlat, startlong**: Latitude and longitude of the upstream endpoint of the segment
- **endlat, endlong**: Latitude and longitude of the downstream endpoint of the segment

Event Data

Crash

- **CRSHDATE**: Date on which the crash occurred
- **CRSHTIME**: Time at which the crash occurred (HHMM)
- **INJSVR**: Injury severity: K (fatal), A (suspected serious), B (suspected minor), C (possible), O (none)
- **LOCTYPE**: Location type: I (intersection), N (non-intersection), PL (parking lot), PP (private property)
- **LATDECDG, LONDECDG**: Latitude and longitude in decimal degrees of the first harmful event
- **ONHWY, ONHWYDIR, ONHWYSYS**: Name of the highway on which the crash occurred, signed direction, and highway system (IH, USH, STH, CTH)
- **ONSTR, ATSTR**: Street name on which the crash occurred and intersecting-street name
- **TRVLDIR1, TRVLDIR2**: Directions of travel of involved vehicles (NB, SB, EB, WB)

Non-crash Incident

- **Intercad_ID**: Unique InterCAD incident identifier
- **Event_Type**: Incident type (e.g., disabled vehicle, debris, traffic stop)
- **Start_Time, End_Time**: Incident start and end date and time
- **Location**: Roadway location text (road name(s) and travel direction)
- **Description**: Narrative description of the incident
- **Latitude, Longitude**: Incident location in decimal degrees

Lane Closure

- **ClosureID**: Unique identifier for each lane closure record
- **ClosureType**: Closure category (construction, maintenance, permit, emergency, special event)
- **BeginDate, BeginTime, EndDate, EndTime**: Closure start and end date and time
- **Highway**: Affected roadway or route
- **RoadwayStatus**: Roadway status (e.g., full closure, lane or shoulder closure)
- **Lane Description**: Text description of the lane configuration and restrictions
- **ClosureLength**: Reported closure length (miles)
- **BeginLatitude, BeginLongitude**: Latitude and longitude of the closure start
- **EndLatitude, EndLongitude**: Latitude and longitude of the closure end

Weather

- **id**: NOAA weather station identifier

- **date**: Observation date (YYYYMMDD)
- **PRCP**: Daily precipitation (tenths of mm)
- **SNOW**: Daily snowfall (mm)
- **SNWD**: Snow depth (mm)
- **latitude, longitude**: Station latitude and longitude
- **mindate, maxdate**: Station period of record (temporal data availability)

Traffic Signal: WisDOT Inventory

- **int_id:** Unique intersection identifier
- **ix_name:** Intersection name, typically the cross-street pair
- **lat, lon:** Latitude and longitude of the signal in decimal degrees

Traffic Signal: OSM Inventory

- **way_id:** OSM way ID of the road the signal node sits on
- **name:** OSM street/way name
- **highway:** OSM road class of the parent way (tertiary, motorway_link, etc.); used to distinguish ramps from mainline
- **ref_name:** OSM route reference (e.g., WI 66)
- **signal_node_ids:** OSM node ID of the traffic-signal node
- **lat, lon:** Latitude and longitude of the signal node in decimal degrees

Delay-Cause Matching Data

Core identifiers and traffic state

- **TMC_CODE**: Unique Traffic Message Channel (TMC) identifier
- **TSTAMP**: Timestamp at 15-minute resolution
- **HOUR**: Hour of day (0–23)
- **HOURLY_VOLUME**: Estimated hourly traffic volume (vehicles/hour), derived from AADT × CCS hourly profile factors
- **RAW_VHD**: Raw vehicle-hours of delay (veh-hr), computed using free-flow speed benchmark
- **VHD**: Vehicle-hours of delay (veh-hr), computed using the 60% free-flow speed benchmark
- **IMPUTE_FLAG**: Imputation flag (observed; linearly interpolated)
- **HV_RATIO**: Heavy vehicle ratio (share of single-unit and combination trucks)

Crash

- **CRASH_FLAG**: Crash indicator (0: no crash; 1: crash)
- **CRASH_SEV**: Crash severity category: K (fatal), A (suspected serious), B (suspected minor), C (possible injury), O (no apparent injury)

- **CRASH_UP_FLAG**: Upstream-impact indicator for crashes (0: crash on the same TMC; 1: crash occurred within 3 miles upstream)
- **CRASH_COUNT**: Number of overlapping crashes

Non-crash incident

- **INCIDENT_FLAG**: Non-crash incident indicator (0: no incident; 1: incident)
- **INCIDENT**: Incident type (categorical)
- **INCIDENT_UP_FLAG**: Upstream-impact indicator for incidents (0: incident on the same TMC; 1: incident occurred within 3 miles upstream)

Lane closure (work zone / emergency / special event)

- **WZ_FLAG**: Work zone indicator (0: no work zone; 1: lane closure due to work zone activity)
- **WZ**: Work zone roadway status (categorical)
- **EMERGENCY_FLAG**: Emergency lane-closure indicator (0: no emergency closure; 1: lane closure due to emergency activity)
- **EMERGENCY**: Emergency roadway status (categorical)
- **LC_OPPO_TMC**: Opposing-direction TMC affected by the lane closure (if applicable)
- **LC_UP_FLAG**: Upstream-impact indicator for lane closures (0: closure on the same TMC; 1: closure occurred within 3 miles upstream)
- **SPECIAL_FLAG**: Special-event lane-closure indicator (0: no special event closure; 1: lane closure due to a special event)
- **SPECIAL**: Special event type (categorical)

Weather

- **WEATHER_RAIN_FLAG**: Rain intensity category (0: none; 1: light < 0.1 mm/h; 2: moderate 0.1–8 mm/h; 3: heavy 8–16 mm/h; 4: extreme > 16 mm/h)
- **WEATHER_RAIN_MM**: Daily precipitation (mm)
- **WEATHER_SNOW_FLAG**: Snow intensity category (0: none; 1: light < 0.1 mm/h; 2: moderate 0.1–1.5 mm/h; 3: heavy 1.5–3 mm/h; 4: extreme > 3 mm/h)
- **WEATHER_SNOW_MM**: Daily snowfall (mm)
- **WEATHER_SNWD_MM**: Daily snow depth (mm)

Holiday

- **HOLIDAY_FLAG**: Holiday indicator (0: non-holiday; 1: holiday)

Traffic signal

- **SIGNAL_FLAG**: Traffic signal indicator (0: no signal; 1: signal located within 50 meters)

Recurrent vs. Non-Recurrent Delay Classification Data

Core identifiers and traffic state

- **REC_VHD**: Recurrent delay
- **NONREC_VHD**: Non-recurrent delay

Aggregation Data

Core identifiers

- **REGION**: WisDOT region name (e.g., NORTHCENTRAL, NORTHEAST, SOUTHEAST, SOUTHWEST, NORTHWEST)
- **MONTH**: Calendar month (1–12)
- **CAUSE_FLAG_COMBINATION**: Flag-based category describing which causal-factor indicators were active for the underlying 15-minute observations.
  - NONE: No event-related flags active
  - Otherwise, a concatenation of flag names separated by underscores (e.g., WZ_FLAG_SIGNAL_FLAG, SIGNAL_FLAG_WEATHER_SNOW_ACTIVE).
  - This field allows multiple active flags to be represented in a single label.

Aggregation counts

- **N_ROWS**: Number of underlying 15-minute TMC observations aggregated into the row for the given (REGION, MONTH, CAUSE_FLAG_COMBINATION)

Delay metrics (veh-hr)

- **TOTAL_VHD**: Total vehicle-hours of delay aggregated over the N_ROWS observations
- **TOTAL_RECURRENT_VHD**: Portion of TOTAL_VHD classified as recurrent delay using the event-free baseline approach
- **TOTAL_NONRECURRENT_VHD**: Portion of TOTAL_VHD classified as non-recurrent delay (excess above the recurrent baseline during periods with recorded disruptions)

Consistency check:

TOTAL_VHD ≈ TOTAL_RECURRENT_VHD + TOTAL_NONRECURRENT_VHD (minor rounding differences may occur)

Notes

- Rows represent monthly regional summaries of 15-minute TMC-level delay after causal-factor matching and recurrent/non-recurrent decomposition.
- Because CAUSE_FLAG_COMBINATION is flag-based, some categories reflect simultaneous conditions (e.g., work zone + weather + signal presence).
- Signal presence is typically a static segment attribute, so many combinations include SIGNAL_FLAG.

Summary Data

Core identifiers

- **REGION**: WisDOT region name (e.g., NORTHCENTRAL, NORTHEAST, SOUTHEAST, SOUTHWEST, NORTHWEST)
- **MONTH**: Calendar month (1–12)
- **CAUSE_FLAG**: Recoded, report-friendly cause category for the underlying 15-minute observations (e.g., No Event, Signal, Work Zone, Signal & Work Zone, Signal & Weather, Special Event & Holiday & Signal).
- This field represents a single assigned category per observation after recoding, and may include combined labels when multiple conditions are jointly represented.

Aggregation counts

- **N_ROWS**: Number of underlying 15-minute TMC observations aggregated into the row for the given (REGION, MONTH, CAUSE_FLAG)

Delay metrics (veh-hr)

- **TOTAL_VHD**: Total vehicle-hours of delay aggregated over the N_ROWS observations
- **TOTAL_RECURRENT_VHD**: Portion of TOTAL_VHD classified as recurrent delay using the event-free baseline approach
- **TOTAL_NONRECURRENT_VHD**: Portion of TOTAL_VHD classified as non-recurrent delay (excess above the recurrent baseline during periods with recorded disruptions)

Consistency check:

TOTAL_VHD ≈ TOTAL_RECURRENT_VHD + TOTAL_NONRECURRENT_VHD (minor rounding differences may occur)

Share metrics (% of total regional-month delay)

Shares are reported as percentages and are computed within each REGION × MONTH.

- TOTAL_SHARE_%: Share of total delay contributed by the category
  TOTAL_VHD / Σ(TOTAL_VHD over CAUSE_FLAG) × 100

- REC_SHARE_%: Share of total delay contributed by the recurrent portion of this category
  TOTAL_RECURRENT_VHD / Σ(TOTAL_VHD over CAUSE_FLAG) × 100
- NONREC_SHARE_%: Share of total delay contributed by the non-recurrent portion of this category
  TOTAL_NONRECURRENT_VHD / Σ(TOTAL_VHD over CAUSE_FLAG) × 100

Notes

- Rows represent monthly regional summaries of 15-minute TMC-level delay after causal-factor matching and recurrent/non-recurrent decomposition.
- CAUSE_FLAG is a recoded/aggregated label intended for reporting and plotting (e.g., stacked-bar monthly compositions). It differs from the raw flag-combination field in `raw_monthly_region_flag_2024.csv`, which preserves the original multi-flag combinations.

9.4. <u>**Analysis Examples**</u>

<u>Analysis Data Structure Example</u>

Table 9-3 provides an example of the 15-minute TMC-level analysis dataset used in the delay causation methodology. Each row represents one TMC segment during one 15-minute interval and includes the timestamp, estimated hourly traffic volume, calculated delay measures, imputation status, heavy vehicle ratio, and matched causal factor indicators. The delay fields include raw VHD, 60% threshold-based VHD, recurrent VHD, and non-recurrent VHD. The remaining columns indicate whether crashes, non-crash incidents, work zones, emergencies, weather events, special events, holidays, or traffic signals are associated with the corresponding TMC-time observation. This example illustrates the structure of the analysis-ready dataset before aggregation into daily, monthly, annual, corridor-level, MPA-level, regional, or statewide outputs.

Table 9-3: 15-Minute TMC-Level Analysis Data Structure Example.

TMC_CODE	TSTAMP	HOUR	HOURLY_VOLUME	RAW_VHD	VHD	REC_VHD	NONREC_VHD	IMPUTE_FLAG	HV_RATIO	CRASH_FLAG	CRASH_SEV
107-25656	2024-10-01 0:00	0	42.91775	0.01827	0	0	0	OBSERVED	0.14319	0	NONE
107N09466	2024-10-01 0:00	0	70.69729	0.002111	0	0	0	OBSERVED	0.106081	0	NONE
107-04666	2024-10-01 0:00	0	81.00034	0.021488	0	0	0	OBSERVED	0.077937	0	NONE
107-09178	2024-10-01 0:00	0	40.31294	0	0	0	0	OBSERVED	0.158166	0	NONE
107N09178	2024-10-01 0:00	0	41.72815	0	0	0	0	OBSERVED	0.161403	0	NONE
107-09177	2024-10-01 0:00	0	42.91775	0.003904	0	0	0	OBSERVED	0.164158	0	NONE

CRASH_UP_FLAG	CRASH_COUNT	INCIDENT_FLAG	INCIDENT	INCIDENT_UP_FLAG	WZ_FLAG	WZ	EMERGENCY_FLAG	EMERGENCY	LC_OPPO_TMC	LC_UP_FLAG
0	0	0	NONE	0	0	NONE	0	NONE	NONE	0
0	0	0	NONE	0	0	NONE	0	NONE	NONE	0
0	0	0	NONE	0	0	NONE	0	NONE	NONE	0
0	0	0	NONE	0	0	NONE	0	NONE	NONE	0
0	0	0	NONE	0	0	NONE	0	NONE	NONE	0
0	0	0	NONE	0	0	NONE	0	NONE	NONE	0

WEATHER_RAIN_FLAG	WEATHER_RAIN_MM	WEATHER_SNOW_FLAG	WEATHER_SNOW_MM	WEATHER_SNWD_MM	SPECIAL_FLAG	SPECIAL	HOLIDAY_FLAG	SIGNAL_FLAG
0	0	0	0	0	0	NONE	0	0
0	0	0	0	0	0	NONE	0	0
0	0	0	0	0	0	NONE	0	0
0	0	0	0	0	0	NONE	0	0
0	0	0	0	0	0	NONE	0	0
0	0	0	0	0	0	NONE	0	0

Cause-Based Reporting Output Example

Table 9-4 and Table 9-5 illustrate the cause-based reporting outputs generated from the 15-minute TMC-level delay records. The raw cause-combination table preserves the original combination of active causal factor indicators for each region and month. This format is useful for checking how multiple conditions overlap, such as crashes overlapping with holidays, signals, weather, or work zones. The reporting summary table converts these raw flag combinations into more readable cause categories for interpretation and visualization. It reports the number of underlying observation rows, total VHD, recurrent VHD, non-recurrent VHD, and the corresponding recurrent and non-recurrent delay shares. These summary outputs are used to compare delay composition across months and regions and to generate cause-based figures for statewide, regional, MPA-level, corridor-level, and selected-section reporting.

Table 9-4: Raw Cause-Combination Table Example.

REGION	MONTH	CAUSE_FLAG_COMBINATION	N_ROWS	TOTAL_VHD	TOTAL_RECURRENT_VHD	TOTAL_NONRECURRENT_VHD
NORTHCENTRAL	1	CRASH_FLAG	501	115.3973	3.857471	111.5399
NORTHCENTRAL	1	CRASH_FLAG_CRASH_UP_FLAG	906	134.1262	3.677604	130.4486
NORTHCENTRAL	1	CRASH_FLAG_CRASH_UP_FLAG_HOLIDAY_FLAG	173	11.71008	0.012777	11.69731
NORTHCENTRAL	1	CRASH_FLAG_CRASH_UP_FLAG_HOLIDAY_FLAG_SIGNAL_FLAG	142	37.5969	3.676251	33.92065
NORTHCENTRAL	1	CRASH_FLAG_CRASH_UP_FLAG_SIGNAL_FLAG	886	96.22027	20.04828	76.17199
NORTHCENTRAL	1	CRASH_FLAG_CRASH_UP_FLAG_WEATHER_SNOW_ACTIVE	113	0.822633	0.149074	0.673559
NORTHCENTRAL	1	CRASH_FLAG_CRASH_UP_FLAG_WZ_FLAG	123	0	0	0
NORTHCENTRAL	1	CRASH_FLAG_CRASH_UP_FLAG_WZ_FLAG_LC_UP_FLAG	13	0.567189	0.079098	0.488091
NORTHCENTRAL	1	CRASH_FLAG_HOLIDAY_FLAG	95	28.18043	0	28.18043
NORTHCENTRAL	1	CRASH_FLAG_SIGNAL_FLAG	447	124.3317	13.87587	110.4558
NORTHCENTRAL	1	CRASH_FLAG_WEATHER_SNOW_ACTIVE	90	11.51834	0	11.51834
NORTHCENTRAL	1	CRASH_FLAG_WZ_FLAG	80	0.035115	0	0.035115

Note: In this example, CRASH_FLAG without any additional flag indicates records where only the crash flag is active among the reported cause flags.

Table 9-5: Reporting Summary Table Example.

REGION	MONTH	CAUSE_FLAG	N_ROWS	TOTAL_VHD	TOTAL_RECURRENT_VHD	TOTAL_NONRECURRENT_VHD	TOTAL_SHARE_%	REC_SHARE_%	NONREC_SHARE_%
NORTHCENTRAL	1	Signal	308194	63366.73	12206.63	51160.11	51.1	9.84	41.26
NORTHCENTRAL	1	No Event	857639	26670.13	2725.761	23944.37	21.51	2.2	19.31
NORTHCENTRAL	1	Holiday & Signal	30862	7450.186	1041.283	6408.903	6.01	0.84	5.17
NORTHCENTRAL	1	Signal & Work Zone	22544	5758.257	597.4854	5160.772	4.64	0.48	4.16
NORTHCENTRAL	1	Signal & Weather	23238	5719.544	812.2395	4907.304	4.61	0.66	3.96
NORTHCENTRAL	1	Holiday	89511	5074.081	228.4442	4845.637	4.09	0.18	3.91
NORTHCENTRAL	1	Work Zone	172686	4219.454	344.8325	3874.622	3.4	0.28	3.12
NORTHCENTRAL	1	Weather	71800	2725.285	132.2094	2593.076	2.2	0.11	2.09
NORTHCENTRAL	1	Holiday & Signal & Work Zone	1234	796.7782	69.4895	727.2886	0.64	0.06	0.59
NORTHCENTRAL	1	Holiday & Weather	3102	544.1918	0.761501	543.4303	0.44	0	0.44
NORTHCENTRAL	1	Holiday & Work Zone	11235	529.696	14.12419	515.5718	0.43	0.01	0.42
NORTHCENTRAL	1	Signal & Weather & Work Zone	981	283.0057	34.28696	248.7188	0.23	0.03	0.2
NORTHCENTRAL	1	Crash	1407	249.5236	7.535075	241.9885	0.2	0.01	0.2
NORTHCENTRAL	1	Crash & Signal	1333	220.552	33.92415	186.6278	0.18	0.03	0.15
NORTHCENTRAL	1	Crash & Holiday & Work Zone	217	121.7321	0	121.7322	0.1	0	0.1
NORTHCENTRAL	1	Crash & Holiday & Signal	220	78.77492	4.870526	73.90439	0.06	0	0.06
NORTHCENTRAL	1	Weather & Work Zone	10680	75.27004	19.94843	55.32161	0.06	0.02	0.04
NORTHCENTRAL	1	Crash & Holiday	268	39.89052	0.012777	39.87774	0.03	0	0.03
NORTHCENTRAL	1	Holiday & Signal & Weather	115	11.98727512	0	11.98727544	0.01	0	0.01
NORTHCENTRAL	1	Crash & Signal & Work Zone	30	1.010112137	0.039942309	0.970169865	0	0	0
…	…	…	…	…	…	…	…	…	…

Figure Output Examples

Figures 9-1 through 9-4 provide examples of the main visualization outputs generated from the delay causation methodology. These figures illustrate how the delay records can be summarized and interpreted across different spatial and temporal resolutions.

Figure 9-1 shows monthly recurrent and non-recurrent delay. This figure is generated from the reporting summary table by summing recurrent VHD and non-recurrent VHD by month, without separating records by cause category. The figure can be used to identify monthly and seasonal delay patterns, as well as changes in the relative contribution of recurrent and non-recurrent delay over time. The same figure can be generated for different spatial resolutions, including statewide, regional, MPA-level, corridor-level, and selected-section summaries.

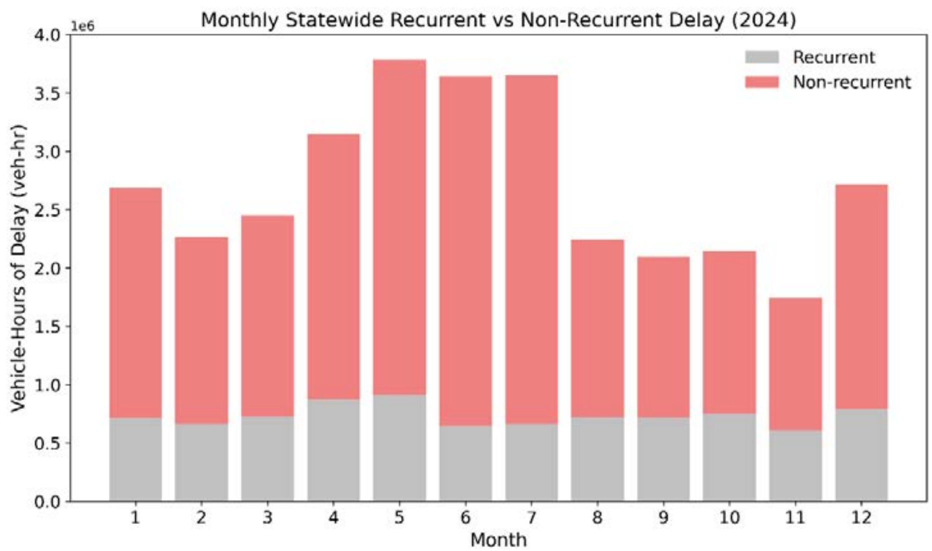

Figure 9-1: Example Monthly Recurrent and Non-Recurrent Delay Output.

Figure 9-2 shows delay composition by cause. This figure is generated from the reporting summary table by aggregating across months and summarizing the share of recurrent delay and cause-specific non-recurrent delay. The figure allows users to compare the relative contribution of recurrent delay, unclassified delay, and delay associated with specific causal factors such as crashes, non-crash incidents, work zones, special events, weather, and holidays. If the same summary is produced by month, the output can also be used to examine monthly delay composition by cause. This type of figure can be generated for different spatial resolutions, allowing comparisons across regions, MPAs, corridors, and selected sections to identify how the dominant delay contributors vary by geography or roadway context.

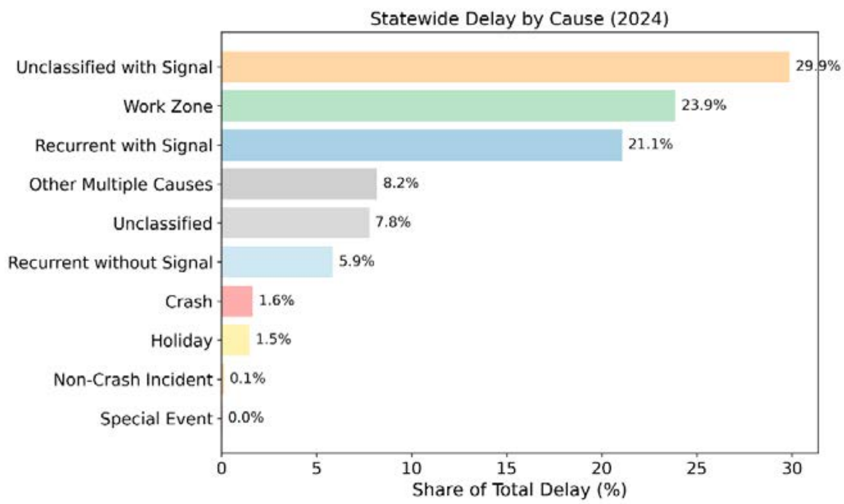

Figure 9-2: Example Delay Composition by Cause Output.

Figure 9-3 shows the spatial distribution of annual TMC-level delay. This map is generated by joining yearly TMC-level VHD summaries to the NPMRDS TMC shapefile. The map is used to identify high-delay hotspots and examine how delay is distributed across the roadway network. When generated at the monthly level, this type of map can also be used to compare seasonal changes in delay concentration and identify locations where delay is concentrated during specific times of year.

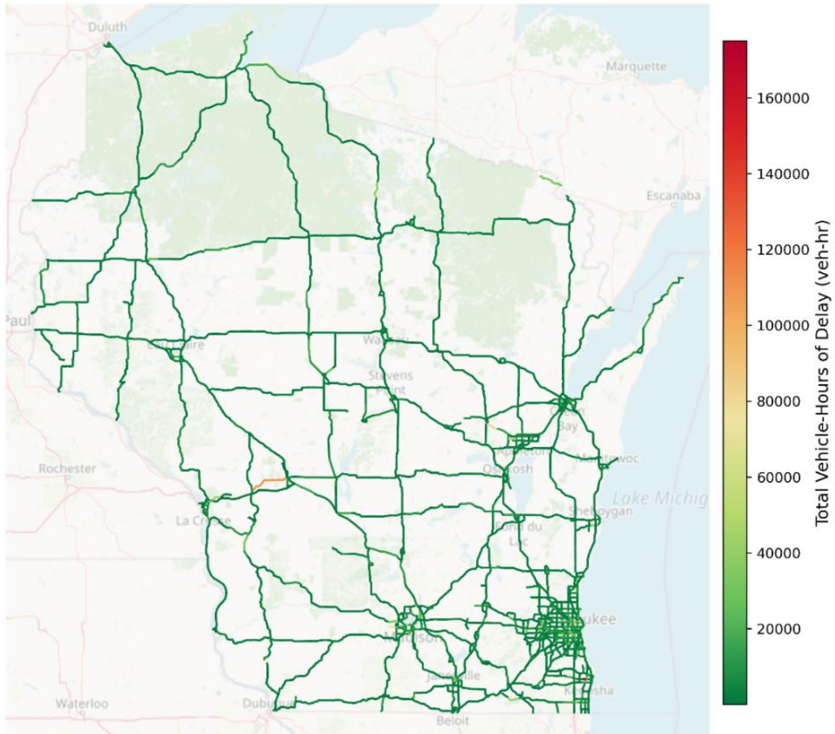

Figure 9-3: Example Annual TMC-Level Delay Map Output.

Figure 9-4 shows a case-study space-time contour for a selected corridor section. This figure is generated from the 15-minute TMC-level analysis dataset, with delay represented by color intensity across time of day and ordered TMC segments. Reported events, such as crashes or incidents, can be overlaid on the contour to examine whether the timing and location of the event coincide with observed delay. This output supports detailed corridor diagnostics by showing the temporal duration, spatial extent, and upstream or downstream propagation of delay. It is especially useful for interpreting event-driven delay, recurrent bottlenecks, and localized disturbances within selected corridor sections.

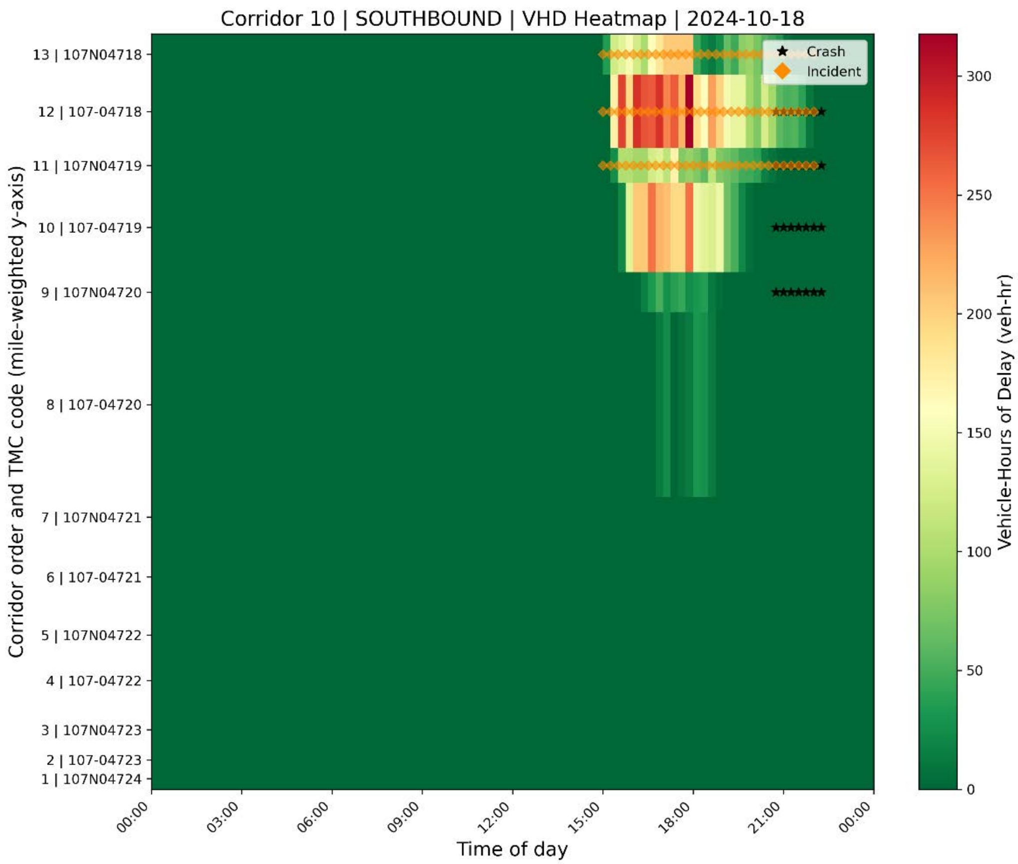

Figure 9-4: Example Case-Study Space-Time Contour Output.